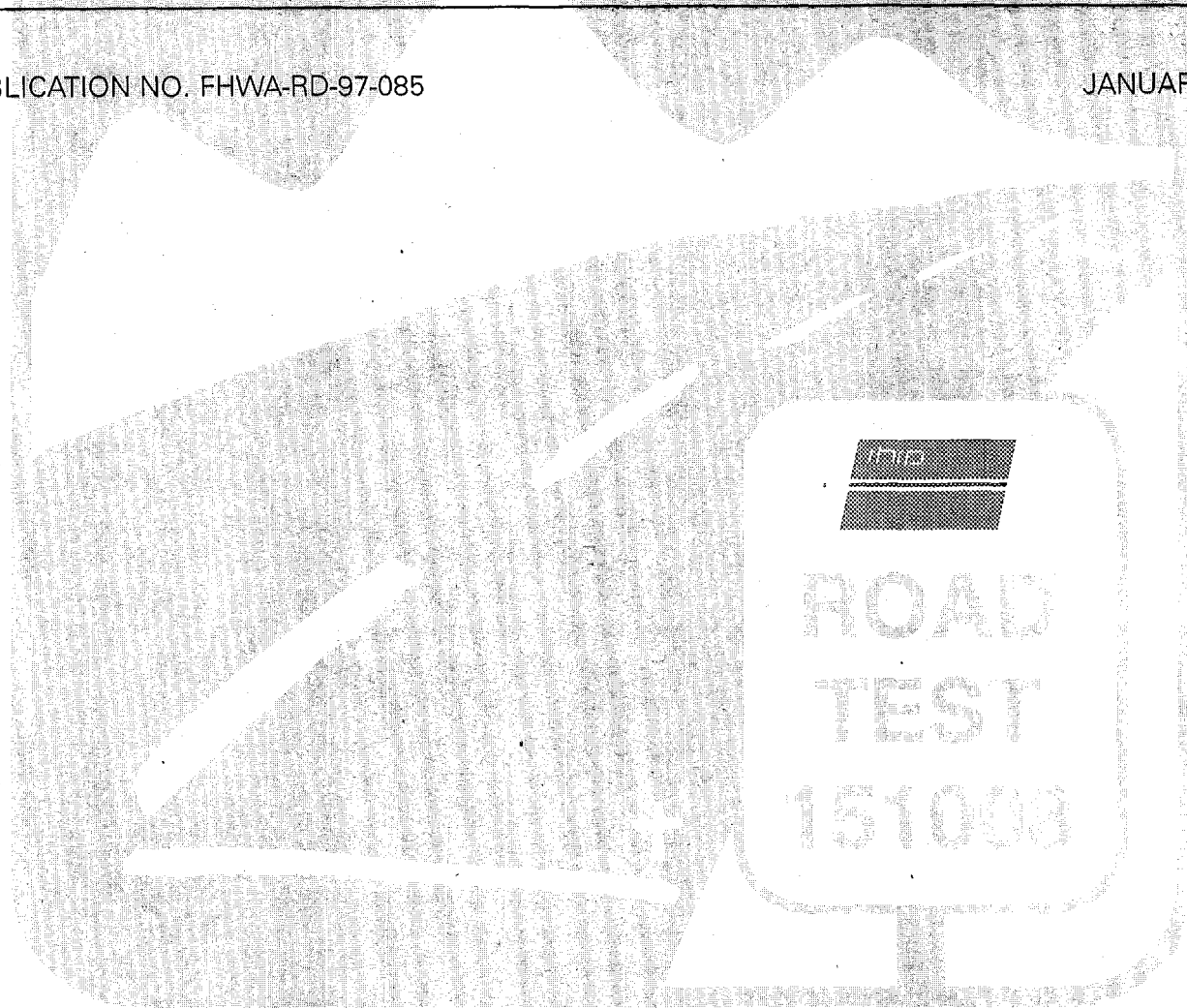


# Analyses Relating To Pavement Material Characterizations And Their Effects On Pavement Performance

PUBLICATION NO. FHWA-RD-97-085

JANUARY 1998



U.S. Department of Transportation  
**Federal Highway Administration**

Research and Development  
Turner-Fairbank Highway Research Center  
6300 Georgetown Pike  
McLean, VA 22101-2296

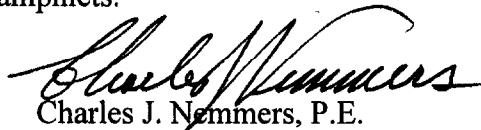


## FOREWORD

A key challenge faced by engineers using the 1993 *AASHTO Guide for Design of Pavement Structures* (AASHTO Guide) is the selection of appropriate design values for the subgrade soil and for the pavement materials. Until now, the information available to help engineers choose appropriate values has been incomplete. This report documents the analysis of the Long-Term Pavement Performance (LTPP) data conducted to develop more complete information on this subject. The specific guidelines and procedures developed through this analysis were presented in a series of three design pamphlets addressing: (1) the selection of appropriate design values to characterize the subgrade soil, (2) interpretation of pavement deflection data, and (3) characterization of the pavement materials. These pamphlets are *Design Pamphlet for the Determination of Design Subgrade Moduli in Support of the 1993 AASHTO Guide for the Design of Pavement Structures (FHWA-RD-97-083)*, *Design Pamphlet for the Backcalculation of Pavement Layer Moduli in Support of the 1993 AASHTO Guide for the Design of Pavement Structures (FHWA-RD-97-076)*, and *Design Pamphlet for the Determination of Layered Elastic Moduli for Flexible Pavement Design in Support of the 1993 AASHTO Guide for the Design of Pavement Structures (FHWA-RD-97-077)*.

Application of the procedures and guidelines developed through this analysis will facilitate and improve application of the AASHTO Guide flexible pavement design procedures. Their use will provide: (1) improved designs, (2) more realistic estimates of pavement performance, and (3) more consistent use of the AASHTO design parameters. Furthermore, although the procedures are specifically developed for use with the 1993 AASHTO Guide, their use will give agencies a "leg up" on implementation of the design procedures being developed for inclusion in the 2002 *AASHTO Guide For Design of New and Rehabilitated Pavement Structures*.

This report will be of interest to those involved in the development of new procedures for pavement design and material characterization, as well as those who wish to understand the technical basis for the referenced design pamphlets.



Charles J. Nemmers, P.E.

Director

Office of Engineering Research & Development

## NOTICE

This document is disseminated under the sponsorship of the Department of Transportation in the interest of information exchange. The United States Government assumes no liability for its contents or use thereof. This report does not constitute a standard, specification, or regulation.

The United States Government does not endorse products or manufacturers. Trade or manufacturers' names appear herein only because they are considered essential to the objective of this document.

**TECHNICAL REPORT DOCUMENTATION PAGE**

1. Report No. <b>FHWA-RD-97-085</b>		2. Government Accession No.		3. Recipient's Catalog No.	
4. Title and Subtitle <b>ANALYSES RELATING TO PAVEMENT MATERIAL CHARACTERIZATIONS AND THEIR EFFECTS ON PAVEMENT PERFORMANCE</b>				5. Report Date <b>January 1998</b>	
				6. Performing Organization Code	
7. Author(s) <b>Harold Von Quintus and Brian Killingsworth</b>				8. Performing Organization Report No. <b>BR95-01/J</b>	
9. Performing Organization Name and Address <b>Brent Rauhut Engineering Inc. 8240 Mopac, Suite 220 Austin, Texas 78759</b>				10. Work Unit No. (TRAIS) <b>C6B</b>	
				11. Contract or Grant No. <b>DTFH61-95-C-00029</b>	
12. Sponsoring Agency Name and Address <b>Office of Engineering R &amp; D Federal Highway Administration 6300 Georgetown Pike McLean, VA 22101-2296</b>				13. Type of Report and Period Covered <b>Final Report 4/95 - 8/96</b>	
				14. Sponsoring Agency Code <b>HCP30-C</b>	
15. Supplementary Notes <b>Contracting Officer's Technical Representative (COTR): Cheryl Allen Richter, HNR-30. BRE staff: Amy Simpson, Tim Martin, Mark Sargent, and Jerry Daleiden.</b>					
16. Abstract <b>This report presents the analysis conducted on relating pavement performance or response measures and design considerations to specific pavement layers utilizing data contained in the Long Term Pavement Performance Program National Information Management System. The goal of this research activity was to enhance implementation and use of the 1993 AASHTO Design Guide through improved materials characterizations. Specifically, the focus of this research activity was to identify the differences that exist between laboratory measured and backcalculated resilient moduli; determine the applicability of the C values, drainage coefficients, and relative damage factors that are included in the Design Guide; and provide procedures to adequately consider the seasonal variation of material properties as related to flexible pavement designs. Based on these results, design pamphlets have been prepared in support of the AASHTO Design Guide. These design pamphlets are documented and included in other reports. The results reported here form the basis and background for those design pamphlets.</b>					
17. Key Words <b>Pavement Performance, Backcalculation, LTPP Data Base, Resilient Modulus, Deflection, AASHTO Guide, Drainage, Subgrade Stabilization</b>				18. Distribution Statement <b>No restrictions. This document is available to the public through the National Technical Information Service, Springfield, Virginia 22161.</b>	
19. Security Classif. (of this report) <b>Unclassified</b>		20. Security Classif. (of this page) <b>Unclassified</b>		21. Number of Pages <b>223</b>	22. Price

# SI\* (MODERN METRIC) CONVERSION FACTORS

## APPROXIMATE CONVERSIONS TO SI UNITS

## APPROXIMATE CONVERSIONS FROM SI UNITS

Symbol	When You Know	Multiply By	To Find	Symbol	Symbol	When You Know	Multiply By	To Find	Symbol
<b>LENGTH</b>					<b>LENGTH</b>				
in	inches	25.4	millimeters	mm	mm	millimeters	0.039	inches	in
ft	feet	0.305	meters	m	m	meters	3.28	feet	ft
yd	yards	0.914	meters	m	m	meters	1.09	yards	yd
mi	miles	1.61	kilometers	km	km	kilometers	0.621	miles	mi
<b>AREA</b>					<b>AREA</b>				
in <sup>2</sup>	square inches	645.2	square millimeters	mm <sup>2</sup>	mm <sup>2</sup>	square millimeters	0.0016	square inches	in <sup>2</sup>
ft <sup>2</sup>	square feet	0.093	square meters	m <sup>2</sup>	m <sup>2</sup>	square meters	10.764	square feet	ft <sup>2</sup>
yd <sup>2</sup>	square yards	0.836	square meters	m <sup>2</sup>	m <sup>2</sup>	square meters	1.195	square yards	yd <sup>2</sup>
ac	acres	0.405	hectares	ha	ha	hectares	2.47	acres	ac
mi <sup>2</sup>	square miles	2.59	square kilometers	km <sup>2</sup>	km <sup>2</sup>	square kilometers	0.386	square miles	mi <sup>2</sup>
<b>VOLUME</b>					<b>VOLUME</b>				
fl oz	fluid ounces	29.57	milliliters	mL	mL	milliliters	0.034	fluid ounces	fl oz
gal	gallons	3.785	liters	L	L	liters	0.264	gallons	gal
ft <sup>3</sup>	cubic feet	0.028	cubic meters	m <sup>3</sup>	m <sup>3</sup>	cubic meters	35.71	cubic feet	ft <sup>3</sup>
yd <sup>3</sup>	cubic yards	0.765	cubic meters	m <sup>3</sup>	m <sup>3</sup>	cubic meters	1.307	cubic yards	yd <sup>3</sup>
NOTE: Volumes greater than 1000 l shall be shown in m <sup>3</sup> .									
<b>MASS</b>					<b>MASS</b>				
oz	ounces	28.35	grams	g	g	grams	0.035	ounces	oz
lb	pounds	0.454	kilograms	kg	kg	kilograms	2.202	pounds	lb
T	short tons (2000 lb)	0.907	megagrams (or "metric ton")	Mg (or "t")	Mg (or "t")	megagrams (or "metric ton")	1.103	short tons (2000 lb)	T
<b>TEMPERATURE (exact)</b>					<b>TEMPERATURE (exact)</b>				
°F	Fahrenheit temperature	5(F-32)/9 or (F-32)/1.8	Celsius temperature	°C	°C	Celsius temperature	1.8C + 32	Fahrenheit temperature	°F
<b>ILLUMINATION</b>					<b>ILLUMINATION</b>				
fc	foot-candles	10.76	lux	lx	lx	lux	0.0929	foot-candles	fc
fl	foot-Lamberts	3.426	candela/m <sup>2</sup>	cd/m <sup>2</sup>	cd/m <sup>2</sup>	candela/m <sup>2</sup>	0.2919	foot-Lamberts	fl
<b>FORCE and PRESSURE or STRESS</b>					<b>FORCE and PRESSURE or STRESS</b>				
lbf	poundforce	4.45	newtons	N	N	newtons	0.225	poundforce	lbf
lbf/in <sup>2</sup>	poundforce per square inch	6.89	kilopascals	kPa	kPa	kilopascals	0.145	poundforce per square inch	lbf/in <sup>2</sup>

\* SI is the symbol for the International System of Units. Appropriate rounding should be made to comply with Section 4 of ASTM E380.

# TABLE OF CONTENTS

	<u>Page No.</u>
1. INTRODUCTION .....	1
1.1 Background .....	1
1.2 Study Objectives .....	3
1.3 Scope of Report .....	4
2. LTPP DATA FOR STUDY ANALYSES .....	5
2.1 Data Request .....	5
2.2 Data Availability .....	11
2.2.1 Traffic Data .....	11
2.2.2 Environmental Data .....	12
2.2.3 Materials Test Data .....	12
2.2.4 Monitoring Data .....	13
2.2.5 Maintenance/Rehabilitation Data .....	13
2.3 Data Not in the Data Base .....	14
2.4 Problems With Data Available From the Data Base .....	15
2.5 Data Organization and Processing .....	22
3. DETERMINATION OF LAYERED ELASTIC MODULI - LABORATORY TESTS .....	24
3.1 Laboratory Resilient Modulus Test Results .....	27
3.2 Dense-Graded Asphalt Concrete Mixtures .....	27
3.3 Unbound Materials .....	39
3.4 Nonlinear Elastic Coefficient/Exponents Determined From Physical Properties .....	47
4. DETERMINATION OF LAYERED ELASTIC MODULI - BACKCALCULATED FROM DEFLECTION BASINS .....	57
4.1 Application and Use of Deflection Measurements .....	57
4.1.1 Data Consistency and Accuracy .....	58
4.1.2 Deflection Data Interpretation .....	59
4.2 Backcalculation Process .....	61
4.2.1 "Problem" Deflection Basins .....	62
4.2.2 Reduction of Deflection Matching Error Term .....	78
4.2.3 Modulus Ratios .....	80
4.3 Differences Between Laboratory Determined and Backcalculated Elastic Moduli .....	87
4.3.1 Laboratory and In Situ Conditions .....	88
4.3.2 Temperature Gradient Considerations for Asphalt Concrete Mixtures .....	89
4.3.3 Stress-State Considerations for Unbound Materials .....	96
4.3.4 Stress Sensitivity of Pavement Structure .....	107
4.3.5 Dissipate Work Considerations .....	108
5. MOISTURE EFFECTS AND DRAINAGE COEFFICIENTS .....	115
5.1 Drainage Systems .....	117
5.1.1 Base/Subbase Layers .....	117
5.1.2 Subgrade Layers .....	117
5.2 Data Used in Analyses .....	118

## TABLE OF CONTENTS (Continued)

	<u>Page No.</u>
5.3 Moisture Effects on Pavement Performance .....	119
5.4 AASHTO Drainage Coefficients .....	134
5.4.1 Flexible .....	134
5.4.2 Rigid .....	135
5.4.3 Evaluation of the Drainage Coefficients .....	135
5.5 Reduction of Layer Moduli During Saturated Conditions .....	136
6. SUBGRADE CHARACTERIZATION AND STABILIZATION .....	137
6.1 Available Data From the LTPP Data Base .....	137
6.1.1 Types and Number of Projects .....	137
6.1.2 Traffic Data .....	139
6.2 Subgrade Characterization for Design .....	140
6.2.1 Determination of Effective Resilient Modulus .....	140
6.2.2 Use of the Damage Concept. ....	141
6.3 Effect of Stabilized Subgrade on Performance of Flexible Pavements .....	143
6.3.1 IRI vs. Age .....	143
6.3.2 IRI vs. Fatigue Cracking .....	149
6.4 Effect of Stabilized Subgrades on Pavement Properties .....	150
7. SEASONAL VARIATION OF PAVEMENT MATERIALS .....	156
7.1 Seasonal Effects on Pavement Materials .....	158
7.1.1 Data Used in Evaluations .....	158
7.1.2 Limitations of Evaluation .....	162
7.2 Asphalt Concrete Materials .....	162
7.3 Unbound Base and Subbase Materials .....	166
7.4 Subgrade Soils .....	171
8. FWD DEFLECTION-TIME DATA AND PAVEMENT PERFORMANCE .....	177
8.1 Background .....	177
8.2 Load-Deflection Response Data .....	177
8.2.1 Application of Impact Load .....	177
8.2.2 Peak Deflection Time .....	178
8.2.3 Response Recovery Time .....	178
8.3 Dissipated Work .....	187
8.3.1 Pavement Structural Characteristics .....	188
8.3.2 Pavement Performance Comparisons .....	188
8.4 Summary .....	196
9. CONCLUSIONS AND RECOMMENDATIONS .....	197
9.1 Findings From the Data Analyses .....	197
9.1.1 Material Testing and Characterization Issues .....	197
9.1.2 Backcalculation of Layer Moduli for Design Purposes .....	199
9.2 Potential Concerns/Problems With the LTPP Data Base .....	201
REFERENCES .....	203

## List of Figures

<b><u>Figure</u></b>	<b><u>Page No.</u></b>
1. Design procedures used on a routine basis by State Highway Agencies across the United States (2) .....	2
2. Subgrade parameters used for flexible pavement designs across the United States (2) .....	25
3. Comparison of total and instantaneous resilient modulus for dense-graded asphalt concrete materials recovered and tested from the GPS sites .....	28
4. Histogram of the indirect tensile strengths measured at 25 °C (77 °F) for dense-graded asphalt concrete mixtures recovered from the GPS sites .....	30
5. Relationship between indirect tensile strength and total resilient modulus for asphalt concrete materials/mixtures .....	31
6. Histogram of the total resilient modulus of asphalt concrete materials measured at the three test temperatures .....	32
7. Histogram of Poisson's ratios for each test temperature for the asphalt concrete mixtures .....	34
8. Chart for the total resilient modulus vs. temperature using indirect tensile loading conditions .....	35
9. Vertical and horizontal deformations measured during repeated-load indirect tensile testing at 5 °C (41 °F) .....	36
10. Vertical and horizontal deformations measured during repeated-load indirect tensile testing at 25 °C (77 °F) .....	37
11. Vertical and horizontal deformations measured during repeated-load indirect tensile testing at 40 °C (104 °F) .....	38
12. Results from repeated-load triaxial resilient modulus tests performed on unbound base materials and subgrade soils .....	40
13. Histogram of resilient modulus at specific stress states for unbound coarse- and fine-grained soils .....	41
14. Histogram of the $R^2$ term using equation 5 to fit the laboratory repeated-load resilient modulus test data for unbound materials and soils .....	43

## List of Figures (Continued)

<u>Figure</u>	<u>Page No.</u>
15. Histogram of the $K_1$ elastic coefficient for the unbound materials and subgrade soils .....	44
16. Histogram of the $K_2$ elastic exponent for the unbound materials and subgrade soils .....	45
17. Histogram of the $K_3$ elastic exponent for the unbound materials and subgrade soils .....	46
18. Typical normalized deflection basins with low error terms (i.e., the use of elastic layer theory is applicable for analyzing these basins) .....	64
19. Type I normalized deflection basins .....	64
20. Type II normalized deflection basins .....	65
21. Type III normalized deflection basins .....	65
22. Limiting modulus criteria of unbound base and subbase layers (26) .....	81
23. Histogram of the calculated modulus ratios between adjacent unbound pavement/subgrade layers .....	82
24. Comparison of test results between unconfined compression and indirect tensile tests (8) .....	91
25. Comparison of temperatures measured at the surface to those measured below the surface for the GPS-1 and 2 sites .....	92
26. Graphical illustration of procedure used to determine the depth at which the temperature is to be determined for use in the laboratory so that the measured and backcalculated moduli are equal .....	93
27. Comparison of laboratory measured values determined at the mid-depth temperature to the backcalculated moduli .....	94
28. Graphical illustration for procedure used to determine the stress states to be used in the laboratory so that the measured and backcalculated moduli are equal .....	100
29. Graphical illustration of the vertical profile of stresses in a layer for equating laboratory measured to backcalculated moduli .....	101



## List of Figures (Continued)

<b><u>Figure</u></b>	<b><u>Page No.</u></b>
30. Graphical comparison of backcalculated and laboratory measured moduli for the base and subbase layers . . . . .	105
31. Graphical comparison of backcalculated and laboratory measured moduli for subgrade soils . . . . .	106
32. Typical deflection-time history data collected during FWD testing and the associated dissipated work for a GPS site that has elastic behavior . . . . .	109
33. Typical deflection-time history data collected during FWD testing and the associated dissipated work for a GPS site that has viscoelastic behavior . . . . .	110
34. Typical deflection-time history data collected during FWD testing and the associated dissipated work for a GPS site that has viscoelastic and plastic behavior . . . . .	111
35. Frequency of difference between optimum and actual moisture contents for granular base layers in GPS sections with no positive drainage system . . . . .	124
36. Frequency of difference between optimum and actual moisture contents for granular base layers in GPS sections with positive drainage systems . . . . .	125
37. Comparison of difference between optimum and actual moisture contents for subgrade soils in GPS-1 and GPS-2 sections with no positive drainage system . . . . .	126
38. Comparison of difference between optimum and actual moisture contents for subgrade soils in GPS-1 and GPS-2 sections with positive drainage systems . . . . .	127
39. Minnesota seasonal site measurements for precipitation and moisture contents from 1994 . . . . .	128
40. Minnesota seasonal site measurements for base and subgrade moisture contents from 1994 . . . . .	129
41. Minnesota seasonal site measurements in the granular base, including backcalculated resilient modulus from 1994 . . . . .	130
42. Texas seasonal site measurements for precipitation and moisture contents from 1994 . . . . .	131
43. Texas seasonal site measurements for base and subgrade moisture contents from 1994 . . . . .	132
44. Texas seasonal site measurements in the granular base, including backcalculated resilient modulus from 1994 . . . . .	133

## List of Figures (Continued)

<b><u>Figure</u></b>	<b><u>Page No.</u></b>
45. Chart for estimating effective roadbed soil resilient modulus for flexible pavements designed using the serviceability criteria (1) .....	138
46. Example of IRI versus time for GPS sites with clay subgrades .....	145
47. Example of IRI versus time for GPS sites with silt subgrades .....	146
48. Example of IRI versus time for GPS sites with sand subgrades .....	147
49. Example of IRI versus time for GPS sites with gravel subgrades .....	148
50. Histogram and comparison of selected volumetric properties of subgrade soils beneath a stabilized subgrade layer .....	151
51. Histogram and comparison of selected volumetric properties of sandy subgrades supporting pavements without any stabilized subgrade layer .....	152
52. Histogram and comparison of selected volumetric properties of clay subgrades supporting pavements without any stabilized subgrade layer .....	153
53. Examples of the dissipated work determined from the deflection-time histories recorded during deflection testing on a pavement without a stabilized subgrade layer as compared to a pavement with a stabilized subgrade .....	155
54. Range and average values for layer strength coefficients of those SHA's using the 1972 or 1986/93 AASHTO procedures for flexible pavement design .....	157
55. Seasonal variation of the normalized backcalculated layer moduli for asphalt concrete mixture at three of the seasonal sites .....	159
56. Seasonal variation of the normalized backcalculated layer moduli for unbound granular base/subbase materials at three of the seasonal sites .....	160
57. Seasonal variation of the normalized backcalculated layer moduli for the subgrade soils at three of the seasonal sites .....	161
58. Relationship between asphalt concrete tensile strains calculated with elastic layer theory of the total number of 80-kN (18-kip) ESAL's' .....	165
59. Plots of base stiffness coefficient by season .....	169
60. Ratio of SN based on seasonal subgrade Mr to SN based on guide .....	174

## List of Figures (Continued)

<b><u>Figure</u></b>	<b><u>Page No.</u></b>
61. FWD load pulse type "A" and the deflections measured by each sensor at GPS site 481174 .....	179
62. FWD load pulse type "B" and the deflections measured by each sensor at GPS site 483589 .....	180
63. FWD load pulse type "C" and the deflections measured by each sensor at GPS site 4810481 .....	180
64. FWD load pulse type "D" and the deflections measured by each sensor at GPS site 011001 .....	181
65. Average slope or speed (in inches per ms) of the peak deflections measured by each sensor during FWD testing of selected SMP and GPS test sections .....	182
66. Typical FWD deflection-time data from testing performed on an asphalt concrete pavement with elastic behavior, GPS site 481056 .....	184
67. Typical FWD deflection-time data from testing performed on an asphalt concrete pavement with some viscoelastic behavior, GPS site 481060 .....	185
68. Typical FWD deflection-time data from testing performed on a PCC pavement with viscoelastic behavior, GPS site 484143 .....	186
69. Hysteresis loop as measured by the FWD at GPS site 481122 (asphalt concrete-surfaced pavement) in July .....	189
70. Hysteresis loop as measured by the FWD at GPS site 484143 (PCC-surfaced pavement) in July .....	190
71. Hysteresis loop as measured by the FWD at GPS site 481060 (asphalt concrete-surfaced pavement) in July .....	191
72. Dissipated work by month, as measured during FWD deflection testing at three seasonal sites in the southern region .....	194
73. Comparison of dissipated work to pavement condition for different traffic levels for selected GPS sites in the southern region .....	195

## List of Tables

<b><u>Table</u></b>		<b><u>Page No.</u></b>
1.	Data elements collected and used in the different studies . . . . .	6
2.	GPS sites having resilient modulus test data for 90 percent or more of the pavement cross section . . . . .	17
3.	Summary of GPS sections with repeated-load resilient modulus tests for the unbound pavement materials and subgrade soils . . . . .	21
4.	Examples of relationships used to calculate the design resilient modulus for subgrade soils from other properties . . . . .	26
5.	Summary of average elastic coefficients and exponents (K values) determined from regression studies of the repeated-load triaxial compression tests of unbound pavement materials and subgrade soils . . . . .	42
6.	Relationships previously developed between the nonlinear elastic coefficient/exponents and physical properties of soils (10) . . . . .	49
7.	Relationships or correlations between the nonlinear elastic coefficients/exponents using equation 5 and physical properties of soils obtained from the LTPP data base . . . . .	53
8.	Listing of sections with problem deflection basins that are not compatible with elastic layer theory . . . . .	66
9.	GPS section ends that exceed the modulus ratio set by figure 22 . . . . .	83
10.	Regression of K values based on stress states and resilient moduli using equation 5 . . . . .	103
11.	Example of backcalculated layer moduli for the different FWD load levels used, ksi . . . . .	112
12.	AASHTO drainage coefficients, $m_1(1)$ . . . . .	116
13.	Listing of GPS sites that contain some type of drainage system . . . . .	120
14.	Calculated base stiffness coefficients . . . . .	168
15.	Backcalculated subgrade moduli and associated data (see footnote 5) . . . . .	173

## List of Tables (Continued)

<b><u>Table</u></b>		<b><u>Page No.</u></b>
16.	Average slope of the relationship between sensor distance from the load and time to peak deflection .....	183
17.	Dissipated work calculated from the loading and unloading (the hysteresis loop) of the pavement structure during FWD testing by type of surface .....	192

## List of Abbreviations and Symbols

AASHTO	-	American Association of State Highway and Transportation Officials
AC	-	Asphalt concrete
ASTM	-	American Society for Testing and Materials
CBR	-	California bearing ratio
CRCP	-	Continuously reinforced concrete pavement
ESAL	-	Equivalent single-axle loads
FHWA	-	Federal Highway Administration
FWD	-	Falling Weight Deflectometer
GPS	-	General Pavement Studies
HMAC	-	Hot mix asphalt concrete
IMS	-	Information management system
JPCP	-	Jointed plain concrete pavement
JRCP	-	Jointed reinforced concrete pavement
LTPP	-	Long Term Pavement Performance
NIMS	-	National Information Management System
PCC	-	Portland cement concrete
PSI	-	Present serviceability index
QA	-	Quality assurance
QC	-	Quality control
RCOs	-	Regional coordinating offices
RIMs	-	Regional information management system
SHAs	-	State Highway Agencies
SHRP	-	Strategic Highway Research Program
SSV	-	Soil support value
TAC	-	Technical assistance contractor
TB	-	Treated base
TRB	-	Transportation Research Board
WIM	-	Weigh in motion
$w_{act}$	-	In situ water content of unbound aggregate bases/subbases or subgrade soils
$w_{opt}$	-	Optimum water content
$w_s$	-	Water content of the test specimen
$a_2$	-	AASHTO structural layer coefficient for the granular base/materials
C	-	Cohesion of the soil
C Value	-	A factor converting backcalculated layer moduli to laboratory measured values
$D_p$	-	Layer thickness
$D_s$	-	Depth into the subgrade, below pavement layers
DI	-	Damage index
E	-	Modulus of elasticity backcalculated from deflection basin measurements
$E^*$	-	Complex modulus of asphalt concrete mixtures

## List of Abbreviations and Symbols (Continued)

$E_{RI}$	-	Instantaneous resilient modulus
$E_{RT}$	-	Total resilient modulus of asphalt concrete mixtures and/or asphalt stabilized base mixtures, as measured in the laboratory
$j$	-	Number of seasons
$K_1, K_2, K_3, K_5$	-	Nonlinear elastic constants and coefficients of the material response constitutive equation for unbound pavement materials and subgrade soils
$k_o$	-	At-rest earth pressure coefficient
$k_p$	-	Passive earth pressure coefficient
LL	-	Liquid limit
$M_R$	-	Resilient modulus of the unbound pavement layer, stabilized subgrade, and/or subgrade or roadbed soil, configuration and tire pressure
$N$	-	Number of allowable equivalent load repetitions to a specific distress extent and severity
$n$	-	Actual number of equivalent load repetitions
$p_a$	-	Atmospheric pressure
$p_o$	-	At-rest lateral earth pressure in the subgrade at a depth of $D_s$
PI	-	Plasticity index
$P_{40}$	-	Percentage passing the No. 40 sieve
$S$	-	Degree of saturation
SN	-	Structural number
$T$	-	Pavement temperature
$t$	-	Layer thickness
$U_f$	-	Damage factor based on a serviceability design criteria
$\theta$	-	Bulk stress
$\phi$	-	Angle of shearing resistance
$\gamma_{ds}$	-	Dry density or unit weight of the test specimen
$\gamma_{dmax}$	-	Maximum dry unit weight of the soil
$\gamma_p$	-	Weighted average unit weight of the pavement structure and stabilized subgrade, if present
$\gamma_s$	-	Unit weight of the subgrade or roadbed soil
$\epsilon_t$	-	Tensile strain at the bottom of the asphalt concrete layer
$\epsilon_c$	-	Vertical compressive strain at the top of the subgrade
$\sigma_d$	-	Deviator stress
$\sigma_3$	-	Confining pressure
$\sigma_x, \sigma_y$	-	Normal horizontal or lateral stresses
$\sigma_z$	-	Normal vertical stress
$\nu$	-	Poisson's ratio
% Clay	-	Percentage of clay in the soil
% Shrinkage	-	Percentage of shrinkage of the soil
% Silt	-	Percentage of silt in the soil
% Swell	-	Percentage swell of the soil

# **PAVEMENT MATERIAL CHARACTERIZATIONS AND PAVEMENT PERFORMANCE**

## **EXECUTIVE SUMMARY**

There have been major efforts in the last several decades towards advancing pavement technology in the areas of structural design and materials characterization. Unfortunately, much of this research has yet to find its way into routine use by practicing engineers. A classic example of this reluctance to use relatively new technology is the AASHTO Design Guide. Fewer than half of the State Highway Agencies (SHA's) have adopted or use the Guide for routine pavement design some 10 years after its initial publication in 1986.

One answer for this limited use and acceptance may be due to the increased complexity over the relatively small and simple 1972 AASHTO "Blue" Book. Another answer may be related to the difficulty in using and understanding (or not having confidence in) some of these new inputs, such as resilient modulus, reliability and drainage coefficients. For example, resilient modulus testing for pavement design was available and being used more than 10 years before publication of the 1986 AASHTO Design Guide. However, most SHA's still do not actually use the resilient modulus test to determine the design modulus of the roadbed soil, but rather estimate this value using correlations that are simple, but highly inaccurate.

Another major research effort in the pavement performance area was initiated in 1987 through the creation of the Strategic Highway Research Program (SHRP), and was entitled the Long Term Pavement Performance (LTPP) program. This program set up hundreds of experimental test sites across the U.S. and initiated the data collection effort for each site. One of the goals of the LTPP program was to create an extensive, but well-structured, data base that would help confirm and validate these new technologies and design procedures, but more importantly, build confidence in their use. This LTPP data base, referred to as the National Information Management System (NIMS), was a key product of SHRP in which all of the data are being stored and updated on a continual basis for use by the pavement industry. The Federal Highway Administration (FHWA) has assumed responsibility for managing this data base and to continue with the data collection and monitoring effort to ensure that there are sufficient data to support the continued development and implementation of new technologies.

To begin capitalizing on this massive data collection effort, FHWA initiated several data analysis contracts, one of which was in the materials characterization area for pavement design. Specifically, the overall goal of this contract, entitled "Analyses Relating to Pavement Material



Characterizations and Their Effects on Pavement Performance" (Contract No. DTFH61-95-C-00029) was to use the LTPP data base to enhance implementation of the 1993 AASHTO Design Guide through improved material characterization. This contract has resulted in four reports and three design pamphlets in support of the 1993 AASHTO Design Guide. The reports and design pamphlets are listed below:

**Reports:**

1. *Analyses Relating to Pavement Material Characterizations and Their Effects on Pavement Performance.*
2. *Backcalculation of Layer Moduli of LTPP General Pavement Study Sites.*
3. *Evaluation of IRI Decreases With Time in the LTPP Southern Region.*
4. *LTPP FWD Deflection-Time Data for Characterizing Pavement Structures and Pavement Response.*

**Design Pamphlets:**

1. "Backcalculation of Pavement Layer Moduli in Support of the 1993 AASHTO Guide for the Design of Pavement Structures."
2. "Determination of Design Subgrade Moduli in Support of the 1993 AASHTO Guide for Design of Pavement Structures."
3. "Determination of Layered Elastic Moduli in Support of the 1993 AASHTO Guide for the Design of Pavement Structures."

In summary, the reports noted above provide the background and a discussion of the work conducted, while the design pamphlets are intended to support the determination of selected design inputs that are required by the AASHTO Design Guide. Key findings from the overall study are listed below:

**Backcalculated Layer Moduli for Structural Design:**

1. Backcalculation of layer moduli using elastic layer theory can be used to determine the resilient modulus of different pavement layers. However, the in situ moduli must be adjusted to represent or equal the laboratory measured values for those design procedures developed with laboratory measured moduli (which includes the AASHTO Design Guide). Layer moduli backcalculated with different programs should not be used interchangeably, because of the differences found between the various backcalculation programs. The adjustments converting field calculated moduli to laboratory measured

values (as reported in this study) are only applicable to the "MODULUS" and "WESDEF" programs. Both of these programs use a linear elastic layered response model to calculate a deflection basin.

2. Elastic layer theory is not applicable to all types of measured deflection basins. Some deflection basins are considered or identified as "problem" basins, because they do not fit the "standard" deflection basin profile calculated with elastic layer theory. Although layer moduli can be determined from problem deflection basins, the elastic moduli may not be representative of the actual in situ material.
3. Backcalculated layer moduli are almost always greater than the laboratory measured values at comparable stress states and/or temperatures.
4. There is no unique solution for a specific deflection basin. The error term should be as low as possible, but less than a value of 2½-percent error per sensor when using the backcalculated moduli for design.

#### **Subgrade Characterization for Structural Design:**

1. Determination of the design subgrade modulus utilizing the relative damage factors based on the AASHTO serviceability criteria, tends to be greater than the design subgrade modulus calculated using damage factors based on minimizing the subgrade vertical compressive strain at the top of the subgrade. All pavement designs generated with the AASHTO Design Guide should be checked using the response criteria of minimizing subgrade vertical compressive strains, especially for lower volume roadways.
2. Correlations should not be used to estimate the design resilient modulus for pavement structural design for high-volume roadways. The design resilient modulus should be determined from laboratory resilient modulus tests, or backcalculated from deflection basins. The possibility of large errors is simply too high when using gross correlations between physical properties or strength values (such as CBR) and resilient modulus.

#### **Drainage Considerations:**

1. The AASHTO drainage coefficients are not recommended for use in structural design. Instead, the design process should account for a reduction in the resilient

modulus to account for saturated conditions through the calculation of a design modulus using relative damage factors for all unbound moisture-sensitive materials.

2. The use of positive drainage features in both asphalt concrete- and portland cement concrete-surfaced pavements was not qualified through the use of the LTPP data base. Some of the problems in identifying the potential benefit of subsurface drainage features may be related to the assumption that the positive drainage system is functioning properly. As such, it is recommended that those sites with positive drainage features (i.e., edge drain systems) be inspected by video inspection techniques to confirm that these drainage features are, in fact, functioning.

#### **Determination of Design Layer Moduli:**

1. Seasonal variations of layer moduli (estimated through moisture and/or temperature differences between the seasons) must be considered in determining the design modulus of different materials so that the structural layer coefficients can be determined for use with the AASHTO Design Guide. The design modulus can be determined using a damage concept similar to that used in determination of an effective resilient modulus of the roadbed soil. More specifically, structural designs based on a serviceability criteria should be checked using other pavement response criteria (i.e., asphalt concrete tensile strains, subgrade vertical compressive strains, layer modulus ratios, etc.).

Specific discussion on each of these key findings are given in the reports listed above. Application and use of these findings are expected to provide improved designs and a more realistic estimate of pavement behavior and performance. In addition, implementation of these studies should provide a more consistent use of the design parameters. These studies also attempt to merge and compare designs based on new technology using pavement response criteria that are required for mechanistic-empirical procedures and those using the serviceability concept.



# PAVEMENT MATERIAL CHARACTERIZATIONS AND PAVEMENT PERFORMANCE

## 1. INTRODUCTION

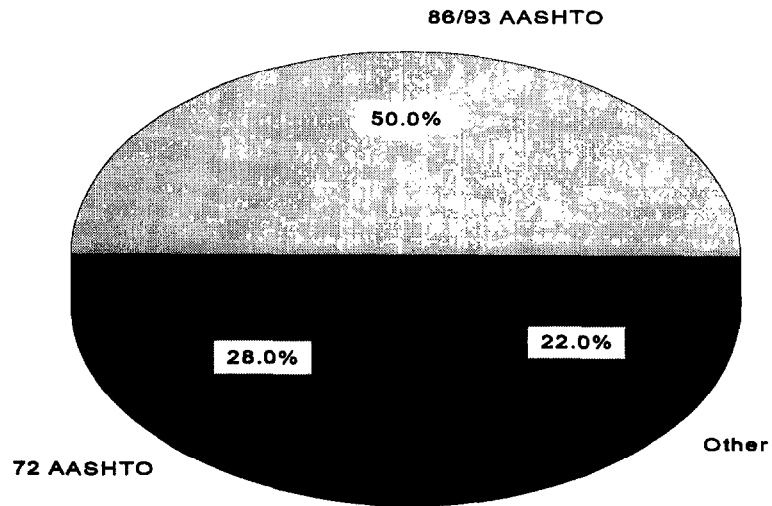
### 1.1 Background

While there have been major efforts in the last several decades towards advancing pavement technology, much of this research has not found its way into the daily design procedures used by practicing engineers. A classic example of this would be the limited use of the 1986 AASHTO Design Guide (1) for routine pavement design 10 years after its initial publication. Only about half of the State Highway Agencies (SHA's) have formally incorporated or use the 1986/1993 AASHTO Guide for flexible pavement design (figure 1). This statement is based on the Phase I findings of NCHRP Project 1-32 entitled "Systems for Design of Highway Pavements"(2). This percentage of use seems low, since an enormous effort was put into the 1986 Design Guide to provide more design capabilities than were included in the 1972 Interim Guide.

One cause for this limited use and acceptance may be the increased number of pages in the new manual over the relatively small and simple 1972 AASHTO "Blue" Book. The increased size may have led to a perceived increase in complexity for the new guide. Another cause may be the difficulty in obtaining and demonstrating the applicability of some of these new inputs, such as resilient modulus of the subgrade soil, reliability and the drainage coefficients. The guide provides inadequate direction for obtaining these and other important inputs and, as a result, engineers are selecting ranges of values for input, some of which may be inaccurate. No matter how good the design procedure, if erroneous inputs are used, the final result will be erroneous.

The analyses conducted under this contract were focused on relating pavement performance and design considerations to specific pavement layers and material characterizations utilizing data contained in the Long Term Pavement Performance (LTPP) National Information Management System (NIMS). In addition, they demonstrate the usefulness of this data base for answering pavement engineering questions.

**a. Design Procedures Used for Flexible Pavements**



**b. Design Procedures Used for Rigid Pavements**

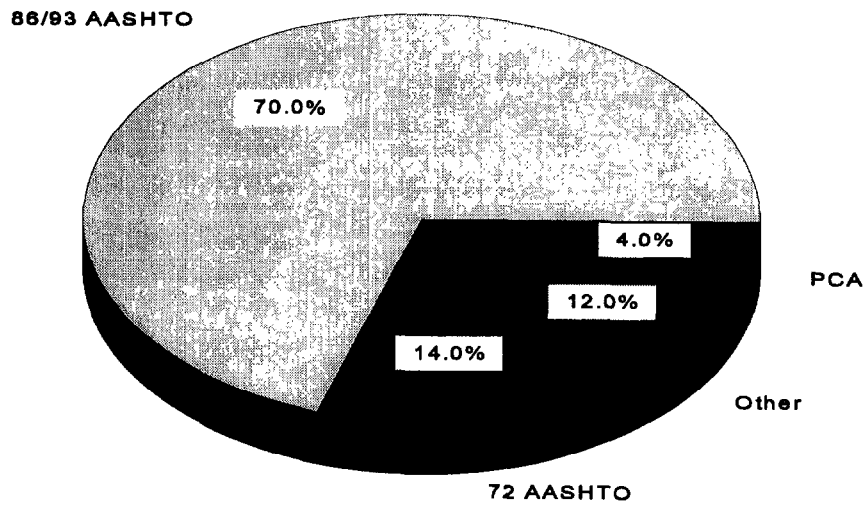


**Figure 1. Design procedures used on a routine basis by State Highway Agencies across the United States (2).**

## **1.2 Study Objectives**

The overall goal of this research effort was to enhance implementation of the 1993 AASHTO Design Guide through improved material characterization for those inputs required by the 1993 Design Guide, which are not well defined. As stated, the LTPP data base was used as the primary data source for improving the material characterizations required for pavement design. The goal of this study was subdivided into two objectives. The first objective was to identify and provide procedures for determining layered elastic or resilient moduli in support of the AASHTO Design Guide for new pavement design and rehabilitation design. The second objective was to investigate the importance of selected pavement design features for improving pavement performance through the LTPP data base. To accomplish the overall goal, the two project objectives were further subdivided into five research activities. The focus of the research activities were as follows:

1. Investigate relationships or differences that exist between laboratory measured and backcalculated pavement layer moduli for individual pavement layers, including the subgrade.
2. Investigate and identify a relationship (or predictive equations) for estimating pavement layer moduli utilizing material properties obtained from the laboratory and/or field.
3. Provide supporting data on the applicability of the drainage coefficients, and the recommended ranges. Also, evaluate the effect of moisture (or drainage design features) on pavement performance.
4. Provide supporting data on the use of stabilized subgrades (i.e., for use with swelling soils, frost susceptible soils, and moisture sensitive soils) for increasing pavement life, and evaluate the design concept of limiting subgrade vertical compressive strains.
5. Provide supporting data on the adequacy and applicability of using resilient modulus to estimate layer coefficients for different pavement materials, while taking into consideration the seasonal variation of material properties.

### **1.3 Scope of Report**

This report is divided into nine chapters, which includes the introduction as chapter 1. Chapter 2 discusses the data collection effort and requirements for the different study analyses; chapter 3 provides a detailed discussion on the determination of layered elastic moduli for use in design from laboratory tests, while chapter 4 discusses the backcalculation of layer moduli and differences between the laboratory measured and backcalculated values. Chapter 5 provides a discussion on the effects of moisture effects on pavement performance and the applicability of drainage coefficients included in the AASHTO Design Guide; chapter 6 discusses the data analysis effort regarding subgrade characterization and stabilization as related to improved pavement performance; chapter 7 presents the findings and discussion on the seasonal variation of material properties, determination of layer coefficients from resilient moduli and determining equivalent layer moduli for use in pavement design; chapter 8 briefly overviews use of the dissipated work concept to assist in estimating remaining life and predicting pavement performance; and chapter 9 is a summary of all results conducted within this study and the conclusions and observations reached.



## **2. LTPP DATA FOR STUDY ANALYSES**

Since 1989, data have been collected under the LTPP project on inservice highway pavements and stored in a data base to be used by researchers worldwide for a better understanding of pavements. The LTPP NIMS now occupies a 10-gigabyte computer in Oak Ridge, Tennessee. To begin capitalizing on this massive data collection effort and examine some of the pavement design issues, the FHWA initiated numerous data analysis efforts. One of these analysis contracts (which is the focus of this report) evaluated material characterization methodologies and their relationship to pavement performance and design. Through these analyses, the usefulness of this data base was demonstrated for answering pavement engineering questions. With the knowledge gained from earlier studies, personnel on this project began assessing the data that would be available for analysis and the mechanisms by which the data would be collected. The rest of this chapter overviews the data collection process and the data requested from LTPP for this project.

Initially, various pavement design procedures, sensitivity studies and performance studies were reviewed to identify those data elements that were believed to be necessary in achieving the overall goals of this project, which include evaluating selected material properties and pavement features in relation to pavement performance. A listing of these different data elements selected for the various research activities of this project are included in table 1. Each of these data elements were obtained either through the LTPP data base directly, or indirectly through correlations using other data elements found in the data base.

### **2.1 Data Request**

A subsidiary objective of this project was to help FHWA evaluate the current version of the LTPP data request software. This subsection deals with all aspects of one data request and provides some evaluation comments regarding the software. All data were originally requested from the Transportation Research Board (TRB) using the standard request procedure and the LTPP data request software. The data request software is used to select particular sections, view their position on a map of the U.S., determine the amount of data available for that section, and complete a data request form for that data. The software is self-explanatory, and was put together in a well-organized and complete software package. It provides clear guidance on where to begin the process of selecting sections and determining the amount of data items available.

**Table 1. Data elements collected and used in the different studies.**

<b>Research Activity</b>	<b>Backcalculation of Layer Moduli (Task B)</b>	<b>Comparison of Backcalculated &amp; Lab Values (Task C)</b>	<b>Moduli &amp; Physical Properties (Task D)</b>	<b>Drainage Coefficients &amp; Moisture Effects (Task E)</b>	<b>Subgrade Charact. &amp; Stabilization (Task F)</b>	<b>Seasonal Variation Effects (Task G)</b>
AASHTO Soil Classification		✓	✓	✓	✓	
Age of Pavement at Time of Materials Sampling & Deflection Testing				✓	✓	✓
Air Voids, HMAC Layers		✓	✓	✓		✓
Asphalt Content, HMAC Layers		✓	✓			
Atterberg Limits - Unbound Layers & Subgrade Soils		✓	✓	✓	✓	✓
Compaction, Percent		✓	✓	✓	✓	
Deflection Data, 1st Round at Test Pit & Sampling Locations	✓					
Deflection Data - Seasonal				✓	✓	✓
Density, Bound Layers		✓				
Density, Maximum Lab Value			✓		✓	✓

**Table 1. Data elements collected and used in the different studies (continued).**

<b>Research Activity</b>	<b>Backcalculation of Layer Moduli (Task B)</b>	<b>Comparison of Backcalculated &amp; Lab Values (Task C)</b>	<b>Moduli &amp; Physical Properties (Task D)</b>	<b>Drainage Coefficients &amp; Moisture Effects (Task E)</b>	<b>Subgrade Charact. &amp; Stabilization (Task F)</b>	<b>Seasonal Variation Effects (Task G)</b>
Density, Unbound Layers Wet & Dry		✓	✓	✓	✓	
Depth to Rigid Layer		✓				
Depth to Water Table	✓			✓	✓	
Distress Data - Amount of Cracking & Rutting	✓			✓	✓	✓
Depth to Frost Penetration					✓	✓
Freeze/Thaw Cycles, Annual			✓	✓		
Freeze/Thaw Cycles, Monthly					✓	✓
Frost Heave Probability						✓
Frost Heave Rate						✓
Gradations, HMAC		✓	✓			
Gradations, Unbound Materials & Subgrade Soils		✓	✓	✓	✓	✓
Material Description		✓	✓	✓	✓	
Modulus, Backcalculated	✓	✓		✓	✓	✓

**Table 1. Data elements collected and used in the different studies (continued).**

<b>Research Activity</b>	<b>Backcalculation of Layer Moduli (Task B)</b>	<b>Comparison of Backcalculated &amp; Lab Values (Task C)</b>	<b>Moduli &amp; Physical Properties (Task D)</b>	<b>Drainage Coefficients &amp; Moisture Effects (Task E)</b>	<b>Subgrade Charact. &amp; Stabilization (Task F)</b>	<b>Seasonal Variation Effects (Task G)</b>
Modulus, Resilient Laboratory		✓	✓		✓	✓
Moisture Content, In Situ		✓	✓	✓	✓	
Moisture Content, Optimum			✓		✓	
Moisture Susceptibility, HMAC				✓		
Pavement Structure, Layer Material Type	✓	✓			✓	
Permeability, Unbound Layers				✓	✓	
Potential Vertical Rise					✓	✓
Precipitation, Annual		✓	✓			
Precipitation, Monthly				✓	✓	✓
Profiles, Longitudinal					✓	✓
PSI, Initial					✓	✓
Saturation, Percent		✓	✓	✓		
Shoulder Information				✓		
Soil Profile	✓	✓				
Soil Suction, Subgrade				✓		

**Table 1. Data elements collected and used in the different studies (continued).**

<b>Research Activity</b>	<b>Backcalculation of Layer Moduli (Task B)</b>	<b>Comparison of Backcalculated &amp; Lab Values (Task C)</b>	<b>Moduli &amp; Physical Properties (Task D)</b>	<b>Drainage Coefficients &amp; Moisture Effects (Task E)</b>	<b>Subgrade Charact. &amp; Stabilization (Task F)</b>	<b>Seasonal Variation Effects (Task G)</b>
Specific Gravity, Unbound Layers		✓	✓			
Specific Gravity, HMAC			✓			
Strength, Compressive		✓	✓		✓	
Strength, Indirect Tensile		✓				
Subdrainage Details				✓		
Sunshine, Percent				✓		
Swell Probability						✓
Swell Rate Constant						✓
Temperature, FWD Testing		✓			✓	
Temperature, Average Annual				✓		
Temperature, Average Monthly					✓	✓
Temperature, Days Below 0 °C						✓
Temperature, Days Above 32 °C						✓
Thickness, Pavement Layer	✓	✓	✓	✓	✓	✓

**Table 1. Data elements collected and used in the different studies (continued).**

<b>Research Activity</b>	<b>Backcalculation of Layer Moduli (Task B)</b>	<b>Comparison of Backcalculated &amp; Lab Values (Task C)</b>	<b>Moduli &amp; Physical Properties (Task D)</b>	<b>Drainage Coefficients &amp; Moisture Effects (Task E)</b>	<b>Subgrade Charact. &amp; Stabilization (Task F)</b>	<b>Seasonal Variation Effects (Task G)</b>
Traffic, 80-kN (18-kip) ESAL's				✓	✓	✓
Traffic, No. of Heavy Axle Loads & Magnitudes					✓	
Viscosity, HMAC		✓	✓			
Wind Speed, Average Annual				✓		

The data request software requires that sections be selected or identified to begin the data retrieval process. Upon selection of sections, a listing of data availability is automatically provided. This screen provides essential information allowing the user to ascertain the effectiveness of the data to be requested.

The software then visually leads the user to the selection of tables that contain the data they have identified. This process is very straightforward and provides the number of records contained in each table based on a subset of selected sections. One drawback to the software is the fact that selecting portions of a table is not possible. Obtaining every element from each table may not be necessary in many instances. For example, Table TST\_SS04\_UG08 contains the AASHTO soil classification among several other data elements, and was the only element required from this table for use in this study. It would have been much easier in the data manipulation phase to only have received those data elements requested for this table.

The instructions for filling out the data request form were easily followed, but another difficulty was encountered with the software. Due to the nature of this project, there were two separate sets of sections which were examined: one was for the tasks related to backcalculation and another set for the tasks related to pavement performance. In order to handle these two subsets of sections, it was necessary to complete two data requests. To complete the two data requests it was necessary to exit the software to clear the previous selection. An option for clearing a previous request should be added to the software for just such cases.

In receiving the data back from TRB, a final difficulty was encountered. Since the size of the data requested was quite large, suitable media transfer had to be found that was compatible at both ends. At the time, the options were 4-Mb DAT tape or Everex tape, which limited the transfer of data, and the use of diskettes was not a practical solution. However, since this incident, the FHWA has worked to find a solution to this problem so that future requests will not face the same difficulty.

## **2.2 Data Availability**

The LTPP NIMS currently houses five different kinds of data, which include traffic, environmental, materials, monitoring, and maintenance and rehabilitation. The first four data elements are directly applicable to this project, and were obtained either from the NIMS or were requested directly from the regional coordination offices.

**2.2.1 Traffic Data.** Traffic data contained in the LTPP Information Management System (IMS) for General Pavement Study (GPS) Test sections consist of both SHA historical estimates and

actual monitored traffic data using Weigh In Motion (WIM) equipment. The historical estimates were provided by the States based on the time from the last major rehabilitation conducted on the GPS section to 1989. The monitored data begins in 1989 and is to be collected throughout the LTPP program.

At the time of this project, there were some questions regarding the quality of both the historical estimates and the monitored traffic data. Specifically, the monitored traffic data were found to have some problems when processed through the quality control (QC) software. Also, a version of the software that was being used early in the analysis was unable to provide Equivalent Single-Axle Load (ESAL) estimates, which also slowed down the analysis process. Eventually, 80-kN (18-kip) ESAL estimates were obtained and used in some of the research activities. However, these estimates did contain errors that were not corrected through the quality assurance (QA) process (see discussion in section 2.4). The effect of these errors on the various research activities is still unknown.

**2.2.2 Environmental Data.** Environmental data were collected from the National Oceanic and Atmospheric Association. Four or five weather stations around each GPS section were selected based on proximity and similarity in climate. The data are collected from these stations and then a weighted average is calculated where the weights are based upon the distance of the station from the site, with closer stations having a greater weight (and more influence) than stations that are farther from the site. The data collected begin in the year the site was last rehabilitated to 1989. No data are currently available past 1989.

Environmental data in the LTPP IMS consists of annual rainfall, annual freeze/thaw cycles, annual freeze index, number of days with temperature less than 0 °C (32 °F) by month, number of days with temperature greater than 32 °C (90 °F) by month, monthly averages of minimum and maximum temperature, monthly precipitation for all 12 months, average number of days with temperature below freezing, average number of days with temperature greater than 32 °C (90 °F), annual freeze index, average daily temperature range determined from the monthly average, monthly maximum and minimum temperatures, the average daily maximum temperature for the summer, and the average daily minimum temperature for the winter.

**2.2.3 Materials Test Data.** In 1989 and 1990, samples were collected from each end of the 152-m (500-ft) GPS test sections and were tested in the laboratory. From this testing, the asphalt content, air void content, and gradation of the aggregate in the hot mix asphalt concrete (HMAC) layers were determined. In addition, the Atterberg limits, optimum moisture, maximum density, in situ moisture content, and gradations were collected on the unbound materials. Finally, resilient modulus testing was conducted for both the unbound and asphalt concrete materials.



Other materials data were collected for each section from the individual SHA's, which included the test section location, information about the construction of the test section, the mix design and materials information about the base and subgrade. However, this inventory materials data were not used or considered when actual laboratory test results were available.

Materials data are generally available for each pavement layer included in the layer table in the IMS. These data are present for the approach end and for the leave end of each test section. When multiple values are provided in the NIMS for each end of the test section (e.g., HMAC resilient moduli), the values were averaged in the project data base so that there is one representative value. Those GPS sections that have significant differences between both ends were separated and considered as different structures.

**2.2.4 Monitoring Data.** Each GPS test section is monitored on a regular basis. This routine information includes deflections measured with the Falling Weight Deflectometer (FWD), longitudinal profile, distress, cross-profile, and friction. The friction data are provided by the individual SHA's. Distress information is collected via two methods. One method is a standard manual survey involving trained personnel collecting the data, and the other method is automated. PASCO USA has a unit that collects both the distress and cross-profile information, by filming each section at night with lights mounted on the vehicle that provide a high-intensity light source. The films are taken back to the office and the data are collected from the film.<sup>1</sup> However, the manual distress surveys were used in this study when available.

**2.2.5 Maintenance/Rehabilitation Data.** Maintenance and rehabilitation data are also collected by the SHA's for LTPP. As a maintenance or rehabilitation event occurs, general information regarding construction, materials and date of completion are all collected and stored. This data was important to this project when analyses were being conducted on the pavement roughness and the rate of distress development.

---

Note: Considerable differences have been found between the manual and automated distress surveys for some distress types. These differences are primarily attributable to the resolution limits of the hardware used in the initial interpretation of the film and to the evolution of the *Distress Identification Manual for the LTPP Project* (report number SHRP-P-338, dated 1993) subsequent to the film interpretation.

### 2.3 Data Not in the Data Base

Several data items required for the analyses were not directly available from the NIMS, but were requested from the Regional Coordinating Offices (RCO's) or the Technical Assistance Contractor (TAC). Each of these are briefly listed and noted below:

- Backcalculated moduli are not available from the data base. However, the backcalculations have been completed twice prior to this analysis, once by the individual RCO's and once by the TAC. These backcalculated modulus values were obtained from the TAC.
- Seasonal FWD deflection data are not currently in the NIMS or the Regional Information Management System (RIMS). However, each of the RCO's have been tasked with preparing this data for entry into the RIMS. These data were requested and obtained from the individual RCO's.
- Several of the data elements noted in table 1 are not available in the NIMS or the RIMS. In particular, subgrade compressive strength, saturation, specific gravity, and K coefficients of the resilient modulus equation for coarse- and fine-grained soils are not currently available. However, each of these elements were measured during repeated-load resilient modulus testing for the Southern and North Atlantic regions at Law Laboratories. In addition, a confined compression test was conducted on each resilient modulus sample after resilient modulus testing was completed. All of these data elements were identified as being necessary for at least one of the analysis efforts. These strength data were obtained from the testing forms completed by Law Laboratories in Atlanta, Georgia.
- Initial Present Serviceability Index (PSI) data, although considered to be critical historical information, currently has no space allocated for storage in the data base. These data were collected from each of the States prior to the early analyses conducted under the SHRP, and can be found in the reports from those studies (3, 4).
- Rut depths using a 1.2-m (4-ft) straight edge are no longer commonly used. Equations for the calculation of PSI values were generated expressly for the incorporation of these rut depths, but these data are not currently available in the data base nor are rut depths being collected using a 1.2-m (4-ft) straight edge in the NIMS. However, full cross-profiles are being collected, and a program has been created to calculate rut depths from these cross-profiles for both 1.2-m (4-ft) and 1.8-m (6-ft) straight edges.

- Distress information is limited for a few of the GPS test sections in that only one to two rounds of distress data collected by PASCOS have been filtered into the data base for all GPS sections, and there are some sections where no manual surveys have been conducted. As previously mentioned (see footnote 1, page 13), it has been found that significant differences between the available distress data sources exist. Therefore, use of these data sets were kept separate to avoid conflicts and misrepresentation.
- Certain data are also not available in the IMS because they are considered to be calculated data. Hence, some of the data (such as air, void content or percent compaction) were calculated from the raw data.

#### **2.4 Problems With Data Available From the Data Base**

Several data elements noted as being required for these analyses were unavailable or severely limited for use on this project. Each of these are briefly listed below:

- As stated, samples were collected on each of the sections at the initiation of the LTPP study. Asphalt layers were tested only if they were greater than 38 mm (1.5 in) thick. While most asphalt layers for the GPS sections are greater than 38 mm (1.5 in), some sections have one or two layers that were thinner than 38 mm. This may lead to some asphalt sections (i.e., thin sections) without materials characterization for a large portion of the HMAC material. Finally, there are some sections for which all of the asphalt layers are less than 38 mm (1.5 in). These sections have no laboratory testing data for the asphalt concrete materials.
- Resilient modulus of the pavement materials was a very important and critical part of this overall research effort. Unfortunately, not all of the repeated-load resilient modulus testing has been completed. In fact, the GPS sites in the western part of the U.S. have no resilient moduli currently available and the unbound materials have not yet been tested in the north central part of the U.S. As resilient modulus was a key data element, those GPS section ends where most of the pavement layers had been tested for resilient modulus were used more extensively in the data analysis. The following summarizes the number of GPS sites for which resilient modulus tests were conducted on most of the pavement layers and subgrade.

---

GPS Sites:	Subgrade soil resilient modulus tests completed.....	220
GPS Sites:	Unbound granular base/subbase modulus tests completed.....	181
GPS Sites:	Subgrade soil/unbound base and/or subbase tests completed.....	133

---

Table 2 lists those GPS sites for which most of the layers in the pavement cross section and subgrade were tested for resilient modulus, and identifies those layers with resilient modulus test data. The percentage of pavement cross section tested for resilient modulus was calculated to quantify those GPS sections with insufficient materials data. Only those sections having 90 percent or more of their cross-sectional thickness (surface, base, subbase layers) tested for resilient modulus were used for these analyses. Table 3 summarizes the number of GPS sites with repeated-load resilient modulus testing of the embankment and subgrade soils by material and type of test specimen.

- None of the stabilized layers received resilient modulus testing with the exception of the asphalt stabilized material. This testing was not originally planned for any of the treated materials, except the asphalt stabilized bases, and there currently is no plan for testing these materials in the future.
- HMAC viscosity, subdrainage information, subgrade soil suction, shoulder information, potential vertical rise, swell probability, swell rate constant, frost heave probability, maximum potential loss, and frost heave rate were initially requested from the SHA's as inventory data. While the viscosity information is fairly complete, all of the other data elements are severely limited.
- In situ wet/dry densities are only available for sections that had test-pit sampling. Test-pit sampling was only performed on the asphalt sections and not all of these sections had a test pit. Test-pit sampling was not conducted on sections that were curbed or had utility lines in the way. Therefore, densities and compaction (calculated from the density) are not available for every section. These densities and compaction data were available for a limited number of test sections from the inventory data, but were generally unavailable, like many other inventory data elements.
- In processing traffic data, the data are run through a QC process. The QC process flags data that appear to be in error. The data may be out of calibration or could have any

**Table 2. GPS sites having resilient modulus test data for 90 percent or more of the pavement cross section.**

<b>Subgrade St SHRP End</b>	<b>Both Base &amp; Subgrade St SHRP End</b>	<b>Base St SHRP End</b>	<b>Subgrade St SHRP End</b>	<b>Both Base &amp; Subgrade St SHRP End</b>	<b>Base St SHRP End</b>
110111	110111	110012	1239962	1240991	1239961
110211	110211	110012	1239971	1240992	1239962
110212	110212	110012	1239972	1241001	1239962
130281	130281	110111	1240571	1241001	1239971
130282	130282	110111	1240571	1241002	1239971
140071	140071	110112	1240572	1241002	1239972
140072	140072	110191	1240572	1241021	1239972
140732	140732	110192	1240591	1241022	1240571
140841	140841	110211	1240592	1241031	1240572
140842	140842	110212	1240961	1241032	1240591
141251	141251	130281	1240961	1241051	1240592
141251	141251	130281	1240962	1241052	1240961
141252	141252	130282	1240962	1241061	1240962
141252	141252	130282	1240991	1241062	1240991
141261	141261	140071	1240992	1241071	1240991
141261	141261	140071	1241001	1241071	1240992
141262	141262	140072	1241001	2310121	1241001
141262	141262	140072	1241002	2810011	1241002
150082	160191	140732	1241002	2810011	1241021
160191	160191	140841	1241021	2810012	1241021
160191	160192	140841	1241022	2810012	1241022
160192	160192	140842	1241031	2810161	1241022
160192	530732	140842	1241032	2810161	1241031
410221	540211	141251	1241051	2810162	1241031
530582	540212	141252	1241052	2810162	1241032
530582	1210301	141261	1241061	2850251	1241032
530731	1210302	141262	1241062	2850252	1241051
530732	1210601	160191	1241071	2858051	1241051
540211	1210601	160192	1241071	2858052	1241052
540212	1238041	530732	1241362	3510022	1241052
558051	1238041	530732	2010051	3510031	1241061
558052	1238042	540211	2010051	3510051	1241061
940081	1238042	540211	2010092	3510051	1241062
940081	1239951	540212	2010092	3510052	1241062
940082	1239952	540212	2010101	3510052	1241071
940082	1239961	940201	2010101	3511121	1241081
950011	1239962	1210301	2010102	3511121	1241082
950011	1239971	1210301	2010102	3511122	1290542
1210301	1239972	1210302	2310121	3511122	1310011
1210302	1240571	1210302	2310122	3520061	1310012
1210601	1240571	1210601	2310262	3520062	1310041
1210601	1240572	1210602	2310262	3521181	1310042
1238041	1240572	1213702	2330141	3521182	1310051
1238041	1240591	1213702	2330141	3530101	1310052
1238042	1240592	1238041	2370231	3530101	1310311
1238042	1240961	1238042	2370232	3530102	1310312
1239951	1240961	1239951	2510022	3530102	1330071
1239952	1240962	1239952	2810011	3560331	1330072
1239961	1240962	1239952	2810011	3560332	1330161

**Table 2. GPS sites having resilient modulus test data for 90 percent or more of the pavement cross section (continued).**

<b>Subgrade St SHRP End</b>	<b>Both Base &amp; Subgrade St SHRP End</b>	<b>Base St SHRP End</b>	<b>Subgrade St SHRP End</b>	<b>Both Base &amp; Subgrade St SHRP End</b>	<b>Base St SHRP End</b>
2810012	4041601	1330191	3718171	4811742	4510111
2810161	4041602	1330192	3718172	4811742	4510112
2810161	4270252	1341111	3719921	4811812	4510241
2810162	4270371	1341112	3750371	4811832	4510242
2810162	4270372	2140251	3750372	4811832	4510252
2830911	4510081	2310121	3750372	4835592	4710232
2830911	4510081	2330131	3758271	4835891	4710281
2830912	4510111	2810011	3758271	4835891	4710282
2830912	4510111	2810012	3758272	4835892	4731011
2850251	4510112	2810161	3758272	4835892	4731012
2850252	4510241	2810162	4010151	4836091	4731041
2858051	4510242	2850251	4010151	4836092	4731081
2858052	4510242	2850252	4010152	4836092	4731082
3410112	4510252	2858051	4010152	4837691	4731102
3410311	4510252	2858052	4010171	4837691	4760151
3410311	4710232	3440421	4010171	4837692	4760152
3410312	4710281	3510022	4010172	4837692	4790241
3410331	4710281	3510031	4010172	4837791	4790242
3410331	4710282	3510032	4041571	4837791	4810561
3410332	4731011	3510051	4041572	4837792	4810562
3410332	4731011	3510052	4041581	4837792	4810772
3510022	4731012	3511121	4041581	4838651	4810871
3510031	4731012	3511122	4041582	4838651	4810872
3510051	4731081	3520061	4041582	4838652	4810931
3510051	4731081	3520062	4041601	4838652	4810961
3510052	4731082	3521181	4041602	4841421	4810962
3510052	4731082	3521181	4041621	4853281	4811161
3511121	4760151	3521182	4041621	4853282	4811221
3511121	4760152	3521182	4041622	4860791	4811221
3511122	4810561	3530101	4041622	4860791	4811222
3511122	4810562	3530102	4050212	4860792	4811222
3520061	4810772	3560331	4050212	4860792	4811231
3520062	4810772	3560332	4060101	4861791	4811232
3521181	4810871	3710241	4060101	4861792	4811681
3521182	4810872	3710401	4060101	5016822	4811741
3530101	4810931	3710402	4060102	5120211	4811742
3530101	4810931	3718031	4060102	5120211	4811812
3530102	4810961	3718032	4070242	5120212	4811832
3530102	4810961	3730441	4215971	5120212	4835592
3560331	4810962	3730442	4215972	5470081	4835891
3560332	4810962	4041601	4215982	7241212	4835892
3610111	4811161	4041602	4215982	8716221	4836091
3610112	4811161	4050211	4215992	8716802	4836092
3710062	4811221	4050211	4215992		4837691
3710062	4811222	4216131	4216061		4837692
3710242	4811681	4270252	4216062		4837791
3713522	4811681	4270371	4216901		4837792
3713522	4811741	4270372	4216901		4838651

**Table 2. GPS sites having resilient modulus test data for 90 percent or more of the pavement cross section (continued).**

<b>Subgrade St SHRP End</b>	<b>Both Base &amp; Subgrade St SHRP End</b>	<b>Base St SHRP End</b>	<b>Subgrade St SHRP End</b>	<b>Both Base &amp; Subgrade St SHRP End</b>	<b>Base St SHRP End</b>
4216902		4838652	4810771		
4216902		4841421	4810772		
4230441		4853281	4810772		
4230441		4853282	4810871		
4250202		4860791	4810872		
4250202		4860792	4810931		
4270251		4861791	4810931		
4270252		4861791	4810961		
4270371		4861792	4810961		
4270372		4861792	4810962		
4510081		5016822	4810962		
4510081		5016831	4811161		
4510111		5016832	4811161		
4510111		5120211	4811221		
4510112		5120212	4811222		
4510241		5470081	4811681		
4510242		7230081	4811681		
4510242		7230082	4811741		
4510252		7241212	4811741		
4510252		8716221	4811742		
4570191		8716802	4811742		
4570191			4811812		
4710231			4811832		
4710232			4811832		
4710281			4835592		
4710281			4835891		
4710282			4835891		
4730751			4835892		
4730751			4835892		
4731011			4836091		
4731011			4836092		
4731012			4836092		
4731012			4837691		
4731081			4837691		
4731081			4837692		
4731082			4837692		
4731082			4837791		
4760151			4837791		
4760152			4837792		
4810481			4837792		
4810481			4838651		
4810482			4838651		
4810482			4838652		
4810561			4838652		
4810562			4841421		
4810761			4841422		
4810762			4850351		
4810762			4850351		
4810771			4852781		

**Table 2. GPS sites having resilient modulus test data for 90 percent or more of the pavement cross section (continued).**

<b>Subgrade St SHRP End</b>	<b>Both Base &amp; Subgrade St SHRP End</b>	<b>Base St SHRP End</b>
4852782		
4853281		
4853282		
4853361		
4853361		
4860791		
4860791		
4860792		
4860792		
4861791		
4861792		
5016821		
5016822		
5110021		
5120211		
5120211		
5120212		
5120212		
5440031		
5440032		
5440042		
5470081		
7241211		
7241212		
8716221		
8716222		
8716801		
8716802		



**Table 3. Summary of GPS sections with repeated-load resilient modulus tests for unbound pavement materials and subgrade soils.**

<b>Number of Sections</b>	<b>Total # of GPS Sections</b>	<b># of Clay</b>	<b># of Silt</b>	<b># of Sand</b>	<b># of Gravel</b>
All Regions/All Types (AC & PCC)	793	233	68	331	125
Total GPS Sections Analyzed	572	177	45	258	80
Total GPS Sections Used for the Analysis (>90% X-Section Tested)	324	75	26	163	51
Containing Moduli Data	125	20	10	78	15
Field Condition (Shelby)	37	14	2	20	1
Recompacted Specimen (Bulk)	88	6	8	58	14
<b>Percentage of Sections</b>	<b>% GPS Sections</b>	<b>% with Clay</b>	<b>% with Silt</b>	<b>% with Sand</b>	<b>% with Gravel</b>
All Regions/All Types (AC & PCC)	100	29	9	42	16
Total GPS Sections Analyzed	72	22	6	33	10
Total GPS Sections Used for the Analysis (>90% X-Section Tested)	41	9	3	21	6
Containing Moduli Data	16	3	1	10	2
Field Condition (Shelby)	5	2	0	3	0
Recompacted Specimen (Bulk)	11	1	1	7	2

Note: Cumulative values for the various material types that do not equal 100 percent were caused by missing data and/or roundoff error.

number of other problems. The flagged data are then left out of the estimate of the number of ESAL's for that year. In preparing the data for analysis, it was determined that not all of the flagged data were kept out of the ESAL estimate. It was not possible to determine how many of the sections suffered from this problem without examining the data closely section by section. The problem was reported to the FHWA, but due to time limitations, any analysis requiring traffic data had to be performed with the data as they existed.

- Currently, the individual RCO's collect the data and enter it into their RIMS. Once the data are collected and entered, QC programs are run on the data and the output is examined to identify and eliminate apparent errors. These data (or a portion thereof) are uploaded annually to the NIMS. The last upload of GPS distress, FWD, and profile data to the NIMS was 6 months prior to the commencement of this study. The rest of the GPS data were uploaded 1½ years prior to the beginning of this study. Therefore, the data used may not have been as up-to-date as possible. In addition, maintenance or rehabilitation events may have taken place in between available monitoring events without the knowledge of the user of the data base.

## **2.5 Data Organization and Processing**

Once all of the data were obtained from the LTPP NIMS and the RCO's, it was necessary to organize the data into a format that could be used for all of the analyses. Prior to breaking the data into separate categories or research areas (table 1), there were several steps that had to be accomplished. When examining the data, it can be seen that there are differences between layer thicknesses and material properties of the ends of the same test section. These differences are slight in some cases and very large in others. Backcalculation of layer moduli was conducted using the FWD data collected over each of the sampling areas just prior to sampling. For this reason, analyses were conducted not on a test-section basis, but rather on data collected past the test-section ends where material sampling actually occurred. Hence, for each test section, generally two observations will be found for each layer within the data base used to conduct the analyses.

For some of the analyses conducted within this study, some layers of similar materials were combined into one layer. For these combined layers, the bulk specific gravities of the asphalt layers, the resilient moduli of the asphalt layers, the indirect tensile or diametral strengths of the asphalt concrete layers and the moisture contents of the unbound layers, each had more than one

value per layer, per test-section end. Therefore, comparable data were averaged for the combined layer before inclusion into the data base used for this study.

For the purposes of comparing laboratory to backcalculated moduli (discussed in subsection 4.3), laboratory data for some layers of similar materials were combined to force the laboratory layer configuration to be the same as the layer configuration used in the backcalculation process. The materials data for the combined layers were combined using a weighted average where the weights were proportional to the thickness of the original layer. For example, the combinations of the resilient moduli used cubes of the thicknesses for the weight rather than just the thickness to result in equivalent stiffnesses, as shown below:

$$E_R (\text{Combined Layer}) = \frac{E_{R1} t_1^3 + E_{R2} t_2^3}{t_1^3 + t_2^3} \quad (1)$$

where:

$E_R$  = Resilient modulus measured in the laboratory for asphalt concrete mixtures or layers;  $M_R$  is generally used for the resilient modulus for unbound aggregate bases and subbases and subgrade soils.

$t$  = Layer thickness

In some cases, the subgrade was separated into two layers for the backcalculation process. In these cases, the subgrade laboratory data were only used to represent the top subgrade layer. As stated previously, the “Percentage of Pavement Section Tested” was calculated to quantify sections which lacked materials data. Only those sections having 90 percent or more of their cross-sectional thickness (surface, base, subbase layers) tested for resilient modulus were used for these analyses.

Before the data elements were included in the analysis data base, the data were examined to ensure proper use of the data. After the quality checks were completed, all data were subdivided or separated into smaller data sets for the individual research study areas. Each of these sets are discussed in the following chapters of the report for the different study areas.

### **3. DETERMINATION OF LAYERED ELASTIC MODULI - LABORATORY TESTS**

Resilient modulus is the primary material property that is used to characterize the roadbed soil and other structural layers for flexible pavement design in the 1986 and 1993 *AASHTO Guide for Design of Pavement Structures*. Resilient modulus is simply a measure or estimate of the elastic modulus of the material at a given stress state or temperature (i.e., assumed to be the modulus of elasticity). It is mathematically defined as the applied stress (or deviator stress change for triaxial testing of unbound materials) divided by the "recoverable" strain that occurs when the applied repeated-load is removed from the test specimen. Resilient modulus is generally measured in the laboratory using repeated-load triaxial and/or indirect tensile tests depending on the type of material being tested. However, another way of determining the resilient modulus can be through backcalculation of layer moduli from deflection basin tests performed on the pavement's surface.

In practice, less than 20 percent of the SHA's actually use the laboratory resilient modulus test to determine those values for use in design. Most use some type of correlation between resilient modulus and other physical properties or strength measures. Figure 2 shows the distribution of subgrade strength values used for design of flexible pavements by SHA's in the United States, and table 4 includes some examples of those relationships that various SHA's have developed for subgrade soils.

Within the AASHTO Design Guide, resilient modulus is also used to determine and/or estimate the structural layer coefficients for different pavement materials. The methods to determine the layer coefficient vary extensively across the U.S. Some States have determined the layer coefficients from previous performance observations, while others have generated relationships between resilient modulus of various materials and layer coefficients. Thus, resilient modulus is an important and critical parameter used within the AASHTO Design Guide.

It is extremely important that the highway industry be confident in determining and using resilient modulus when characterizing pavement materials and subgrade soils. Currently, that confidence in and understanding of resilient modulus simply does not exist in many SHA's for day-to-day design practices. Reasons for this low confidence are related to the extensive variability in the test results, the perceived difficulty in using the equipment, the time required to run the test, and the test does not result in one single value to be used in design.

Both chapters 3 and 4 investigate the determination of resilient modulus for use in design and evaluation, and summarize the analyses conducted with the LTPP data base. The intent of this

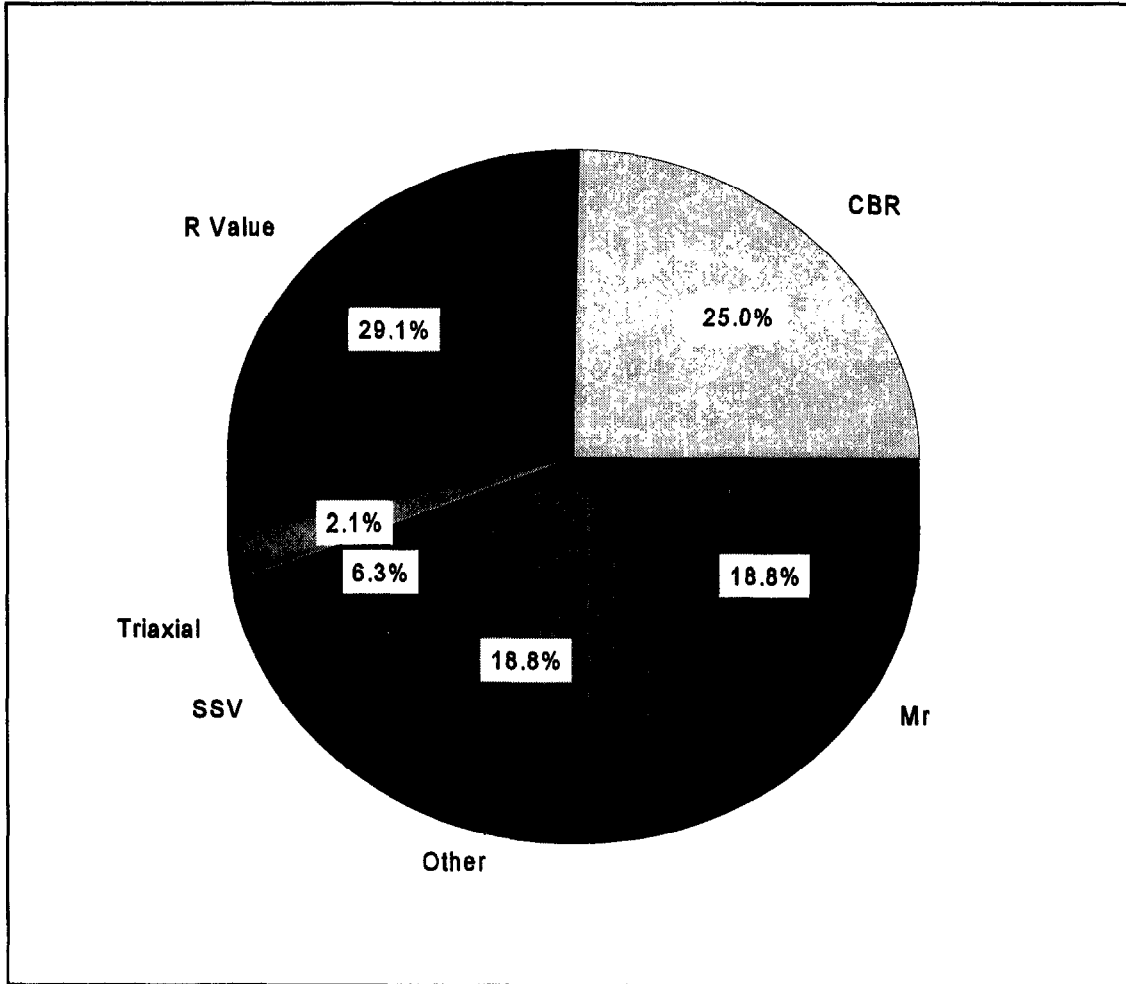


**Figure 2. Subgrade parameters used for flexible pavement designs across the United States (2).**

**Table 4. Examples of relationships used to calculate the design resilient modulus for subgrade soils from other properties.**

State	Relationship
Arizona	<p>log R value @ 300 psi = 2.0 - 0.006 (% pass 200) - 0.017 (PI)</p> $M_r = \frac{1815 + 225 (R_{mean}) + 2.40 (R_{mean})^2}{0.6 (SVF)^{0.6}}$ <p>where <math>M_r</math> = Resilient Modulus (psi)  <math>R_{mean}</math> = Mean value of correlated and actual resistance values (R values)  SVF = Seasonal Variation Factor  PI = Plasticity Index  % Pass 200 = Percent passing the number 200 sieve</p>
Colorado	<p><math>S_1 = [(R-5)/11.29] + 3</math></p> $M_r = 10^{\left[ \frac{S_1 + 18.72}{6.24} \right]}$ <p>where R = Resistance value  <math>S_1</math> = Soil support value  <math>M_r</math> = Resilient Modulus (psi)</p>
Nebraska	<p><math>M_r = 100 (b_0 + B_1G + B_2G^2 + B_3G^3 + B_4G^4)</math></p> <p>where <math>m_r</math> = Resilient Modulus (psi)  G = Nebraska Group Index  <math>B_i</math> = Regression coefficients (function of moisture contained in soil)</p>

$$Pa = psi \times (6.89 \times 10^3)$$

Note: All of the above equations were developed using English units. As such, English units must be used in calculating the design resilient modulus in psi. After the design resilient modulus is calculated in psi, it then can be converted to SI units.

effort is to demonstrate and build confidence in the use of resilient modulus for design and evaluation, and identify critical differences between laboratory measured and backcalculated moduli. Chapter 3 focuses on laboratory measured moduli, while chapter 4 is on backcalculation of layer moduli from deflection measurements. Chapter 4 also identifies and discusses those differences found between laboratory determined and backcalculated moduli.

### **3.1 Laboratory Resilient Modulus Test Results**

Various laboratory procedures and equipment have been used for measuring resilient moduli on both bound and unbound pavement materials, including subgrade soils. As part of the LTPP program, resilient moduli were measured on selected pavement layers and subgrade soils recovered from the ends of most GPS projects. Table 2 listed those GPS projects for which repeated-load resilient modulus tests have been completed on at least a portion of the pavement layers/materials and/or subgrade soils. This list of GPS projects includes less than 300 of the more than 780 available GPS test sections. The following discusses the laboratory test results for the asphalt concrete mixtures, unbound granular base/subbase materials and subgrade soils that have been tested. Repeated-load resilient modulus tests were not performed on the Portland Cement Concrete (PCC) materials nor any of the treated base and stabilized subgrade materials.

### **3.2 Dense-Graded Asphalt Concrete Mixtures**

Indirect tensile resilient modulus tests for dense-graded asphalt concrete surface and base materials were conducted at three temperatures. These temperatures were 5 °C (41 °F), 25 °C (77 °F), and 40 °C (104 °F). Two modulus values were calculated for each test temperature, an instantaneous and total resilient modulus. The instantaneous modulus is calculated using the recoverable strain at the time when all of the repeated load is removed, and the total modulus is calculated using the total recoverable strain from peak strains until the next load pulse is applied.

Figure 3 shows a comparison of the total and instantaneous resilient modulus for all dense-graded asphalt concrete mixtures included in the LTPP data base. As shown, the difference between the instantaneous and total resilient moduli decreases with decreasing test temperatures, because the material is becoming more elastic. This observation is consistent with the findings from other material studies. In summary, the following lists the average ratio between the total and instantaneous resilient moduli ( $E_{RT}/E_{RI}$ ) for the three test temperatures.

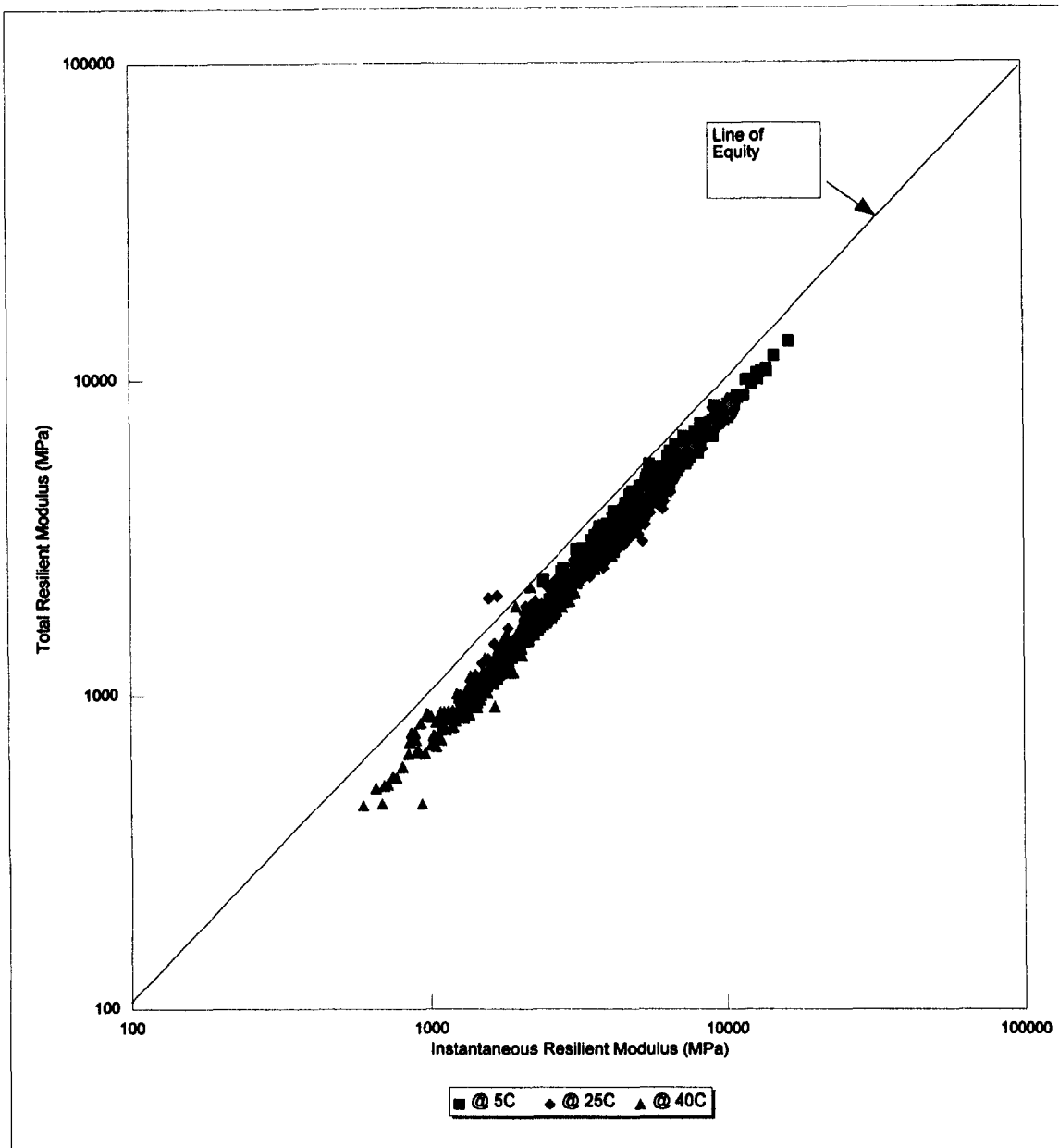


**Figure 3. Comparison of total and instantaneous resilient modulus for dense-graded asphalt concrete materials recovered and tested from the GPS sites.**



Test Temperature, °C (°F)	*E <sub>RT</sub> /E <sub>RI</sub> Ratios	
	Other Studies (3, 4)	LTPP Data
5 (41)	0.88 (.82-.92)**	0.85 (.78-.90)
25 (77)	0.75 (.65-.82)	0.76 (.68-.80)
40 (104)	0.62 (.58-.67)	0.71 (.66-.82)

\*E<sub>RI</sub> = Instantaneous Resilient Modulus

E<sub>RT</sub> = Total Resilient Modulus

\*\*Numbers in the ( ) are the typical range of the moduli ratios reported in other studies (5, 6).

Indirect tensile strengths were also measured on each of these mixtures at 25 °C (77 °F). Figure 4 shows the histogram of indirect tensile strengths measured at this temperature. Previous laboratory studies completed on asphalt concrete materials have reported relationships between the indirect tensile resilient modulus and strength. Figure 5 graphically shows the range of typical relationships between indirect tensile strength and total resilient modulus that have been measured on cores, and compares those relationships to the strength-modulus values measured from asphalt concrete cores recovered from the GPS sites. As shown, significant differences do exist between the LTPP data and results from other studies. Reasons for this substantial difference are unknown.

**Observation:** The indirect tensile strength-total resilient modulus relationship measured on cores recovered from the GPS sites are significantly different from those reported in other material research studies (figure 5).

Another important point to note is the greater variability of the instantaneous resilient modulus data than for total resilient modulus. This observation is consistent with other material study findings and is a result of the fact that the instantaneous recovered deformations are not well defined, whereas the total recovered displacements are easily defined. As a result, the total resilient modulus was used, in most cases, for the data analyses discussed in this report.

Figure 6 is a histogram of the total resilient moduli measured at each of the three test temperatures. As shown, the range or dispersion of values significantly increases with decreasing test temperatures, which is inconsistent with previous study results. The other more important point to note is that the total resilient moduli measured at 5 °C (41 °F) are consistently

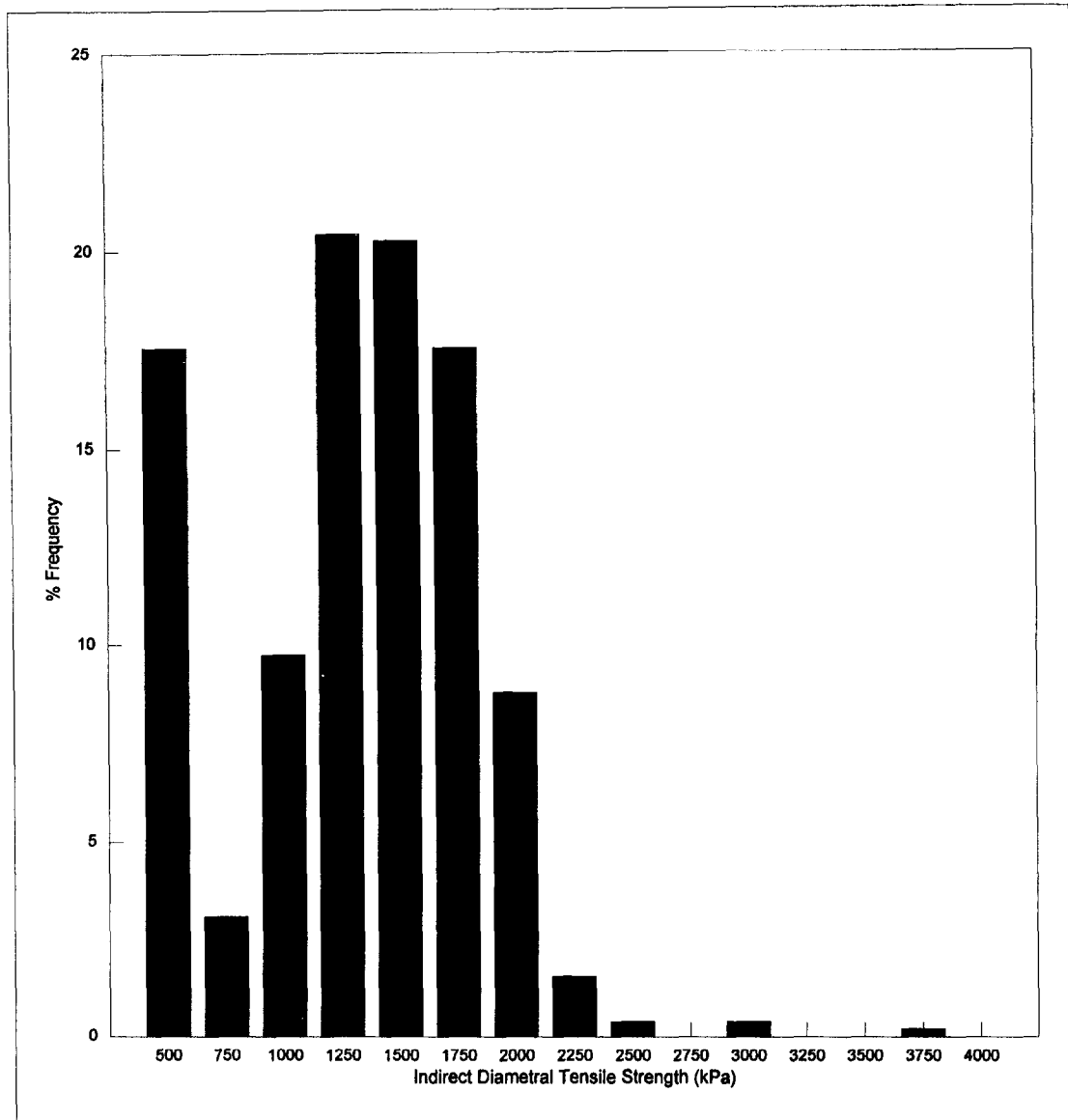


**Figure 4. Histogram of the indirect tensile strengths measured at 25 °C (77 °F) for dense-graded asphalt concrete mixtures recovered from the GPS sites.**

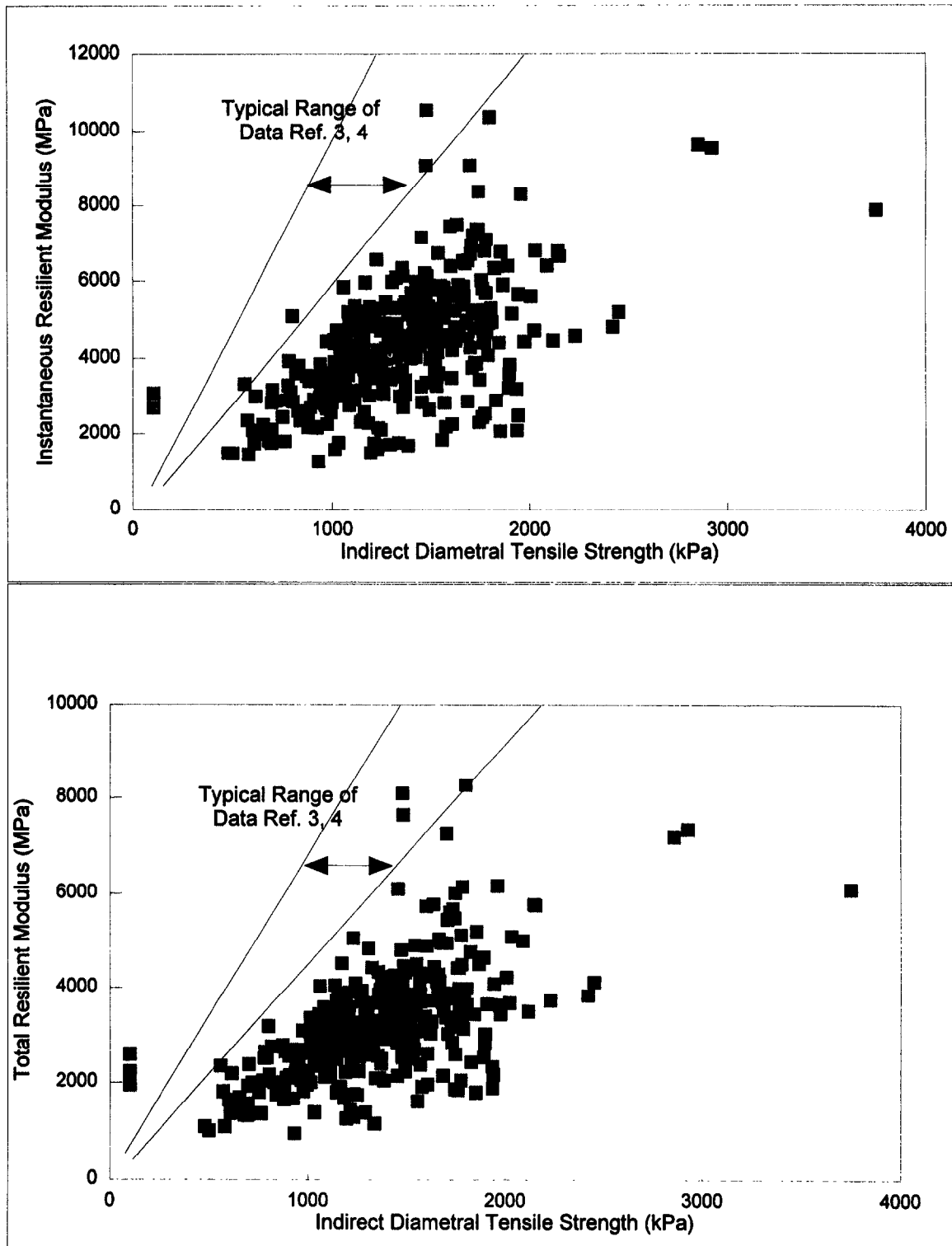


**Figure 5. Relationship between indirect tensile strength and total resilient modulus for asphalt concrete materials/mixtures.**

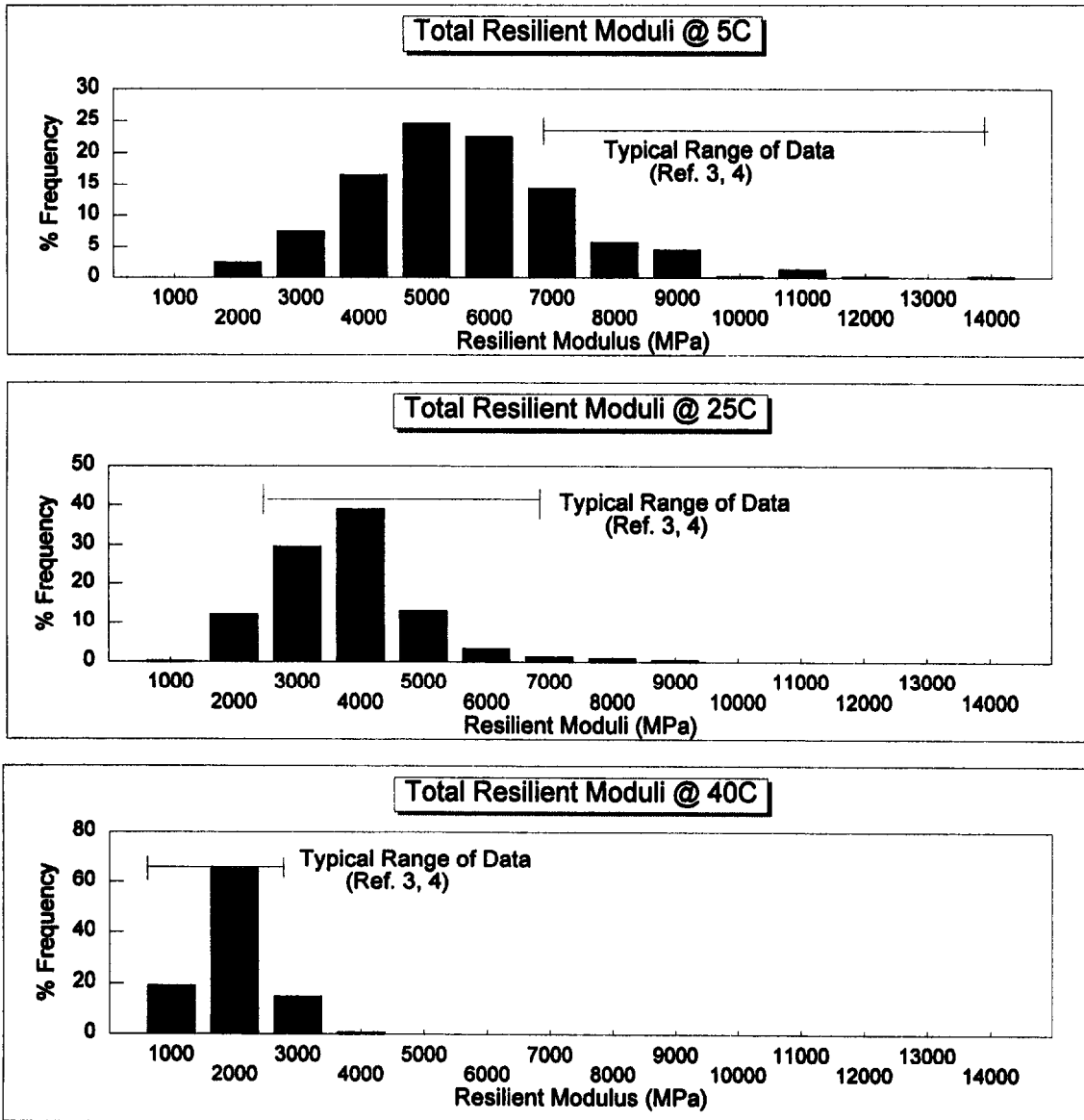


**Figure 6. Histogram of the total resilient modulus of asphalt concrete materials measured at the three test temperatures.**

low when compared to the moduli measured at 25 °C (77 °F) (especially for aged asphalt concrete mixtures). In fact, the range of values reported from other studies (5, 6, 7, 8) are included in the histograms in figure 6, and show that the moduli measured at 5 °C (41 °F) within the LTPP program are significantly less than moduli reported from other studies at the same test temperature.

Poisson's ratio is an important parameter that affects the calculation of resilient modulus using repeated-load indirect tensile tests. Figure 7 is a histogram of Poisson's ratio measured at each test temperature. These values are reasonable and consistent with those reported from other studies. Thus, Poisson's ratio is not believed to be the cause of this substantial difference in resilient modulus values at 5 °C (41 °F) , as compared to the results from other test programs.

**Observation:** The resilient moduli measured at 5 °C (41 °F) on asphalt concrete cores are consistently low and are believed to be in error when compared to the moduli measured on those same cores at 25 °C (77 °F) and 40 °C (104 °F).

This observation is more clearly shown in figure 8, which shows the range of typical values reported from different studies as compared to those moduli obtained from the LTPP data base. In summary, the moduli measured at 25 and 40 °C (77 and 104 °F) are within the same range of reported values, but at 5 °C (41 °F) the LTPP results differ by a factor of about two, as compared to other values reported in the literature. In addition, the temperature effect on resilient modulus from the LTPP data base is slightly less than reported from other studies.

Figures 9 through 11 show an example of the vertical and horizontal deformations measured at 5, 25 and 40 °C (41, 77 and 104 °F), respectively, during indirect tensile repeated-load resilient modulus testing of the LTPP cores. These data were reviewed in an attempt to identify the reasons for this significant difference, but with no conclusive results. However, one important item to note is the magnitude of the noise in the data, which is present at all temperatures. This noise increases the variability of the calculated resilient modulus and makes it difficult to graphically visualize determination of the resilient modulus, especially the instantaneous resilient modulus.

As a result of this observation (figure 8), the resilient moduli measured at 5 °C (41 °F) were excluded from use in the detailed studies discussed within the report. The resilient moduli measured at 5 °C (41 °F) should be checked for potential errors and/or to identify the reason(s) that the reported resilient moduli are significantly different than those reported in other studies.

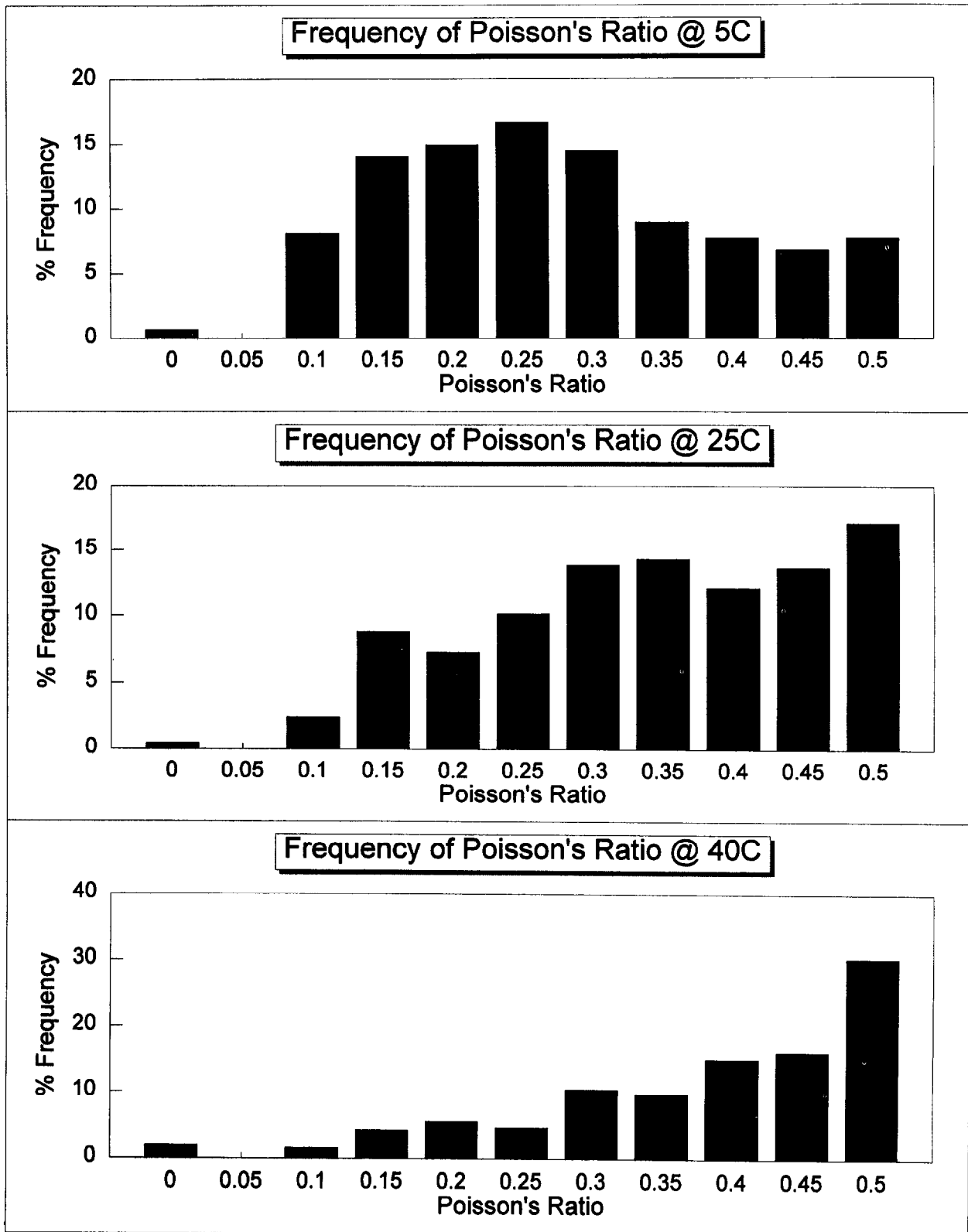


**Figure 7. Histogram of Poisson's ratios for each test temperature for the asphalt concrete mixtures.**

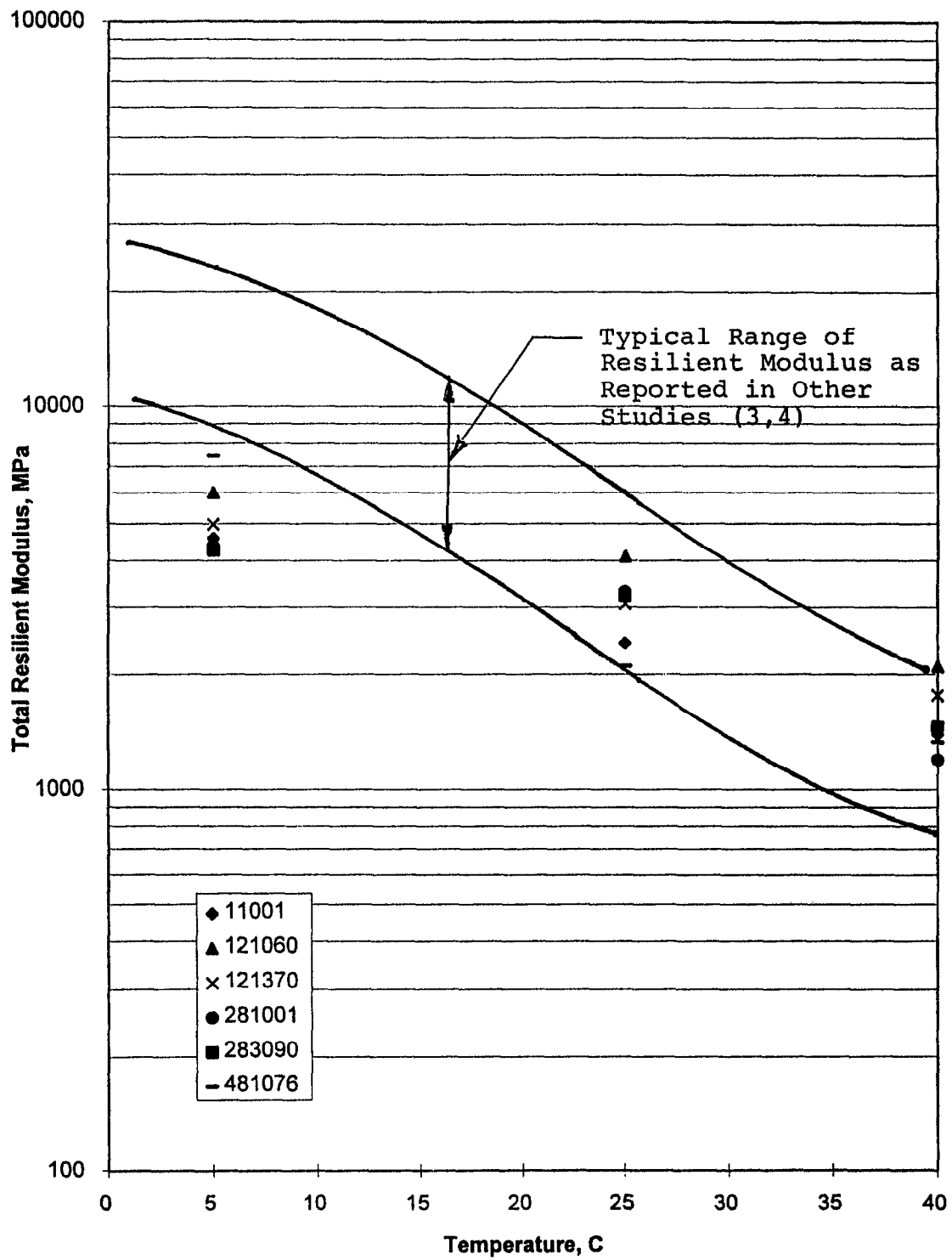
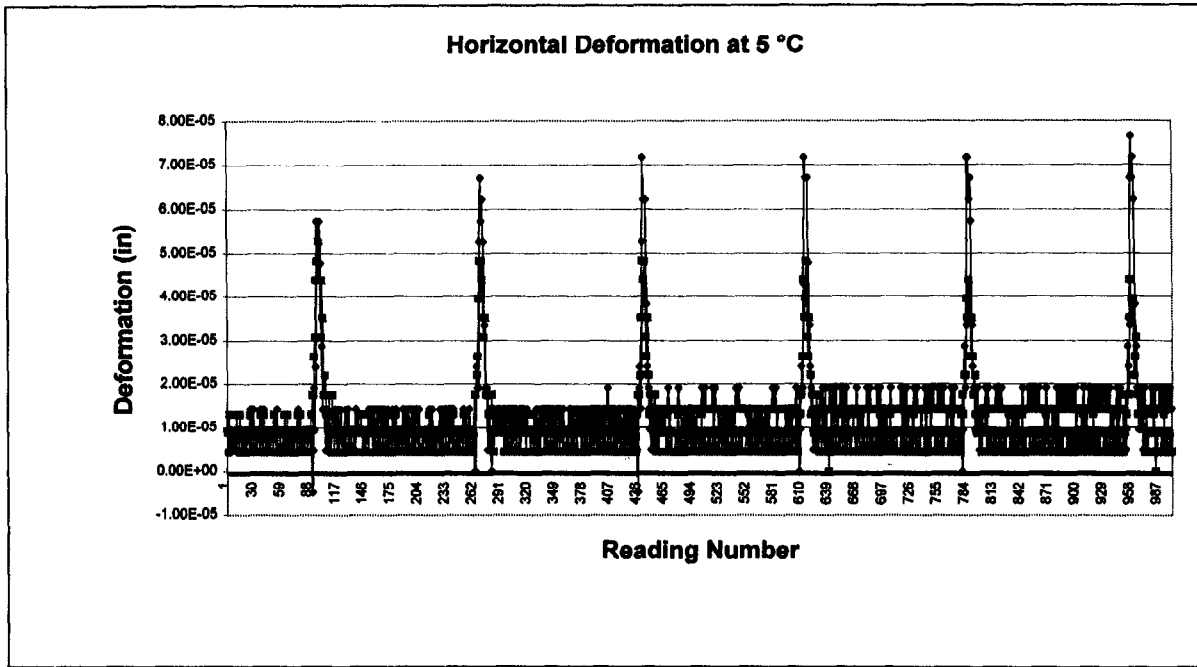
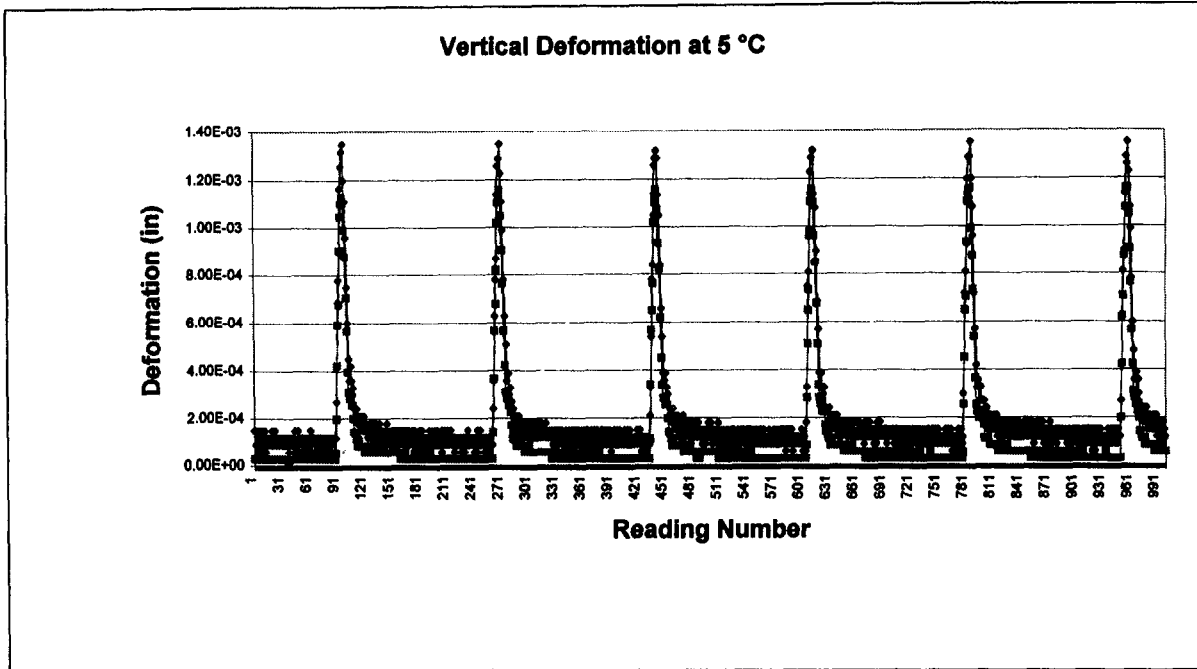


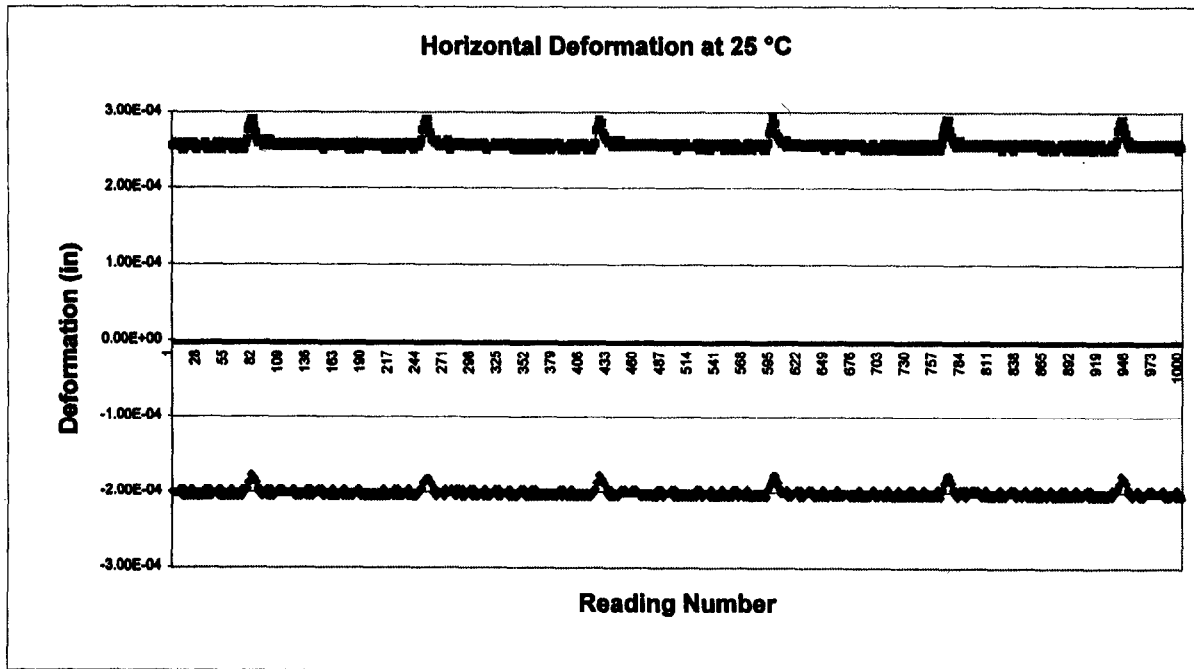
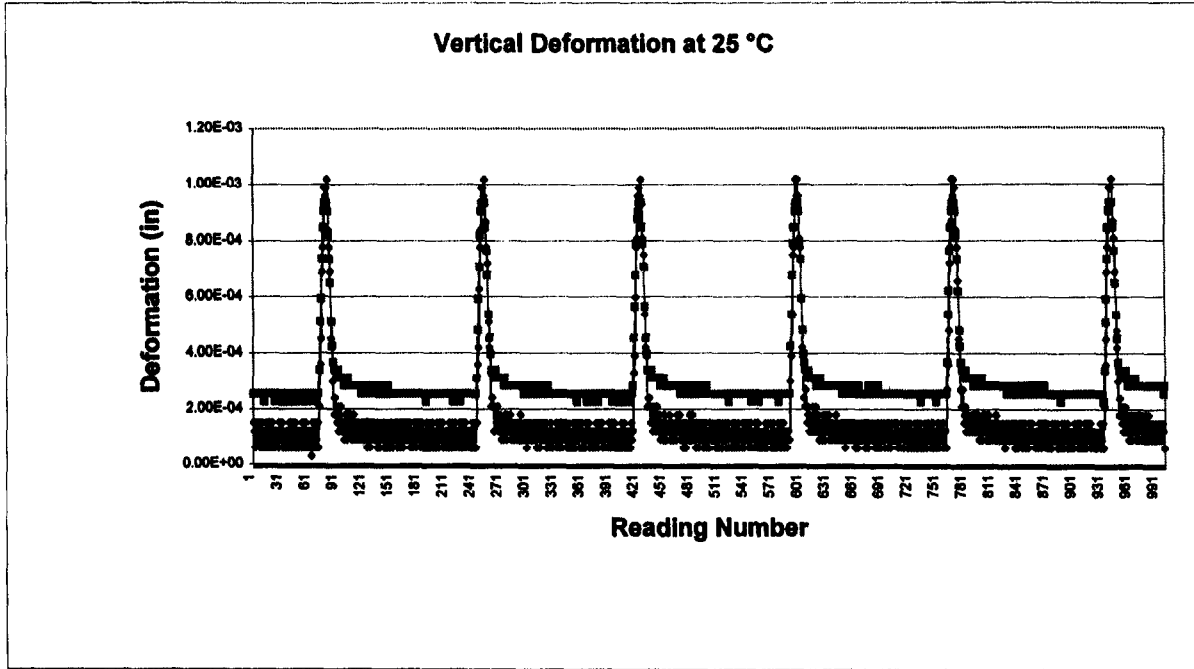
**Figure 8. Chart for the total resilient modulus vs. temperature using indirect tensile loading conditions.**



1 in = 2.54 cm

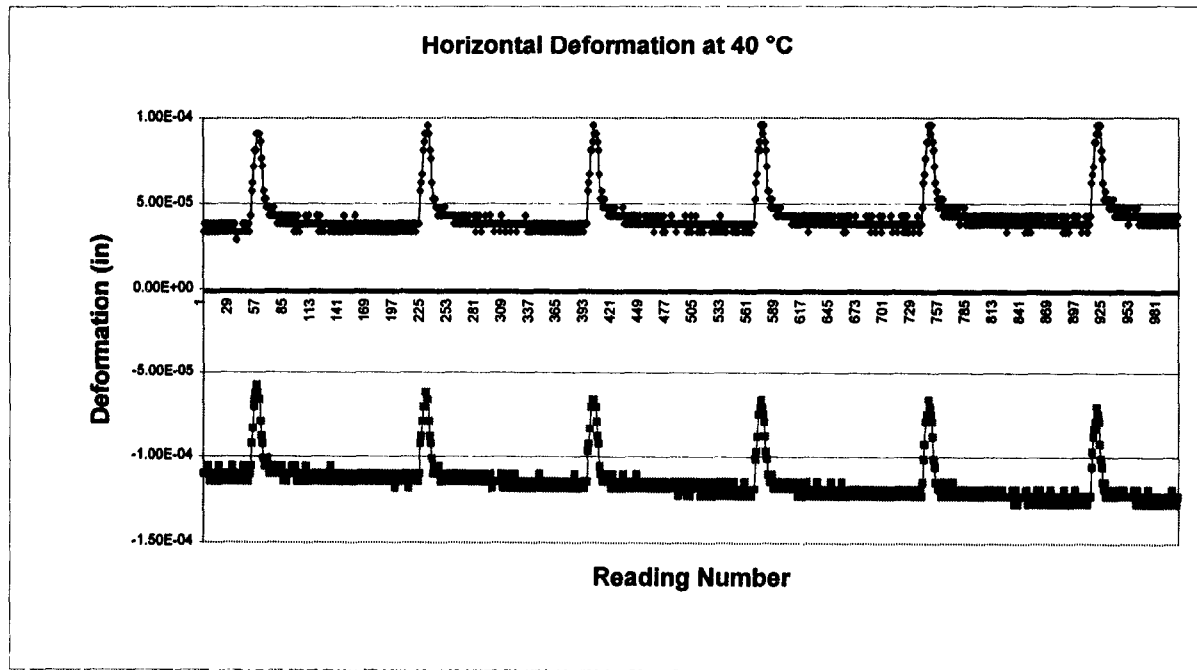
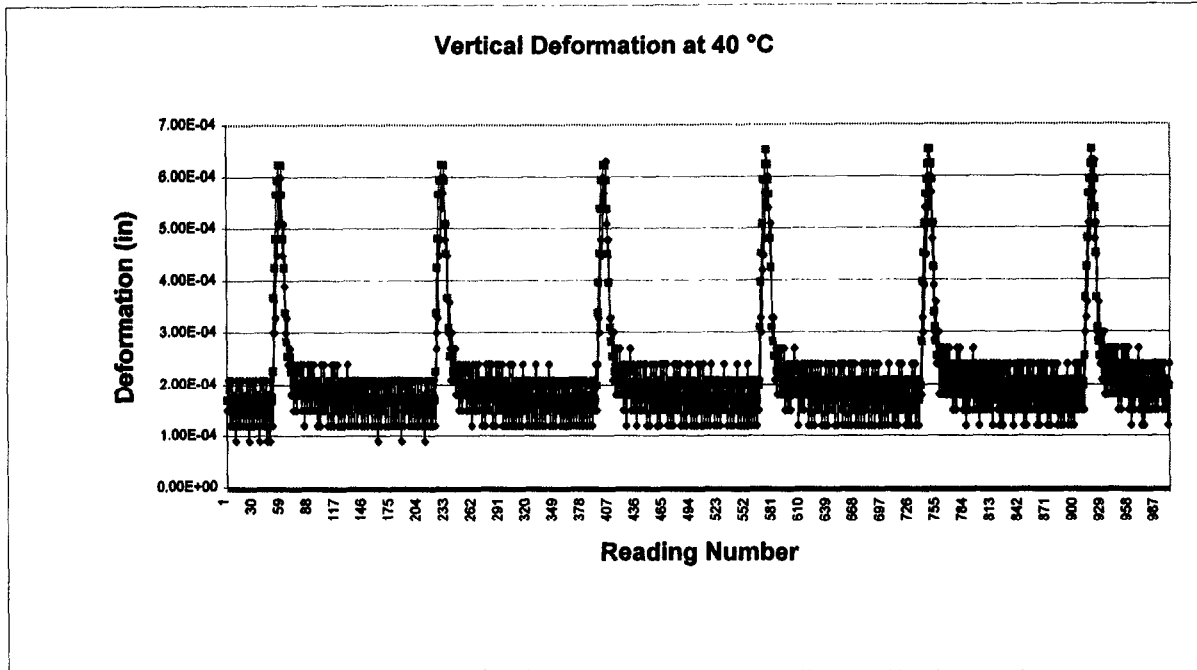
**Figure 9. Vertical and horizontal deformations measured during repeated-load indirect tensile testing at 5 °C (41 °F).**





1 in = 2.54 cm

**Figure 10. Vertical and horizontal deformations measured during repeated-load indirect tensile testing at 25 °C (77 °F).**



1 in = 2.54 cm

**Figure 11. Vertical and horizontal deformations measured during repeated-load indirect tensile testing at 40 °C (104 °F).**

### 3.3 Unbound Materials

Repeated-load triaxial compression tests were used to measure the resilient moduli of unbound granular base/subbase materials and subgrade soils. These tests are performed over a range of stress states and confining pressures to evaluate the nonlinear elastic behavior of these materials. Figure 12 graphically presents an example of the test results of repeated-load resilient modulus tests on unbound granular base materials and subgrade soils recovered from selected GPS sites. Figure 13 shows the distribution of resilient moduli measured at a specific stress state for unbound granular base/subbase materials and coarse- and fine-grained subgrade soils recovered and tested within the LTPP program.

Various types of relationships have been used to represent the repeated-load resilient modulus test results of coarse-grained and fine-grained soils (figure 12). Some of the more common relationships that have been used are listed below:

For coarse-grained soils:  $M_r = K_1 (\theta)^{K_2}$  (2)  
 where:  $\theta$  = bulk stress  
 $K_1$  and  $K_2$  are regression constants

For fine-grained soils:  $M_R = K_1 (\sigma_d)^{K_3}$  (3)  
 where:  $\sigma_d$  = deviator stress

More recently, other constitutive relationships have been used to represent the laboratory test results of all unbound pavement materials and subgrade soils. Two of these relationships are listed below:

$$M_R = K_1 (\sigma_d)^{K_2} (1 + \sigma_3)^{K_5} \quad (4)$$

where:  $\sigma_3$  = confining pressure

$$M_R = K_1 p_a \left[ \frac{\theta}{p_a} \right]^{k_2} \left[ \frac{\sigma_d}{p_a} \right]^{k_3} \quad (5)$$

where:  $p_a$  = atmospheric pressure

Since equations 4 and 5 are independent of soil type, these relationships were used to determine the coefficients and exponents in the resilient modulus equation to fit the LTPP laboratory test results.

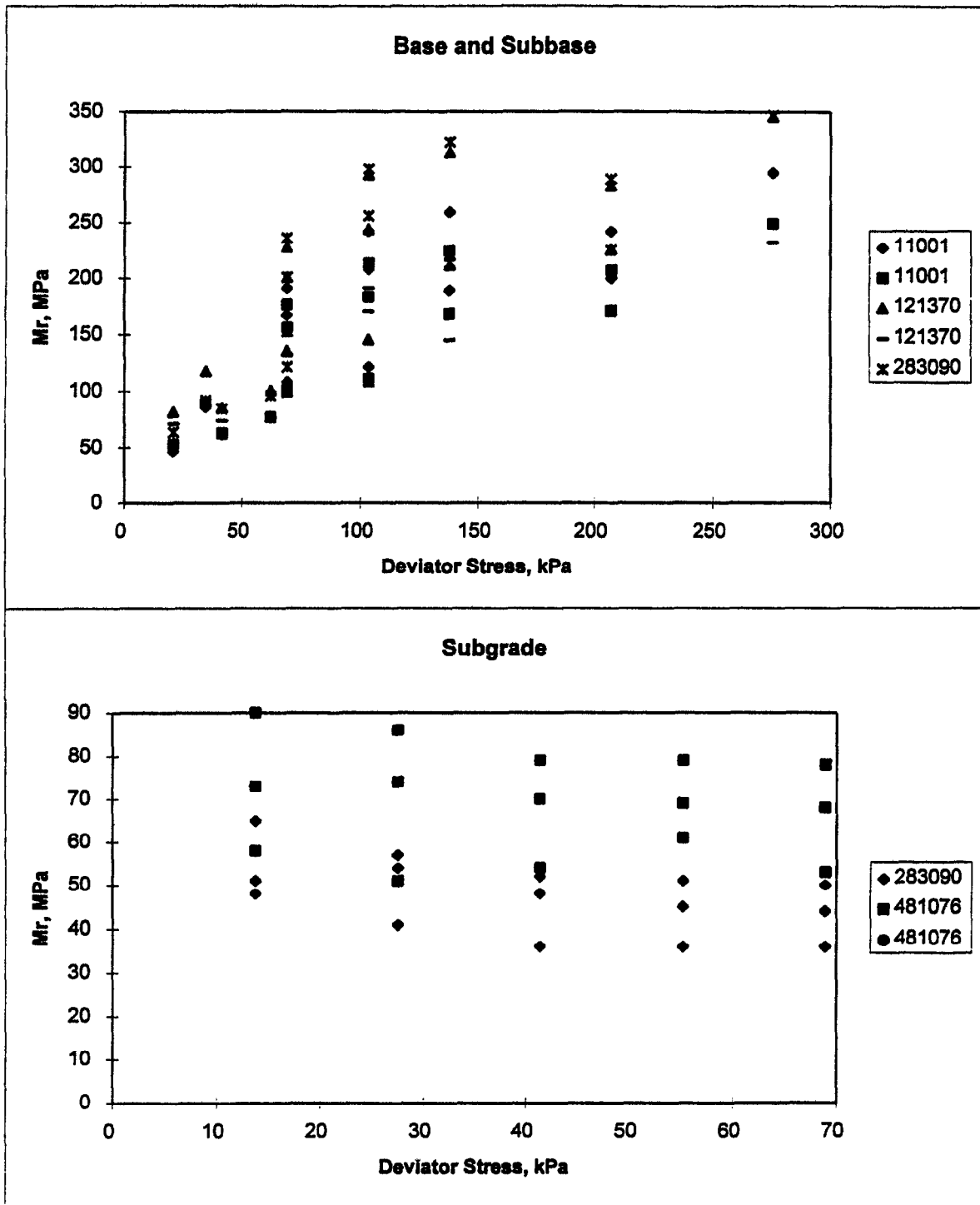


**Figure 12. Results from repeated-load triaxial resilient modulus tests performed on unbound base materials and subgrade soils.**

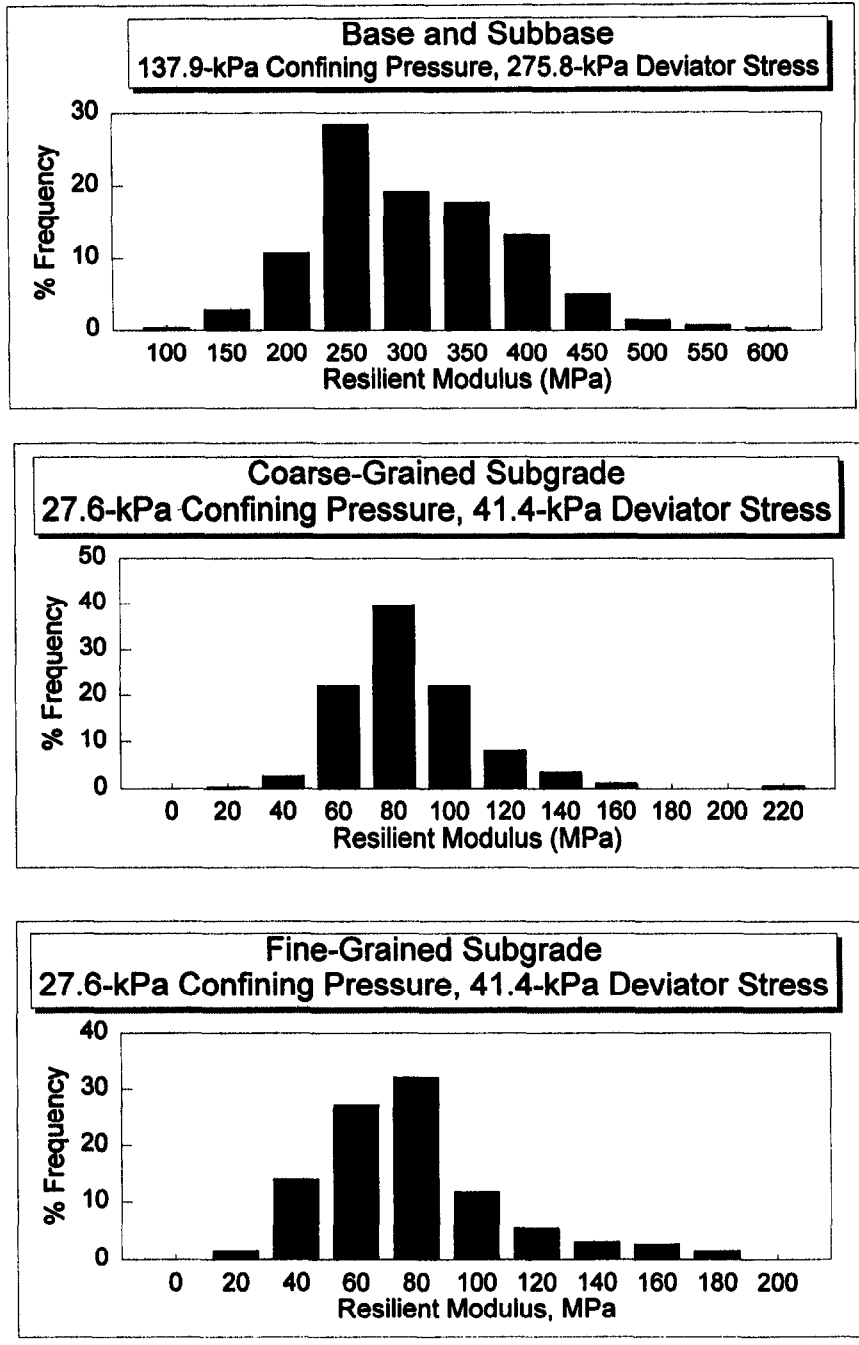


**Figure 13. Histogram of resilient modulus at specific stress states for unbound coarse- and fine-grained soils.**

Table 5 summarizes the average nonlinear elastic coefficients and exponents (K values) that were determined from regression analyses of the resilient moduli test data of the unbound granular base/subbase materials and subgrade soils. As expected, the K values do vary, depending upon the type of equation used to represent the nonlinear elastic response. However, the error terms and multiple correlation coefficients (resulting from the use of linear regression analyses) for both equations are similar. In fact, there is no significant difference between how well each of the relationships (equations 4 and 5) fit the laboratory data. The average R<sup>2</sup> term (multiple-correlation coefficient) for both relationships exceed 0.85 for the GPS repeated-load resilient modulus data.

**Table 5. Summary of average elastic coefficients and exponents (K values) determined from regression studies of the repeated-load triaxial compression tests of unbound pavement materials and subgrade soils.**

Material/ Soil Type	Equation 4			Equation 5		
	K <sub>1</sub>	K <sub>2</sub>	K <sub>3</sub>	K <sub>1</sub>	K <sub>2</sub>	K <sub>3</sub>
Clay	8,300	-0.08	0.26	594	0.44	-0.19
Silts	5,800	0.08	0.48	426	0.42	-0.23
Sands	5,400	0.14	0.45	598	0.44	-0.12
Gravels	8,100	-0.02	0.46	836	0.23	-0.08
Base	5,500	0.21	0.59	869	0.65	-0.04

Equation 4: 
$$M_R = K_1 (\sigma_d)^{K_2} (1 + \sigma_3)^{K_3}$$

Equation 5: 
$$M_R = K_1 p_a \left[ \frac{\theta}{p_a} \right]^{k_2} \left[ \frac{\sigma_d}{P_a} \right]^{k_3}$$

Figure 14 is a histogram of the multiple-correlation coefficient for how well the test data fits equation 5. As such, equation 5 is the relationship that was selected for use on this project to represent the nonlinear elastic response of unbound pavement materials and subgrade soils. Equation 5 is also similar to the constitutive equation used within the Superpave program (as developed by SHRP, [9]) to represent the response of unbound materials and soils for evaluating asphalt concrete pavements and mixtures. Figures 15 through 17 show the distribution of the nonlinear elastic coefficients and exponents of equation 5 (K<sub>1</sub>, K<sub>2</sub>, K<sub>3</sub>) by material type for the unbound materials recovered and tested from the GPS sites.

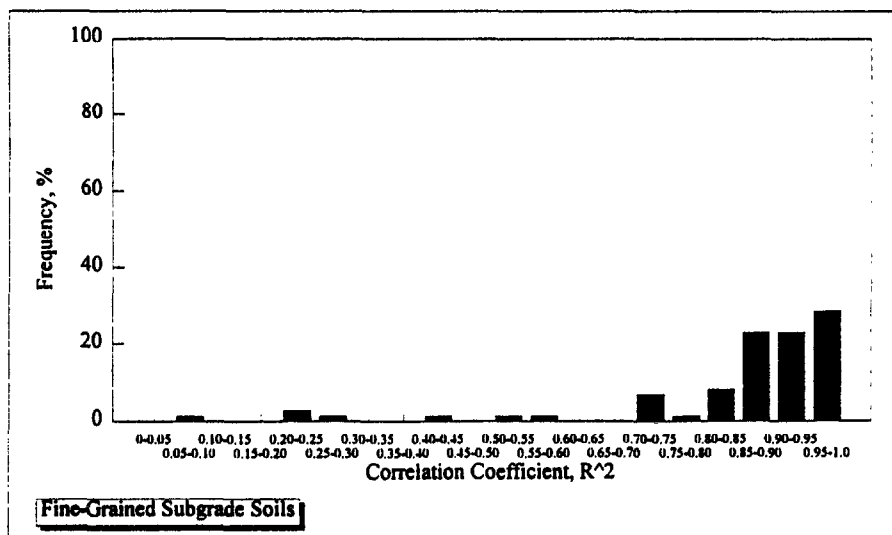
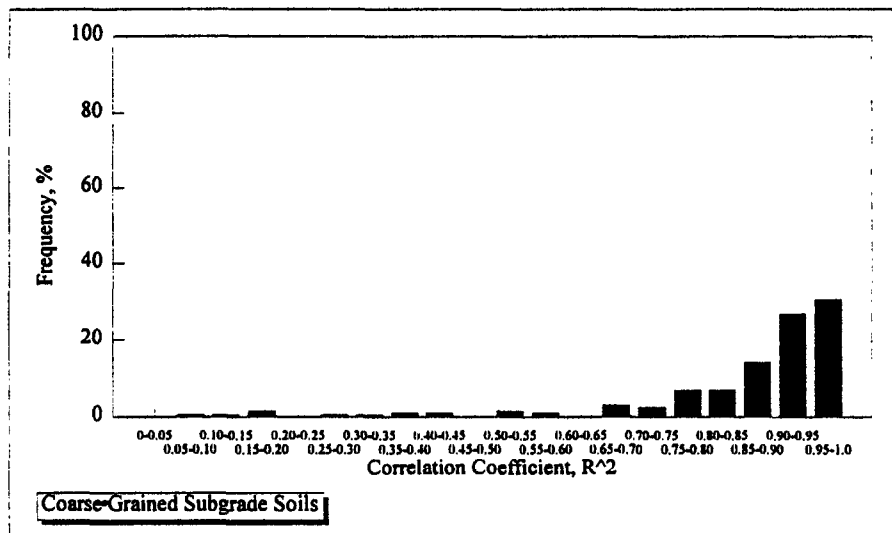
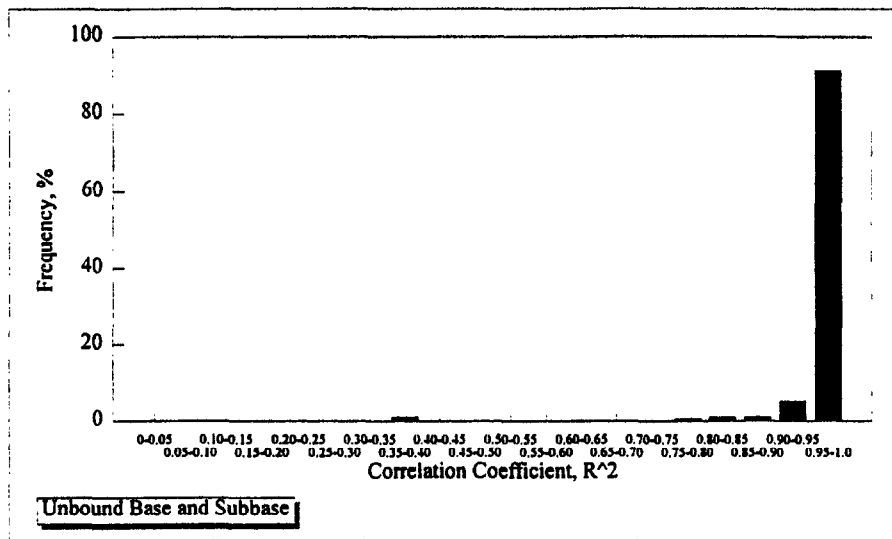


**Figure 14. Histogram of the R<sup>2</sup> term using equation 5 to fit the laboratory repeated-load resilient modulus test data for unbound materials and soils.**

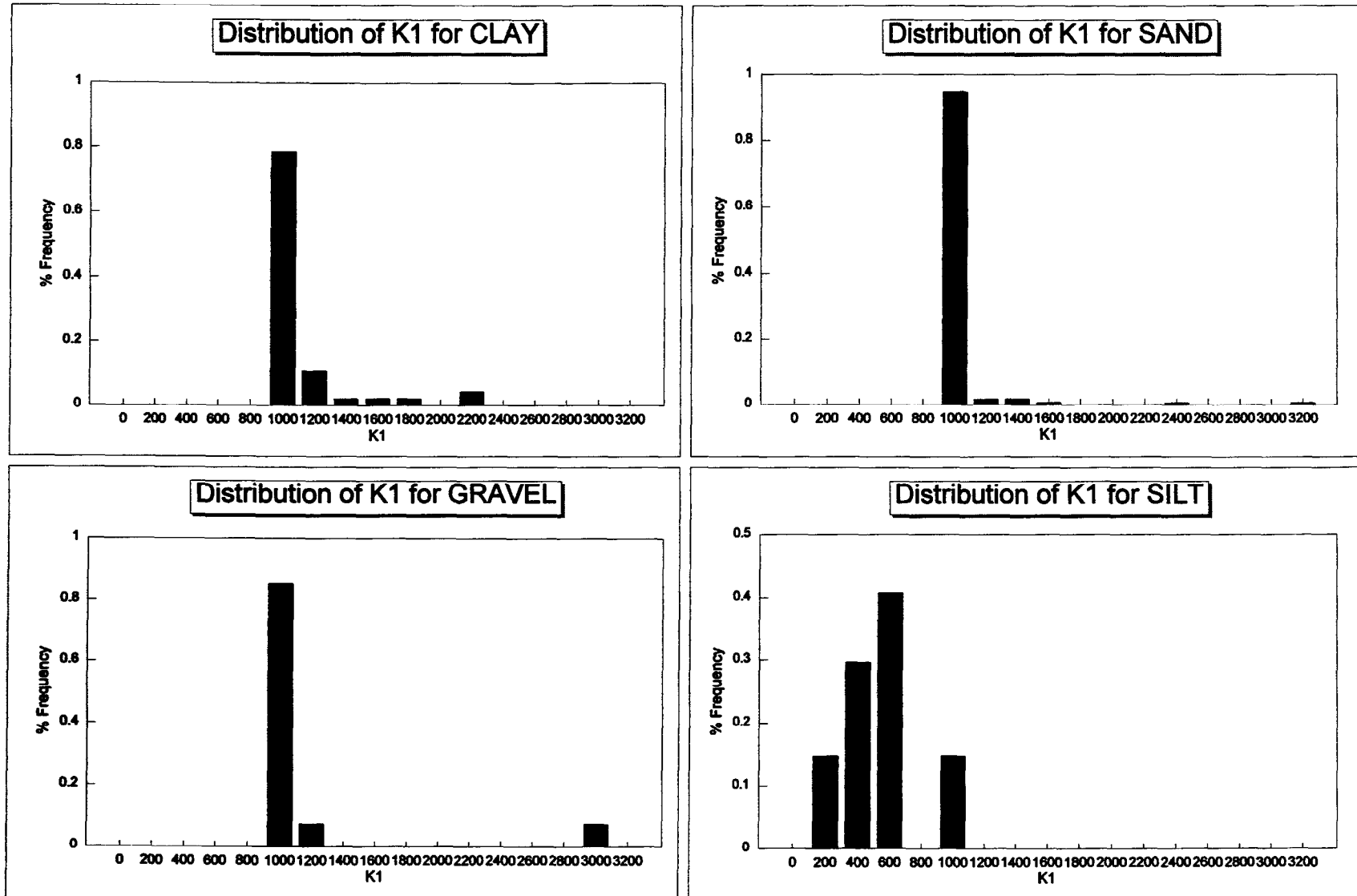


**Figure 15. Histogram of the  $K_1$  elastic coefficient for the unbound materials and subgrade soils.**



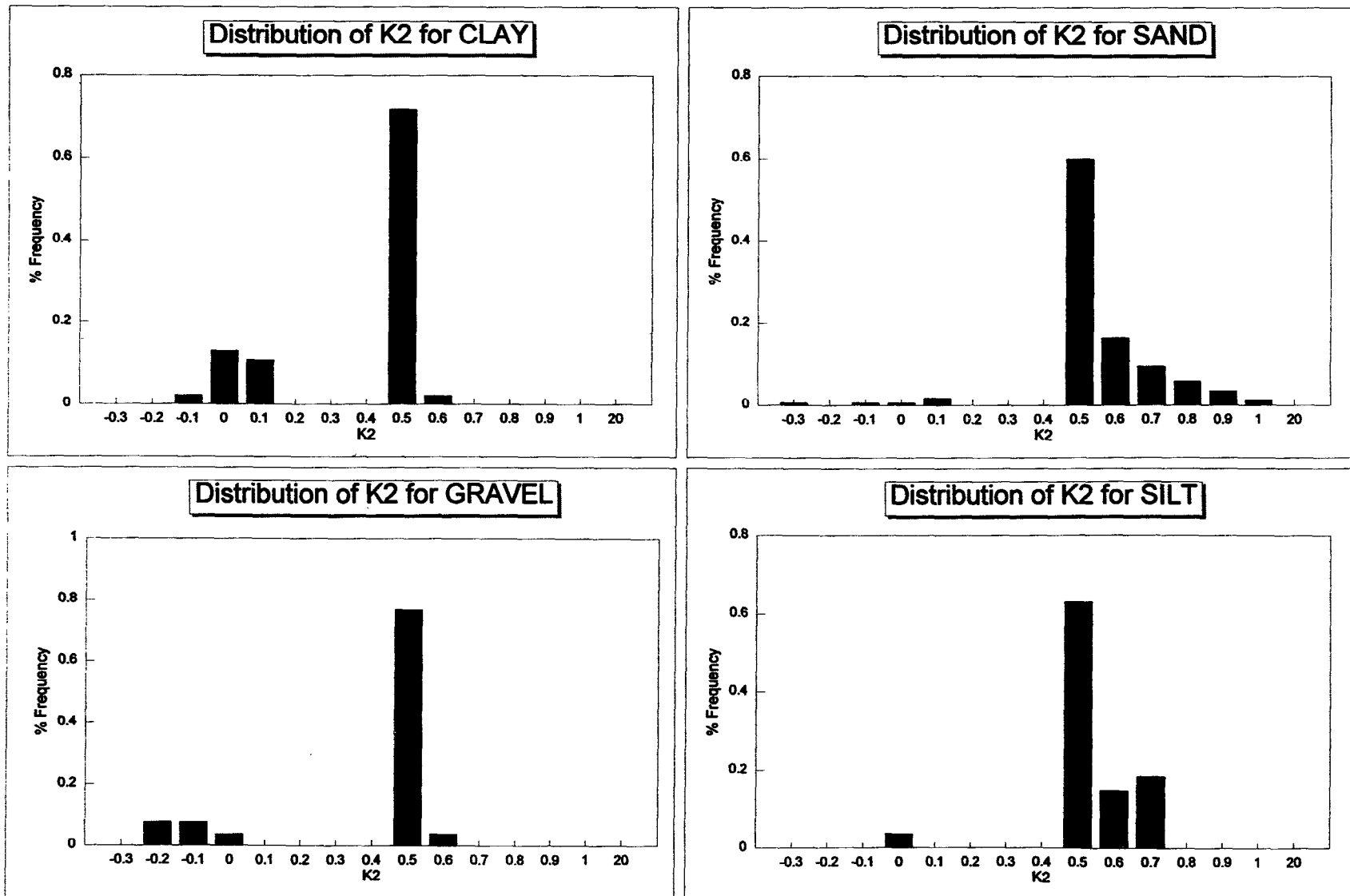


**Figure 16. Histogram of the  $K_2$  elastic exponent for the unbound materials and subgrade soils.**

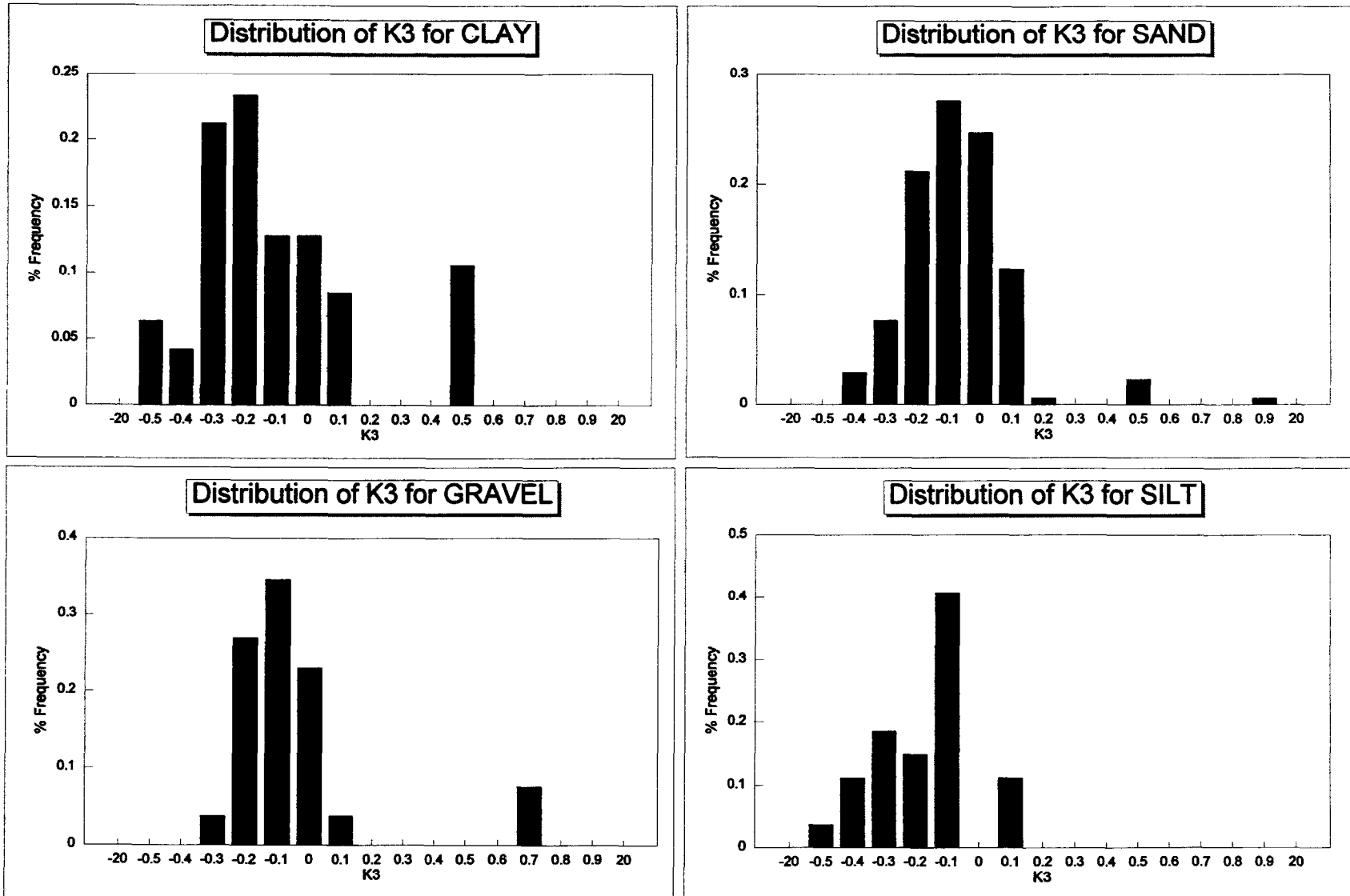


**Figure 17. Histogram of the  $K_3$  elastic exponent for the unbound materials and subgrade soils.**

**Observation:** Equation 5 can be used to accurately fit or represent the laboratory test results of repeated-load triaxial compression tests for resilient modulus testing of unbound pavement materials and subgrade soils.

### **3.4 Nonlinear Elastic Coefficient/Exponents Determined From Physical Properties**

About half of the SHA's use the 1986/1993 *AASHTO Guide for Design of Pavement Structures*, but less than 20 percent actually measure the resilient modulus of the pavement materials and subgrade soils. Most SHA's use other properties to predict the design resilient modulus from correlations published in the literature or developed directly by the SHA. An example of some of these correlations were given in table 4, and others have been published in the AASHTO Guide.

From past experiences in developing predictive models for resilient modulus utilizing materials data, very poor correlations have been found to exist between the resilient modulus and physical properties. Physical properties in this sense refer to density, moisture content, plasticity index, gradation, clay content, etc. One of the reasons that the resilient modulus has been found to be poorly correlated to physical properties is that the resilient modulus for most unbound pavement materials and subgrade soils changes with the applied stress. Trying to correlate physical properties that do not change with stress state to a resilient modulus that changes at different rates with stress state becomes very difficult, if not impossible. Therefore, the K values noted in equation 5 (repeated below) were instead regressed with the physical properties of those materials as independent variables in an attempt to increase the reliability in estimating the resilient modulus from physical properties of those materials.

One of the potential benefits from an ability to determine resilient modulus from the physical properties would be to consider seasonal variations of resilient modulus resulting from seasonal changes in the material's physical properties. Seasonal variations are critical for determining the design resilient moduli for a particular project. Estimating the effect of variations in moisture content and other such physical properties on resilient moduli becomes very important. A relationship based upon changes in physical properties could then be used to estimate the equivalent annual moduli to be used in design based upon conducting limited subgrade resilient moduli testing. In fact, it is standard practice by many SHA's to only determine the resilient modulus or to conduct repeated-load triaxial testing of the subgrade soils and/or base materials at the optimum conditions, but this is generally non-conservative when saturated or partially saturated conditions occur.

During laboratory testing, the resilient moduli were related to the bulk stress and deviator stress in accordance with equation 5. The values of  $K_1$ ,  $K_2$ , and  $K_3$  were included in the data base and correlated to other physical properties of the material. In this manner, the difference in pavement types, environment, and other such parameters were initially excluded from the analyses. Figures 15 through 17 showed the histograms of the K values for the different materials and subgrade soils included in the LTPP data base. As shown, many of these K values are material type-dependent.

The material types identified in these figures were based on physical properties that were also measured on soils recovered from each of these sites. The extremely important point to recognize, however, is that testing for resilient modulus and other physical properties may have been conducted on samples from different depths and soils. Therefore, data from those sites where the subgrade test specimen used for resilient modulus testing was recovered 30 cm (12 in) or more beneath the top of subgrade, were not included in the multiple regressions. The reason for this omission is that the other laboratory test results may not represent the specific material used for resilient modulus testing, because moisture contents, dry densities, gradation and other physical properties were only measured on soils recovered at the surface of the subgrade.

The LTPP data base contained a variety of laboratory data for various test sections. The data needed for the analysis of the K values had to be extracted and organized to evaluate whether there was sufficient information. Each section contained data for an approach and leave end resulting in two observations for each section. Quality checks were conducted for each section end, such as “Ninety (90 percent) of Section Tested” to ensure that all of the layers (surface and base) combined contained test information for more than 90 percent of the cross-sectional thickness. This data set was divided into material classes containing granular base and clay, silt, sand and gravel subgrades.

Data within the LTPP data base were analyzed to determine correlations and/or potential relationships that could be used to determine each of the K values from physical properties of unbound materials. Others have also attempted to develop these correlations using a similar type approach. One such example is the study completed by Santha in 1994 (10). Results from this study are provided in table 6, which shows the relationships and important physical properties that have been found to be significant to the prediction of the K values for the resilient modulus equation 5. The Santha study was a highly controlled laboratory study, but it only included a limited number of subgrade soil types. Fortunately, the LTPP data base includes results from laboratory resilient modulus tests and other physical property test on various materials and soils, but it is an uncontrolled experiment for relating the nonlinear elastic coefficients/exponents to the physical properties.

**Table 6. Relationships previously developed between the nonlinear elastic coefficient/exponents and physical properties of soils (10).**

---

**K Values for Cohesive Soils**

---

$$\begin{aligned} \bullet \text{ } \log K_1 = & 19.813 - 0.045 (W_{opt}) - 0.131 (W_s) - 9.171 \left( \frac{\gamma_{ds}}{\gamma_{dmax}} \right) \\ & + 0.037 (\% \text{ Silt}) + 0.015 (LL) - 0.016 (PI) \\ & - 0.021 (\% \text{ Swell}) - 0.052 (\gamma_{dmax}) + 0.00001 [(P_{40})(S)] \end{aligned}$$

---


$$R^2 = 0.95$$

$$\bullet \text{ } K_2 = 0$$


---

$$\begin{aligned} \bullet \text{ } K_3 = & 10.274 - 0.097 (W_{opt}) - 1.06 \left( \frac{W_s}{W_{opt}} \right) - 3.471 \left( \frac{\gamma_{ds}}{\gamma_{dmax}} \right) \\ & + 0.0088 (P_{40}) - 0.0087 (PI) + 0.014 (\% \text{ Shrinkage}) \\ & - 0.046 (\gamma_{dmax}) \end{aligned}$$

---


$$R^2 = 0.94$$


---

**Table 6. Relationships previously developed between the nonlinear elastic coefficient/exponents and physical properties of soils (10) (continued).**

**K Values for Noncohesive Soils**

---


$$\bullet \text{Log}K_1 = 3.479 - 0.07(W_a) + 0.24 \left( \frac{W_s}{W_{opt}} \right) + 3.681 \left( \frac{\gamma_s}{\gamma_{dmax}} \right) + 0.011(\% \text{ Silt})$$

$$+ 0.006(\% \text{ Clay}) - 0.025(\% \text{ Swell}) - 0.039(\gamma_{dmax}) + 0.004$$

$$\left[ \frac{(\% \text{ Swell})^2}{(\% \text{ Clay})} \right] + 0.0023 \left[ \frac{\gamma_{dmax}^2}{P_{40}} \right]$$

$R^2 = 0.94$

---


$$\bullet K_2 = 6.044 - 0.053(W_{opt}) - 2.076 \left( \frac{\gamma_{ds}}{\gamma_{dmax}} \right) + 0.0053(S) - 0.0056$$

$$(\% \text{ Clay}) + 0.0088(\% \text{ Swell}) - 0.0069(\% \text{ Shrinkage}) - 0.027(\gamma_{dmax})$$

$$+ 0.012(CBR) + 0.003 \left[ \frac{(\% \text{ Swell})^2}{\% \text{ Clay}} \right] - \left[ \frac{(\% \text{ Swell} + \% \text{ Shrinkage})}{\% \text{ Clay}} \right]$$

$R^2 = 0.96$

---


$$\bullet K_3 = 3.752 - 0.068(W_s) + 0.309 \left( \frac{W_s}{W_{opt}} \right) - 0.006(\% \text{ Silt}) + 0.0053$$

$$(\% \text{ Clay}) + 0.026(\% \text{ Shrinkage}) - 0.033(\gamma_{dmax}) - 0.0009 \left[ \frac{(\% \text{ Swell})^2}{(\% \text{ Clay})} \right]$$

$$+ 0.00004 \left[ \frac{S^2}{\% \text{ Shrinkage}} \right] - 0.0026 \left[ \frac{CBR}{(\% \text{ Shrinkage})} \right]$$

$R^2 = 0.87$

**Table 6. Relationships previously developed between the nonlinear elastic coefficient/exponents and physical properties of soils (10) (continued).**

where:	$W_{opt}$	=	optimum water content
	$W_s$	=	water content of the test specimen
	$\gamma_{ds}$	=	dry density of the test specimen
	$\gamma_{dmax}$	=	maximum dry unit weight of soil
	% silt	=	percentage of silt
	LL	=	liquid limit of soil
	PI	=	plasticity index of soil
	% swell	=	percentage swell of the soil
	$P_{40}$	=	percentage passing the No. 40 sieve
	S	=	degree of saturation
	% shrinkage	=	percentage of shrinkage of the soil
	% clay	=	percentage of clay

---

Results from this study are summarized in table 7, which identifies those parameters which were found to be significantly correlated to each of the K values. Even though correlations do exist, the results were not very promising in terms of estimating the K values from the physical properties at a reasonable confidence level. Potential reasons for these poor correlations may be related to the physical property testing and repeated-load triaxial testing of different soil samples, retaining the undisturbed soil samples in thin-walled shelly tubes for nearly 2 years prior to removal and testing, only one test specimen per section end (no replication), recompacting some of the materials for testing which may have changed some of the physical features of the materials during the re-compaction process, and the variability associated with the repeated-load testing as compared to some of the other physical property test results.

This study attempted to replicate the procedure used by Santha in 1994 (10) using data from the GPS sections in the LTPP data base. Unfortunately, the LTPP data base does not contain data for percent swell, percent shrinkage, and others that were included in the Santha study. Using those properties that were available for all of the sites, both linear and nonlinear regression analyses were performed for each K value for granular bases and clay, silt, sand, and gravel subgrades. These results indicated that the correlation between the K values and the physical parameters contained in the LTPP data base was poor, at best.

The data were further divided into samples that were recompacted and those that were not (Shelby and Bulk) to improve upon the correlation. Unfortunately, these data sets were too limited as to the number of observations for a statistically meaningful regression. Although the correlation significantly improved, the reasons for the improvement are inconclusive and debatable. Obviously, a greater correlation may have resulted because of the smaller sample size. On the other hand, the recompacted test specimens (undisturbed versus recompacted) were more highly correlated to the physical properties, because the materials recovered for physical property and repeated-load testing were from the same bulk sample. Samples recovered from Shelby tubes, may not have been the same as the materials used for physical property testing (i.e., soils taken from different depths).

A nonlinear analysis was attempted to provide an improved model for the calculation of K values using the physical parameters provided by the LTPP data base. The same partitioning of the data used for the linear analysis was used for the nonlinear analysis. The results from our linear regression provided insight on the weight or significance of the various physical parameters. In all cases, the percent of optimum moisture content was the most significant value in obtaining K



**Table 7. Relationships or correlations between the nonlinear elastic coefficients/exponents using equation 5 and physical properties of soils obtained from the LTPP data base.**

---

**K Values for Clay-Type Soils:**

$$\bullet \text{Log}K_1 = 17.662 - 0.2647(W_{opt}) - 0.4430(W_s) + 2.6732 \left( \frac{\gamma_{ds}}{\gamma_{dmax}} \right) + 0.1320(\% \text{ Silt}) + 0.6422(LL) - 0.3742(PI) - 0.1963(\gamma_{dmax}) - 0.00087(P_{40})(S)$$

$R^2 = 1.0$   
Std. Error =  $8.5 \times 10^{-14}$

---


$$\bullet K_2 = 0$$

---


$$\bullet K_3 = 3.3673 - 0.01464(W_{opt}) - 1.7371 \left( \frac{W_s}{W_{opt}} \right) - 0.1264 \left( \frac{\gamma_{ds}}{\gamma_{dmax}} \right) - 0.02400(P_{40}) + 0.03483(PI) + 0.001779(\gamma_{dmax})$$

$R^2 = 0.81$   
Std. Error = 0.115

---

where:

$W_{opt}$	=	Optimum water content
$W_s$	=	Water content of the test specimen (or soil)
$\gamma_{ds}$	=	Dry density of the test specimen (or soil)
$\gamma_{dmax}$	=	Maximum dry unit weight of soil
% silt	=	Percentage of silt
LL	=	Liquid limit
PI	=	Plasticity index
$P_{40}$	=	Percentage passing the No. 40 sieve
S	=	Degree of Saturation

**Table 7. Relationships or correlations between the nonlinear elastic coefficients/exponents using equation 5 and physical properties of soils obtained from the LTPP data base (continued).**

---

**K Values for Silt-Type Soils:**

$$\bullet \text{Log}K_1 = 1.9823 + 0.01394(W_s) - 0.5934 \left( \frac{W_s}{W_{opt}} \right) + 0.1500 \left( \frac{\gamma_{ds}}{\gamma_{dmax}} \right) + 0.00831(\gamma_{dmax}) + 0.000334 \left( \frac{\gamma_{dmax}^2}{P_{40}} \right)$$

$R^2 = 0.810$   
Std. Error = 0.112

---

$$\bullet K_2 = 6.4676 - 0.0861(W_{opt}) - 0.5458 \left( \frac{\gamma_{ds}}{\gamma_{dmax}} \right) + 0.00800(S) - 0.04226(\gamma_{dmax})$$

$R^2 = 0.688$   
Std. Error = 0.117

---

$$\bullet K_3 = 5.7391 + 0.07929(W_s) - 1.1778 \left( \frac{W_s}{W_{opt}} \right) + 0.008037(\%Silt) + 0.04549(\gamma_{dmax})$$

$R^2 = 0.568$   
Std. Error = 0.137

---

**Table 7. Relationships or correlations between the nonlinear elastic coefficients/exponents using equation 5 and physical properties of soils using data from the LTPP data base (continued).**

---

**K Values for Sand-Type Soils:**

$$\bullet \text{ Log } K_1 = 2.7602 - 0.00702(W_s) - 0.08076 \left( \frac{W_s}{W_{opt}} \right) + 0.05750 \left( \frac{\gamma_{ds}}{\gamma_{dmax}} \right) + 0.000279(\gamma_{dmax})$$

$$R^2 = 0.160$$

$$\text{Std. Error} = 0.164$$

---


$$\bullet K_2 = 0.7386 - 0.01497(W_{opt}) + 0.3916 \left( \frac{\gamma_{ds}}{\gamma_{dmax}} \right) - 0.00604(S) - 0.00157(\gamma_{dmax})$$

$$R^2 = 0.2259$$

$$\text{Std. Error} = 0.167$$

---


$$\bullet K_3 = -0.04978 - 0.0092(W_s) + 0.008377 \left( \frac{W_s}{W_{opt}} \right) - 0.0052(\% \text{ Silt}) + 0.000487(\gamma_{dmax})$$

$$R^2 = 0.304$$

$$\text{Std. Error} = 0.112$$


---

**K Values for Gravel-Type Soils:**

Unavailable due to insufficient data in the LTPP data base for these type soils.

---

values. The model used for the nonlinear regression contained the percent optimum moisture content value as shown below:

$$K = \alpha \left( \frac{W_s}{W_{opt}} \right)^\beta$$

The K values predicted from the nonlinear analysis were compared to the actual K values. This comparison indicated that there was too much scatter in the data to have meaningful results. The nonlinear analysis, when convergence was achieved, always predicted the mean value. This is an indication that the results from the nonlinear analysis are invalid.

Use of the relationships given in table 7 can result in large errors in estimating the resilient moduli compared to the values from laboratory resilient modulus testing. Therefore, it is recommended that repeated-load laboratory test results be used in determining resilient modulus for design purposes. The equations shown in tables 6 and 7 should only be used for planning purposes and adjusting the measured moduli to account for seasonal variations, such as variations in moisture content of subgrade soils throughout the year.

**Observation:** Using the LTPP data base, poor correlations were found between the physical properties of the soil and the nonlinear elastic coefficients and exponents of equation 5. For pavement design, repeated-load triaxial comparison tests should be performed to determine the resilient modulus of pavement materials and subgrade soils. Physical properties (such as moisture content), however, can be used to make adjustments to the laboratory measured moduli to account for seasonal variations.

#### **4. DETERMINATION OF LAYERED ELASTIC MODULI - BACKCALCULATED FROM DEFLECTION BASINS**

##### **4.1 Application and Use of Deflection Measurements**

The use of nondestructive deflection testing is an integral part of the AASHTO structural evaluation and rehabilitation design process. Although nondestructive testing has been used for a long time by the pavement industry, there has been an explosion within the last decade in the use of this equipment for pavement structural evaluation and rehabilitation design. One reason for this increase in use is that it has become essential from the engineer's point of view to know the behavior or response of the pavement structure and subgrade and the interaction of the various layers under wheel loads. Results of deflection tests have been and are being utilized in the following areas:

1. Assistance in the location of borings along existing roadways so that the maximum amount of material and subsurface data can be obtained with a limited number of bore holes . This is achieved by strategically locating cores and borings in areas with statistically different measured deflection basins.
2. Determination of the structural capacity and remaining life of existing pavements based on deflection criteria developed from performance data. This also includes determination of structural overlay thickness design requirements of existing roadways to reduce the measured deflection below some critical value, and determining effective or equivalent surface layer thicknesses or moduli for cracked pavements.
3. Backcalculation of layer moduli (Young's Modulus) to identify material/layer weaknesses within the pavement structure and to assist the engineer in selecting a reliable rehabilitation alternative to correct some surface distress or pavement deficiency.
4. Void detection and location under PCC pavements and as a quality control check for filling voids or "mudjacking" PCC pavements.
5. Determination of load transfer efficiency of joints in PCC pavements and shear transfer across cracks in asphalt concrete pavements for reflection cracking design requirements.

As part of the ongoing LTPP Program that was originally set up through SHRP, deflection measurements with the FWD are being made on all of the GPS (including the seasonal sites) and Special Pavement Study (SPS) projects across the U.S. These deflection basins were used in this research study to determine elastic layer moduli for the pavement materials and subgrade through the use of backcalculation techniques. These data represent a critical and necessary part of the data base.

**4.1.1 Data Consistency and Accuracy.** Data consistency and accuracy are very important when comparing deflection data from one region or pavement to another, and certainly when trying to distinguish or identify layer condition/features for predicting pavement performance. Several agency procedures and programs (11) were developed under SHRP to ensure that the deflection data stored in the LTPP NIMS were uniform and accurate. The following lists and briefly identifies four of those software programs that are currently in use and were used to collect and process the first round of deflection data.

- **FWDCAL** is the software designed to do calibration checks and adjustments for the geophones used to measure deflection in the FWD test system. This ensures, on a monthly basis, that the sensors are performing within specified tolerances with respect to each other.
- **FWDREFCAL** is a program developed as a means of doing a reference calibration of both the load cell and the geophones within the FWD test system. FWDREFCAL is performed on the FWD's annually. This consists of checking the geophones against a known value (calibrated linear voltage displacement transducer (LVDT) is used in this system) and checking the load cell against another referenced load cell developed by SHRP/LTPP. The purpose of this annual calibration is to ensure that the load-cell system and all the sensors within the FWD test system are within specifications based on a comparison with a known reference load cell and LVDT. This check ensures that the load recorded by the load cell is accurate and that the movement registered by the sensors is also accurate when traced back to a known standard.
- **FWDFSCAN** is the initial check on the FWD data run in the office after it is received from the field. FWDFSCAN was developed by SHRP/LTPP to check the FWD data for completeness and readability. This software ensures that data have been collected in the proper format as defined in the LTPP User's Guide for FWD testing.

- **FWDCHECK** (12) is intended to check the FWD data files for section homogeneity, non-representative test pit in section data and general reasonableness of the structural capacity of the test section being analyzed. The program automatically generates an output files that summarizes the results of the checking process. Preliminary data analysis within the FWDCHECK software includes normalization of the loading to provide a uniform set of data for comparison purposes, temperature correction of the normalized deflections are also computed and various corrected normalized deflection statistics are calculated for the pavement section being analyzed.

**4.1.2 Deflection Data Interpretation.** One of the more common analysis methods of deflection data is to backcalculate material response parameters for each layer within the pavement structure from the deflection basin measurements. These methods and programs can be grouped into four basic categories. These categories are:

1. Static (Load Application) - Linear (Material Characterization) Methods
2. Static (Load Application) - Nonlinear (Material Characterization) Methods
3. Dynamic (Load Application) - Linear (Material Characterization) Methods
4. Dynamic (Load Application) - Nonlinear (Material Characterization) Methods.

Some of the software that has been used to backcalculate layer modulus values over the past several years include BISDEF, CHEVDEF, ELMOD, ELSDEF, EVERCALC, ISSEM4, MODCOMP, MODULUS and WESDEF. At present, interpretation of deflection basin test results is usually performed with static-linear analyses. Dynamic analyses of deflection basins are available (13, 14), but are not in common use by the industry. Although many of the software packages have similarities, the results generated from the same set of data by various programs can be different. These differences are a result of the type of iteration scheme used and the modulus calculation routine employed (15). Moduli can be determined by either backcalculation (16) or forward (17) calculation schemes. As for the deflection testing devices, standardization of analysis procedures is also a key topic within the industry. Presently, the American Society for Testing and Materials (ASTM) has under ballot a procedure (D5858) for analyzing deflection basin test results to determine layer elastic moduli (18).

Most of the backcalculation procedures in use today are based on elastic layer theory to calculate Young's Modulus (modulus of elasticity) for each structural layer within the pavement, such that the difference between the measured and predicted basins is minimal. Some of the programs

based on elastic layer theory have been modified to account for the viscoelastic and/or nonlinear behavior of materials. SHRP, as well as others, studied and evaluated many of these backcalculation procedures to select one method for use in characterizing the subgrade and other pavement layers to evaluate the performance of flexible and rigid pavements. The program entitled "MODULUS 4.0" (19) was selected for flexible and composite pavements; whereas, a new procedure was developed for rigid pavements, as part of the SHRP P-020 Data Analysis Project (3).

Most of these programs are limited by the number of layers within the pavement and the thickness of those layers, and are based on linear elastic materials assumptions. As such, any discontinuity cannot be physically represented by the model. Thus, the calculated layer moduli represent "effective" values that take into account anomalies (such as cracks, voids, etc.) thickness variations within each layer, and a combination of layers with similar materials or thin layers with thick layers. Layer thickness is an extremely important feature when backcalculating layer moduli from deflection basin test results. A 10-percent difference in thickness can result in more than a 20-percent change in the calculated modulus. Therefore, using accurate layer thicknesses becomes critically important. For this reason, only the deflection basins measured at the test pits and other material sampling locations were initially used to backcalculate layer moduli.

The use of deflection testing and analysis methods to evaluate the pavement's response and to determine layer condition or critical properties of that layer has met with varying degrees of success; generally less than that desired (20). In general, there has been reasonable success or confidence in evaluating the modulus of the supporting subgrade soils; whereas, determining the modulus of the pavement layers, especially the surface layers has been suspect. Unfortunately, most of these analysis procedures become less reliable or unstable as the layer evaluation progresses from the subgrade to the surface. In fact, the surface layer modulus that is calculated from the measured deflection basin is normally considered poorly defined by deflection tests.

More importantly, these existing procedures typically are not sensitive enough to adequately determine the condition of each individual pavement layer, especially in relation to the effect that distresses and other pavement features have on pavement structural response to applied wheel loads. This result has spawned the development of dynamic analysis tools and use of other NDT techniques (such as wave propagation) for improving on the accuracy of these predictions or calculations, as compared to moduli measurements made in the laboratory. Two dynamic linear backcalculation programs that have been developed are UTFWIBM (13) and SCALPOT (14),



but both have had very limited use. Thus, for purposes of this research study, MODULUS 4.0 (21) and 4.2 (16) and WESDEF (22) (all based on elastic layer theory) were used to backcalculate the modulus of each pavement structural layer, including the subgrade from the deflection basin measurements.

## **4.2 Backcalculation Process**

The backcalculation process used and results obtained are reported by Von Quintus and Killingsworth (15) and were used in all data analysis topics included within this report. In general, backcalculation of layer moduli was only performed during this study for those GPS sites that had large error terms (greater than 2.0-percent error per sensor) resulting from the original SHRP study (23, 24, 25). ASTM D5858 (Standard Guide for Calculating In Situ Equivalent Elastic Moduli of Pavement Materials Using Layered Elastic Theory) was used as an initial guide for re-backcalculating the problem sections or sites with high error terms. The following briefly summarizes the steps involved in the backcalculation process:

1. Review the measured deflection basins to ensure that the deflections decrease consistently with those sensors farther from the applied load. This step is discussed further in subsection 4.2.1.
2. Review the soils and conditions identified in the 6-m (20-ft) shoulder boring, as well as from the shelly tubes. Separate significantly different subgrade soils or subsurface conditions into different layers (i.e., above and below any water table and at a rigid layer or boundary condition). This step is discussed further in subsection 4.2.2.
3. Review the pavement structure used in the original SHRP backcalculation process and ensure that the layered structure is consistent with the test results and material definitions. Recombine and/or separate layers, if necessary, to decrease the error term. This step is also discussed further in subsection 4.2.2.
4. Identify potential problem layers included in the structure. For example, weak soils above stiffer soils, sandwich sections (a soft layer of material between two strong materials), and thin and thick layers relative to the adjacent layers. This step is discussed further in subsection 4.2.3.

5. Review the moduli ratios between adjacent unbound layers to identify unrealistic or improbable conditions (i.e., high moduli ratios causing large tensile stresses at the bottom of the unbound layer). This step is also discussed further in subsection 4.2.3.

After completing the new backcalculation runs and determining if the error terms were reduced, the resulting layer moduli were reviewed for reasonableness. For those basins that consistently hit the upper limit set for a particular material, the structure was again reviewed in an attempt to reduce the error term, while maintaining reasonable values. Values that hit the lower limit were considered less critical and the lower limit was further reduced. Low modulus values may be reasonable, because of contamination of underlying materials, the presence of cracks or internal damage (such as stripping), and/or the weakening of some unbound materials with an increase in moisture and/or decrease in density.

**4.2.1 "Problem" Deflection Basins.** For some of the deflection basins, large error terms (significantly exceeding 2½ percent per sensor) were found using the MODULUS 4.0 and 4.2 and WESDEF programs to backcalculate layer moduli, regardless of the layer combination used to represent the GPS section ends. As a result, a study was initiated to identify the reason(s) for the difference between predicted versus observed deflection basins.

In reviewing the backcalculated layer moduli results, it was noted that many of the GPS sites with the large error terms had deflection basins which are not characteristic of elastic layered theory. These deflection basins are termed "problem" basins. For example, several sections were found to have increasing or identical deflection measurements with increasing sensor number. These sections generally did not provide reasonable results in the backcalculation process, because the theory will not allow a calculated deflection basin to fit this type of measured basin.

To evaluate and compare the different shapes or types of deflection basins to those calculated with elastic layered theory, all basins were first normalized to the deflection measured at sensor number 1, which is directly under the load (i.e., see figure 18). These normalized deflection basin data were divided into four categories or types of basins. These different categories are shown in figures 18 through 21 and defined below.

- Figure 18 shows typical normalized deflection basins where the error terms were very low (generally less than 1½-percent error per sensor) for both PCC- and asphalt concrete-surfaced pavements.

- Figure 19 shows a Type I deflection basin. For this deflection basin, the deflections measured at most of the sensors are greater than the deflection measured by sensor 1, directly under the load. The Type I deflection basins generally had the greatest error terms, as one might expect.
- Figure 20 shows a Type II deflection basin, which included a significant decrease in measured deflections between two adjacent sensors. Depending upon the magnitude of this drop or break in the deflection basin, some of the error terms are large, while others with the smallest differences are close to a value of 2½-percent error per sensor.
- Figure 21 shows a Type III deflection basin. For these basins, the deflection measured at a further, but adjacent sensor was found to be greater than the deflection closer to the load. Some of these deflection basins had error terms ranging from greater than 10 percent to values less than 2½-percent error per sensor. The error obviously depended upon the magnitude of the increase in deflection between two adjacent sensors.

Table 8 summarizes the numbers of sites and section ends which were found to have a Type I, II, or III deflection basin. The following summarizes the number of section ends by pavement types that were found to be characteristic of a "problem" deflection basin.

Pavement Type	Type of Problem Deflection Basin		
	I (Figure 19)	II (Figure 20)	III (Figure 21)
Total Number of GPS Section Ends	71	170	42
PCC-Surfaced Section Ends	65	36	39
Asphalt Concrete-Surfaced Section Ends	6	134	3

As shown, there are a substantial number of section ends with problem deflection basins. In fact, approximately 18 percent of the section ends were found to have one of these problem deflection basins. More importantly, it is interesting to note the type of pavement that has the characteristics of these problem deflection basins. For example, over 90 percent of the section ends that have a Type I and III deflection basin were PCC-surfaced pavements. It is believed that these problem deflection basins may be characteristic of those areas with voids, a loss of

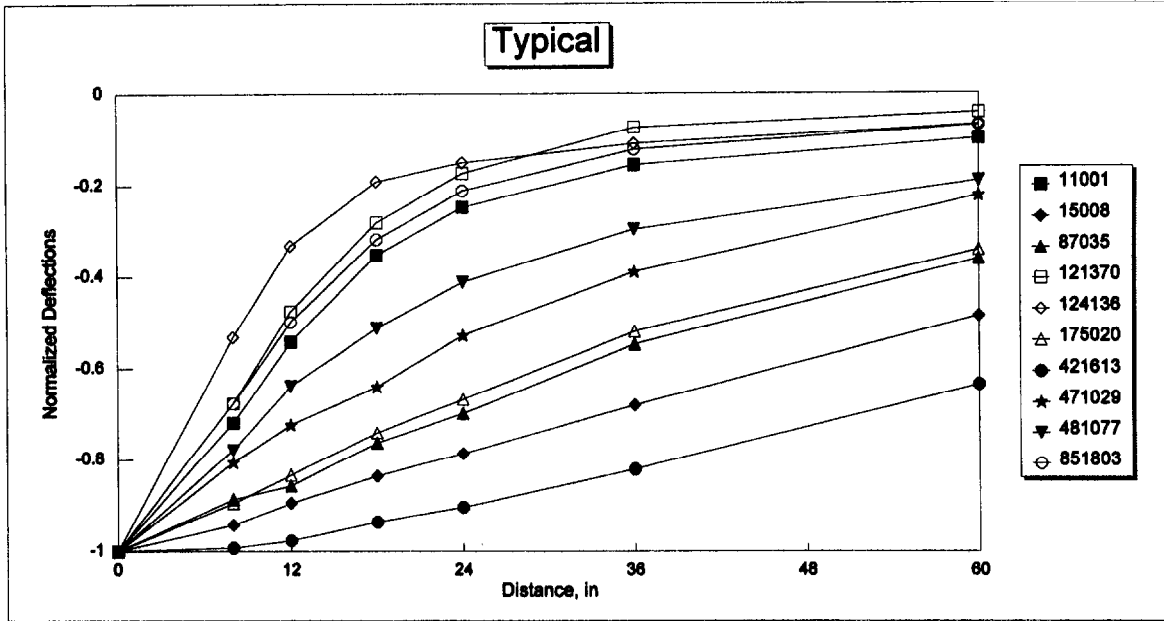


Figure 18. Typical normalized deflection basins with low error terms (i.e., the use of elastic layer theory is applicable for analyzing these basins).

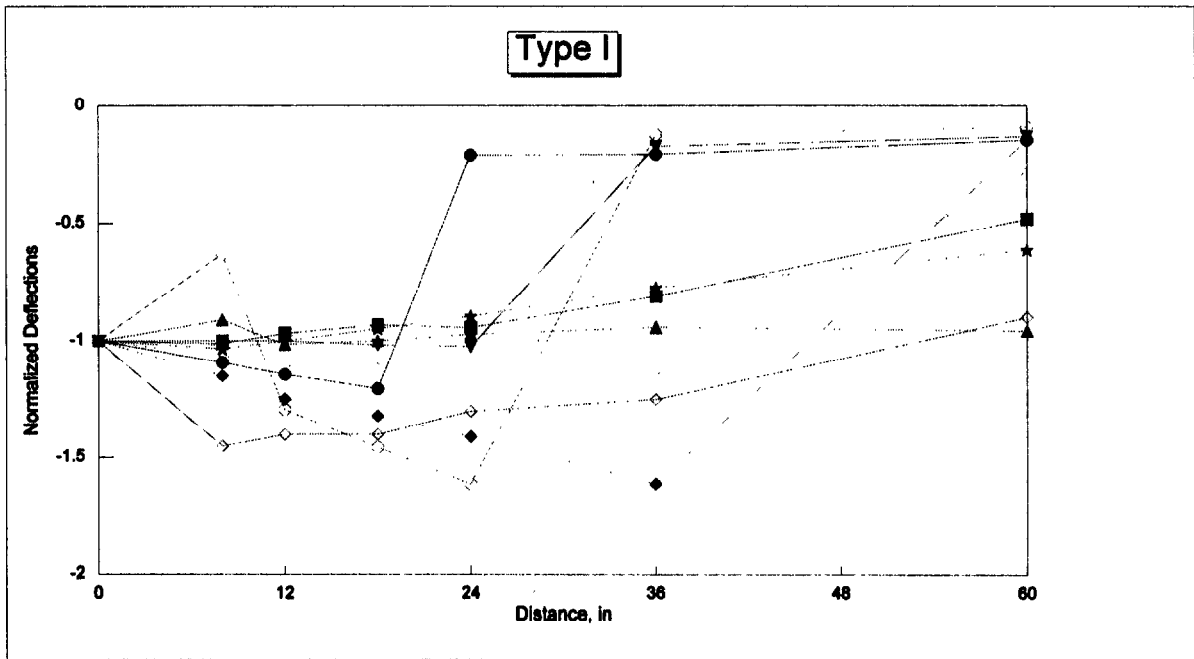
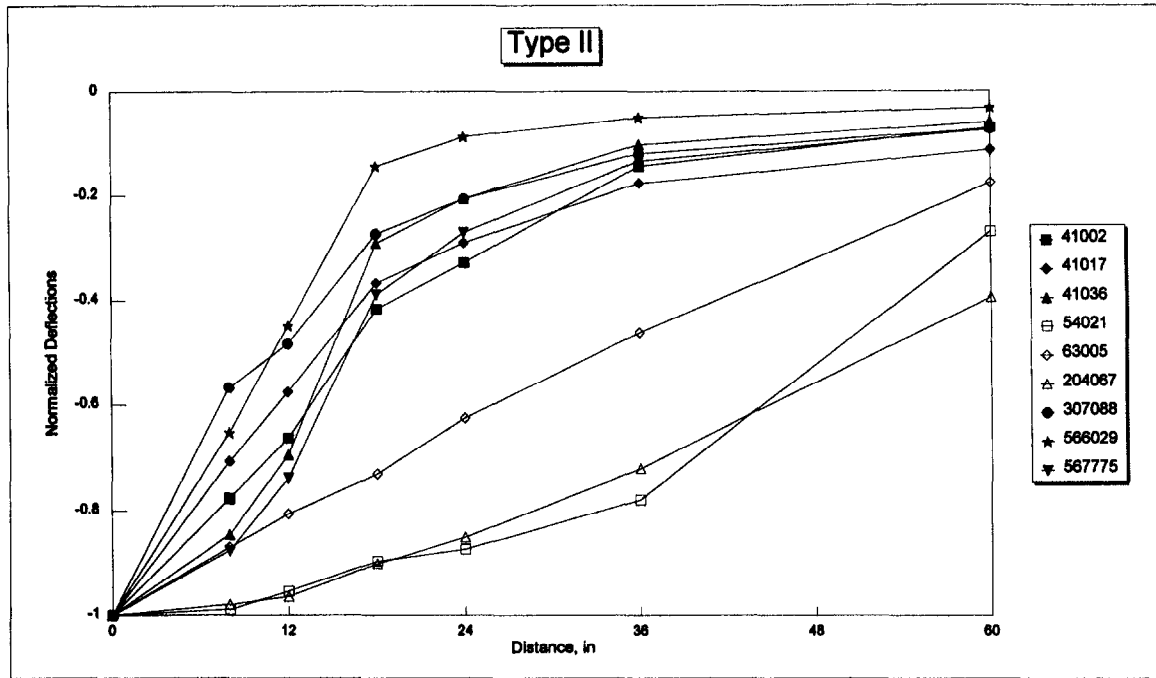
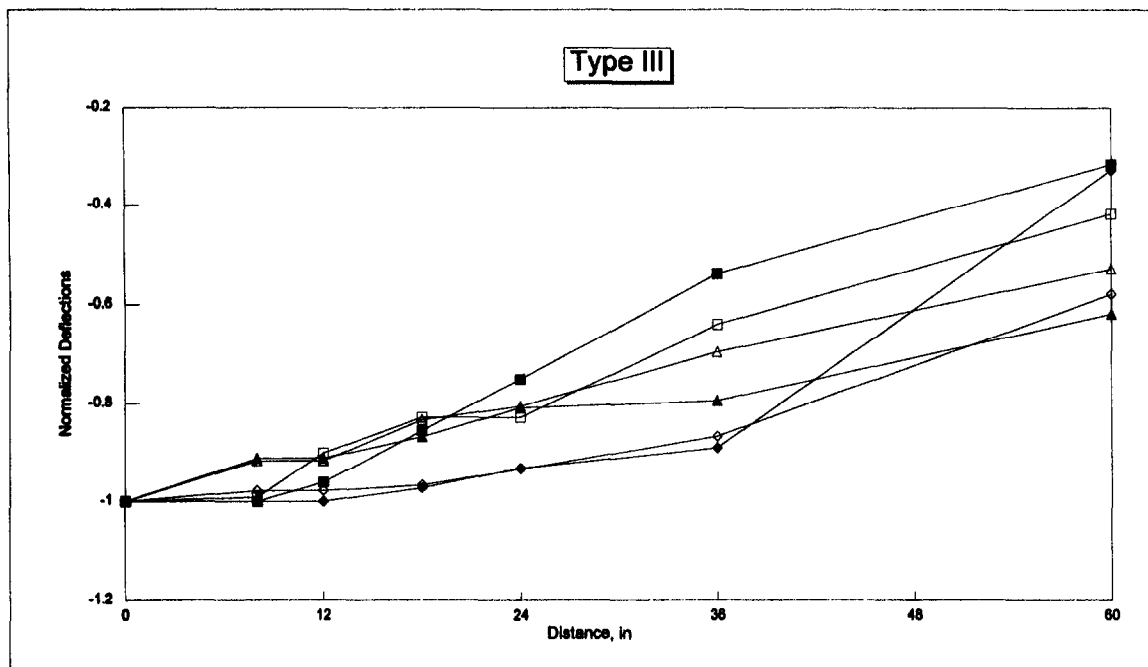


Figure 19. Type I normalized deflection basins.



**Figure 20. Type II normalized deflection basins.**



**Figure 21. Type III normalized deflection basins.**

**Table 8. Listing of sections with problem deflection basins that are not compatible with elastic layer theory.**

Type of Deflection Basin	Sensors Where Problem Characteristics Were Measured	GPS Experiment No.	Pavement Surface Type	State	Section ID No.	Section End
I	2,5	3	JPCP	AR	053011	Appr.
I	5	3	JPCP	AR	053011	Leave
I	3,4	2	AC/TB	CA	062053	Appr.
I	3	3	JPCP	CA	063010	Appr.
I	3	3	JPCP	CA	063010	Leave
I	2-6	3	JPCP	CA	063013	Appr.
I	2-6	3	JPCP	CA	063013	Leave
I	3	3	JPCP	CA	063019	Appr.
I	3	3	JPCP	CA	063019	Leave
I	2-5	3	JPCP	CA	063030	Appr.
I	2	3	JPCP	CA	063042	Appr.
I	3-6	3	JPCP	CA	063042	Leave
I	3,4	3	JPCP	CA	067456	Appr.
I	3,4	3	JPCP	CA	067456	Leave
I	2	7A	AC/PCC	CO	087035	Appr.
I	2,3	9	PCC/PCC	CO	089019	Leave
I	2,3	3	JPCP	FL	123804	Leave
I	2-7	3	JPCP	FL	124057	Leave
I	2	3	JPCP	FL	124109	Leave
I	2-5	3	JPCP	FL	124138	Appr.
I	1	1	HMAC	FL	129054	Leave
I	2	3	JPCP	GA	133007	Appr.
I	2-5	3	JPCP	GA	133011	Appr.
I	3	1	HMAC	ID	161007	Leave
I	2	1	HMAC	ID	161010	Appr.

**Table 8. Listing of sections with problem deflection basins that are not compatible with elastic layer theory (continued).**

Type of Deflection Basin	Sensors Where Problem Characteristics Were Measured	GPS Experiment No.	Pavement Surface Type	State	Section ID No.	Section End
I	2	5	CRCP	IN	185518	Leave
I	2-5	3	JPCP	IA	193006	Appr.
I	3	3	JPCP	IA	193033	Appr.
I	2,3,4	3	JPCP	KY	213016	Appr.
I	2,3	4	JRCP	LA	224001	Appr.
I	2	4	JRCP	MI	264015	Leave
I	2,3	9	PCC/PCC	MN	276300	Leave
I	2-6	3	JPCP	MS	283018	Leave
I	2-5	9	PCC/PCC	MS	289030	Appr.
I	2-6	9	PCC/PCC	MS	289030	Leave
I	2-6	3	JPCP	NB	313018	Appr.
I	2-6	3	JPCP	NB	313018	Leave
I	2	3	JPCP	NV	323010	Appr.
I	3	3	JPCP	NC	373816	Appr.
I	2	5	CRCP	NC	375826	Leave
I	2	9	PCC/PCC	OK	404155	Appr.
I	2-4	3	JPCP	OK	404160	Leave
I	2,3	5	CRCP	OK	404166	Leave
I	2,3	5	CRCP	OR	415005	Appr.
I	2,3	5	CRCP	OR	415006	Appr.
I	2	9	PCC/PCC	PA	421627	Leave
I	2-6	3	JPCP	SD	463013	Appr.
I	3,4	3	JPCP	SD	463053	Appr.
I	2,5	3	JPCP	SD	466600	Appr.
I	5	3	JPCP	TX	483003	Appr.
I	2	3	JPCP	TX	483003	Leave
I	2-4	2	AC/TB	TX	483679	Appr.

**Table 8. Listing of sections with problem deflection basins that are not compatible with elastic layer theory (continued).**

Type of Deflection Basin	Sensors Where Problem Characteristics Were Measured	GPS Experiment No.	Pavement Surface Type	State	Section ID No.	Section End
I	3	5	CRCR	TX	483719	Leave
I	4	9	PCC/PCC	TX	483845	Leave
I	2,3	4	JRCP	TX	484152	Appr.
I	2,5	5	CRCP	TX	485024	Appr.
I	2	5	CRCP	TX	485284	Appr.
I	5	5	CRCP	TX	485284	Leave
I	2	5	CRCP	TX	485301	Leave
I	2,3	3	JPCP	UT	493011	Appr.
I	2,3	5	CRCP	VA	515010	Appr.
I	2-5	3	JPCP	WA	533011	Appr.
I	2-6	3	JPCP	WA	533011	Leave
I	2	3	JPCP	WA	533014	Appr.
I	3-6	3	JPCP	WA	533019	Appr.
I	3-6	3	JPCP	WA	537409	Appr.
I	2	3	JPCP	WA	537409	Leave
I	2-7	4	JRCP	WV	544004	Appr.
I	2-4	3	JPCP	WI	553016	Leave
I	2-6	3	JPCP	WI	553019	Leave
I	2,3	3	JPCP	QB	893001	Leave
II	3-4	5	CRCP	AL	013998	Appr.
II	3-4-5	1	HMAC	AZ	041002	Appr.
II	3-4-5	1	HMAC	AZ	041002	Leave
II	3-4-5	1	HMAC	AZ	041007	Appr.
II	3-4-5	1	HMAC	AZ	041007	Leave
II	3-4-5	1	HMAC	AZ	041015	Appr.
II	3-4-5	1	HMAC	AZ	041015	Leave
II	3-4-5	1	HMAC	AZ	041017	Leave



**Table 8. Listing of sections with problem deflection basins that are not compatible with elastic layer theory (continued).**

Type of Deflection Basin	Sensors Where Problem Characteristics Were Measured	GPS Experiment No.	Pavement Surface Type	State	Section ID No.	Section End
II	2-3-4	1	HMAC	AZ	041018	Appr.
II	2-3-4	1	HMAC	AZ	041018	Leave
II	3-4-5	1	HMAC	AZ	041021	Appr.
II	3-4-5	1	HMAC	AZ	041021	Leave
II	2-3-4	1	HMAC	AZ	041022	Leave
II	2-3-4	1	HMAC	AZ	041024	Leave
II	2-3-4	1	HMAC	AZ	041025	Appr.
II	2-3-4	1	HMAC	AZ	041025	Leave
II	2-3-4	1	HMAC	AZ	041034	Appr.
II	3-4-5	1	HMAC	AZ	041034	Leave
II	3-4-5	1	HMAC	AZ	041036	Appr.
II	3-4-5	1	HMAC	AZ	041036	Leave
II	3-4-5	1	HMAC	AZ	041037	Appr.
II	3-4-5	1	HMAC	AZ	041037	Leave
II	2-3-4-5	2	AC/TB	AZ	041065	Appr.
II	2-3-4-5	2	AC/TB	AZ	041065	Leave
II	3-4-5	6A	AC/AC	AZ	046053	Appr.
II	3-4-5	6A	AC/AC	AZ	046053	Leave
II	3-4-5	6A	AC/AC	AZ	046054	Appr.
II	3-4-5	6A	AC/AC	AZ	046054	Leave
II	2-3-4-5	6A	AC/AC	AZ	046055	Appr.
II	2-3-4-5	6A	AC/AC	AZ	046055	Leave
II	3-4-5	6A	AC/AC	AZ	046060	Appr.
II	3-4-5	6A	AC/AC	AZ	046060	Leave
II	2-3-4	2	AC/TB	AZ	052042	Appr.
II	6-7	4	JRCP	AR	054021	Leave
II	6-7	5	CRCP	AR	055803	Appr.

**Table 8. Listing of sections with problem deflection basins that are not compatible with elastic layer theory (continued).**

Type of Deflection Basin	Sensors Where Problem Characteristics Were Measured	GPS Experiment No.	Pavement Surface Type	State	Section ID No.	Section End
II	2-3-4	5	CRCP	AR	055805	Appr.
II	2-3-4-5	9	PCC/PCC	AR	059100	Leave
II	6-7	2	AC/TB	CA	062004	Leave
II	2-3-4	2	AC/TB	CA	062038	Appr.
II	2-3-4	2	AC/TB	CA	062051	Appr.
II	2-3-4	2	AC/TB	CA	062051	Leave
II	6-7	3	JPCP	CA	063005	Appr.
II	2-3	3	JPCP	CA	063021	Leave
II	3-4-5	2	AC/TB	CA	067452	Leave
II	2-3-4	2	AC/TB	CA	067491	Appr.
II	2-3-4	2	AC/TB	CA	068150	Leave
II	2-3-4	1	HMAC	CA	068153	Leave
II	1-2-3	1	HMAC	CA	068534	Leave
II	3-4-5	1	HMAC	CO	081029	Appr.
II	3-4-5	1	HMAC	CO	081029	Leave
II	3-4-5	1	HMAC	CO	081047	Appr.
II	3-4-5	1	HMAC	CO	081047	Leave
II	3-4-5	1	HMAC	CO	081053	Appr.
II	3-4-5	1	HMAC	CO	081053	Leave
II	3-4-5	1	HMAC	CO	081057	Appr.
II	3-4-5	1	HMAC	CO	081057	Leave
II	3-4-5	2	AC/TB	CO	082008	Appr.
II	3-4-5	2	AC/TB	CO	082008	Leave
II	3-4-5	3	JPCP	CO	083032	Leave
II	3-4-5-6	6A	AC/AC	CO	086002	Appr.
II	3-4-5	6A	AC/AC	CO	086002	Leave
II	3-4-5	6A	AC/AC	CO	086013	Appr.

**Table 8. Listing of sections with problem deflection basins that are not compatible with elastic layer theory (continued).**

Type of Deflection Basin	Sensors Where Problem Characteristics Were Measured	GPS Experiment No.	Pavement Surface Type	State	Section ID No.	Section End
II	3-4-5	6A	AC/AC	CO	086013	Leave
II	2-3-4-5	7A	AC/PCC	CO	087036	Leave
II	3-4-5	3	JPCP	CO	087776	Appr.
II	3-4-5	3	JPCP	CO	087776	Leave
II	3-4-5	1	HMAC	CO	087780	Appr.
II	3-4-5	1	HMAC	CO	087780	Leave
II	3-4-5	2	AC/TB	CO	087781	Appr.
II	3-4-5	2	AC/TB	CO	087781	Leave
II	2-3-4-5	6A	AC/AC	CO	087783	Appr.
II	3-4-5	6A	AC/AC	CO	087783	Leave
II	5-6-7	3	JPCP	FL	124109	Appr.
II	2-3-4	1	HMAC	FL	124154	Appr.
II	2-3-4	1	HMAC	FL	124154	Leave
II	5-6-7	3	JPCP	GA	133017	Leave
II	5-6-7	2	AC/TB	GA	134092	Appr.
II	1-2-3	7A	AC/PCC	GA	137028	Leave
II	3-4-5	1	HMAC	ID	161001	Appr.
II	3-4-5	1	HMAC	ID	161001	Leave
II	3-4-5	1	HMAC	ID	161005	Appr.
II	3-4-5	1	HMAC	ID	161005	Leave
II	1-2-3-4	1	HMAC	ID	161007	Appr.
II	1-2-3-4	1	HMAC	ID	161007	Leave
II	3-4-5	1	HMAC	ID	161010	Leave
II	3-4-5	1	HMAC	ID	161020	Appr.
II	3-4-5	1	HMAC	ID	161020	Leave
II	3-4-5	1	HMAC	ID	161021	Appr.
II	3-4-5	1	HMAC	ID	161021	Leave

**Table 8. Listing of sections with problem deflection basins that are not compatible with elastic layer theory (continued).**

Type of Deflection Basin	Sensors Where Problem Characteristics Were Measured	GPS Experiment No.	Pavement Surface Type	State	Section ID No.	Section End
II	3-4-5	3	JPCP	ID	163017	Leave
II	3-4-5	5	CRCP	ID	165025	Appr.
II	3-4-5	6A	AC/AC	ID	166027	Leave
II	3-4-5	1	HMAC	ID	169032	Appr.
II	3-4-5	1	HMAC	ID	169032	Leave
II	3-4-5	1	HMAC	ID	169034	Appr.
II	3-4-5	1	HMAC	ID	169034	Leave
II	2-3-4-5	4	JRCP	IN	184021	Appr.
II	2-3-4-5	9	PCC/PCC	IN	189020	Leave
II	2-3-4-5	5	CRCP	IA	199116	Leave
II	2-3-4-5	7B	AC/PCC	IA	199126	Appr.
II	3-4-5	3	JPCP	KS	203013	Appr.
II	3-4-5	3	JPCP	KS	203013	Leave
II	4-5-6	4	JPCP	KS	204053	Appr.
II	6-7	4	JRCP	KS	204053	Leave
II	3-4-5	4	JRCP	KS	204054	Appr.
II	4-5-6	4	JRCP	KS	204063	Leave
II	6-7	4	JRCP	KS	204067	Appr.
II	3-4-5-6	1	HMAC	KY	211010	Appr.
II	5-6-7	1	HMAC	MI	261010	Appr.
II	5-6-7	1	HMAC	MI	261010	Leave
II	4-5-6	2	AC/TB	MS	283085	Appr.
II	3-4-5	2	AC/TB	MS	283085	Leave
II	2-3-4	4	JRCP	MO	294031	Appr.
II	5-6-7	4	JRCP	MO	294069	Appr.
II	5-6-7	4	JRCP	MO	294069	Leave
II	3-4-5-6	6A	AC/AC	MT	306004	Appr.

**Table 8. Listing of sections with problem deflection basins that are not compatible with elastic layer theory (continued).**

Type of Deflection Basin	Sensors Where Problem Characteristics Were Measured	GPS Experiment No.	Pavement Surface Type	State	Section ID No.	Section End
II	3-4-5-6	6A	AC/AC	MT	306004	Appr.
II	3-4-5	6A	AC/AC	MT	306004	Leave
II	3-4-5	2	AC/TB	MT	307076	Appr.
II	3-4-5	2	AC/TB	MT	307076	Leave
II	3-4-5	1	HMAC	MT	307088	Appr.
II	3-4-5	1	HMAC	MT	307088	Leave
II	3-4-5	1	HMAC	MT	308129	Appr.
II	3-4-5	1	HMAC	MT	308129	Leave
II	3-4-5-6	1	HMAC	NB	311030	Appr.
II	3-4-5-6	1	HMAC	NB	311030	Leave
II	2-3-4-5	6B	AC/AC	NB	316700	Leave
II	3-4-5	9	PCC/PCC	NB	316701	Appr.
II	3-4-5	2	AC/TB	NV	321030	Leave
II	3-4-5	2	AC/TB	NV	322027	Appr.
II	3-4-5	2	AC/TB	NV	322027	Leave
II	5-6-7	1	HMAC	NC	371817	Leave
II	3-4-5	3	JPCP	NC	373807	Appr.
II	3-4-5	3	JPCP	NC	373807	Leave
II	3-4-5-6	5	CRCP	NC	375827	Leave
II	6-7	3	JPCP	ND	383005	Appr.
II	3-4-5	7A	AC/PCC	OH	397021	Appr.
II	4-5-6	6B	AC/AC	OK	404086	Leave
II	3-4-5-6	2	AC/TB	OK	404088	Appr.
II	3-4-5	2	AC/TB	OK	404164	Leave
II	3-4-5	5	CRCP	OR	415008	Leave
II	3-4-5	7A	AC/PCC	PA	427025	Leave
II	2-7	3	JPCP	SD	463010	Appr.

**Table 8. Listing of sections with problem deflection basins that are not compatible with elastic layer theory (continued).**

Type of Deflection Basin	Sensors Where Problem Characteristics Were Measured	GPS Experiment No.	Pavement Surface Type	State	Section ID No.	Section End
II	3-4-5-6	1	HMAC	TX	481122	Leave
II	4-5-6	2	AC/TB	TX	482133	Appr.
II	4-5-6	2	AC/TB	TX	482133	Leave
II	3-4-5-6	1	HMAC	TX	483579	Appr.
II	6-7	2	AC/TB	TX	483689	Appr.
II	3-4-5-6	1	HMAC	UT	491001	Appr.
II	3-4-5	6A	AC/AC	UT	491004	Appr.
II	3-4-5	1	HMAC	UT	491008	Appr.
II	3-4-5	1	HMAC	UT	491008	Leave
II	3-4-5-6	3	JPCP	UT	493010	Appr.
II	6-7	2	AC/TB	VA	511423	Appr.
II	3-4-5	1	HMAC	WA	531002	Appr.
II	3-4-5	1	HMAC	WA	531002	Leave
II	3-4-5	6B	AC/AC	WA	531005	Appr.
II	3-4-5	6B	AC/AC	WA	531005	Leave
II	3-4-5	1	HMAC	WA	531008	Appr.
II	3-4-5	1	HMAC	WA	531008	Leave
II	3-4-5-6	3	JPCP	WA	533812	Appr.
II	3-4-5	6A	AC/AC	WA	536056	Appr.
II	3-4-5	6A	AC/AC	WA	536056	Leave
II	3-4-5	6A	AC/AC	WA	537322	Appr.
II	3-4-5	6A	AC/AC	WA	537322	Leave
II	3-4-5	2	AC/TB	WY	562015	Leave
II	3-4-5	1	HMAC	WY	566029	Appr.
II	3-4-5	1	HMAC	WY	566029	Leave
II	3-4-5	1	HMAC	WY	567775	Appr.
II	3-4-5	1	HMAC	WY	567775	Leave

**Table 8. Listing of sections with problem deflection basins that are not compatible with elastic layer theory (continued).**

Type of Deflection Basin	Sensors Where Problem Characteristics Were Measured	GPS Experiment No.	Pavement Surface Type	State	Section ID No.	Section End
III	2	5	CRCP	AL	013998	Leave
III	2	4	JRCP	AL	014007	Leave
III	4	4	JRCP	AR	053059	Leave
III	2	4	JRCP	AR	054021	Leave
III	2	4	JRCP	AR	054023	Leave
III	2,3	3	JPCP	CA	063024	Appr.
III	2	3	JPCP	CO	083032	Appr.
III	2,3	3	JPCP	ID	163017	Leave
III	2	3	JPCP	ID	163023	Appr.
III	2	4	JRCP	IL	174074	Leave
III	2	5	CRCP	IL	175843	Appr.
III	2	5	CRCP	IL	175843	Leave
III	2	3	JPCP	IN	183031	Appr.
III	2	4	JRCP	IN	184021	Leave
III	2	5	CRCP	IN	185043	Appr.
III	2,3	9	PCC/PCC	IN	189020	Appr.
III	2	3	JPCP	IA	193009	Leave
III	2	3	JPCP	IA	193055	Appr.
III	3,4	3	JPCP	KS	203060	Appr.
III	2	3	JPCP	MN	273013	Appr.
III	2,3	7A	AC/PCC	MS	283097	Leave
III	2	5	CRCP	MS	285025	Appr.
III	2	5	CRCP	MS	285805	Leave
III	4,5	4	JRCP	MO	295473	Appr.
III	2	4	JRCP	MO	295483	Appr.
III	2,3	2	AC/TB	NV	321030	Appr.
III	2,3	3	AC/TB	NV	323013	Leave

**Table 8. Listing of sections with problem deflection basins that are not compatible with elastic layer theory (continued).**

Type of Deflection Basin	Sensors Where Problem Characteristics Were Measured	GPS Experiment No.	Pavement Surface Type	State	Section ID No.	Section End
III	2	5	CRCP	OK	404158	Leave
III	2,3,4	5	CRCP	OR	415021	Leave
III	2	5	CRCP	OR	415022	Appr.
III	2,3	6A	AC/AC	OR	416011	Leave
III	2,3	5	CRCP	OR	417081	Leave
III	2	3	JRCP	PA	423044	Appr.
III	2,3	5	CRCP	PA	425020	Appr.
III	2,3	9	PCC/PCC	PA	429027	Leave
III	2	5	CRCP	SC	455034	Leave
III	2,3	3	JPCP	TX	483010	Appr.
III	3,4	3	JPCP	TX	483010	Leave
III	2,3	9	PCC/PCC	TX	483569	Appr.
III	2	4	JRCP	TX	484143	Leave
III	2,3	5	CRCP	TX	485026	Leave
III	2,3	3	JPCP	PR	724121	Appr.



support, a severe thermal gradient causing curling and/or warping of the PCC slab, and/or a combination of these conditions.

Conversely, almost 80 percent of those section ends found with a Type II deflection basin were dense-graded, asphalt concrete-surfaced pavements. The reason for these types of deflection basins are unknown. However, the error term for these types of basins were found to decrease when a very stiff layer was incorporated in the pavement structure. For example, at some of the Arizona sites, the error term decreased to a value of less than 3.0-percent error per sensor when the sand subbase was allowed to exceed a modulus well above 690 Pa (100 ksi). Unfortunately, even allowing the sand subbase layer to exceed 6900 Pa (1,000 ksi) did not always reduce the error term to a value less than 2½-percent per sensor.

**Observation:** Numerous GPS section ends were found to have "problem" deflection basins that are not appropriate for use of elastic layer theory for backcalculating layer moduli. As such, programs based upon the theory of elasticity should not be used for analyzing these type of basins.

A further investigation of a few of the sections with problematic deflection basins was conducted for the Southern LTPP Region. For those sites studied, the problems with the deflections appear to be caused by a variety of problems. First, one of the sites has an HMAC surface over a lime-treated base where the lime-treated base set up to the extent that it is now very hard and the HMAC surface layer has exhibited cracking similar to an HMAC overlay of a PCC pavement. Hence, when testing this section, the deflections were very small and were noted at the time to be problematic. Similarly, other sections studied in the southern and western regions were found to have sand subbase layers with extremely high moduli, indicative of a cement-treated material. Various iterations and layer combinations were used to produce lower moduli values. All other combinations resulted in much higher error terms, so the moduli that corresponded to the lowest error term was used.

Another section studied was a PCC section and again the deflections were very small. It was noted that the FWD operator tried moving to different areas to determine if the problem was only at a particular location; however, this was not the case because all of the deflections were very small. It has also been noted that other sections in the GPS-7 experiment (asphalt concrete overlay on PCC pavements) are known to produce problems identified by the FWD software during testing. Based on an initial review in the southern region, it is believed that most of the problems occurring are indicative of some type of material problem rather than a problem in the software or FWD operations.

For the detailed studies on pavement features as related to pavement performance and defining the differences between laboratory determined and backcalculated moduli, only typical deflection basins for which the error term was less than 2½-percent per sensor were used.

**4.2.2 Reduction of Deflection Matching Error Term.** Nondestructive deflection testing (NDT) has been conducted several times on each test section. NDT was conducted only once, however, over the area where the test pit was dug from which the materials data were obtained. Several sections were noted that had varying pavement structures between the two ends of the test section. This did not necessarily affect the backcalculation results; however, it should be noted that one end or the other may or may not represent the actual 152-m (500-ft) pavement test section, or in fact, there may be a homogeneity problem throughout the test section. Therefore, backcalculation results were used from the first round of FWD testing, before the test pit was dug to ensure accurate layer thicknesses and representative materials data were used in the backcalculation process. Table 1 included a list of all of the data elements required for completion of the backcalculation of layer moduli.

A four-layer (or less) pavement structure was used for the backcalculations completed by the SHRP-LTPP program. Combination of layers was carried out automatically by the software according to specific rules established by SHRP. The error term on a per sensor basis for many of these sites was relatively large, exceeding 15 percent in more than just a few cases. These large errors are believed to have been caused in part by the unique deflection basins previously discussed (figures 19 through 21) and by combining various layers and ignoring certain site-specific conditions. In an effort to reduce the unacceptable error terms (greater than 2.5 percent per sensor), each site was studied to confirm or pursue a more appropriate layer structure. The following discusses the review of each material or layer in the pavement, including the subgrade.

***Subgrade Layers.*** The subgrade was divided for this study into two layers for certain conditions. These conditions had to do with the depth to water table, depth to a rigid layer, and the depth to a significant change in material type. Subdividing the subgrade by the depth to the water table significantly improved the match between the calculated and measured deflection basins. Modulus values above the water table are generally greater than those below the water table, as expected (i.e., the effect of moisture on the soil's response to load).

The other condition has to do with a depth to a rigid layer. Obviously, if limestone or rock is encountered at a site, then there is really no question as to the depth to a rigid layer; however, there are cases where different soils were encountered at varying depths. For example, there are some sites where a weak or soft material was encountered near the surface, and was underlain by

a relatively strong or stiffer layer, but not defined as a rigid layer. The question is whether a strong layer (relative to the weaker layer) supporting a weaker layer represents a rigid layer in terms of the measured deflections. For these cases, the subgrade was separated at that depth where those significant changes occur and the error term generally did decrease.

***Unbound Base/Subbase Layers.*** The unbound base and subbase layers were considered two different layers, unless these materials were found to be similar from the laboratory test results. For the rebackcalculation of layer moduli, thick granular base/subbase layers (exceeding 30 cm [12 in] in thickness) were further subdivided into separate layers. In some cases, subdividing thick granular base/subbase layers further reduced the error term. This was especially important for backcalculating layer moduli for sections with a Type II deflection basin. Reduction of the error term for some of these sites required that the subbase modulus be increased to represent a stabilized material. Backcalculated moduli for these GPS sites were identified as questionable when the inventory data, materials sampling forms, and materials test results included in the LTPP data base noted these layers as unbound granular materials, such as a sand subbase. These results were not used in further detailed analyses within this project.

***Asphalt Concrete Layers.*** The asphalt concrete surface and base layers were generally combined into one layer for the backcalculation regime used by the SHRP-LTPP program. Under this study, however, these layers were separated in some cases when there was a significant difference in materials. Separating the asphalt concrete layers, especially for some of the overlaid sections, further reduced the error term below the acceptable value of 2½ percent per sensor. Asphalt, cement and/or lime-treated base layers were nearly always considered different layers in the backcalculation process.

***Number of Structural Layers.*** As discussed in the above paragraphs, there were cases where five or more different structural layers were required to represent those GPS section ends with large error terms from the initial backcalculation results completed by SHRP. Using five layers in the WESDEF program did not always reduce the error term. MODULUS 4.2 is restricted to a maximum of four layers, including the subgrade. For these conditions, an elastic-layered theory program entitled "ELSYM5" was used in a trial-and-error mode separately to match the measured deflection basins. In no case, however, were the number of layers to be backcalculated allowed to exceed six layers. The results of this analysis showed that only a small percentage of the GPS section ends were found to have lower error terms using a five- or six-layer structure.

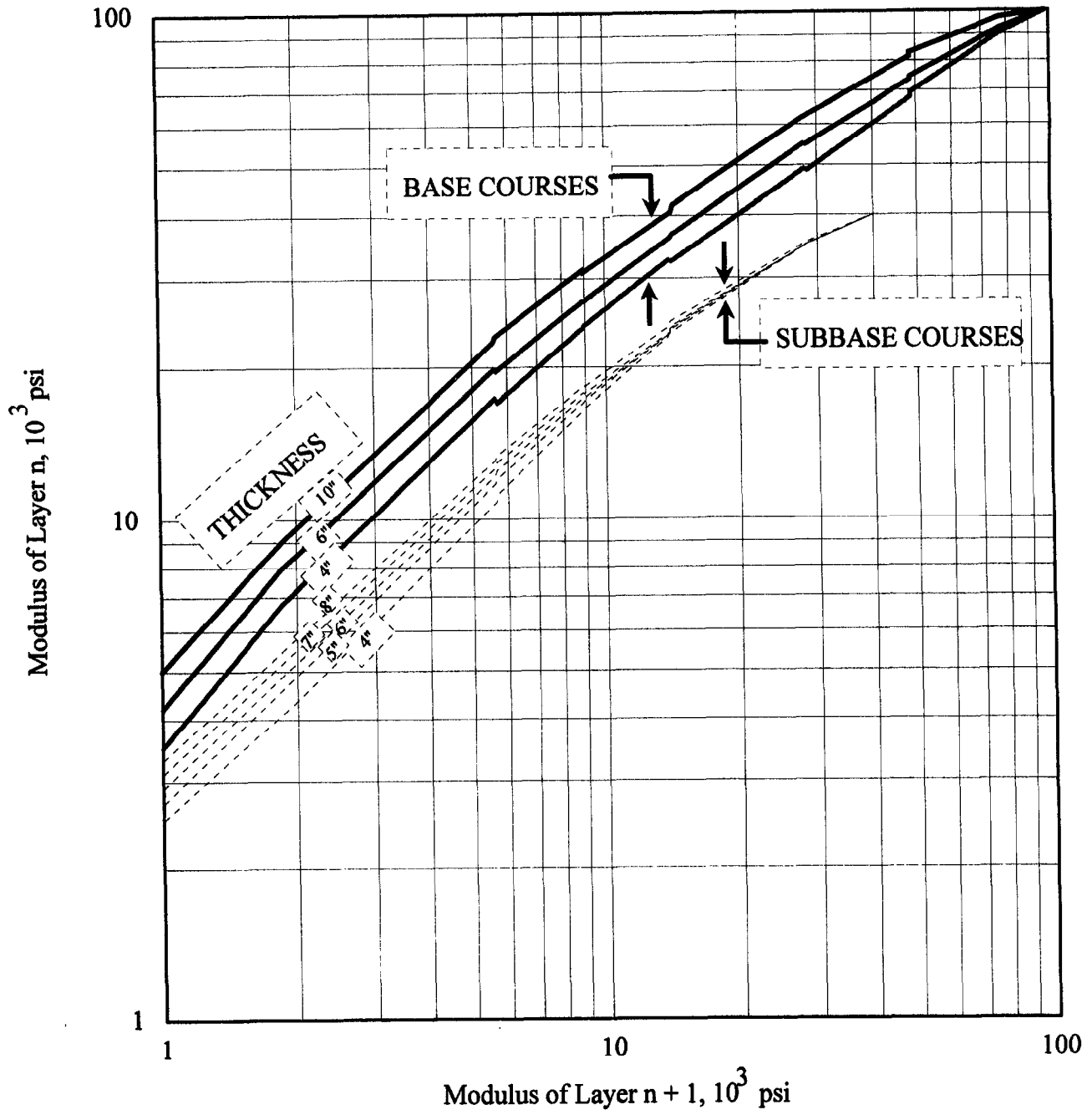
**Observation:** Excluding those GPS section ends with problem deflection basins, the use of a four-layer system consistently resulted in the lowest error term, as compared to the use of three, five or six layers.

**4.2.3 Modulus Ratios.** Elastic moduli were calculated for the 40-kN (9-kip) load to evaluate the in situ response characteristics of each structural layer within each GPS site tested. These layer moduli were further examined for reasonableness based on material type and the overall pavement cross section. Layer moduli were also calculated for all FWD load levels to evaluate the in situ stress sensitivity of each material. The stress sensitivity of the pavement structure and materials is discussed in detail in subsection 4.3.4.

Modulus ratios between two adjacent unbound layers were determined and reviewed for each GPS section end. When moduli ratios of adjacent unbound layers exceed a value of about 3.5, large tensile stresses can occur at the bottom of the upper layer. These tensile stresses can result in decompaction of that layer reducing the modulus. As such, modulus ratios of adjacent unbound layers exceeding 4 are considered unrealistic, or suggest that the unbound material may, in fact, be responding as a bound or stabilized material. The criteria established by the Corps of Engineers (26) were used to identify those section ends with high modulus ratios based on the pavement cross-section or layer thicknesses (figure 22).

Thick granular base and/or subbase layers were further divided into two equal layers for many of the initial backcalculation results with high layer modulus ratios. These divisions resulted in reduced modulus ratios in many cases, while maintaining an acceptable error term for the calculated deflection basin. Figure 23 is a histogram of the modulus ratios between adjacent unbound pavement/subgrade layers for PCC- and asphalt concrete-surfaced pavements. As shown, the modulus ratios for both pavement types have a uniform distribution. More importantly, over 80 percent of the modulus ratios were found to be acceptable. Table 9 notes those GPS section ends where the modulus ratios exceed the allowable value given in figure 22, but have acceptable error terms.

**Observation:** There is no unique solution for a particular deflection basin using programs based on elastic layer theory. Minor changes in the pavement structure, layer combination, and depth to a rigid layer can have a significant effect on the error term (calculated versus measured deflection basins) and/or resulting layer moduli. This effect or difference in computed layer moduli is much greater for surface and base layers than for the subgrade layers.



1 in = 2.54 cm  
 1 psi = 6.89 kPa

**Figure 22. Limiting modulus criteria of unbound base and subbase layers (26).**

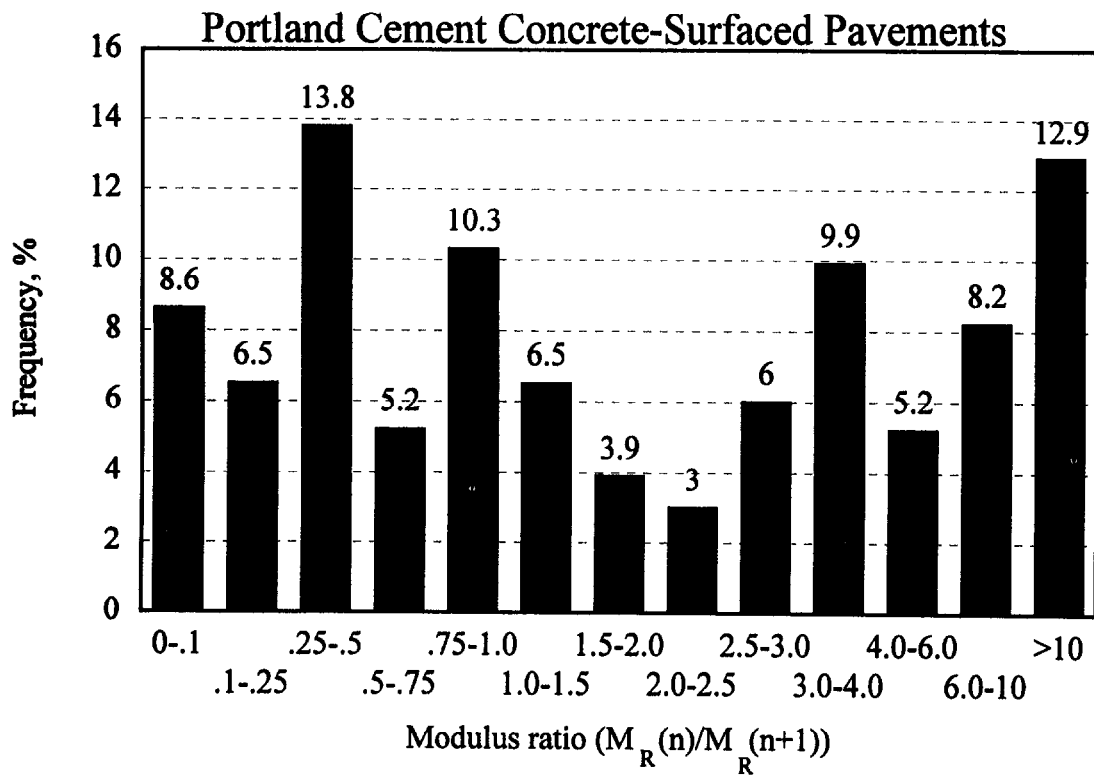
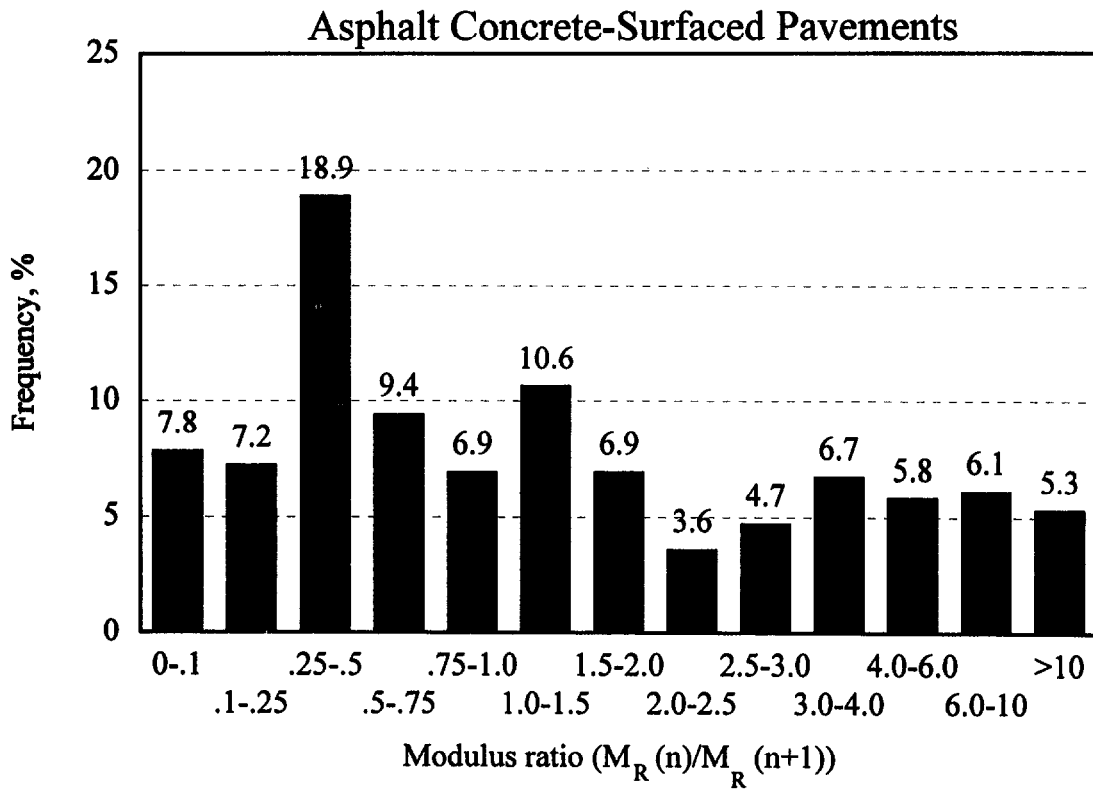


**Figure 23. Histogram of the calculated modulus ratios between adjacent unbound pavement/subgrade layers.**

**Table 9. GPS section ends that exceed the modulus ratio set by figure 22.**

<b>GPS Section No.</b>	<b>Section End</b>	<b>Unbound Layers with Large Ratios</b>
014007	Appr.	Subbase/Base
014007	Leave	Subbase/Base
014084	Appr.	Subgrade/Subbase
021004	Appr.	Subgrade/Subbase
021004	Leave	Subgrade/Subbase
053073	Appr.	Subbase/Base
053073	Leave	Subbase/Base
068150	Appr.	Subgrade/Subbase
068534	Appr.	Subgrade/Subbase
068534	Leave	Subbase/Base
091803	Appr.	Subgrade/Base
091803	Leave	Subgrade/Base
123811	Appr.	Subgrade/Subbase
123995	Appr.	Subbase/Base
123995	Leave	Subbase/Base
123997	Appr.	Subgrade/Subbase
123997	Leave	Subgrade/Subbase
124059	Appr.	Subgrade/Base
124059	Leave	Subgrade/Base
124102	Leave	Subbase/Base
124137	Leave	Subgrade/Subbase
131031	Appr.	Subgrade/Base
133007	Leave	Subgrade/Base

**Table 9. GPS section ends that exceed the modulus ratio set by figure 22 (continued).**

<b>GPS Section No.</b>	<b>Section End</b>	<b>Unbound Layers with Large Ratios</b>
133016	Appr.	Subgrade/Base
133019	Appr.	Subgrade/Base
157080	Leave	Subgrade/Subbase
175217	Leave	Subgrade/Base
176050	Leave	Subgrade/Base
179327	Leave	Subgrade/Base
193055	Leave	Subgrade/Base
196150	Appr.	Subgrade/Base
196150	Leave	Subgrade/Base
204016	Appr.	Subgrade/Base
204016	Leave	Subgrade/Base
214025	Leave	Subgrade/Base
231012	Appr.	Subgrade/Base
231026	Leave	Subgrade/Base
251002	Appr.	Subbase/Base
251002	Leave	Subbase/Base
261013	Appr.	Subbase/Base
265363	Leave	Subbase/Base
266016	Leave	Subgrade/Subbase
271023	Leave	Subbase/Base
273003	Appr.	Subgrade/Base
273007	Leave	Subgrade/Base
274034	Leave	Subgrade/Base
274040	Appr.	Subgrade/Base
274040	Leave	Subgrade/Base
274050	Leave	Subgrade/Base



**Table 9. GPS section ends that exceed the modulus ratio set by figure 22 (continued).**

<b>GPS Section No.</b>	<b>Section End</b>	<b>Unbound Layers with Large Ratios</b>
28106	Appr.	Subgrade/Subbase
281016	Leave	Subgrade/Subbase
291002	Appr.	Subgrade/Base
291008	Appr.	Subgrade/Base
294036	Leave	Subgrade/Base
295000	Appr.	Subgrade/Base
295000	Leave	Subgrade/Base
295393	Appr.	Subgrade/Base
295473	Leave	Subgrade/Base
295483	Leave	Subgrade/Base
297054	Leave	Subgrade/Base
321021	Leave	Subgrade/Subbase
341030	Appr.	Subbase/Base
352006	Leave	Subgrade/Subbase
364017	Appr.	Subgrade/Base
371803	Appr.	Subgrade/Base
371817	Appr.	Subgrade/Base
395003	Appr.	Subgrade/Subbase
401015	Appr.	Subgrade/Base
401015	Leave	Subgrade/Base
415022	Leave	Subgrade/Base
416011	Leave	Subbase/Base
417018	Leave	Subgrade/Base
421613	Appr.	Subgrade/Base
421613	Leave	Subgrade/Base
421691	Leave	Subgrade/Base

**Table 9. GPS section ends that exceed the modulus ratio set by figure 22 (continued).**

<b>GPS Section No.</b>	<b>Section End</b>	<b>Unbound Layers with Large Ratios</b>
423044	Leave	Subgrade/Base
425020	Appr.	Subgrade/Base
425020	Leave	Subgrade/Base
427025	Appr.	Subgrade/Base
463009	Appr.	Subgrade/Base
463012	Appr.	Subgrade/Base
463012	Leave	Subgrade/Base
465040	Appr.	Subgrade/Subbase
465040	Leave	Subgrade/Subbase
469187	Appr.	Subgrade/Subbase
473101	Appr.	Subgrade/Subbase
473109	Appr.	Subgrade/Subbase
473109	Leave	Subgrade/Subbase
476022	Appr.	Subgrade/Subbase
481046	Appr.	Subbase/Base
481065	Appr.	Subbase/Base
482172	Appr.	Subgrade/Subbase
482172	Leave	Subgrade/Subbase
483609	Appr.	Subgrade/Base
483779	Leave	Subgrade/Subbase
486179	Leave	Subgrade/Subbase
489005	Leave	Subgrade/Base
536048	Appr.	Subgrade/Subbase
536048	Leave	Subbase/Base
536049	Appr.	Subgrade/Subbase
544003	Appr.	Subgrade/Base

<b>GPS Section No.</b>	<b>Section End</b>	<b>Unbound Layers with Large Ratios</b>
<b>553010</b>	<b>Appr.</b>	<b>Subgrade/Base</b>
<b>553012</b>	<b>Appr.</b>	<b>Subgrade/Base</b>
<b>553016</b>	<b>Appr.</b>	<b>Subgrade/Base</b>
<b>553019</b>	<b>Appr.</b>	<b>Subgrade/Base</b>
<b>555037</b>	<b>Appr.</b>	<b>Subbase/Base</b>
<b>555037</b>	<b>Leave</b>	<b>Subbase/Base</b>
<b>555040</b>	<b>Leave</b>	<b>Subgrade/Base</b>
<b>556352</b>	<b>Appr.</b>	<b>Subgrade/Subbase</b>
<b>556352</b>	<b>Leave</b>	<b>Subgrade/Subbase</b>
<b>556354</b>	<b>Leave</b>	<b>Subgrade/Subbase</b>
<b>811804</b>	<b>Appr.</b>	<b>Subgrade/Subbase</b>
<b>826006</b>	<b>Appr.</b>	<b>Subgrade/Subbase</b>
<b>831801</b>	<b>Leave</b>	<b>Subgrade/Subbase</b>
<b>836450</b>	<b>Appr.</b>	<b>Subgrade/Subbase</b>
<b>836452</b>	<b>Appr.</b>	<b>Subgrade/Base</b>
<b>871622</b>	<b>Leave</b>	<b>Subgrade/Subbase</b>
<b>871806</b>	<b>Appr.</b>	<b>Subgrade/Subbase</b>

### **4.3 Differences Between Laboratory Determined and Backcalculated Elastic Moduli**

As stated previously, the 1993 AASHTO Design Guide permits the modulus of the different layers of materials to be measured in the laboratory or to be calculated from deflection basin data. However, the guide falls short of adequately explaining potential differences between moduli determined from both techniques and how to select comparable values.

It has been documented in the literature that the moduli calculated from deflection basin tests do not match measurements made in the laboratory. Various papers presented at the 1993 NDT symposium (20) showed the difficulty and problems in correlating laboratory measured and backcalculated moduli. Although some of the papers did show that differences can and do exist between the laboratory measured resilient moduli and backcalculated values from deflection measurements, other papers showed that the laboratory measured and backcalculated values are

correlated. Currently, the NIMS contains sufficient data from the GPS experiments for the purposes of moduli comparisons. Table 1 identified those data elements used for this activity. The initial comparison of modulus values only included those sites with low error terms from backcalculation of layer moduli (less than 2½-percent error per sensor) and those where the laboratory repeated-load resilient modulus test data fit the selected constitutive equation (equation 5).

**4.3.1 Laboratory and In Situ Conditions.** Laboratory measured resilient or elastic moduli of surface layers represent intact, and for the most part, homogeneous specimens; while the backcalculated surface moduli from deflection measurements represent effective or equivalent moduli. This "equivalent" modulus is representative of the surrounding material, thickness variations (caused by rutting in the wheelpaths), and cracks (and/or joints in PCC pavements). Thus, the equivalent surface modulus is not a true property of the material itself, but a property of the load-response characteristic of the overall pavement structure. When there is a difference, the question is, which value is more appropriate for use in determining the structural capacity and/or overlay thickness requirement? There is also concern as to the accuracy of the backcalculated moduli for certain pavement structures. One of these is the so-called "sandwich"-type structure where a lower stiffness material is placed between two materials with significantly higher moduli.

More directly, pavements with cracks or various discontinuities and other such features, which are the main focus of maintenance and rehabilitation efforts, are ill-suited for any backcalculation analysis or moduli determination that is based on elastic layer theory. Some of the more complicated finite element programs used for backcalculation of material properties are more applicable to these actual conditions. While elastic moduli output for these types of pavements are really meaningless, especially using linear elastic theory, these are pavements for which most of the information is needed for evaluation and rehabilitation studies.

Similarly, there are vertical changes in the subgrade soils at each site. This change in the vertical profile is minor at some sites, whereas, at other sites the change is substantial. Resilient modulus testing was performed on material recovered as close to the surface of the subgrade as possible. However, in calculating a resilient modulus from the deflection basin, a composite value is calculated that takes into account all changes in the vertical profile of the subgrade. The question to be answered is then: How does one consider seasonal variations in this composite value (i.e., combining all changes in the subgrade with depth into one modulus value)? This becomes an important question in comparing laboratory measured values to those calculated from deflection basins measured over a period of time.

Unfortunately, repeated-load resilient modulus test results were not performed on different soils encountered beneath the pavement. Those sites for which the subgrade test specimen was recovered 30 cm (12 in) or more beneath the top of subgrade, were separated out and were not included in the initial evaluation. The reason for this omission is that the other laboratory test results may not represent the specific material for resilient modulus testing. Moisture contents, dry densities, gradation and other physical properties were only measured on soils recovered at the surface of the subgrade.

The same response model must be used to both backcalculate resilient modulus from the deflection value and to calculate the stress state under the pavement for these two values to be compared. In addition, there are other important questions which must be considered when comparing laboratory measured and backcalculated moduli. These are listed below and discussed in the following subsections:

- At what depth is the stress state calculated in the pavement layers and subgrade for comparing the calculated and laboratory measured modulus values for the unbound materials?
- How does one represent thin or nonstructural layers that could have an effect on the bond and shear transfer between layers in the calculated model (asphalt concrete over PCC layers)?
- What stress state should be used in the laboratory to match or compare the laboratory resilient modulus to the backcalculated values?

**4.3.2 Temperature Gradient Considerations for Asphalt Concrete Mixtures.** Asphalt concrete is considered to be a viscoelastic material, whose properties are temperature-dependent. The lower the temperature, the higher the modulus and the more elastic the material becomes (figure 8). Many studies have shown that the resilient modulus as measured by repeated-load indirect tensile tests and repeated-load compression type testing approach one another at 5 °C (41 °F) and begin to diverge at the higher test temperatures (figure 24). At higher test temperatures, the materials are much more viscoelastic; whereas, at the colder temperatures, the material begins to approach the assumptions used for an elastic material.

In the laboratory, the specimens are tested at a constant and uniform temperature (i.e., no temperature gradient throughout the test specimen); whereas, the backcalculated moduli values represent a composite modulus of the asphalt concrete layer for which the temperature varies from the surface to the bottom of that layer. Some of the thermal gradients measured during

deflection testing were very large, which results in modulus gradients with depth for the asphalt concrete surface layer. Figure 25 shows an example of the temperatures recorded at the different depths during FWD deflection testing. One of the questions to be answered is: What temperature should be used for comparing the laboratory measured modulus values to those backcalculated from the deflection basins; or stated differently, what depth in the asphalt concrete layer should be used to determine the temperature for equating the laboratory measured and backcalculated moduli?

Previous studies have also focused on this issue. Some studies have recommended that the temperature to be used is that temperature at one-third the depth of the asphalt concrete layer thickness, whereas other studies have recommended that the temperature be determined at mid-depth. Although differences do exist between the studies, none recommend that surface temperatures be used. In the LTPP program, pavement temperatures were recorded at four depths during deflection testing: at the surface, 2.5 cm (1 in) below the surface, mid-depth, and 2.5 cm (1 in) from the bottom of the asphalt concrete layer. The one exception to this rule was for the asphalt concrete overlays. For asphalt concrete overlays, no mid-depth readings were recorded in the overlay.

To decide at what depth the temperature should be determined for comparing lab to field values, the backcalculated layer moduli were used to determine the test temperature in the laboratory, such that the laboratory measured moduli would be equal to the backcalculated moduli. This procedure is graphically demonstrated in figure 26 using some of the GPS sites. Unfortunately, this procedure rarely resulted in equating the test temperature in the laboratory to those measured in the pavement during deflection measurements, as shown by the summary of values included in figure 26 for a few of the GPS sites.

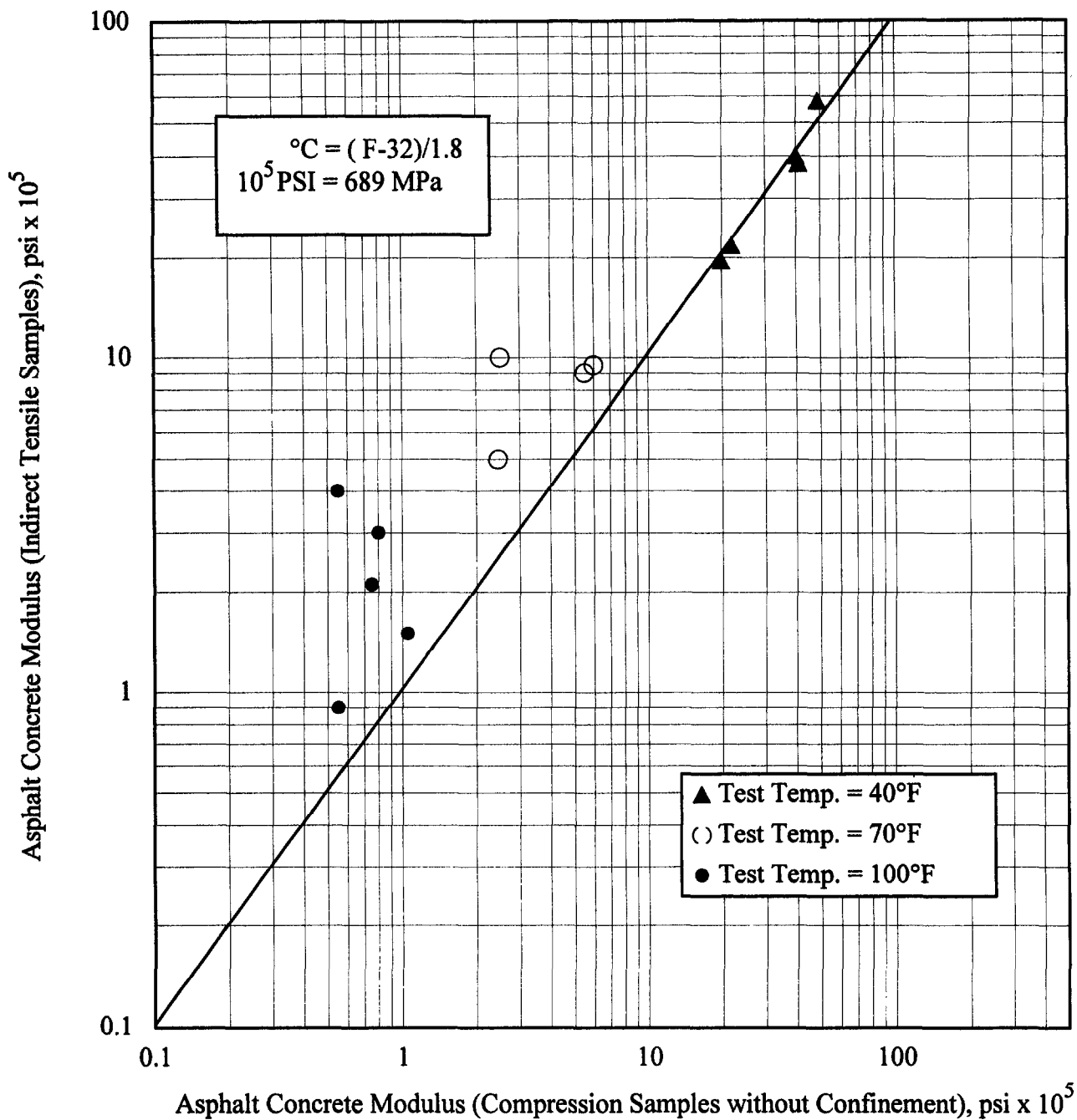
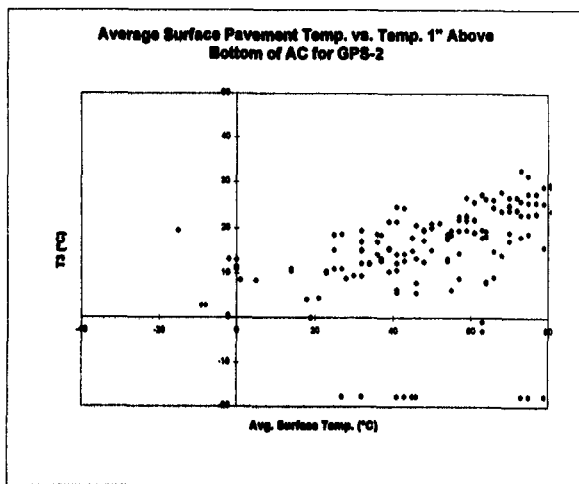
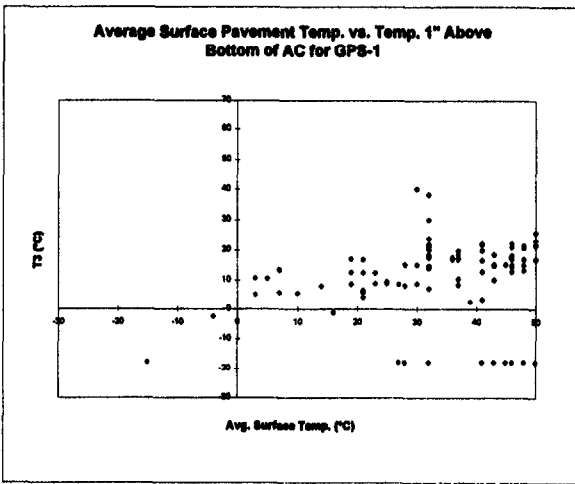
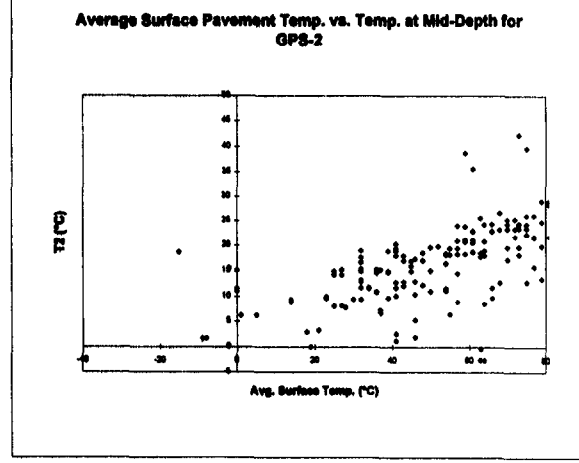
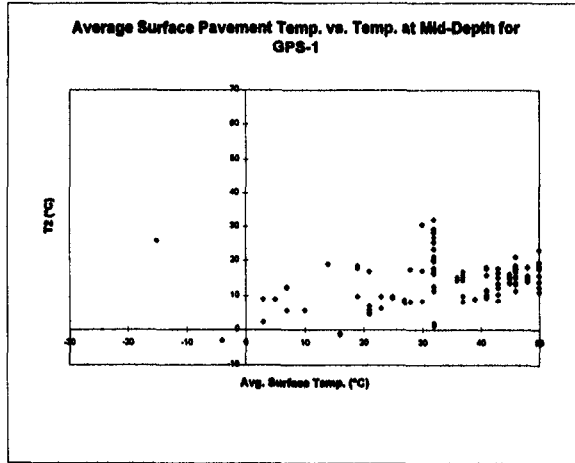
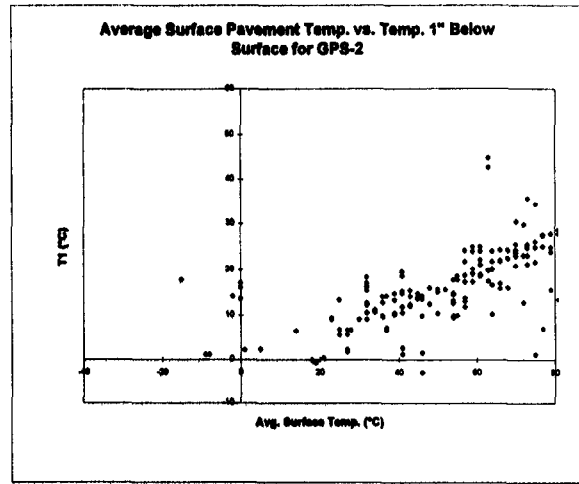
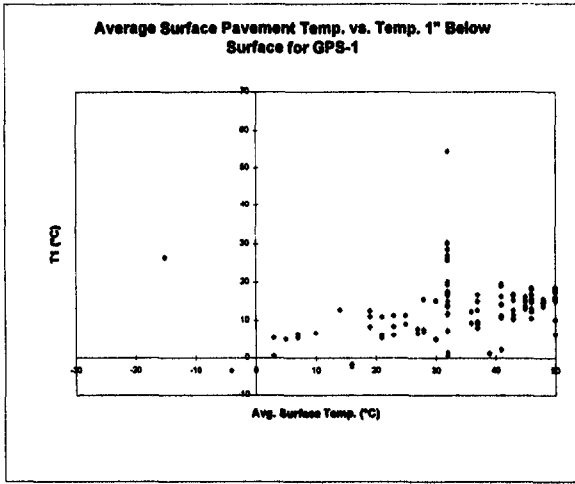


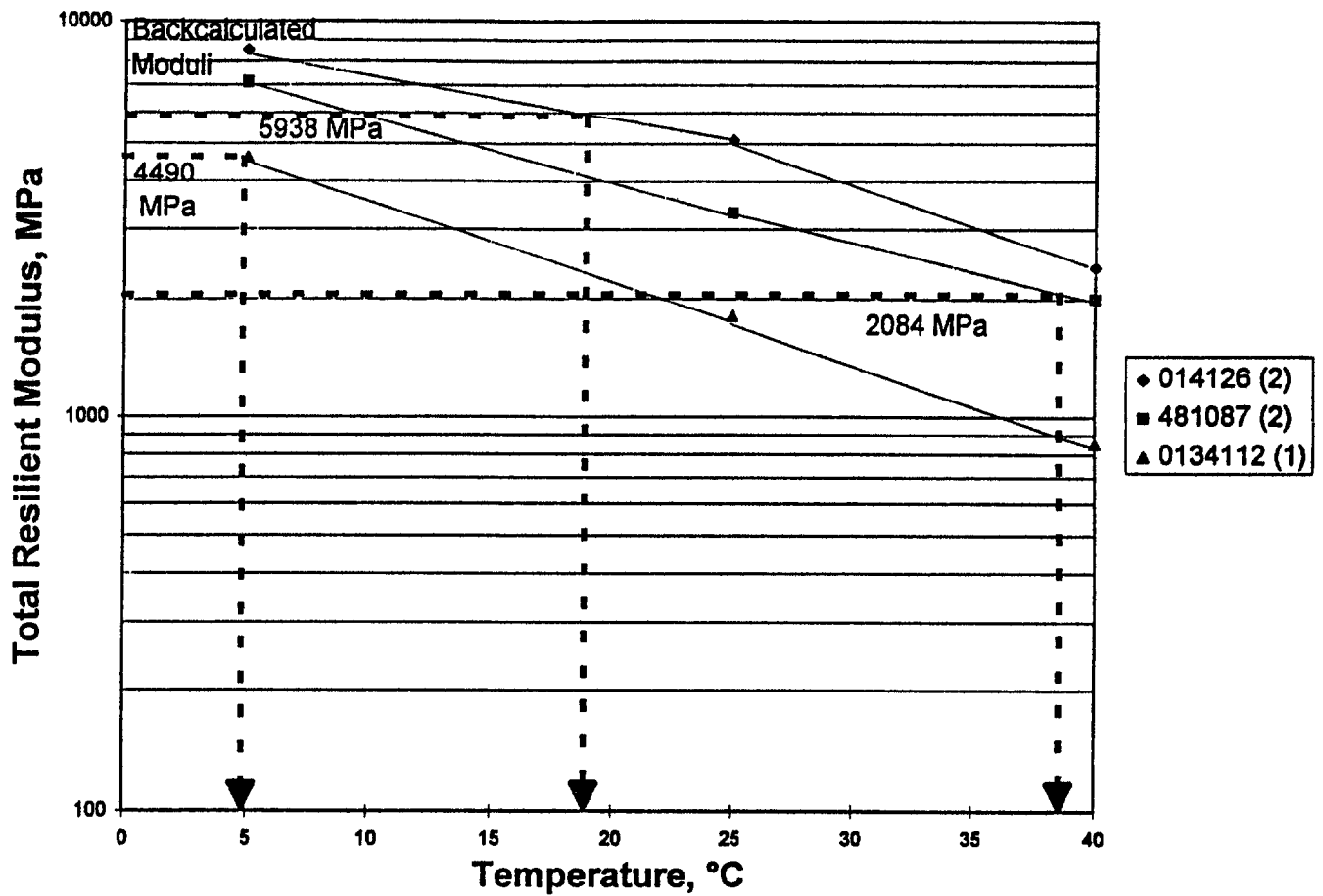
**Figure 24. Comparison of test results between unconfined compression and indirect tensile tests (8).**



1 in = 2.54 cm

**Figure 25. Comparison of temperatures measured at the surface to those measured below the surface for the GPS-1 and 2 sites.**





GPS Section	Backcalculated Equivalent Temperature, °C	Measured Temperatures, °C			
		Surface	2.5 cm	1/2 D	D-2.5 cm
011019(1)	9	20.0	26.8	28.1	20.8
011019(2)	4	21.1	26.8	27.8	20.7
014125(1)	22	0.0	30.1	28.3	30.0
014125(2)	8	0.0	30.4	28.5	30.0
014126(1)	13	8.9	15.2	18.1	21.4
014126(2)	19	10.0	15.4	18.2	21.4
134112(1)	4	42.8	34.7	32.3	27.7
134112(2)	1	42.8	35.1	32.3	27.7
356401(1)	-7	22.8	23.6	27.7	29.9
356401(2)	-40	22.8	23.7	27.6	29.8
481046(1)	14	22.8	23.5	24.9	25.9
481046(2)	18	22.8	23.7	25.0	25.9
481087(1)	54	28.9	32.5	33.2	35.8
481087(2)	38	27.8	32.3	33.0	35.5
481109(1)	*	0.0	15.4	14.8	15.0
481109(2)	-11	0.0	16.1	15.3	15.3
481181(1)	-4	25.0	27.2	30.7	34.3
481181(2)	13	27.8	27.4	30.8	34.3

\*No equivalent temperature

Figure 26. Graphical illustration of procedure used to determine the depth at which the temperature is to be determined for use in the laboratory so that the measured and backcalculated moduli are equal.

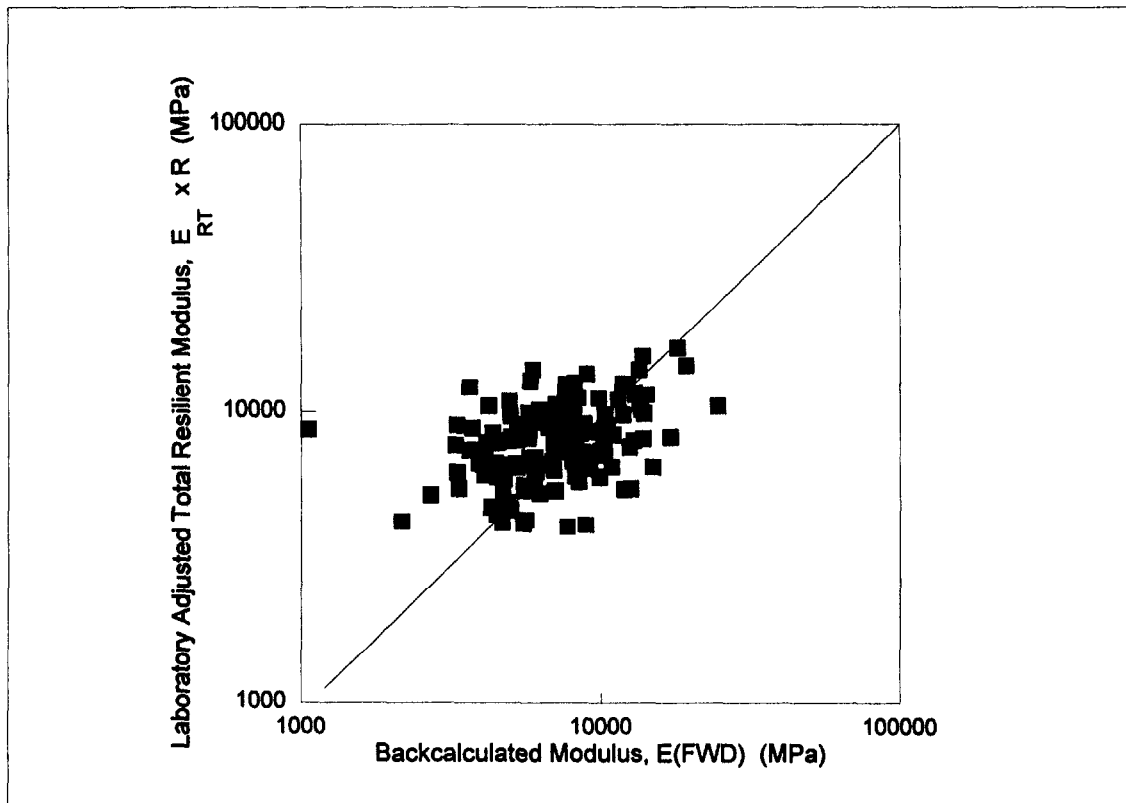
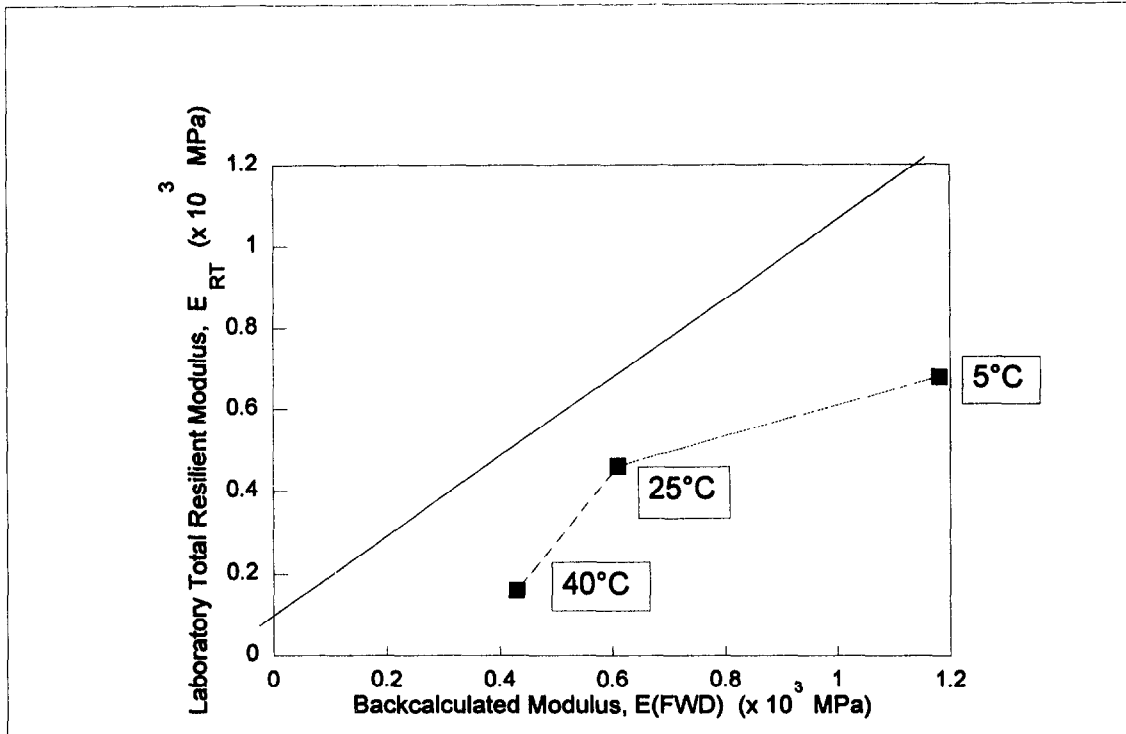


**Figure 27. Comparison of laboratory measured values determined at the mid-depth temperature to the backcalculated moduli.**

The critical or equivalent laboratory temperature related to the backcalculated modulus was, in more than just a few cases, significantly different and, in some cases, completely out of the range of the pavement temperatures measured at various depths during deflection testing. This result suggests that there is no equivalent temperature that can be determined or that other equally important factors need to be considered.

As previously stated, there is some concern whether laboratory moduli measured at a test temperature of 5 °C (41 °F) are reliable. Figure 27 illustrates the average temperature effect on the comparison of laboratory resilient moduli determined at the mid-depth temperature measured during deflection testing to those values backcalculated. As shown, the two moduli diverge more at 40 °C (104 °F) than at 25 °C (77 °F), which is consistent with other findings because of the materials viscoelastic properties. But at 5 °C (41 °F) the moduli also diverge more than at 25 °C (77 °F), which conflicts with studies reported in the literature. This observation also supports the fact that the moduli measured in the laboratory at a test temperature of 5 °C (41 °F) may be in error. Thus, those GPS sites with mid-depth temperatures below 25 °C (77 °F) during the deflection testing were excluded from the comparison of laboratory measured and backcalculated moduli. The viscoelastic effect is discussed in more detail under subsection 4.3.4 and in the following paragraphs.

The discussion in the above paragraphs has centered on determining a critical laboratory temperature so that the backcalculated and laboratory measured moduli are equal. However, there is another equally important factor (especially at the higher temperatures) that must be considered.

Asphalt concrete is a viscoelastic material whose modulus is dependent, not only on temperature, but also time of loading. Thus, there is another question to be considered: Is the type of load and load pulse used in the laboratory compatible or equivalent to the impact load applied by the FWD during deflection testing?

Obviously there is a difference and the effect or importance of that difference is temperature-dependent. Unfortunately, the moduli measured at 5 °C (41 °F) are believed to be in error, as noted above. Thus, evaluating the differences between backcalculated and laboratory measured moduli at different temperatures is not possible using the LTPP data base. Instead, data were used from other studies (i.e., references 5 through 9) to identify those adjustments for loading differences so that the backcalculated and laboratory measured moduli become equal. For most

of these studies, the temperature measured or calculated at the mid-depth of the asphalt concrete layer was used. These adjustments or correction ratios are listed below:

Temperature, °C (°F)	Ratio of Backcalculated to Laboratory Measured Values*
5 (41)	1.00
25 (77)	2.8
40 (104)	4.0

$$*E(\text{FWD})/E_{\text{RT}}(\text{IDT})$$

In other words, the total resilient modulus measured in the laboratory at 40 °C (104 °F) (using the test procedures established by SHRP) should be multiplied by 4.0, on the average, to equal the elastic modulus backcalculated from FWD deflection tests.

Although variation does exist, using a temperature near the mid-depth of the asphalt concrete layer has been found to be acceptable for predicting structural response of the pavement structure. Thus, the mid-depth temperature measured during deflection testing was used to select a value of total resilient modulus measured in the laboratory. A comparison of the backcalculated and laboratory temperatures to equate the laboratory and backcalculated moduli were included in figure 26 for a few of the GPS sites. As shown, the backcalculated moduli are consistently higher than the laboratory values or the backcalculated temperatures are lower than the laboratory temperatures. These laboratory values were then adjusted to account for loading differences, as noted above. A graphical comparison of the backcalculated and adjusted laboratory moduli are included in figure 27, and suggests that the mid-depth temperature and correction ratios can be used to roughly equate backcalculated and laboratory measured moduli for dense-graded asphalt concrete surface mixtures.

**Observation:** For characterizing the structural response of asphalt concrete mixtures, the total resilient modulus measured at the mid-depth temperature of the asphalt concrete layer should be used.

**Observation:** Laboratory measured resilient moduli using the indirect tensile test in accordance with SHRP procedures must be adjusted to account for differences in the applied load between the FWD and laboratory. These adjustments are temperature-dependent.

**4.3.3 Stress-State Considerations for Unbound Materials.** As shown by figure 12, the resilient modulus of the unbound pavement materials and subgrade soils are dependent upon the

stress state of the material, mathematically represented by equation 5. Similar to the temperature dependency of asphalt concrete materials, moduli measured in the laboratory on unbound materials are performed at specific stress states; whereas, in the pavement, the stress state varies both vertically and horizontally. The question becomes: What stress state should be used in the laboratory such that the laboratory measured moduli are comparable or equal to the backcalculated moduli? The laboratory stress state should be equivalent to the stress state calculated and used with the modulus backcalculated from the deflection basins.

As stated previously, the backcalculated modulus ratio between two adjacent layers becomes critical for this case in calculating the stress state at various depths in the unbound pavement layers, because of the computation of tensile stresses near the bottom of those layers. For this study, none of the GPS section ends which exceed the allowable modulus ratio shown in figure 22 were used.

In order to obtain a resilient modulus from repeated-load triaxial tests (AASHTO T294) that is comparable to a backcalculated modulus, lateral and vertical stresses must include the existing in situ pressures within each layer. To determine these values, densities and layer thicknesses of the pavement structure must be considered. The following steps were used to determine a resilient modulus of elasticity that is representative of the particular granular base, subbase, and/or subgrade soil under the pavement structure.

1. Compute the in situ lateral stress. Computation of lateral stresses were made at the mid-depth and quarter-points within each pavement layer, and at various depths of up to 61 cm (24 in) into the subgrade and/or embankment. Lateral stresses were based on load computations made with elastic layer theory for the FWD testing load, and confining pressures estimated from unit weights and thicknesses for each layer in the pavement structure. The total lateral stress for the FWD testing load for a specific layer can be calculated using equation 6.

$$\sigma_3 = \sigma_3^1 + p_n \tag{6}$$

and

$$p_n = K_o (X D_n \gamma_n + \sum_{i=1}^{n-1} \gamma_i D_i) \tag{7}$$

where:

$\sigma_3$	=	In situ confining pressure simulating in-field conditions of layer n.
$\sigma_3^1$	=	Load-related stress computed with elastic layer theory at mid-layer of layer n.
$p_n$	=	At-rest earth pressure at mid-depth of layer n.
$\gamma_i$	=	Unit weight of layer I.
$D_i$	=	Thickness of layer I.
$\gamma_n$	=	Unit weight of layer n.
$D_n$	=	Thickness of layer n.
$K_o$	=	The at-rest earth pressure coefficient.
$X$	=	Percent of layer thickness used for computing the at-rest stress state.

2. Compute the in situ deviator stress. Based on load computations made with elastic layer theory for the FWD testing load, deviator stresses can be computed at varying depths within each layer and the subgrade. Combining these load-related deviator stresses with the at-rest stresses results in an estimation of the actual in-field condition. This can be represented by equation 8.

$$\sigma_d = \sigma_d^1 + p_n (K_o^{-1} - 1) \quad (8)$$

where:

$\sigma_d^1$	=	Load-related deviator stress.
$\sigma_d$	=	In situ deviator stress simulating in-field conditions.

3. Compute the in situ bulk stress. Based on load computations made with elastic layer theory, vertical and horizontal stresses are computed within each layer from the applied load. Combining these load-related stresses with the existing or at-rest stresses results in an estimation of the actual in situ conditions. This can be represented by equation 9.

$$\theta = \sigma_1^1 + \sigma_2^1 + \sigma_3^1 + \sigma_v + 2p_n \quad (9)$$

$$\theta = \sigma_1^1 + \sigma_2^1 + \sigma_3^1 + [1 + 2K_o] [X D_n \gamma_n + \sum_{i=1}^{n-1} \gamma_i D_i] \quad (10)$$

where:

$\sigma^1_1, \sigma^1_2, \sigma^1_3$  = Principle stresses from an applied wheel load.  
 $\sigma_v$  = At-rest vertical stress from the pavement structure and/or embankment (subgrade).

Similar to establishing comparable temperatures for asphalt concrete mixtures, the backcalculated layer moduli for each unbound base/subbase layer and subgrade were used to identify the stress states to be used in the laboratory, such that the laboratory measured modulus equals the backcalculated value from deflection measurements. This is graphically demonstrated in figure 28 for the subgrade at GPS Site 481087.

Considering only those GPS section ends with low error terms and for which resilient modulus testing has been completed, the stress states were calculated at various depths in the pavement structure. As an example, figure 29 shows the change in stress state with depth for each layer in one test section. Backcalculated moduli were used for the ELSYM5 analysis to obtain vertical and lateral stresses at the surface of the subgrade, 15 cm (6 in), 30 cm (12 in), 45 cm (18 in) and 61 cm (24 in) into the subgrade representing the stresses applied by the FWD loads. For the unbound granular base and subbase layers, the mid-depth and quarter-points of the layer were used.

The depth of the rigid base below the subgrade was determined from the shoulder probes. The shoulder probe logs contained information as to the type of material up to 6 m (20 ft) below the surface of the subgrade. (Note: Shoulder probes were conducted some 90 m (295 ft) from the location for deflection measurements, so the subgrade could vary substantially between these locations.) The location where the subgrade material changed dramatically or where a water table was determined was designated and moduli were calculated for each layer. On the other side of the comparison, however, the laboratory test data contained moduli values for only one subgrade soil. Thus, the laboratory measured moduli were compared to the upper subgrade layer, because most laboratory tests were performed on soils recovered from the top 61 cm (24 in).

The at-rest stresses from the pavement layers were calculated and combined with the stresses computed beneath the FWD test loads. The assumptions used for the calculation of the at-rest stresses were:

## GPS Site 481087(2)

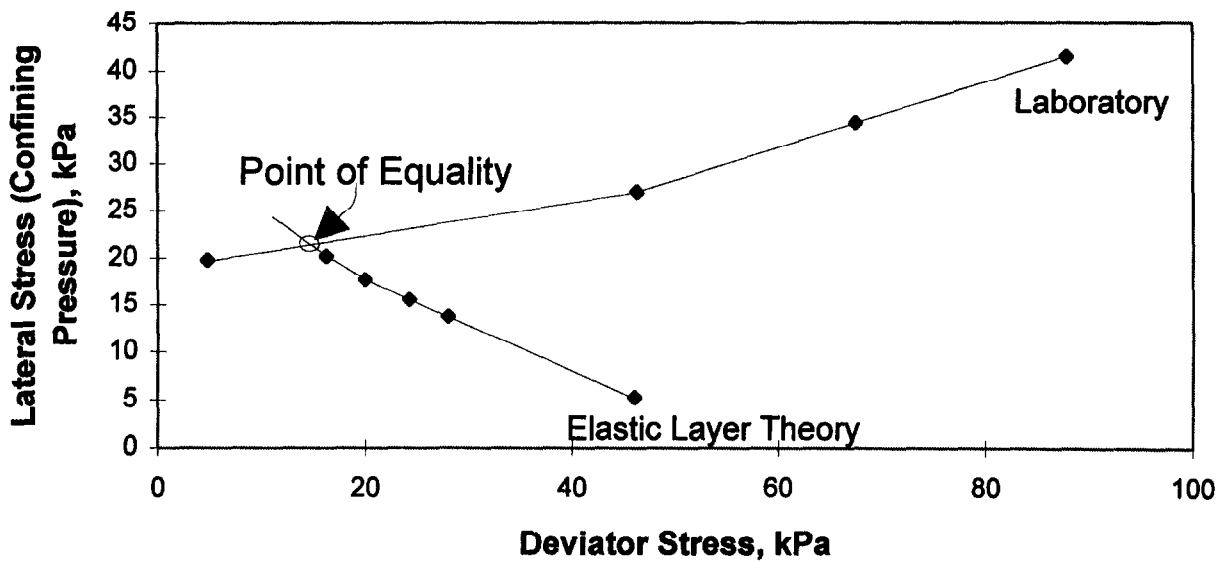
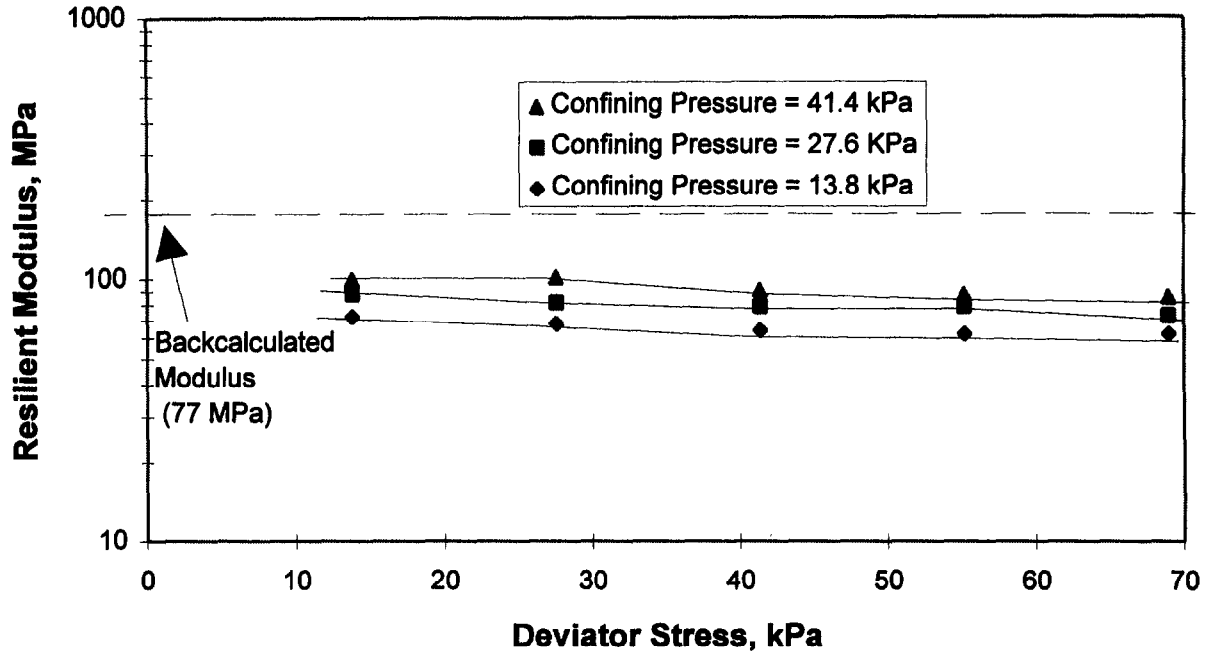


**Figure 28. Graphical illustration for procedure used to determine the stress states to be used in the laboratory so that the measured and backcalculated moduli are equal.**



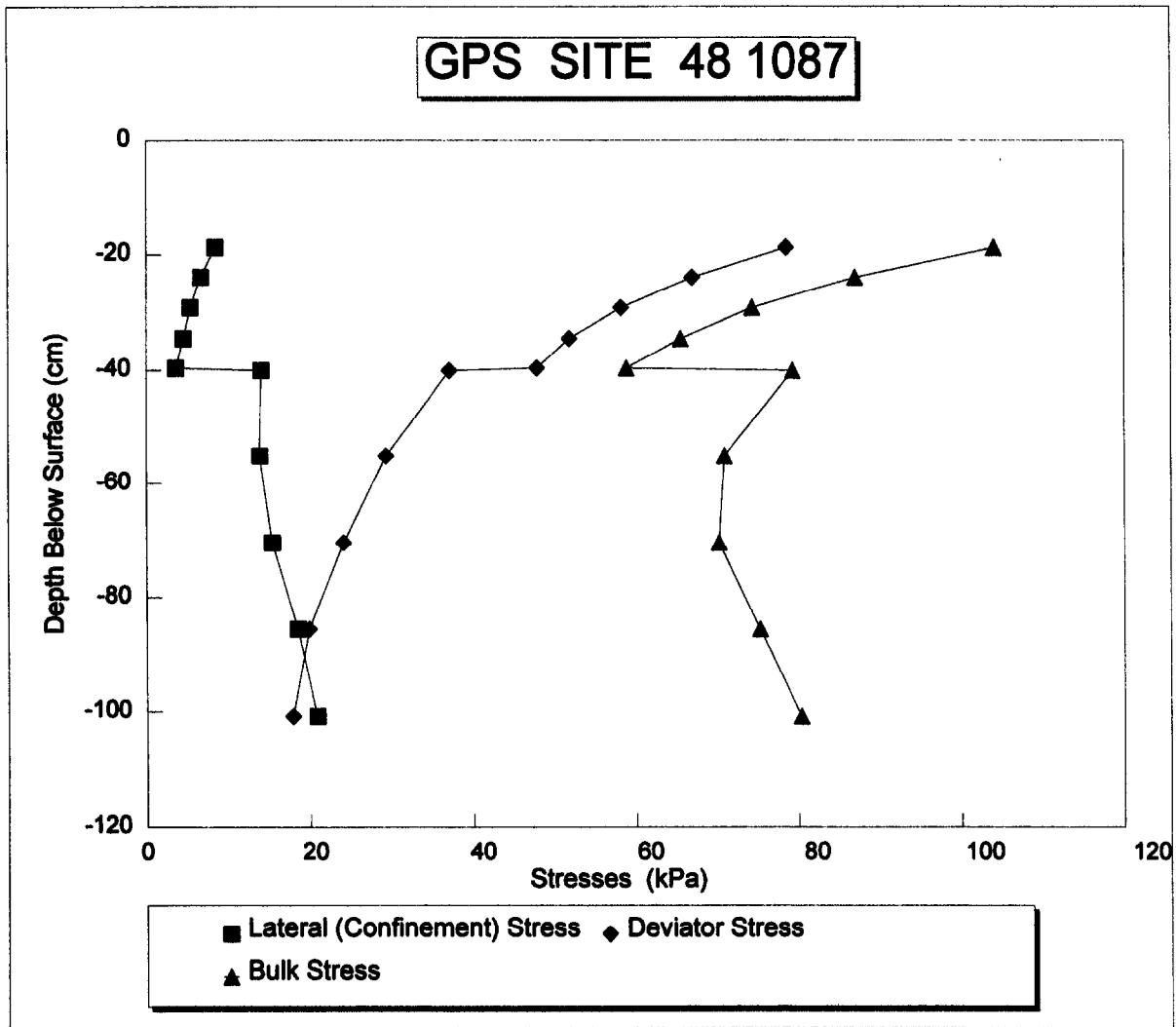


**Figure 29. Graphical illustration of the vertical profile of stresses in a layer for equating laboratory measured to backcalculated moduli.**

- The at-rest earth pressure coefficient for cohesive clay is a function of Poisson's ratio ( $\nu$ ) and is:

$$K_0 = \nu/(1-\nu) \quad (11)$$

- The at-rest earth pressure coefficient for noncohesive soils is a function of the angle of shearing resistance ( $\phi$ ) and is:

$$K_0 = 1 - \sin\phi \quad (12)$$

As Poisson's Ratio and the angle of shearing resistance were not measured, the following values were assumed for different soils: clay,  $\nu = 0.45$ ; silt,  $\phi = 30^\circ$ ; sand,  $\phi = 35^\circ$ ; gravel,  $\phi = 40^\circ$ .

The layer thicknesses and densities were used to calculate a bulk and deviatoric stress for the at-rest condition. These at-rest stresses were combined with the load-related stresses induced by the FWD during testing. The  $K$  values obtained from the linear regression analysis using the laboratory test values for differing stress states were used with the total bulk and deviatoric stresses to calculate the resilient moduli of each unbound layer and the subgrade. The results from the regression analysis at the laboratory repeated-load resilient modulus data are provided in table 10.

**Table 10. Regression of K values based on stress states and resilient moduli using equation 5.**

		<b>K1</b>	<b>K2</b>	<b>K3</b>	<b>r<sup>2</sup></b>
<b>Silt</b>	<b>Average</b>	<b>426</b>	<b>0.42</b>	<b>-0.23</b>	<b>0.87</b>
	<b>Maximum</b>	<b>838</b>	<b>0.66</b>	<b>0.05</b>	<b>0.98</b>
	<b>Minimum</b>	<b>136</b>	<b>-0.05</b>	<b>-0.57</b>	<b>0.09</b>
	<b>Std. Dev.</b>	<b>187</b>	<b>0.17</b>	<b>0.15</b>	<b>0.18*</b>
<b>Clay</b>	<b>Average</b>	<b>594</b>	<b>0.21</b>	<b>-0.19</b>	<b>0.84</b>
	<b>Maximum</b>	<b>2039</b>	<b>0.53</b>	<b>0.30</b>	<b>0.99</b>
	<b>Minimum</b>	<b>87</b>	<b>-0.20</b>	<b>-0.55</b>	<b>0.23</b>
	<b>Std. Dev.</b>	<b>472</b>	<b>0.16</b>	<b>0.22</b>	<b>0.18</b>
<b>Sand</b>	<b>Average</b>	<b>598</b>	<b>0.44</b>	<b>-0.12</b>	<b>0.87</b>
	<b>Maximum</b>	<b>3494</b>	<b>0.99</b>	<b>0.89</b>	<b>0.99</b>
	<b>Minimum</b>	<b>103</b>	<b>-0.33</b>	<b>-0.43</b>	<b>0.08</b>
	<b>Std. Dev.</b>	<b>351</b>	<b>0.21</b>	<b>0.16</b>	<b>0.15</b>
<b>Gravel</b>	<b>Average</b>	<b>836</b>	<b>0.23</b>	<b>-0.08</b>	<b>0.72</b>
	<b>Maximum</b>	<b>3172</b>	<b>0.59</b>	<b>0.67</b>	<b>0.98</b>
	<b>Minimum</b>	<b>229</b>	<b>-0.27</b>	<b>-0.33</b>	<b>0.15</b>
	<b>Std. Dev.</b>	<b>710</b>	<b>0.22</b>	<b>0.23</b>	<b>0.27</b>
<b>Base</b>	<b>Average</b>	<b>869</b>	<b>0.65</b>	<b>-0.04</b>	<b>0.98</b>
	<b>Maximum</b>	<b>2323</b>	<b>1.07</b>	<b>0.61</b>	<b>1.00</b>
	<b>Minimum</b>	<b>250</b>	<b>-0.18</b>	<b>-0.33</b>	<b>0.38</b>
	<b>Std. Dev.</b>	<b>292</b>	<b>0.15</b>	<b>0.13</b>	<b>0.07</b>

\*Note: The standard deviation of the r<sup>2</sup> values from individual test specimens and determined for how well equation 5 fits the laboratory test results.

Unfortunately, there were numerous GPS section ends (almost 75 percent of the section ends) for which the backcalculated values significantly exceed those values measured in the laboratory, such that there is no stress state for which the two moduli are equal. Thus, specific depths were selected, based on the results from other research studies (7), for computing the in situ stress state within each unbound pavement layer. These depths were 45 cm (18 in) into the subgrade and/or embankment soils and at the quarter-depth for the base and subbase layers. At these depths, the laboratory total resilient modulus was determined for the subgrade and any unbound base/subbase layer in the pavement structure. These laboratory moduli were compared to the

backcalculated values and significant differences were found. In fact, the ratio of the laboratory to backcalculated moduli,  $M_R(\text{Lab})/E$  (FWD), varied from 0.1 to 3.5.

These differences were first reviewed by material type, but without any conclusive results, other than that the ratios are independent of material type (i.e., clay, silt, gravel, sand, crushed stone). However, systematic differences in the ratios [ $M_R/E$  (FWD)] were noted by pavement type and layer type. The following summarizes the average  $M_R/E$  (FWD) ratios for specific conditions and pavement types.

Layer Description	Difference Between the Laboratory and Backcalculated Moduli at Equivalent Stress States, $M_R(\text{Lab})/E$ (FWD)		
	Mean	Standard Deviation	Coefficient of Variation, %
Granular Base/Subbase Under a PCC Surface	1.32	0.978	74.1
Granular Base/Subbase Above a Stabilized Material (Sandwich Sections)	1.43	1.14	79.9
Granular Base/Subbase Under an Asphalt Concrete Surface/Base	0.62	0.271	43.8
Subgrade Soil Under a Stabilized Subgrade (Sandwich Section)	0.75	0.095	12.7
Subgrade Soil Under a Pavement Without a Granular Base/Subbase	0.52	0.180	34.6
Subgrade Soil Under a Pavement With a Granular Base/Subbase	0.35	0.183	52.2

Thus, adjustments or correction factors must be applied to the laboratory values for predicting the structural response of pavement structures to wheel loads. Reasons for these differences are believed to be related to the inability of the laboratory tests to simulate the actual confinement and effect of the surrounding materials (laterally and vertically) on the in situ materials' response.

Figures 30 and 31 show the comparison of backcalculated and laboratory measured resilient moduli for different layers using the ratios (correction factors) listed above. As shown, there is much more variability for the unbound granular base/subbase materials than for the subgrade soils. More importantly, since most of the pavement design procedures have been based on laboratory measured values (including the AASHTO Design Guide), backcalculated values should be adjusted for use in the pavement design procedures, such as the AASHTO Design Guide.

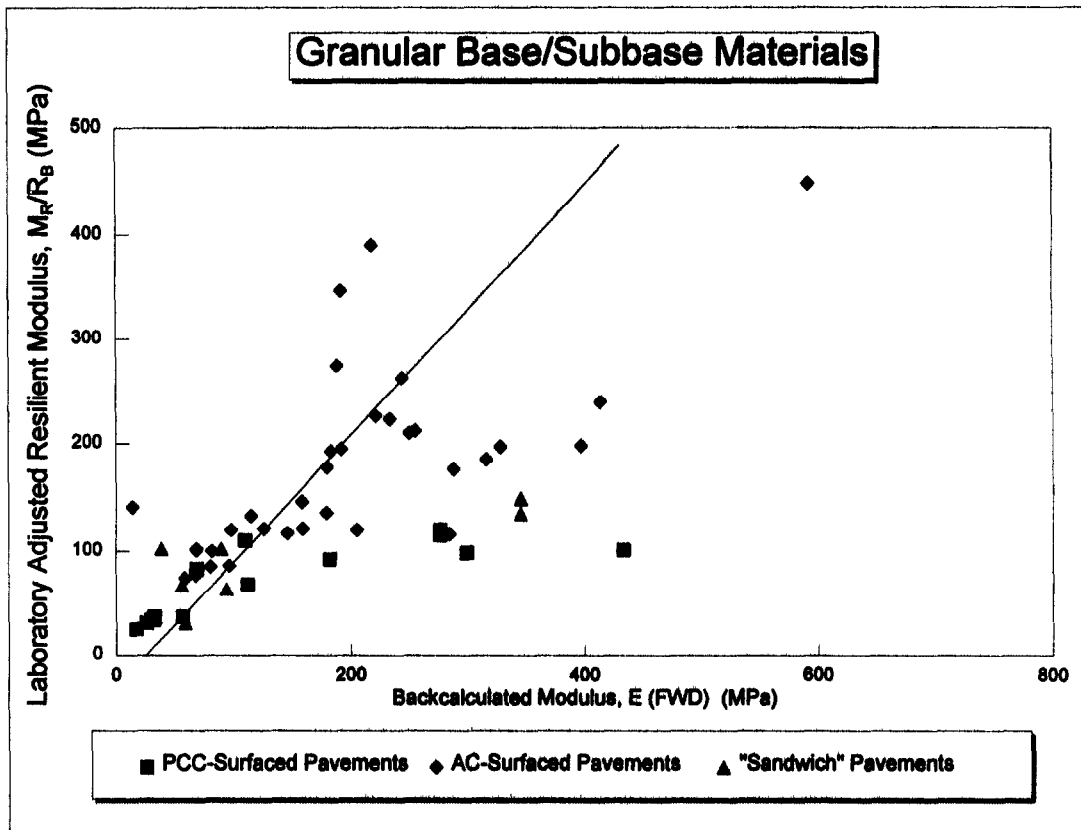


**Figure 30. Graphical comparison of backcalculated and laboratory measured moduli for the base and subbase layers.**

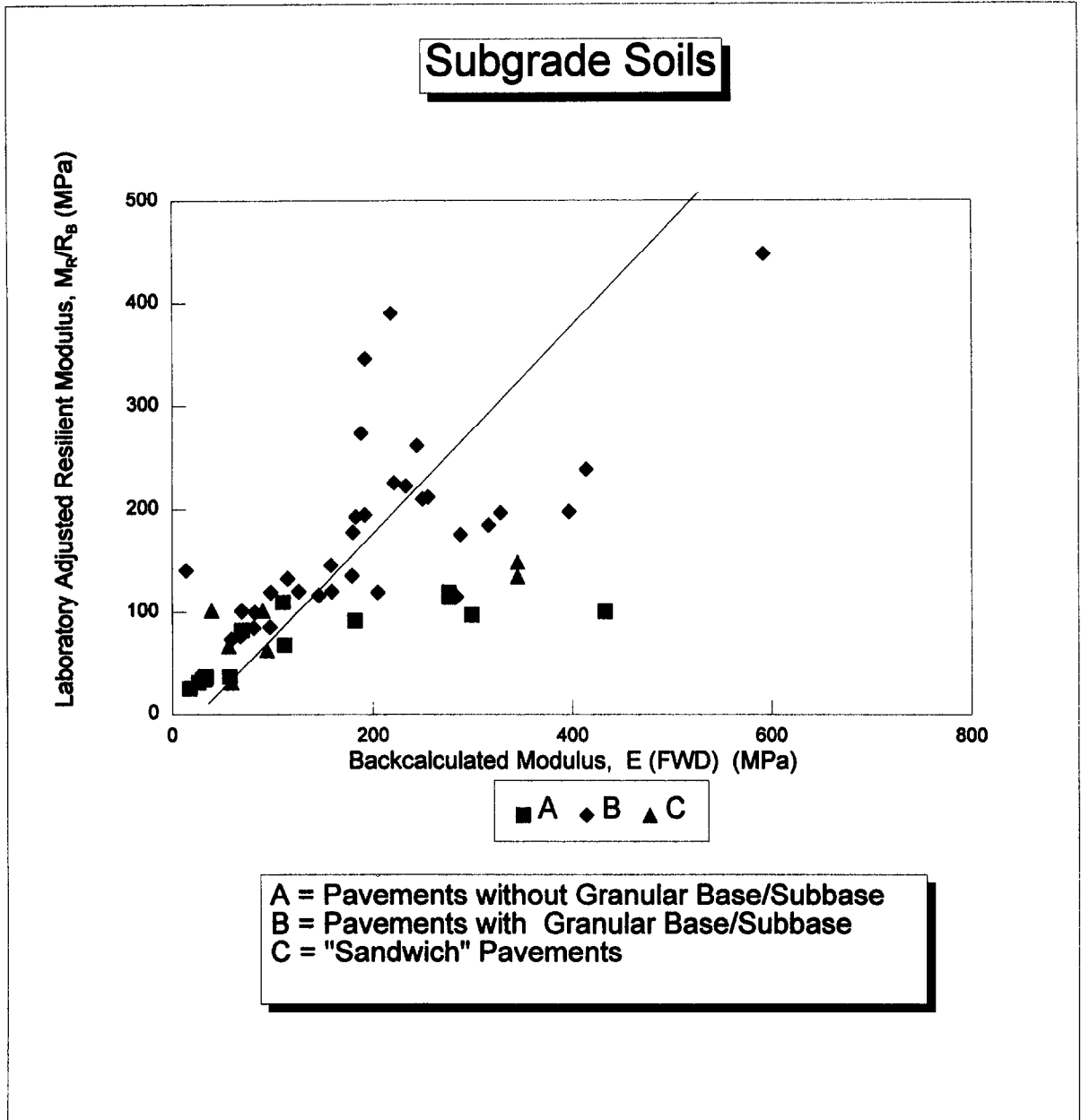


**Figure 31. Graphical comparison of backcalculated and laboratory measured moduli for subgrade soils.**

**Observation:** The stress states determined 45 cm (18 in) into the subgrade and at the quarter-point depth of the base and subbase layers appear to be reasonable for determining the resilient moduli of unbound materials and soils for predicting the structural response of pavements.

**Observation:** Backcalculated layer moduli are consistently higher than laboratory measured moduli at equivalent stress states, and adjustments or corrections must be applied in equating in situ moduli calculated from deflection basin data to moduli measured in the laboratory.

**4.3.4 Stress Sensitivity of Pavement Structure.** To estimate the change in the load-response characteristics of the unbound base materials and subgrade, elastic moduli were calculated for each pavement layer for each load level used in the deflection testing program. This change in the load response or modulus of these materials can be used to estimate the stress sensitivity of the pavement structural layers and subgrade. Examples of the modulus calculated for each load level are given in table 11. As shown, the modulus of the unbound materials increase with increasing load, as expected for coarse-grained materials, and decreased for fine-grained materials. In other cases, the modulus of the base and subgrade remain relatively constant and the modulus of the asphalt concrete surface increases or decreases with load level. Dense-graded asphalt concrete mixtures are not generally considered to be stress sensitive or nonlinear, with the possible exception at high temperatures (40 °C [104 °F] or greater). This nonlinear behavior can be attributed to other factors or conditions, which include:

- The pavement is still “seating” between the surface and unbound base resulting in higher moduli with increasing loads;
- The pavement is beginning to harden or stiffen as a result of surface irregularities, and/or the plastic properties of the pavement structures resulting in the higher moduli with increasing FWD loads;
- The pavement is beginning to soften or weaken as a result of microcracking from the heavier loads and/or viscoelastic properties of the pavement structure, resulting in lower moduli with increasing loads; or
- Questionable backcalculation results, even though tolerances on deflections at the various sensors were satisfied.

Data from the pavement sections included in table 11 were used to evaluate and compare the stress sensitivity measured with the FWD and backcalculated with elastic layer theory to the stress sensitivity as measured in the laboratory using repeated-load triaxial compressions tests. Those unbound pavement layers showing either a softening or hardening effect with increases in the applied load were found to have the same behavioral characteristics as measured in the laboratory, providing some support for use of repeated-load resilient moduli and equation 5.

**4.3.5 Dissipated Work Considerations.** The elastic and viscoelastic properties of the pavement structure can be illustrated by reviewing the deflection-time history data measured with the FWD. Figures 32 through 34 show the different types of pavement response characteristics measured with the FWD. Figure 32 illustrates a pavement section that is highly elastic. In other words, most or all of the induced deflection is recovered immediately after the load pulse reaches zero. On the other hand, Figures 33 and 34 show pavements which are viscoelastic. A viscoelastic pavement will take time to recover the induced deflection after the load pulse reaches zero or, stated differently, the recovery of deflection is time-dependent. The elastic and viscoelastic responses of the pavement structure, as measured by the FWD, may begin to explain those differences noted between the laboratory and backcalculated moduli.

**Observation:** The deflection-time data measured during FWD testing can be used to estimate the elastic and viscoelastic response characteristics of both PCC- and asphalt concrete-surfaced pavements.

Another interesting point to note is the difference in dissipated work, as measured by the FWD, for different types of pavement cross sections. Figures 32 through 34 show the dissipated work as measured with the FWD. This becomes an extremely important parameter in evaluating pavement structures for determining remaining life and rehabilitation requirements. It is believed that the dissipated work measured with the FWD is proportional, if not directly related, to pavement damage for fatigue cracking and other types of distress, excluding permanent deformation and/or rutting that is confined to the surface layer. The use of the dissipated work concept is discussed in greater detail in chapter 8.

**Observation:** Dissipated work can be measured with the FWD. Dissipated work was found to be dependent on the pavement cross section and material types.



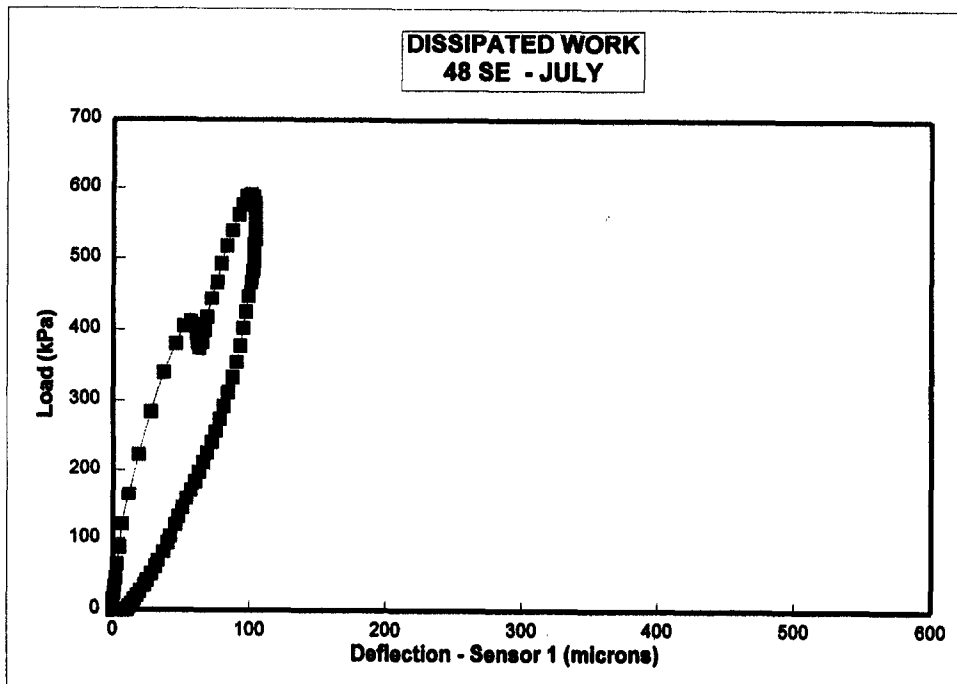
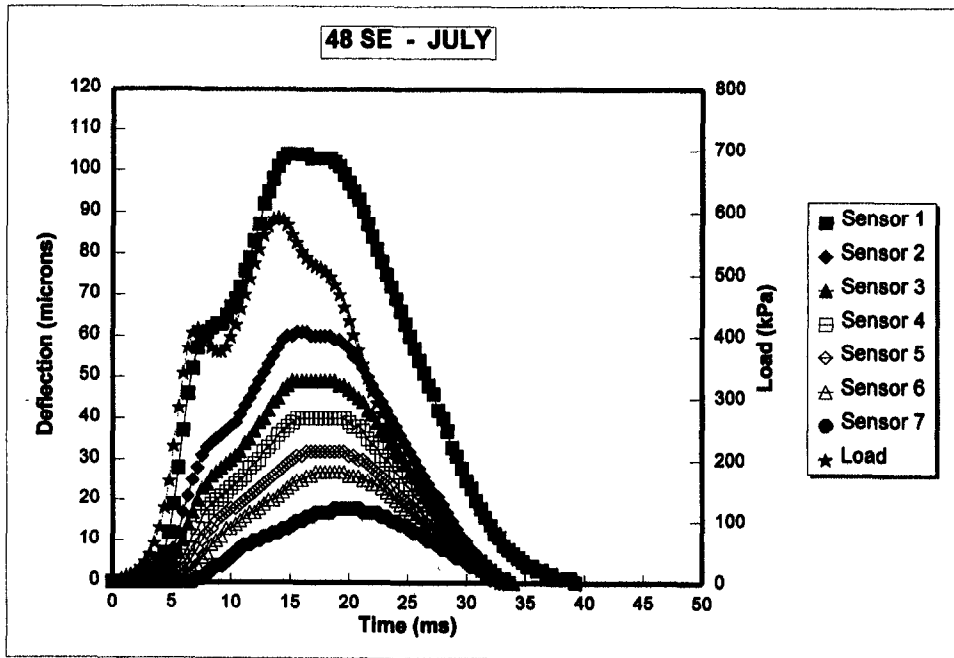


**Figure 32. Typical deflection-time history data collected during FWD testing and the associated dissipated work for a GPS site that has elastic behavior.**

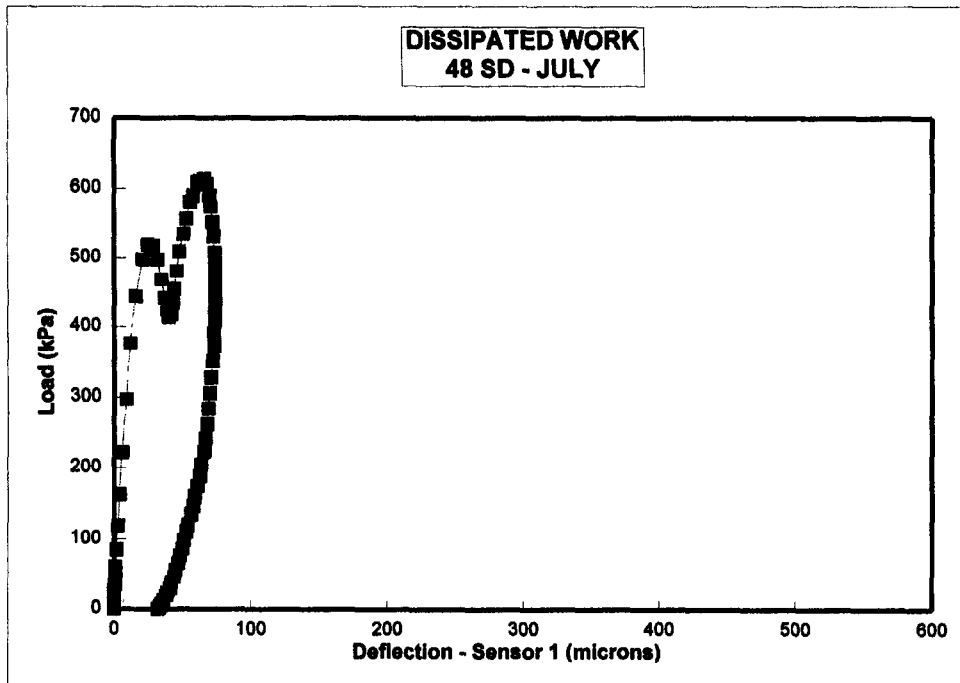
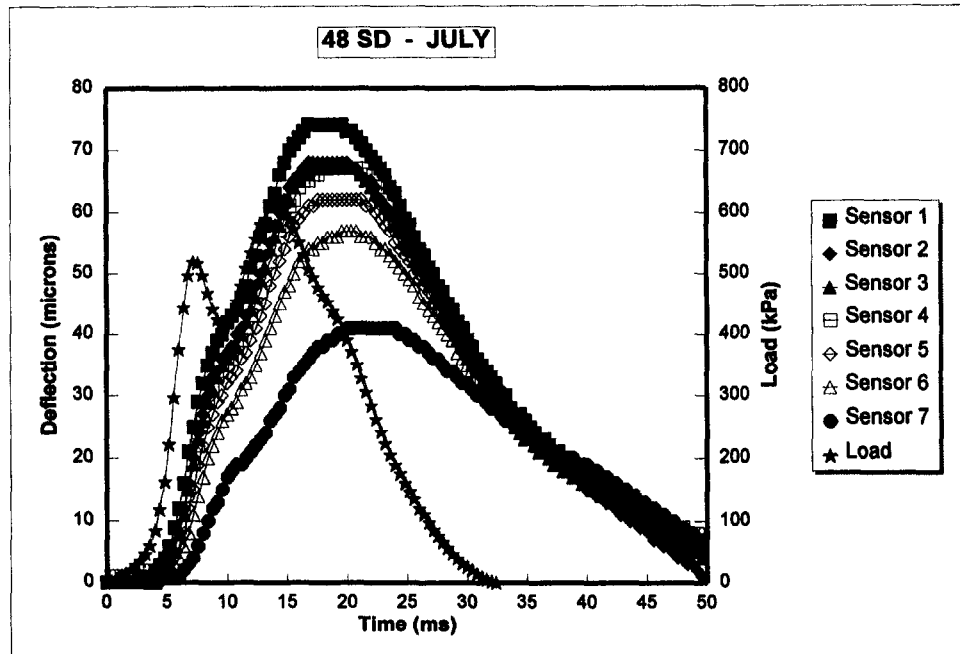


**Figure 33. Typical deflection-time history data collected during FWD testing and the associated dissipated work for a GPS site that has viscoelastic behavior.**

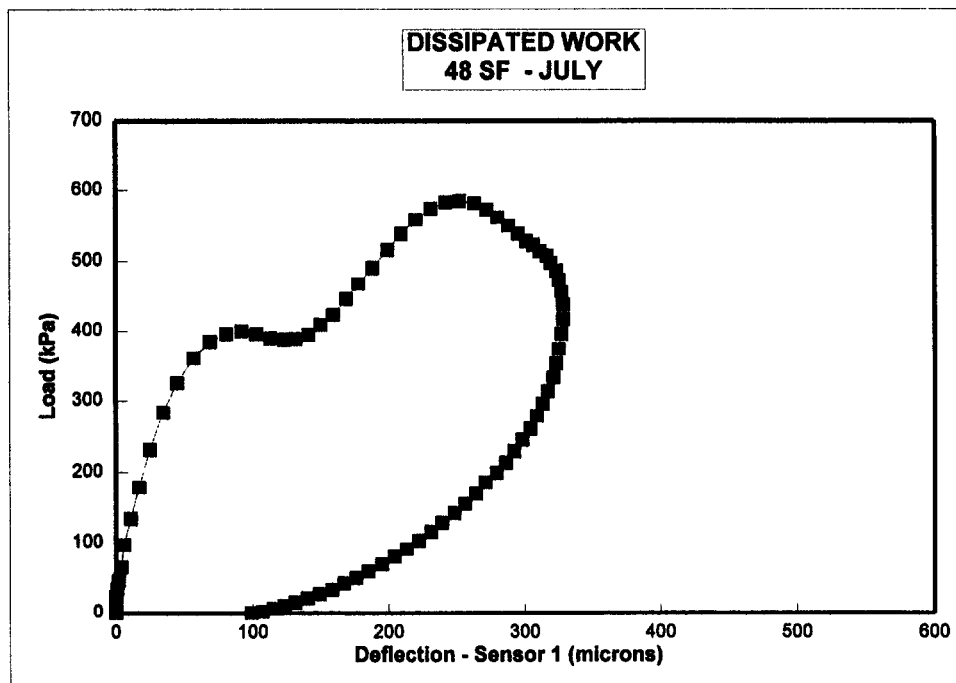
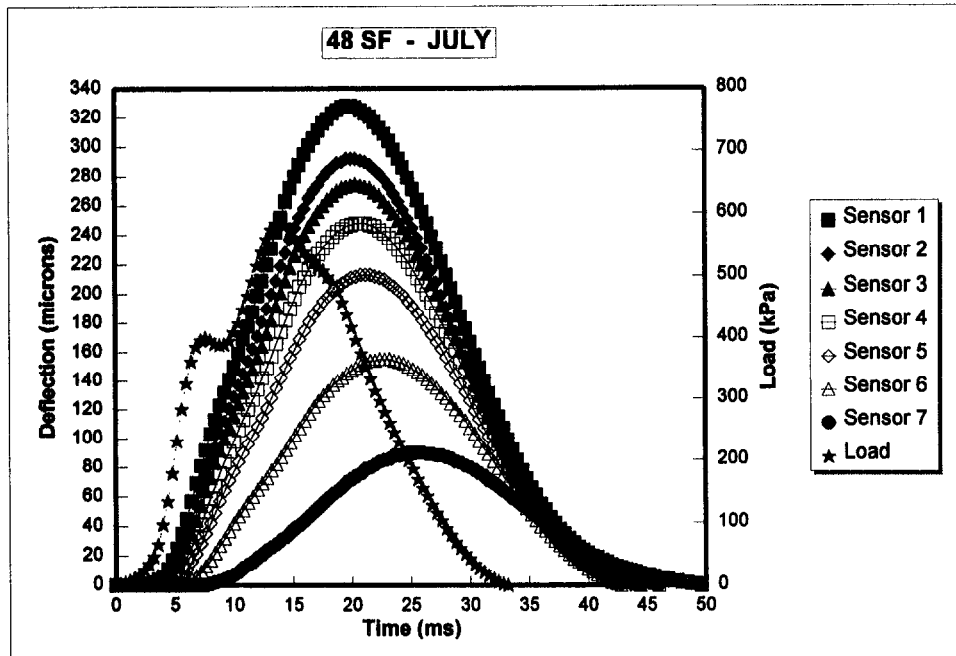


**Figure 34. Typical deflection-time history data collected during FWD testing and the associated dissipated work for a GPS site that has viscoelastic and plastic behavior.**

**Table 11. Example of backcalculated layer moduli for the different FWD load levels used, ksi <sup>(3)</sup>.**

GPS Site	Load Level <sup>(3)</sup> , lb	Pavement Layer				
		Layer 1 Surface	Layer 2	Layer 3	Layer 4	Layer 5
011001 (2)*		HMAC <sup>(1)</sup>	Granular Base	Granular Subbase	Subgrade	Subgrade
	6,000	1,575	36.1	27.9	48.2	28.9
	9,000	2,054	35.9	34.2	46.6	24.1
	12,000	2,040	50.1	29.3	44.1	20.2
	16,000	2,155	61.6	39.7	33.9	43.4
011019 (2)		HMAC	Granular Subbase	Subgrade	Subgrade	
	6,000	934	5.2	88.6	14.1	
	9,000	912	4.6	89.4	13.2	
	12,000	920	4.2	86.7	12.2	
	16,000	1,031	3.3	120.0 <sup>(2)</sup>	10.1	
011019 (2)		HMAC	Granular Subbase	Subgrade	Subgrade	
	6,000	919	4.8	52.7	16.3	
	9,000	1,053	5.4	45.2	18.1	
	12,000	907	5.6	31.2	19.5	
	16,000	1,056	5.2	35.8	21.5	
014126 (1)		HMAC	Granular Subbase	Subgrade	Subgrade	
	6,000	839	23.9	125.4	13.3	
	9,000	842	13.6	126.6	13.0	
	12,000	807	16.4	118.1	8.2	
	16,000	841	17.6	98.3	9.4	

\*Number in ( ) designates the GPS section end. A (1) represents the approach side of the site, and a (2), the leave side.

- (1) For some of the sites, the elastic modulus of the HMAC surface layer was found to consistently decrease or increase with load level. The modulus of dense-graded asphalt concrete mixtures is generally considered to be stress-independent, in relation to the other pavement unbound materials. However, this observation from the backcalculation process is not uncommon.
- (2) Designates a value that represents the upper limit used in the backcalculation process for the material in question.
- (3) The layer moduli backcalculated with both the MODULUS and WESDEF programs are provided in English units (psi); so the results are presented in English units. The conversion to SI units are:  $\text{psi} \times 6.895 \times 10^3 = \text{Pa}$  and  $\text{lbs.} \times 4.448 = \text{N}$ .

**Table 11. Example of backcalculated layer moduli for the different FWD load levels used, ksi<sup>(3)</sup> (continued).**

GPS Site	Load Level <sup>(3)</sup> , lb	Pavement Layer				
		Layer 1 Surface	Layer 2	Layer 3	Layer 4	Layer 5
026010 (2)		HMAC	Granular Base	Granular Subbase	Subgrade	Subgrade
	6,000					
	9,000	1,406	11.0	800.0	37.2	56.8
	12,000	1,560	19.6	601.3	40.0	56.1
	16,000	1,577	24.0	188.7	45.3	39.9
053071 (2)		HMAC	Granular Subbase	Subgrade	Subgrade	
	6,000	2,147	593.4	82.2	57.9	
	9,000	1,012	678.5	50.2	45.6	
	12,000	1,043	520.9	41.9	40.1	
	16,000	783	945.6	20.5	49.1	
121370 (2)		HMAC	Granular Subbase	Subgrade	Subgrade	Subgrade
	6,000	3,093	28.5	9.0	154.4	19.7
	9,000	3,591	31.9	8.6	164.0	17.8
	12,000	4,274	37.8	8.7	192.9	16.4
	16,000	5,366	44.4	8.4	1,532.3	8.9
124136 (1)		HMAC	Granular Subbase	Subgrade	Subgrade	Subgrade
	6,000	2,271	28.0	69.1	55.0	27.8
	9,000	2,917	30.7	64.0	44.7	30.3
	12,000	3,371	35.8	64.3	37.7	34.4
	16,000	3,949	41.1	84.4	37.4	42.8
283083 (2)		HMAC	Treated Base	Subgrade	Subgrade	
	6,000	8,206	430.8	7.0	20.7	
	9,000	6,082	516.0	8.3	17.5	
	12,000	6,617	532.8	7.7	19.9	
	16,000	4,161	675.9	8.8	20.7	

**Table 11. Example of backcalculated layer moduli for the different FWD load levels used, ksi<sup>(3)</sup> (continued).**

GPS Site	Load Level <sup>(3)</sup> , lb	Pavement Layer				
		Layer 1 Surface	Layer 2	Layer 3	Layer 4	Layer 5
351002 (1)		HMAC	HMAC	Granular Base	Subgrade	Subgrade
	6,000	3,776	329.4	16.2	54.3	31.1
	9,000	901	389.6	24.6	39.3	28.9
	12,000	528	460.0	20.7	37.0	26.7
	16,000	570	451.8	25.4	37.9	30.2
294036 (2)		PCC	Granular Base	Subgrade	Subgrade	
	6,000					
	9,000	4,833	100.0 <sup>(2)</sup>	4.1	18.4	
	12,000	4,484	100.0 <sup>(2)</sup>	4.4	16.9	
	16,000	4,415	100.0 <sup>(2)</sup>	7.5	14.5	

## 5. MOISTURE EFFECTS AND DRAINAGE COEFFICIENTS

Premature distress or accelerated deterioration in both flexible and rigid pavements is generally caused by exposure to heavy truck traffic when the pavement layers are in a saturated condition. Saturation of underlying foundation materials generally results in a decrease in strength or the materials inability to support heavy truck loads. Other potential problems associated with saturation of the pavement and subgrade foundation include popouts, differential expansion, frost and freeze-thaw damage, erosion or piping of fine-grained materials creating a loss of support, and stripping of the asphalt binder from the aggregates.

Rapid drainage of the pavement structural section is essential to minimize the length of time the structural section is in a saturated condition. The rapid removal of water from the structural section generally requires the inclusion of a positive drainage system. Drainage of water from pavements is an important consideration in pavement design. Unfortunately, current methods of design have often resulted in base courses that do not drain well because water can enter the pavement structure several different ways (i.e., through cracks, joints, or pavement infiltration, or as groundwater from high water table).

Prior editions of the 1986 *AASHTO Guide for Design of Pavement Structures* have not directly treated the effects of drainage on pavement performance. Drainage effects were only considered in terms of reducing subgrade soil and base strength for flexible pavement design, and the effect of moisture on strength and base erodability for rigid pavement design. The 1986 *AASHTO Guide for the Design of Pavement Structures* included drainage directly as one of the design inputs for both flexible and rigid pavements. The guide considers drainage for flexible pavements through the inclusion of coefficients that account for the effect of moisture on base and subbase strength. Drainage (specifically moisture damage) is considered for the subgrade by seasonally adjusting the subgrade moduli and converting these values to an average annual value based on damage concepts. Determination of the design subgrade resilient modulus is discussed in more detail in chapter 6. A coefficient that adjusts the stress in the PCC slab is included in the rigid pavement design equation. This coefficient considers the effect of moisture on subgrade strength and subbase erodability and adjusts the PCC slab stress accordingly for the design equation.

When designing a new pavement with the AASHTO Design Guide, drainage effects are considered in the design process based on two separate criteria. The first criterion is how well the pavement structure, including the subgrade, drains water away from the pavement. This *quality of drainage* is determined by the estimated time required for the water to drain from the pavement. The second criterion is the estimated percent time that the pavement structure is

exposed to moisture levels approaching saturation. Coefficients are selected on the basis of these two criteria.

Design of flexible pavements provides for layer thickness adjustment for a drainable layer by increasing the design coefficient of that layer. This process effectively reduces the total required thickness for the flexible pavement. Those drainage coefficients recommended in the AASHTO Design Guide are shown in table 12. The guide also recommends drainage coefficient values to be a function of the quality of the drainage and the percent of time during the year that the pavement structure is expected to be exposed to moisture levels approaching saturation. As stated in the guide, the coefficients are dependent on the average yearly rainfall and the prevailing drainage conditions. More importantly, these drainage coefficient values apply only to the effects of drainage on untreated base and subbase layers. Therefore, one of the objectives of this research activity was to investigate the effects of moisture on the drainage coefficients and to determine the effect of inadequate drainage on pavement performance. Values for the different materials were calculated to minimize the difference between the design equation results and the actual observations for the change in pavement distresses and performance; performance being defined by IRI values.

Analysis of the existing design procedure, with relation to drainage, has been completed using data from the FHWA LTPP National Information Management System as it existed in the Spring of 1996. Original development of both the rigid and flexible pavement design coefficients for incorporation of drainage can be found in appendix DD, volume II of the guide. Guidelines for application of the coefficients to the design equations can be found in volume I, sections 1.8 and 2.4.1.

**Table 12. AASHTO drainage coefficients,  $m_i$  (1).**  
 $S_N = A_1 D_1 + a_2 D_2 m_2 + a_3 D_3 m_3$

Quality of Drainage	Percent of Time Pavement Structure is Exposed to Moisture Levels Approaching Saturation			
	Less than 1%	1-5%	5-25%	Greater Than 25%
Excellent	1.40-1.35	1.35-1.30	1.30-1.20	1.20
Good	1.35-1.25	1.25-1.15	1.15-1.00	1.00
Fair	1.25-1.15	1.15-1.05	1.00-0.80	0.80
Poor	1.15-1.05	1.05-0.80	0.80-0.60	0.60
Very Poor	1.05-0.95	0.95-0.75	0.75-0.40	0.40



## 5.1 Drainage Systems

The AASHTO Design Guide discusses various drainage conditions that can exist with pavements and the types of positive drainage systems that can be incorporated to help alleviate drainage problems. These discussions can be found in volume II of the guide and specifically appendix AA. In summary, the guide divides problem drainage conditions into the following two categories:

1. Moisture induction into the pavement through cracks and joints over an impervious subgrade that causes the pavement to exist in a “bathtub” condition.
2. Moisture introduced into the subgrade through high groundwater table or free water existing in pavement due to temporary lower layer saturated conditions.

**5.1.1 Base/Subbase Layers.** Moisture that is allowed to stay in the base and subbase of a pavement and does not freely drain can cause a myriad of problems in terms of overall pavement performance. These include:

1. Breakup of surface layers from pore water pressures,
2. Premature aging and stripping of asphalt pavements,
3. Increased distress development from loss of underlying strength,
4. Increased faulting of concrete pavement joints and cracks, and
5. Erosion of underlying base layers.

Traditionally, design of pavement structures has primarily focused on achieving specific volumetric properties and strength and not on the concept of draining water from the structure. If excess water or moisture was a problem, then the common fix seemed to be adding layer thickness instead of removing the detrimental water.

**5.1.2 Subgrade Layers.** Moisture contained in the subgrade usually is caused by a high groundwater table or the fact that the subgrade will not freely let go of the water (capillary action) in a generally wet environment. If a pavement is properly designed and the moisture in the subgrade does not vary that much over the year, this type of problem may not be that

significant. However, most environments fluctuate, which, in turn, causes a change in the groundwater table and/or the amount of moisture held within the subgrade layer.

Increases in moisture contained in a subgrade can cause a significant loss of underlying pavement strength and will also cause heaving of clay soils. This heaving will increase pavement roughness and may also cause an increased rate of pavement deterioration. Also, ice lenses can form in the unbound pavement layers when water is captured in these layers and freezing occurs. This phenomenon can be very detrimental to the pavement surface layer and will cause an overall loss of strength throughout the pavement's life.

These problems can usually be reduced or avoided entirely through the use of a positive internal drainage system. Typically, these drainage systems include all or part of the following:

- Underdrain pipes,
- Geotextiles (i.e., filter fabrics), and
- Open-graded aggregates (both treated and untreated).

In general, design of these systems consist of selecting the most cost-effective means of removing water from a particular pavement structure. A single material or a combination of materials may be used in developing a positive drainage system, depending on the economics of the situation and the materials available.

## **5.2 Data Used in Analyses**

LTPP data extracted from the NIMS (including several of the Seasonal Monitoring Program (SMP) test sections) were used in this analysis of drainage effects. Several data elements were used including the actual and optimum moisture contents for the underlying pavement layers (including the subgrade), the precipitation at the pavement site and other pavement layer materials data. Table 1 identified those data elements required for this research activity. Some of the more important material properties required were unavailable, so other properties and data elements were used. For example, permeability tests were not included in the SHRP test program for the GPS sites. Thus, permeabilities are unavailable to confirm that drainable bases are, in fact, drainable. For this case, the gradations were reviewed to determine if the aggregate size distribution was compatible with those used for drainable bases.

Sections were divided based on whether or not they had a positive drainage system in place and then were further subdivided to see if other factors influenced the effect of drainage on performance. Unfortunately, there are relatively few GPS sections with a positive drainage

system incorporated in the structure. The limited number of available sites severely restricted the analysis to determine effects on pavement performance. These GPS sites are listed in table 13.

### **5.3 Moisture Effects on Pavement Performance**

The performance, as defined by the IRI values, fatigue cracking and rut depths, of those GPS sites with subsurface drainage features were compared to the performance of GPS sites with similar conditions, but without drainage features. Due to the limited number of pavements with drainage systems and the diversity of the onsite conditions and materials included in the LTPP data base, no statistically sound conclusions could be made regarding the benefit of the drainage system. Therefore, the data analysis for this activity took a much closer look at the condition of the materials/layers within the pavement structure. These conditions or parameters included changes in moisture content and densities from the optimum values, and the resilient modulus of the pavement layers.

Figures 35 through 38 illustrate the change in moisture content from the optimum values for various GPS sections with and without drainage separated by environmental condition and by GPS experiment number. As expected, pavements with different environmental conditions and pavement base layers increase and decrease above the optimum moisture contents. More importantly, the distribution of these properties is comparable between pavements with and without positive drainage systems. As these results were inconclusive, these data were additionally analyzed using only the GPS seasonal sites to evaluate the effect of rainfall on the moisture contents of the pavement materials and subgrade soils over time in relation to the optimum condition and resilient moduli.

Sample results are shown for two GPS seasonal sites with very different environmental conditions on figures 39 through 44. The one clear trend noted for these two sites was that the moisture contents of the base materials were generally well above the optimum content, while the moisture content for the subgrade soils experienced much less change in moisture content from the optimum. While this was not always the case for all other pavements, it does appear to be a general trend. These graphs indicate that as precipitation increases, there are generally increases in the moisture contents of the unbound base and subgrade. However, there are not clear trends when comparing the backcalculated modulus and precipitation or moisture. In other words, those sites with higher moisture contents with relation to optimum are not statistically related to areas of high rainfall.

**Table 13. Listing of GPS sites that contain some type of drainage system.**

State Code	SHRP ID	Drainage System	State Code	SHRP ID	Drainage System
1	1011	4	17	5843	2
1	3028	4	17	5854	2
1	4007	4	17	5869	2
1	4073	2	17	5908	7
1	4129	4	17	9267	2
1	6012	4	18	1028	2
6	2002	2	18	1037	2
6	2053	6	18	2008	7
6	3005	2	18	3003	2
6	3013	2	18	3031	2
6	3019	2	18	4021	6
6	3024	2	18	4042	2
6	3030	2	18	5022	4
6	9107	2	18	5043	2
9	4008	2	18	5518	2
11	1400	4	18	5538	2
12	3811	2	18	6012	2
12	4057	6	18	9020	7
12	4059	2	19	3009	2
12	4109	2	19	3028	2
13	3011	4	19	3033	2

- \*2 = Longitudinal Drains
- 3 = Transverse Drains
- 4 = Drainage Blanket
- 6 = Drainage Blanket w/  
Longitudinal Drains
- 7 = Other

**Table 13. Listing of GPS sites that contain some type of drainage system (continued).**

State Code	SHRP ID	Drainage System	State Code	SHRP ID	Drainage System
13	3015	2	19	5042	2
13	3016	2	19	9116	2
13	3017	4	19	9126	2
13	3018	4	20	4016	3
16	3017	7	23	1009	2
16	6027	7	23	1026	2
16	9032	4	24	1634	4
16	9034	4	24	2401	2
17	1003	2	24	2805	2
17	4074	2	26	1004	2
17	4082	2	26	1013	2
17	5020	2	26	3068	2
17	5151	2	26	4015	2
17	5423	2	26	7072	2
17	5453	2	26	9029	2
26	9030	2	41	7025	2
27	5076	2	42	1597	2
27	6064	2	42	1599	2
27	6250	2	42	1605	2
27	6300	2	42	1606	2
28	9030	2	42	1608	2

\*2 = Longitudinal Drains

3 = Transverse Drains

4 = Drainage Blanket

6 = Drainage Blanket w/  
Longitudinal Drains

7 = Other

**Table 13. Listing of GPS sites that contain some type of drainage system (continued).**

State Code	SHRP ID	Drainage System	State Code	SHRP ID	Drainage System
29	1010	3	42	1613	2
29	5393	3	42	1614	3
29	5483	7	42	1617	3
29	7054	3	42	1618	2
33	1001	3	42	1623	2
34	1003	3	42	1627	2
34	1011	3	42	3044	2
34	1030	7	42	5020	2
34	1031	3	42	7025	3
34	4042	3	42	7037	2
37	1006	2	42	9027	2
37	2824	2	44	7401	3
37	3011	7	46	6600	7
37	3044	7	48	2133	2
37	5037	7	48	5035	2
37	5826	7	48	5336	3
38	6004	2	48	7165	2
39	3801	2	49	1007	3
39	4031	2	49	3010	3
39	5003	2	49	7083	3
39	9006	2	49	7086	6

\*2 = Longitudinal Drains

3 = Transverse Drains

4 = Drainage Blanket

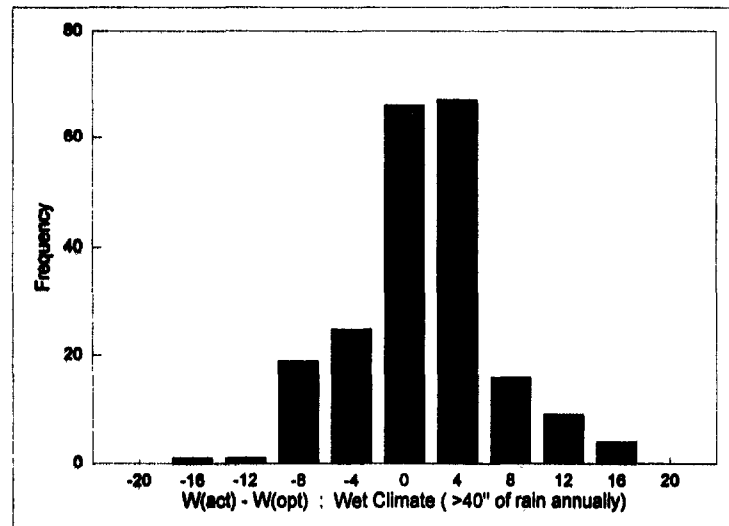
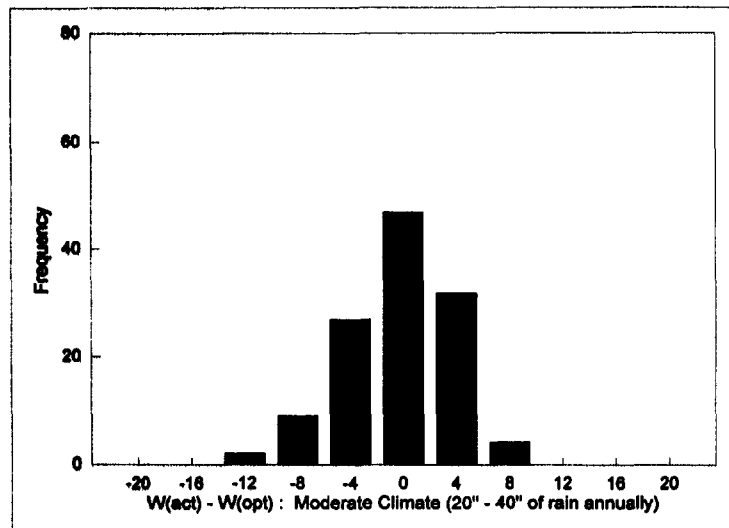
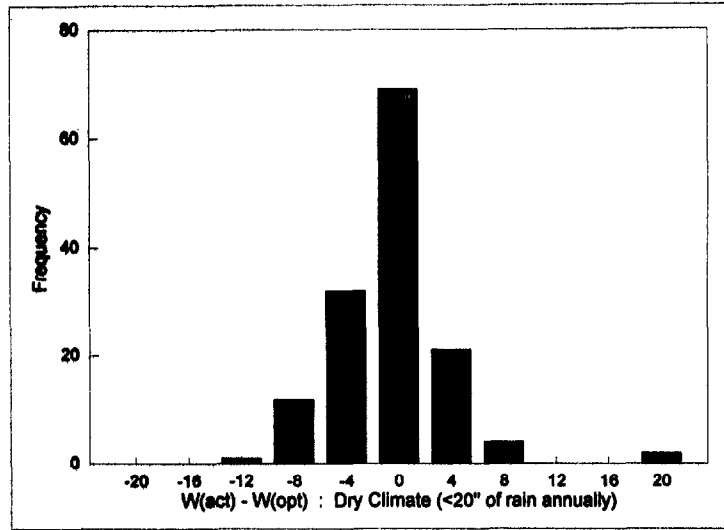
6 = Drainage Blanket w/  
Longitudinal Drains

7 = Other

**Table 13. Listing of GPS sites that contain some type of drainage system (continued).**

State Code	SHRP ID	Drainage System	State Code	SHRP ID	Drainage System
39	9022	2	50	1004	2
40	4155	2	50	1681	3
40	4158	2	50	1682	7
40	4166	6	50	1683	3
41	2002	3	51	1023	2
41	5005	2	51	1464	2
41	5021	2	51	5009	2
41	7018	2	53	3011	2
41	7019	6	55	6351	2
55	6352	3	55	6352	3
55	6353	2	55	6353	2
55	6354	2	55	6354	2
55	6355	2	55	6355	2
82	9017	2	82	9017	2
87	2812	2	87	2812	2
89	3002	2	89	3002	2
89	3016	3	89	3016	3

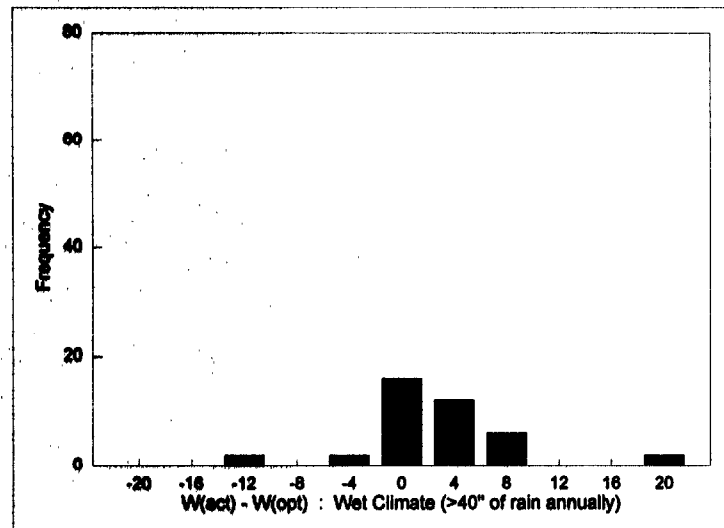
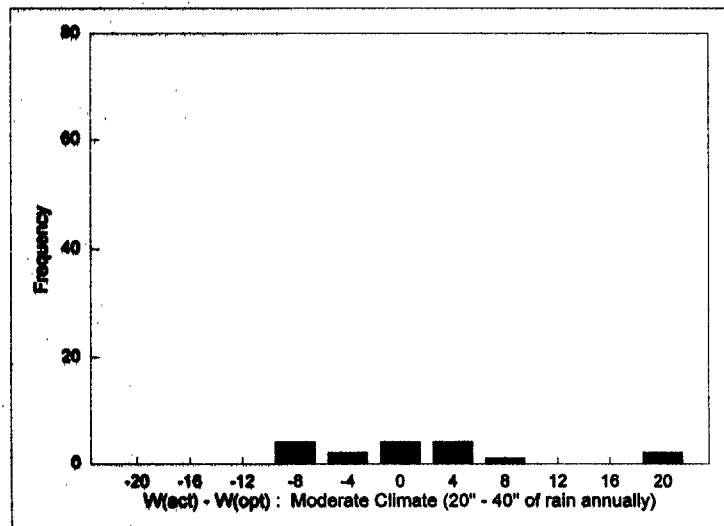
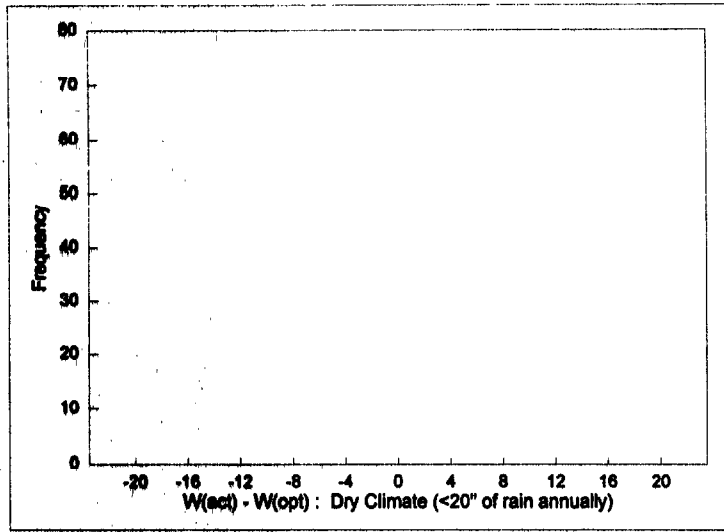
- \*2 = Longitudinal Drains
- 3 = Transverse Drains
- 4 = Drainage Blanket
- 6 = Drainage Blanket w/  
Longitudinal Drains
- 7 = Other



1 in = 2.54 cm

**Figure 35. Frequency of difference between optimum and actual moisture contents for granular base layers in GPS sections with no positive drainage system.**





1 in = 2.54 cm

**Figure 36. Frequency of difference between optimum and actual moisture contents for granular base layers in GPS sections with positive drainage systems.**

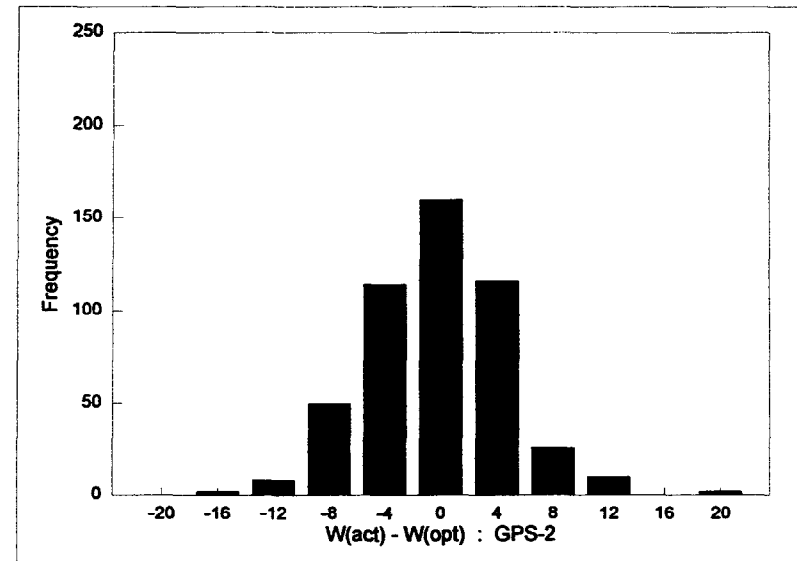
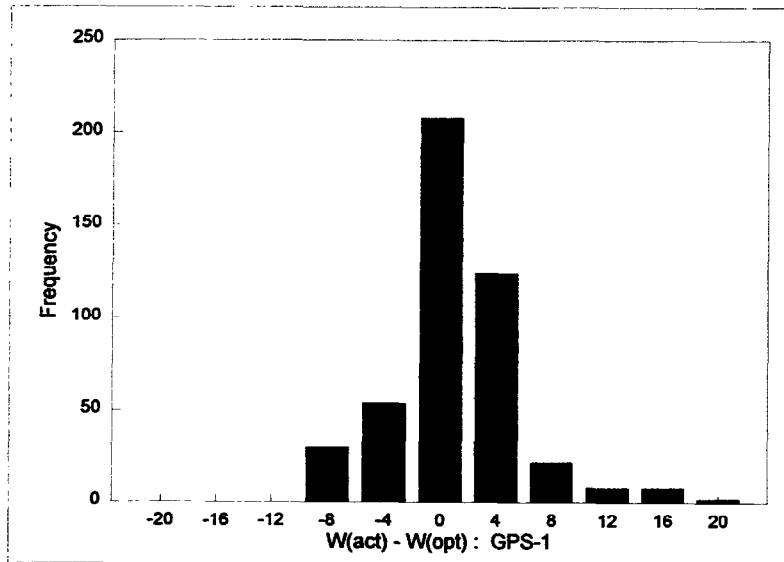


**Figure 37. Comparison of difference between optimum and actual moisture contents for subgrade soils in GPS-1 and GPS-2 sections with no positive drainage system.**

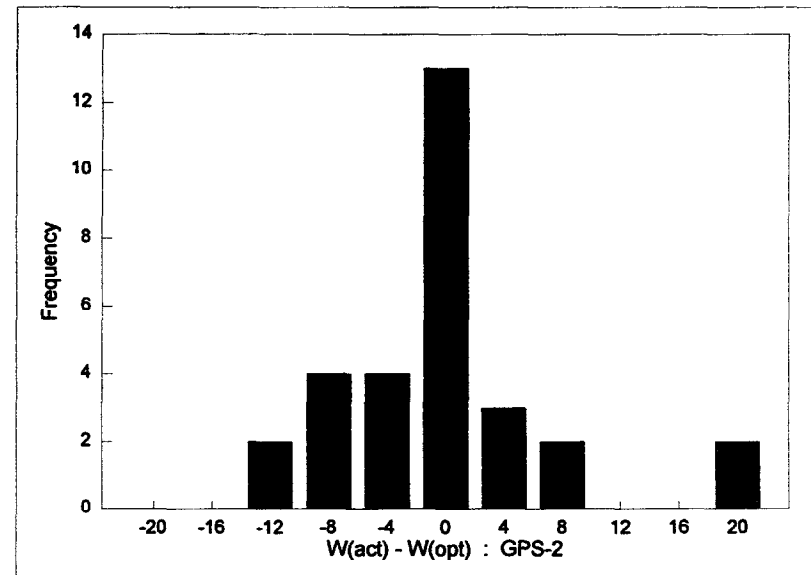
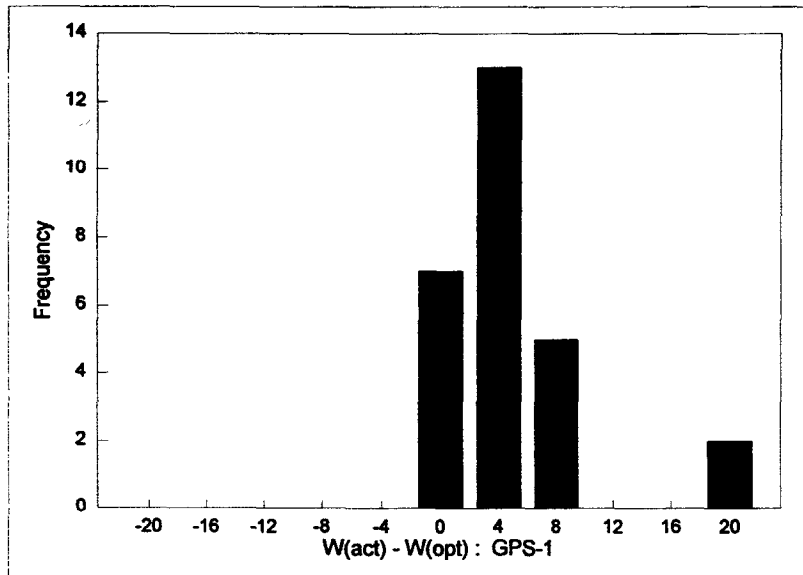


**Figure 38. Comparison of difference between optimum and actual moisture contents for subgrade soils in GPS-1 and GPS-2 sections with positive drainage systems.**

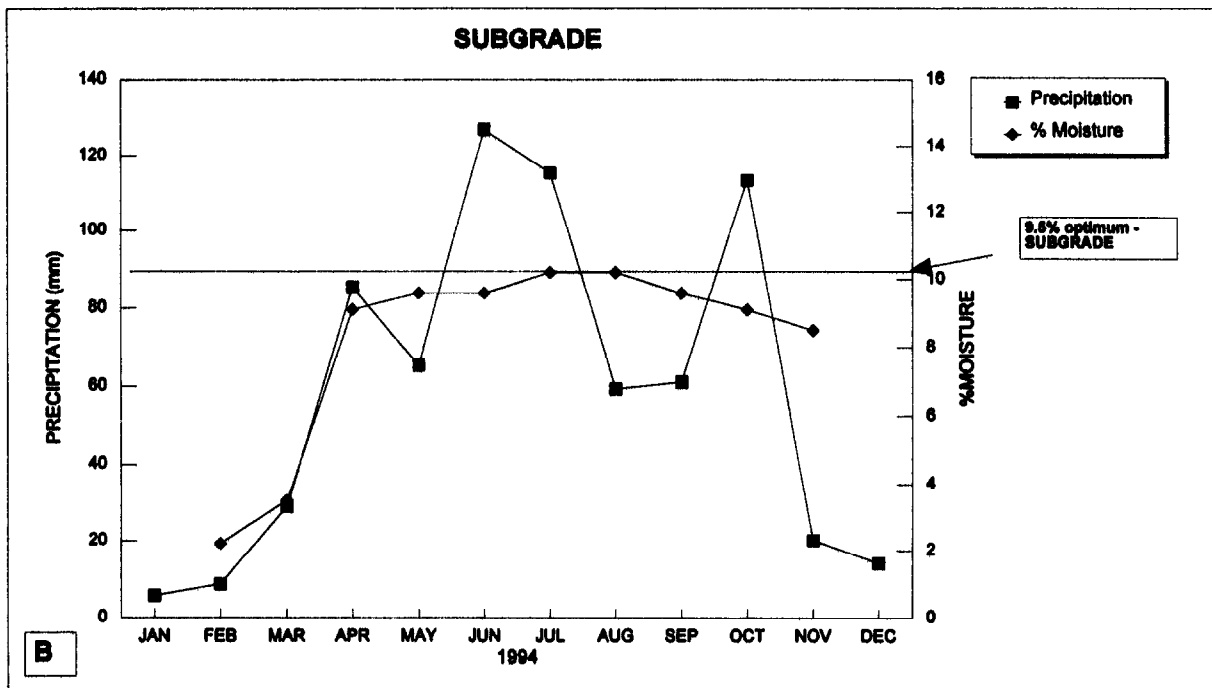
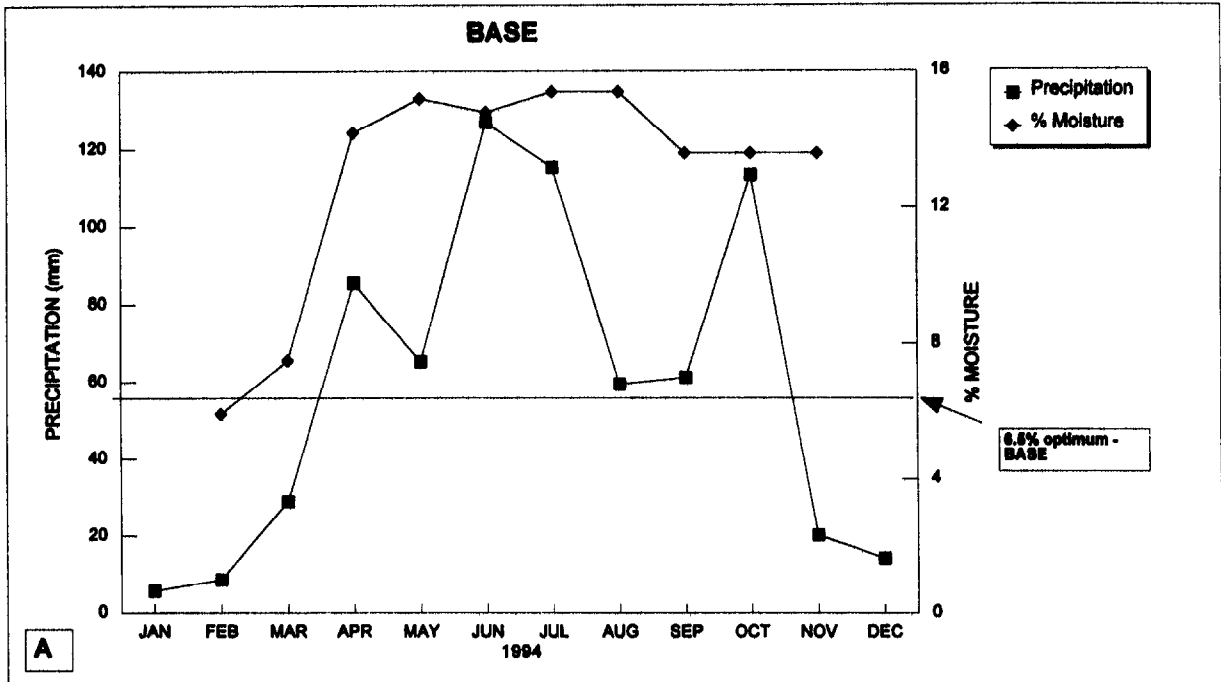


**Figure 39. Minnesota seasonal site measurements for precipitation and moisture contents from 1994.**

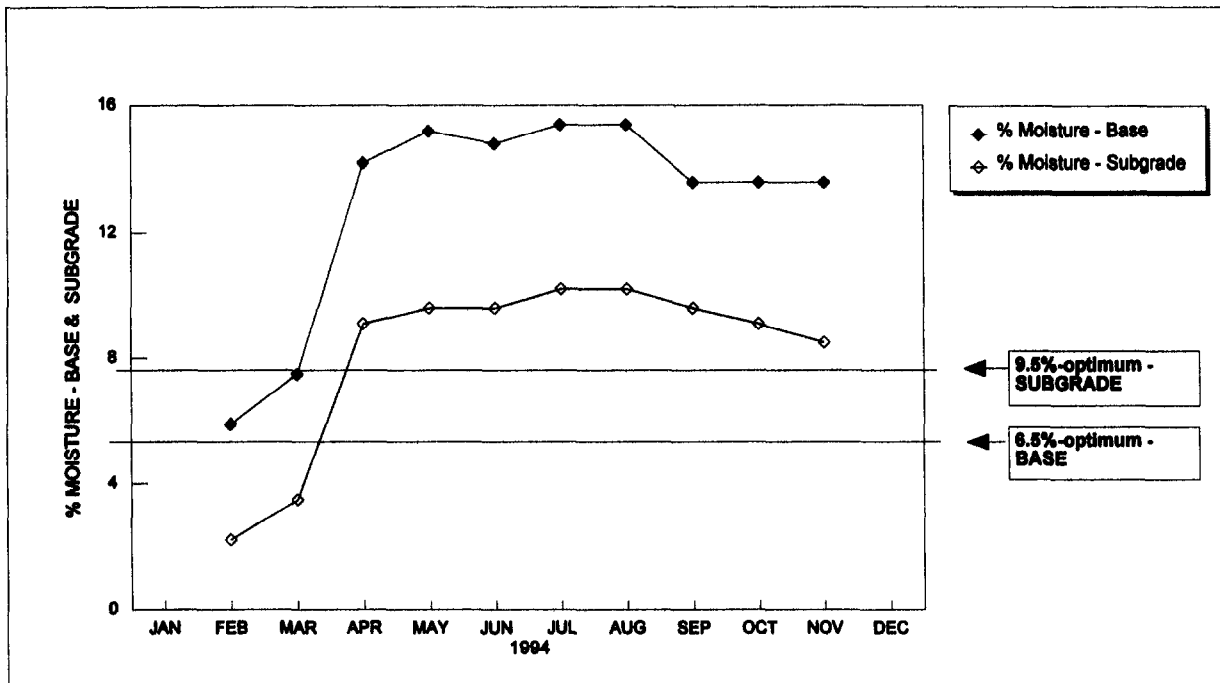


**Figure 40. Minnesota seasonal site measurements for base and subgrade moisture contents from 1994.**

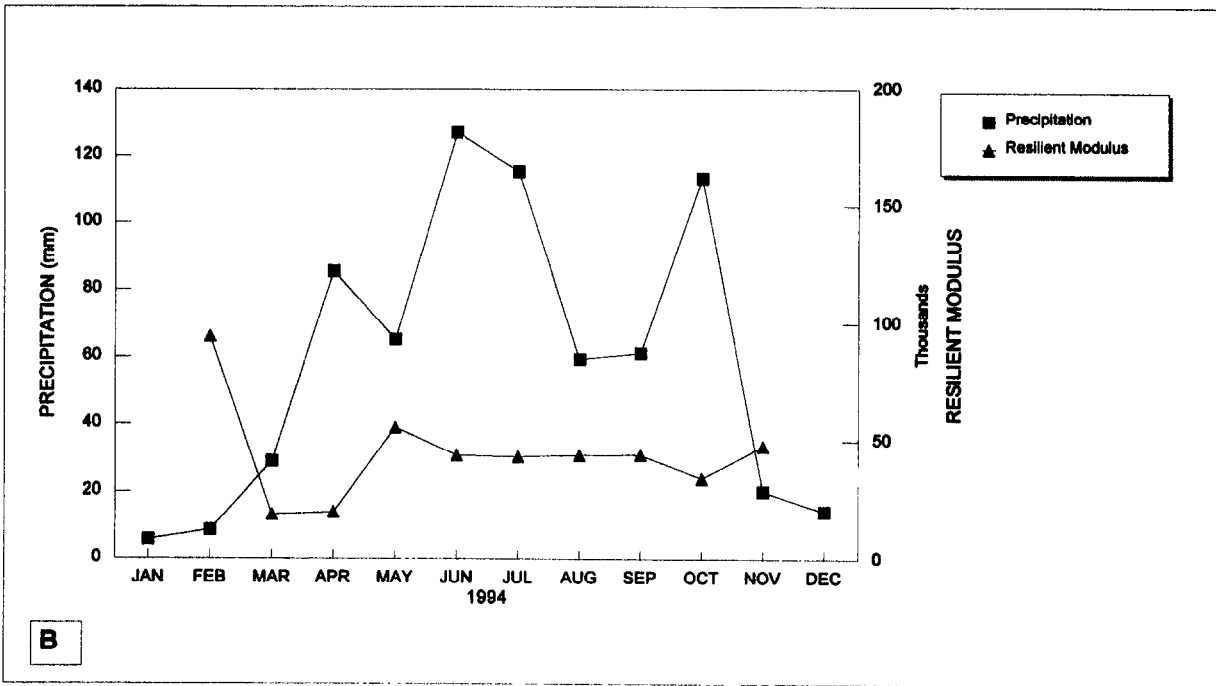
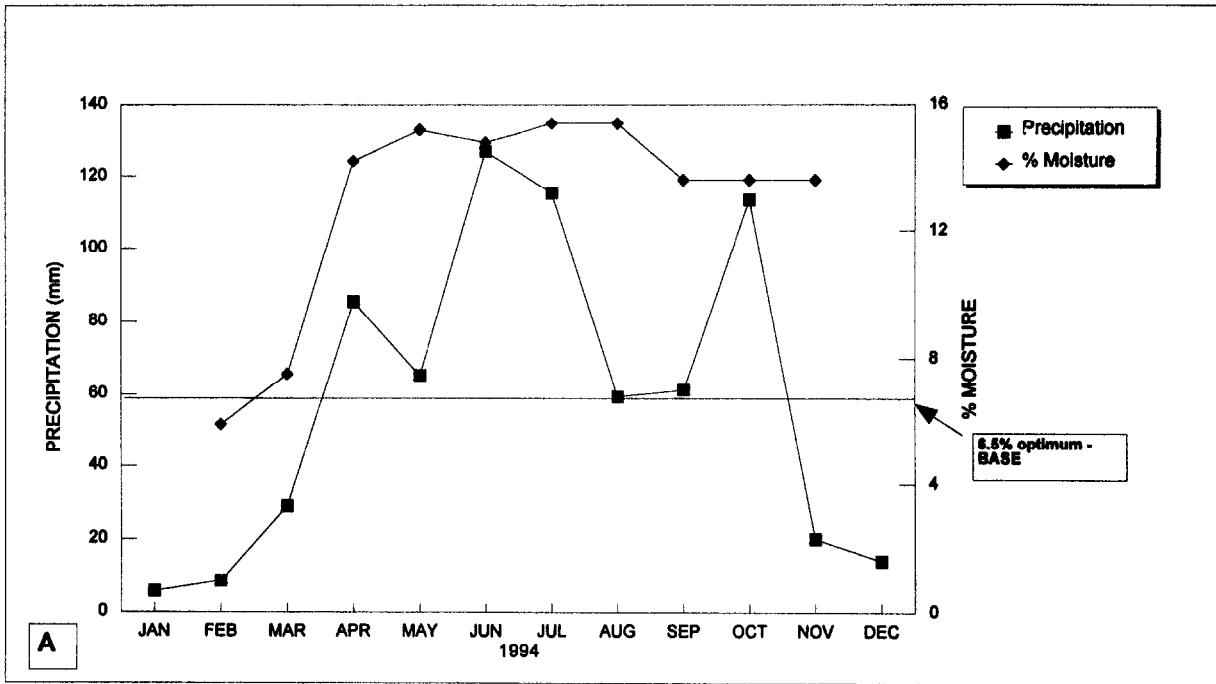


**Figure 41. Minnesota seasonal site measurements in the granular base, including backcalculated resilient modulus from 1994.**

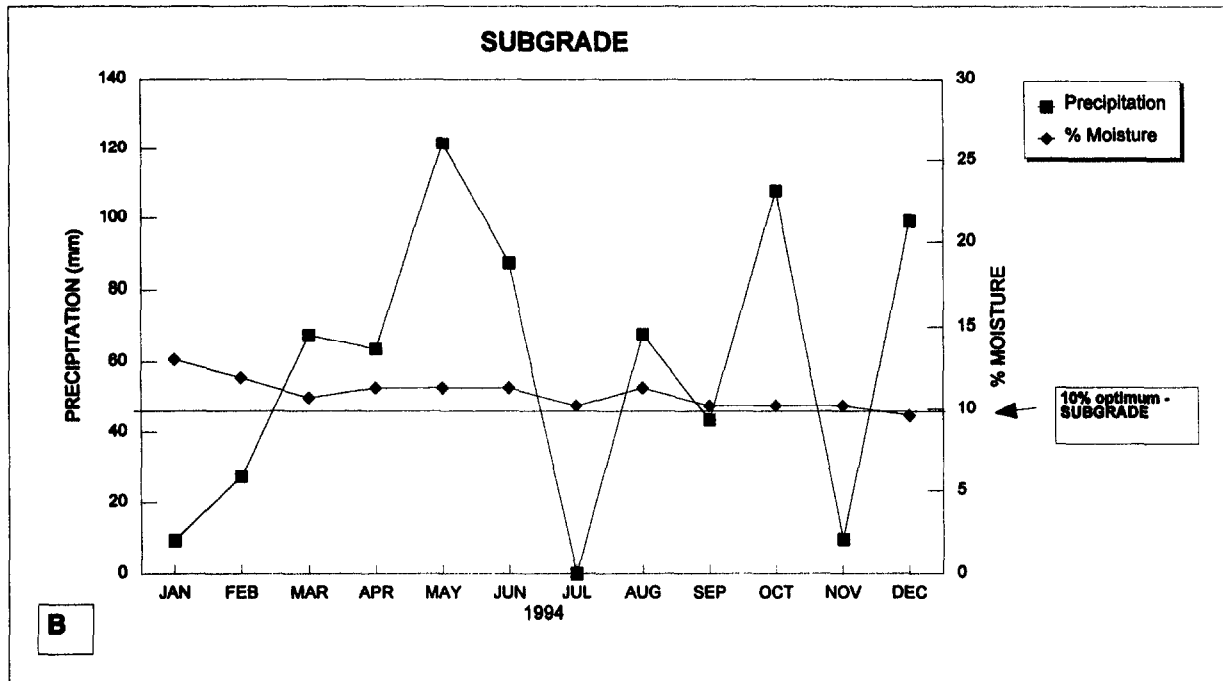
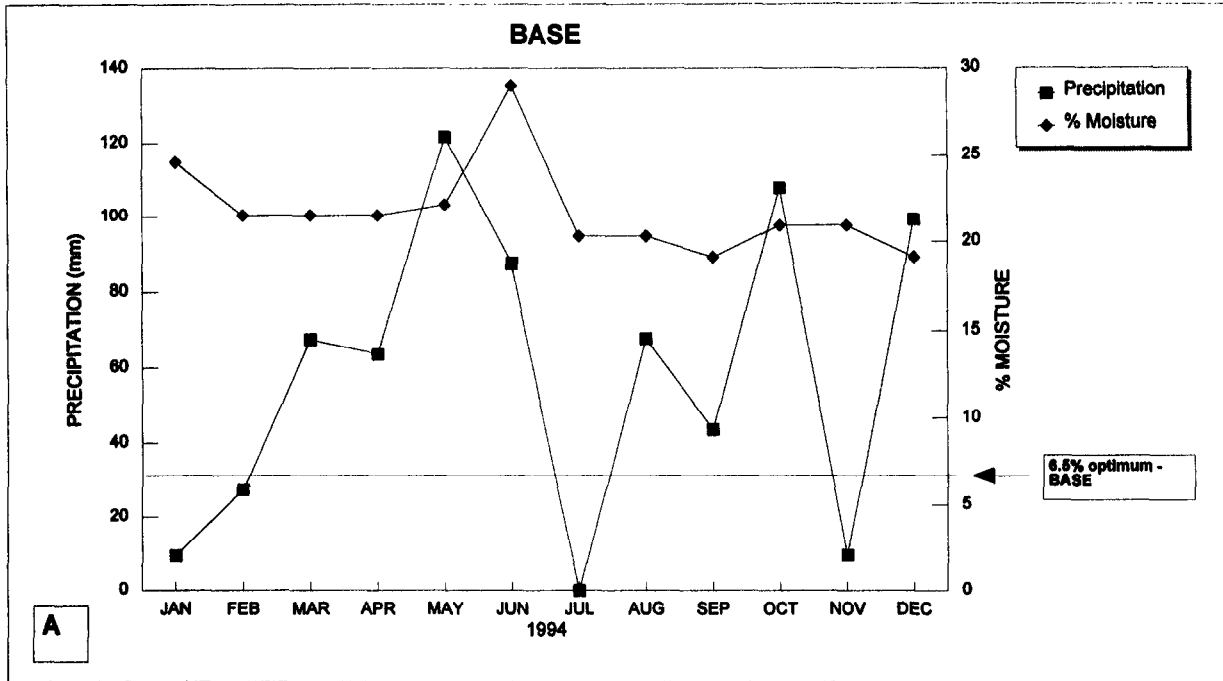


**Figure 42. Texas seasonal site measurements for precipitation and moisture contents from 1994.**

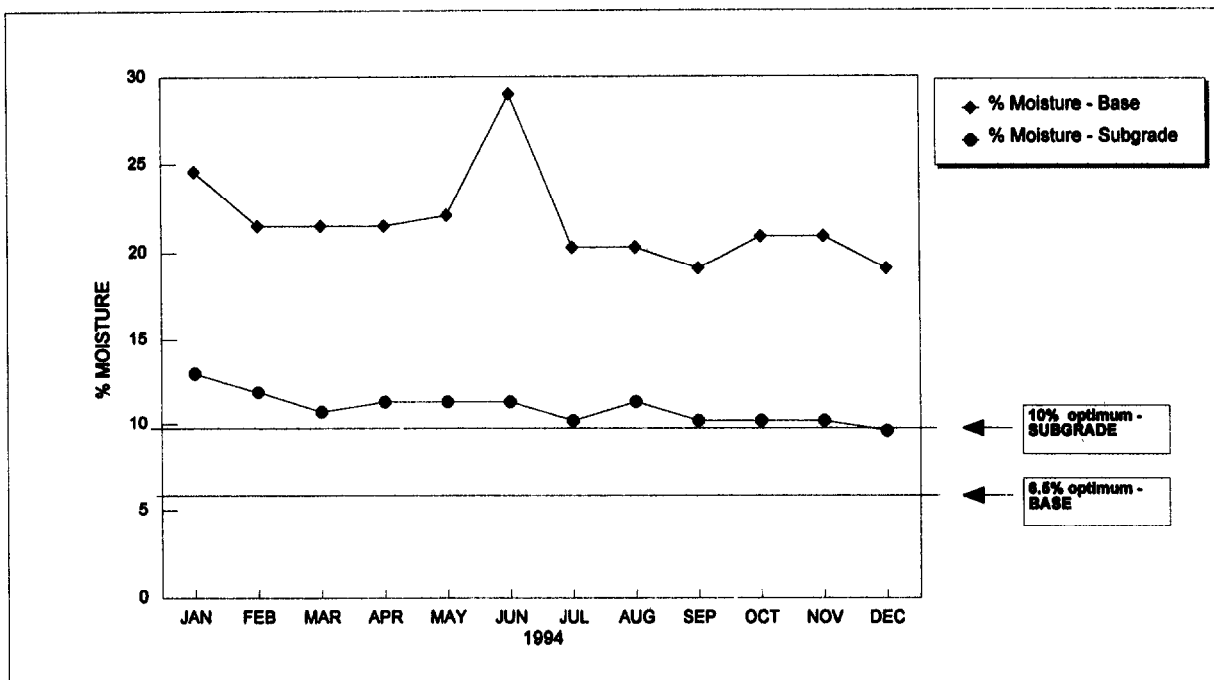


**Figure 43. Texas seasonal site measurements for base and subgrade moisture contents from 1994.**



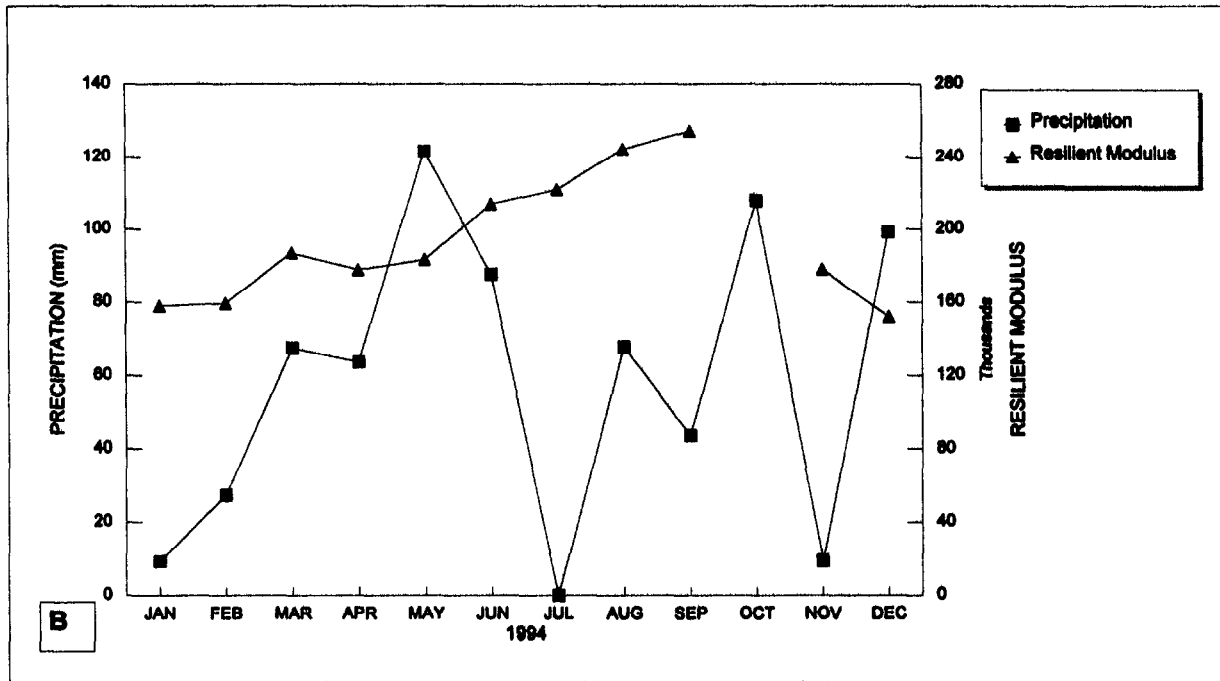
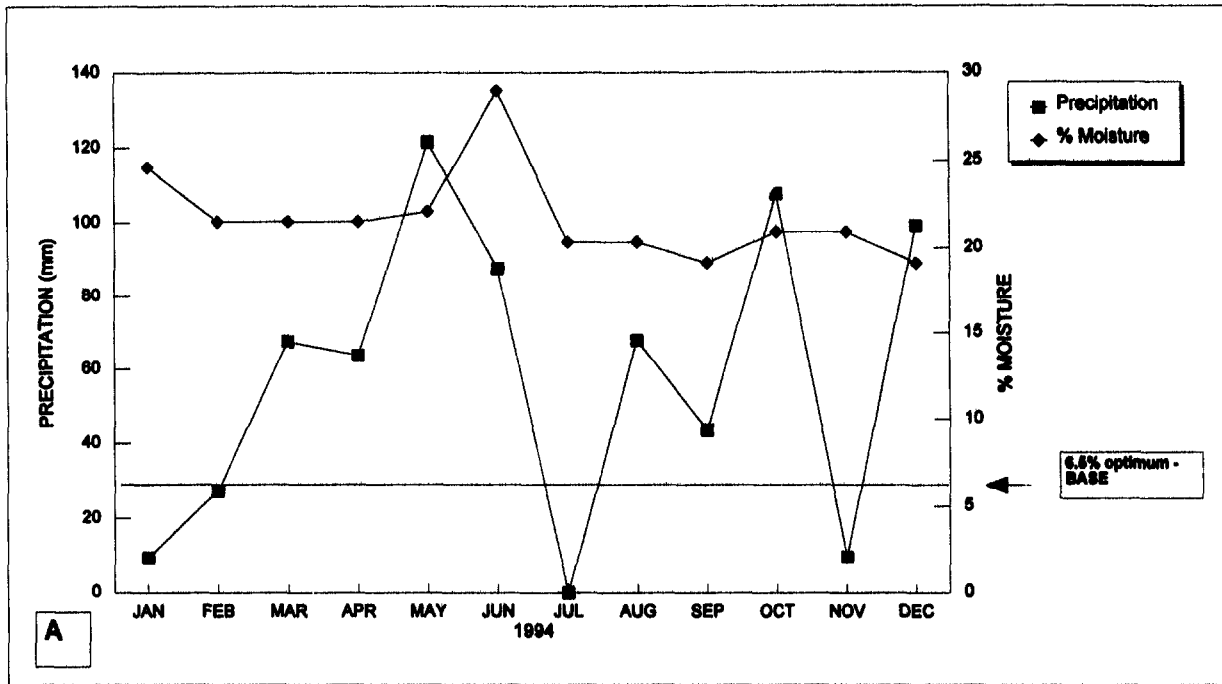


**Figure 44. Texas seasonal site measurements in the granular base, including backcalculated resilient modulus from 1994.**

It should be understood, however, that the optimum moisture contents and maximum unit weight of the materials were assumed to exist at the time of construction, which may or may not be a correct assumption. In addition, it was assumed for this analysis that the drainage systems are functioning properly, which may also be a poor assumption.

One important study and demonstration project that is currently ongoing is FHWA Contract No. DTFH61-95-C-00005, entitled "Video Inspection of Highway Edge Drain Systems." The purpose of this demonstration project is to visually inspect, using video inspection equipment, the internal drainage system of various pavement structures. One of the important findings of this study is that these drainage systems are not being maintained and, in fact, have sometimes been constructed with defects, such as crushed pipes and pipes filled with debris. Thus, it may be expected that the drainage systems for some LTPP test sections may also not be functioning properly. One important preliminary finding from this contract is that if free-draining systems are not inspected and/or maintained, there is a high probability that they are not functioning as originally designed.

Therefore, it is highly recommended that these GPS sites with positive drainage systems be inspected to confirm that the systems are functioning properly. This confirmation will definitely assist future users of the data base regarding the effects and benefit of positive drainage.

## **5.4 AASHTO Drainage Coefficients**

**5.4.1 Flexible.** The approach incorporated in the current AASHTO Design Guide for including drainage effects in flexible pavements consists of applying a drainage coefficient to the *unbound* base and subbase layers in the structural number determination (see table 12). These adjustment factors modify the layer stiffness coefficients based on the expected level of moisture at the pavement site. Essentially, the drainage coefficient is used to quantify the effect of water (moisture) on the stiffness of each of the underlying materials (excluding the subgrade). The drainage factors are chosen based upon the expected time the pavement will be in a near-saturated or saturated condition and the expected rate at which water will drain from the pavement structure.

Development of the drainage coefficients was based upon a mechanistic type of analysis. However, there were several assumptions and conditions made that may have a negative effect on the ability of the coefficients to realistically model the effect on overall pavement performance. For example, the analysis used to develop the design coefficients was based upon elastic layer theory to determine equal deflections between pavements with and without improved drainage (high stiffness vs. low stiffness base layers). This logically would make

sense, even knowing the limitations of characterizing the pavement system as an elastic layered system, but the computations from the guide were never verified using actual field data, because there was no field data available with which to check it.

Another limitation exists in the transformation or expansion of the coefficients from being classified based on the quality of drainage provided (i.e., how well the pavement drains free water) to also being considered to represent the percent of time the pavement is at or near saturation. Very little background is given in the guide on this transformation and how it was developed, and even more importantly, it was also never verified with field data.

**5.4.2 Rigid.** The effect of drainage on pavement performance has been incorporated in the rigid pavement design equation by introduction of the  $C_d$  coefficient. This coefficient is part of the design equation that considers slab strength, stress and underlying support. Development of this coefficient is not rooted in mechanistic concepts like the flexible pavement design coefficients, but was based on the expected minimum effects that drainage would have on the slab thickness. In other words, a 2.5-cm (1-in) reduction in slab thickness was assumed to correspond to an excellent drainage condition and a 3.8-cm (1.5-in) increase in slab thickness was assumed to correspond to a very poor drainage condition. The real effect that a positive drainage system or poor drainage conditions has on the stress conditions of the slab was never verified with actual field data or even a mechanistic analysis. In fact, the guide states:

“It is recommended ... that data from field experiments and long-term pavement performance monitoring be used to validate and/or improve these values.”

As with the flexible pavement drainage coefficients, the selection of a drainage value for the rigid pavement design equation is based upon the percent of time the pavement structure is exposed to moisture levels at or near saturated conditions and the expected quality of drainage at the pavement site.

**5.4.3 Evaluation of the Drainage Coefficients.** One of the goals of this research activity was to validate, or at least confirm, the applicability of these drainage coefficients. Unfortunately, this goal was not achieved because of the following reasons:

- For the traffic data, only historical 80-kN (18-kip) ESAL's were available from the data base and the accuracy of these data was questionable.
- Assumptions had to be made regarding material properties and the functionality of the drainage system, which may or may not be good assumptions applicable to the GPS sites.

- Too few GPS sections exist to make any statistically valid conclusions, given the diversity of the onsite conditions in combination with the two reasons noted above.

## **5.5 Reduction of Layer Moduli During Saturated Conditions**

Seasonal fluctuations in rainfall and frost penetration have a significant effect on the modulus of all underlying pavement layers, especially if these layers are unbound and become saturated for substantial periods of time. The effects of moisture on the resilient moduli of subgrade soils and unbound granular base and subbase layers are fairly well understood, and can be measured in the laboratory using repeated-load triaxial compression tests. In fact, the moisture content (in reference to the optimum value) was found to be one of the most important parameters or properties in estimating resilient modulus from the physical properties. This was previously explained in subsection 3.4.

Resilient modulus of the subgrade soil, as well as for the base and subbase materials, is a critical design parameter which does influence pavement performance. This influence is discussed in much greater detail in chapter 7 which discusses seasonal variations of materials. Seasonal variations include changes in moisture contents caused by poor drainage conditions, which can have an effect on the design resilient modulus for base and subbase layers.

As a result, it is suggested that seasonal variations of resilient moduli for the base and subbase materials be used (similar to determining the subgrade design resilient modulus through use of the damage concept) instead of the drainage coefficients, because the effect of moisture on the pavement materials and subgrade soils (resilient modulus) can be measured directly in the laboratory.

## 6. SUBGRADE CHARACTERIZATION AND STABILIZATION

The basis for soils characterization in the 1986/1993 Design Guide is resilient modulus, which is determined for each different moisture season within a year. The purpose of identifying seasonal moduli is to quantify the relative damage that the pavement is subjected to during each season of the year. This seasonal variation is dependent upon the changes in moisture and other freeze/thaw conditions. The 1986/1993 AASHTO Design Guide includes a chart for calculating the "effective" or equivalent annual resilient modulus for flexible pavement design (figure 45)<sup>1</sup>. The guide clearly emphasizes that this "effective" resilient modulus value to be used in design should be used only for the design of flexible pavements based upon serviceability criteria.

Another objective of this study was to confirm or validate the relative damage concept, or the procedure used to calculate the effective annual resilient modulus for the subgrade soils, using other criteria. For example, subgrade vertical compressive strains are used by some agencies to ensure that there is sufficient cover of pavement materials to prevent an overstressing of the subgrade soils. This study would then tie the serviceability relative damage coefficients to those using subgrade vertical compressive strain criteria. Within the same area, the effects of subgrade stabilization were also investigated using the GPS sites to determine if there is any increase in performance for those pavement structures with stabilized subgrades, as compared to those pavements without stabilized subgrades.

### 6.1 Available Data From the LTPP Data Base

**6.1.1 Types and Number of Projects.** Approximately 370 flexible GPS test sections exist nationwide, including Canada and Puerto Rico. For this task, the data obtained were confined to those sites in the North Atlantic and Southern regions, because these regions were the only ones having resilient modulus test results for unbound soils at the time of this study. Although there are nine GPS experiments, each having some sites with stabilized subgrades, only GPS-1 and GPS-2 studies were used for this research activity. GPS-1 and GPS-2 sites represent original pavements without overlay or other rehabilitation efforts which would interrupt a given history of pavement performance and severely complicate the data analyses. Subgrade types at these sites were broken down into four categories: clays, silts, sands and gravels. Review of the 261 GPS-1 and GPS-2 test section data resulted in the following categorical breakdown and associated number of GPS sections:

---

Note 1: Figure 45 is extracted from the 1993 AASHTO Design Guide, and was derived using English units. As such, it is required that psi be used with figure 45 to determine the relative damage index. The relative damage index is dimensionless.

Month	Roadbed Soil Modulus, $M_R$ (psi)	Relative Damage, $u_f$
Jan.		
Feb.		
Mar.		
Apr.		
May		
June		
July		
Aug.		
Sept.		
Oct.		
Nov.		
Dec.		
Summation: $\Sigma u_f =$		

Average:  $\bar{u}_f = \frac{\Sigma u_f}{n} = \underline{\hspace{2cm}}$

Effective Roadbed Soil Resilient Modulus,  $M_R$  (psi) =  $\underline{\hspace{2cm}}$  (corresponds to  $\bar{u}_f$ )

1 psi = 6.89 kPa

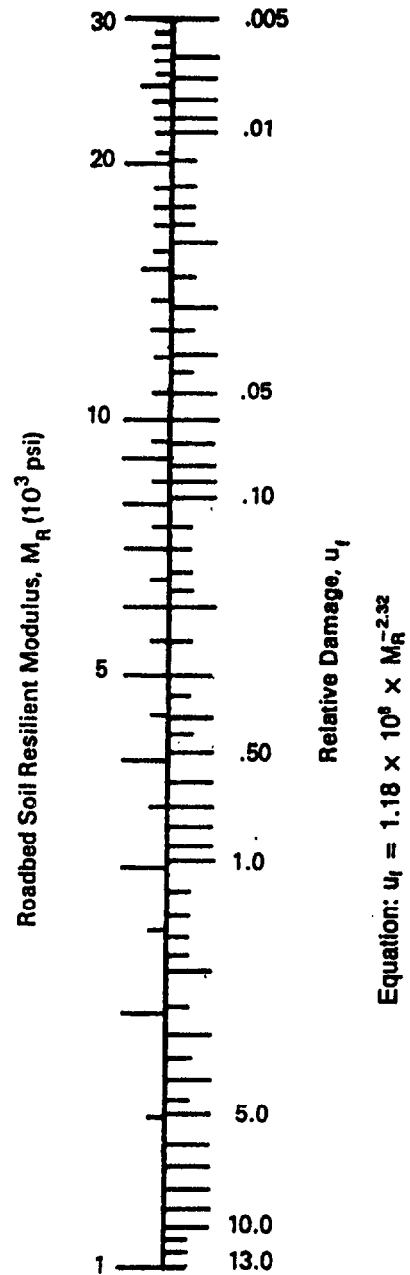


**Figure 45. Chart for estimating effective roadbed soil resilient modulus for flexible pavements designed using the serviceability criteria (1).**

Subgrade	No. of GPS Sites
Clay	73
Silt	23
Sand	128
Gravel	37

These sites were further broken down into those with stabilized versus unstabilized subgrades, which is reflected in the following summary.

Subgrade	No. of Stabilized	No. of Unstabilized
Clay	14	59
Silt	1	22
Sand	14	114
Gravel	0	37

Review of the data shows that a much fewer number of sections have stabilized subgrades. More importantly, a large proportion of the stabilized sections are logically on "problem" subgrades. These disparities made comparisons between subgrades with and without stabilization difficult at best.

**6.1.2 Traffic Data.** Historical traffic data were required to accomplish this research activity and were available from the LTPP data base. However, the historical traffic data are based on estimates that may not accurately reflect the existing traffic levels (both in number of applications and wheel-load magnitudes). Monitored traffic data were also available and were considered acceptable, so comparisons were made between the historical and monitored traffic data. These comparisons revealed large discrepancies between the two values. Further analysis of the monitored traffic data revealed that those data previously flagged for one reason or another were included in the process for calculation of ESAL's. Causes for flagging data included equipment calibration problems, unusual or elevated ESAL values, etc. As a result of these discrepancies, the confidence level in the monitored traffic data was diminished and these data were not used in the analysis.

Traffic data, and more specifically the number and magnitude of the heavier truck loads, were key data elements for accomplishing this research activity to evaluate the higher strain levels induced in the subgrade from the heavier wheel loads. Ideally, traffic data were to have provided a necessary part for comparing and predicting performance (cracking, roughness, and rutting) and not just categorizing the GPS sites with similar traffic levels. More importantly, the number of 80-kN(18-kip) ESAL's included in the data base were calculated using the AASHTO equivalency factors based on the serviceability concept and the questionable traffic data. Equivalency factors based on a serviceability criteria are different from those based on a fatigue cracking or rutting criteria. These comparisons would have provided insight into benefits of subgrade stabilization over nonstabilization through performance characteristics of each site. Use of 80-kN (18-kip) ESAL's severely restricted the analysis for this activity.

## 6.2 Subgrade Characterization for Design

**6.2.1 Determination of Effective Resilient Modulus.** Two different procedures are discussed in the guide for determining the seasonal variation of the modulus. One of these methods involves obtaining a laboratory relationship between resilient modulus and moisture content of the soil. The resilient modulus is then varied for each of the different seasons within a year by the expected change in moisture content of the soil. An alternate procedure is to backcalculate the resilient modulus for different seasons using deflection basins measured on the pavement surface. The guide allows the use of both procedures to determine the seasonal variation of subgrade moduli and relative damage values for calculating the design resilient modulus (figure 45).

However, subsection 4.3 in chapter 3 (Differences Between Laboratory Determined and Backcalculated Elastic Moduli) identified and explained significant differences in the moduli determined from these alternate procedures. If the seasonal moduli are determined through the use of backcalculation techniques, then those subgrade moduli must be divided by the ratios,  $M_R(\text{Lab})/E(\text{FWD})$ , given in subsection 4.3.3. The reason for this adjustment is that the design procedure is based on laboratory measured moduli, and the use of backcalculated moduli will result in an insufficient pavement thickness for the serviceability criteria. The AASHTO Design Guide suggests the use of ratios or C values ranging from 0.15 to 0.24 for clay-type soils, and 0.33 for coarse-grained soils. These values are much lower than those determined from this study (0.35 to 0.75, as tabulated in subsection 4.3.3).

**Observation:** The C values or ratios determined within this study were found to be dependent on pavement type and independent of material type, and were found to be significantly higher than those values mentioned in the AASHTO Design Guide.



**6.2.2 Use of the Damage Concept.** As stated above, the magnitude and number of the heaviest axle loads were key data elements for confirming the use of the relative damage concept to determine the equivalent annual resilient modulus of the subgrade for design. These data elements from the monitored traffic data were not used because they had not passed the quality checks implemented within the data base. For this part of the research activity, only 80-kN (18-kip) ESAL's were used.

Vertical compressive strains at the top of the subgrade have been used in design to ensure that there is sufficient cover to prevent overstressing of the subgrade soils for a specified level of traffic. Two of the relationships<sup>2</sup> that have been developed are listed below (26, 28):

$$\text{Log } N = -6.211 - 4.0 \text{ Log } \epsilon_v \quad (13)$$

$$\text{Log } N = 0.955 (\text{Log } M_R) - 4.082 (\text{Log } \epsilon_v) - 10.90 \quad (14)^{(2)}$$

where:

- N = The allowable number of load applications for a specific axle weight and configuration.
- $\epsilon_v$  = Vertical compressive strain at the top of the subgrade.
- $M_R$  = Resilient Modulus of the subgrade soil, as measured in the laboratory using repeated-load triaxial compression tests in psi.

Both of the above subgrade vertical compressive strain criteria were used to determine the number of allowable 80-kN (18-kip) ESAL's (N) for each end of the GPS section included in this part of the study. These GPS sites were subdivided into two basic categories: (1) GPS sites where the rutting is expected to be confined to the pavement layers, and (2) GPS sites where the rutting is expected to be in the subgrade. The procedure for using the geometry of the rut depth

---

Note 2: Equation 14 was developed using English units. As such, it is required that psi be used in equation 14 to calculate the number of allowable load repetitions.

to predict the layer of its cause was that developed from LTPP data (29). A damage index (D.I.) was then calculated for each section end as follows:

$$D.I. (\epsilon_v) = n/N \quad (15)$$

where:

n = The number of estimated 80-kN (18-kip) ESAL's that are included in the historical traffic data in the LTPP data base.

These damage indices were then compared to the distresses observed (rutting and fatigue cracking) and the values of IRI (International Roughness Index) for each GPS site to evaluate the applicability of the subgrade vertical compressive strain criterion. However, it was determined that the damage indices were not related to the distresses nor IRI values. Possible reasons for these findings are briefly listed below:

- There were too few GPS sites with severe rutting (greater than 1.3 cm (0.5 in)) in the subgrade.
- No trench studies were conducted within the SHRP program to validate and confirm the accuracy of the procedure used to predict the cause of rutting from the geometry of the measured rut depth.
- There were too few sections with moderate to severe fatigue cracking.
- The accuracy of the historical traffic data in the data base is questionable. The historical traffic data are only estimates and are not actual measured values.
- The backcalculated moduli (corrected or adjusted to laboratory values) used for each pavement layer and the subgrade only represent one point in time, which may not be representative of the typical conditions.

Thus, the validity of the damage concept and applicability of the subgrade vertical compressive strain criterion were not confirmed through the use of the LTPP data base. The subgrade modulus in the original AASHTO equation, however, represents the soil in its weakest condition (during spring thaw), and did not account for seasonal variations. Thus, these analyses could be indicating that use of the equivalent annual resilient modulus under the serviceability criteria may be inappropriate. However, it is possible that continued testing and monitoring of the GPS

and seasonal sites and improvements in the accuracy of the monitored traffic data will provide the data needed to eventually accomplish this activity.

### **6.3 Effect of Stabilized Subgrade on Performance of Flexible Pavements**

It is widely accepted that pavement performance is directly affected by the physical properties of underlying subgrade soils. It is theorized that protection of these subgrade soils through stabilization should increase performance of the pavement structure.

Lime stabilization, or the introduction of select materials into poor and unstable subgrade soils, is often conducted to establish a working platform during the construction of subsequent structural layers. Lime stabilization, however, is thought to help reduce the potential for moisture penetration, as well as to increase the stiffness of the underlying subgrade soils. The potential for overstressing those subgrade soils is then reduced, increasing the potential for better pavement performance. Unfortunately, the backcalculated subgrade moduli for the GPS sites with stabilized subgrades were found to be consistently lower than the moduli for those sites without stabilized subgrades. This comparison only suggests that stabilized subgrades have been used in areas with weaker soils, which would be expected, and does not relate to the overall ineffectiveness of the stabilized subgrade layer. The average subgrade moduli backcalculated for each group of pavements are listed below:

GPS Sites with Stabilized Subgrade,  $E(FWD) = 150 \text{ MPa}$

GPS Sites without Stabilized Subgrade,  $E(FWD) = 190 \text{ MPa}$

Investigation of GPS test section data regarding the performance comparisons of GPS sites with stabilized subgrades versus unstabilized subgrades has also provided little insight at this time towards substantiating an increase in performance. The reasons for this inconclusive finding are the same as previously mentioned and discussed in chapter 5 on Moisture Effects and Drainage Coefficients. The following subsections briefly overview some of the comparisons and observations made from these data.

**6.3.1 IRI vs. Age.** A number of comparisons were made to identify any consistent differences in distresses occurring between pavements with subgrade stabilization and those without. The first comparisons were for the IRI versus Age of the pavement. These comparisons were developed for each of the four soil categories in consideration of stabilized versus unstabilized subgrades.

During the initial investigation, several of the plots of IRI vs. Age showed roughness increasing at a given slope, but then experiencing a significant decrease in IRI. Further investigation revealed that a number of these cases could be attributed to the placement of an overlay. These sites were then eliminated from further evaluation within this research activity. The number of test sites affected accounted for almost 5 percent of the original data set considered. The following briefly reviews the comparisons for each soil group considered.

- Clay Subgrades (figure 46). IRI vs. Age comparisons were inconclusive regarding the benefit of one practice over the other. Similar aged pavements appeared to reflect a similar rate of increase in IRI vs. Age (similar slopes), and that rate of increase for both groups of pavements was relatively small. However, those sites with the higher rates of increase (greater slopes) were generally from the unstabilized clay group.
- Silt Subgrades (figure 47). Only one test section having a stabilized silt subgrade was available. The unstabilized silt subgrades of similar aged pavements were found to have similar IRI values. More importantly, those GPS test sections constructed on unstabilized silt subgrades generally have lower IRI values than the other GPS sites included in these analyses.
- Sand Subgrades (figure 48). The comparisons for the sand subgrades are inconclusive as to any benefit from stabilized subgrades. However, the rate of increase of the IRI values with time was generally greater for those sites with stabilized subgrades as compared to sites without subgrade stabilization. More importantly, it was observed that similar aged pavements reflected lower IRI values overall for unstabilized subgrades when compared to GPS test sections with stabilized subgrades. This would indicate that a stabilized subgrade layer has no long-term benefit, or that too much structural value was assigned to the stabilized subgrade layer during design.
- Gravel Subgrades (figure 49). There were no stabilized gravel subgrades for comparison with unstabilized subgrades. It was evident, however, that those GPS test sections with gravel subgrades reflected trends in a more unpredictable manner, as compared to the other groups. Similar aged pavements reflected different slopes, some showing positive trends and others showing negative trends.

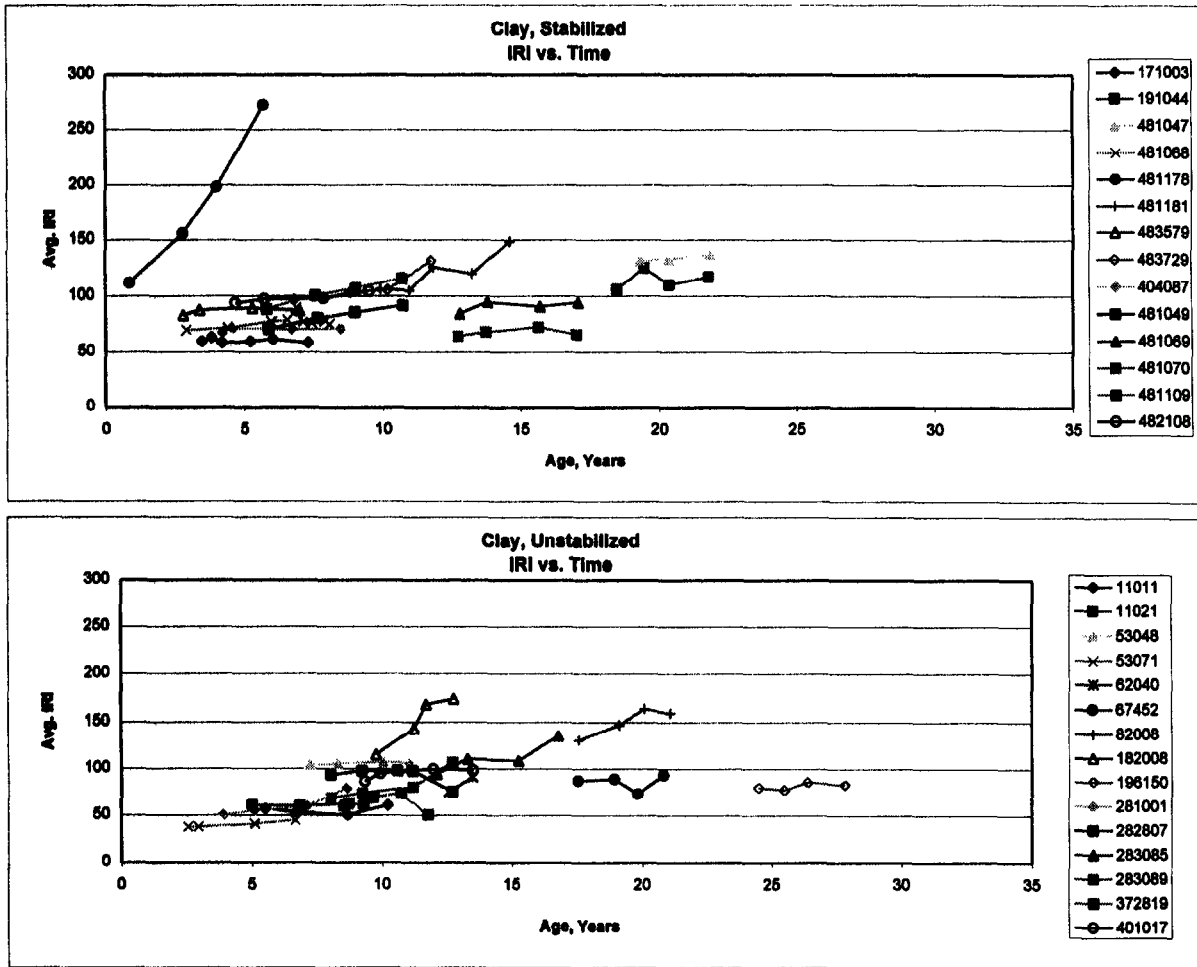


**Figure 46. Example of IRI versus time for GPS sites with clay subgrades.**

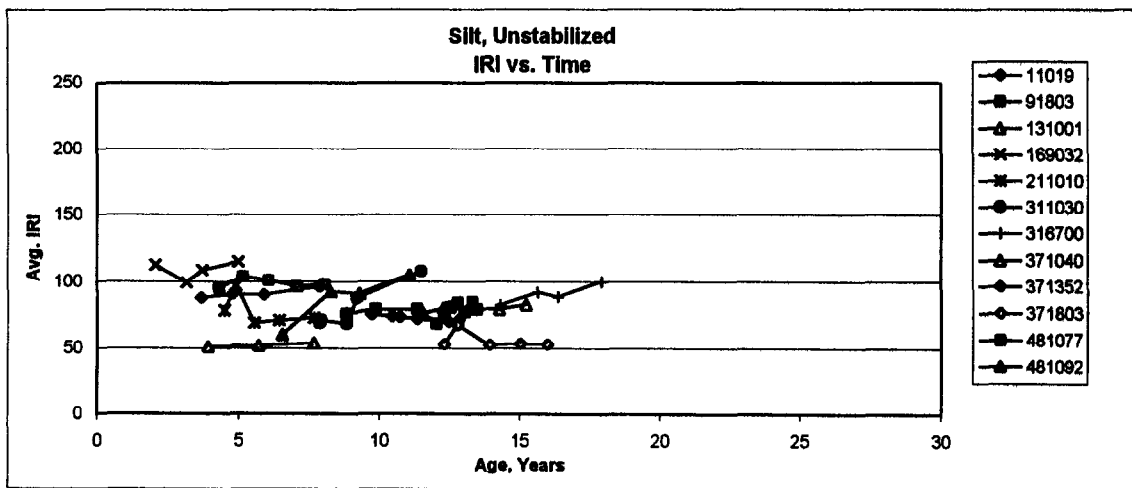
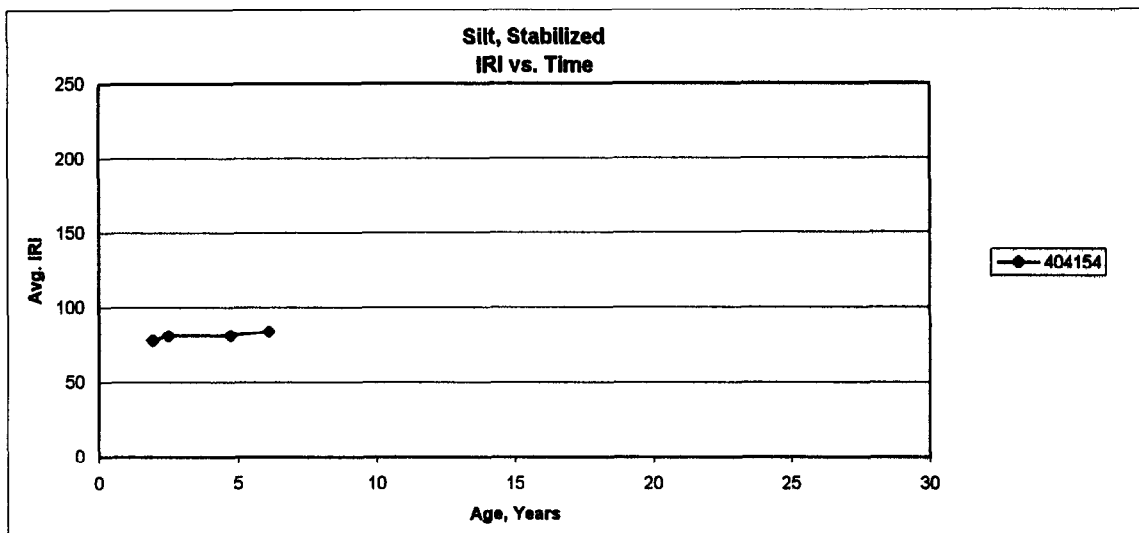


**Figure 47. Example of IRI versus time for GPS sites with silt subgrades.**

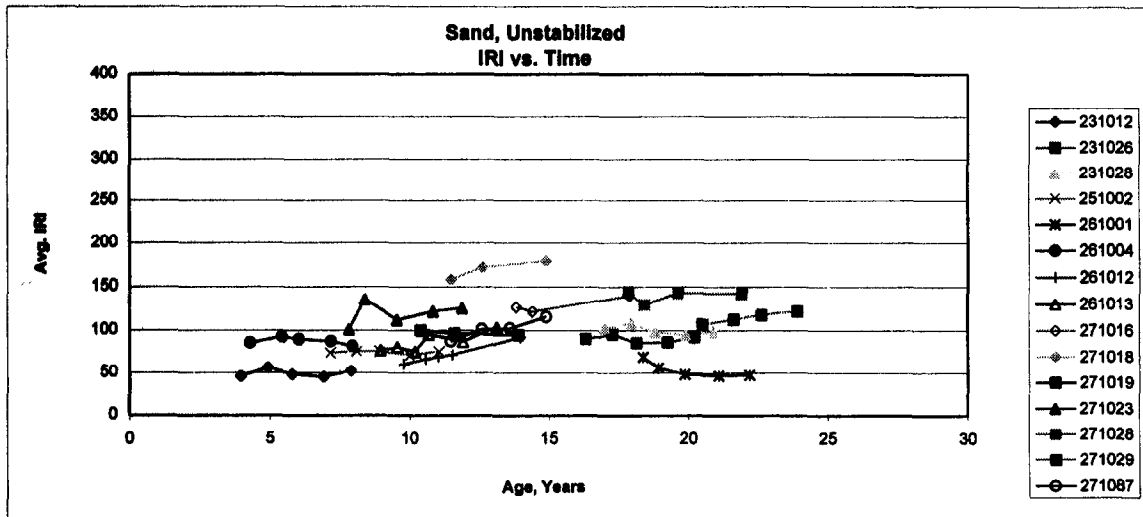
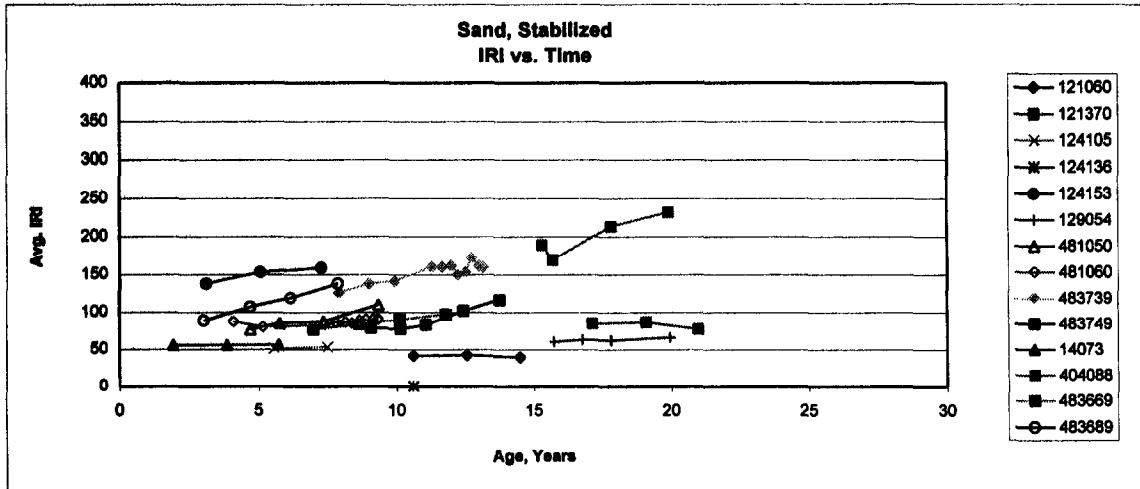


**Figure 48. Example of IRI versus time for GPS sites with sand subgrades.**

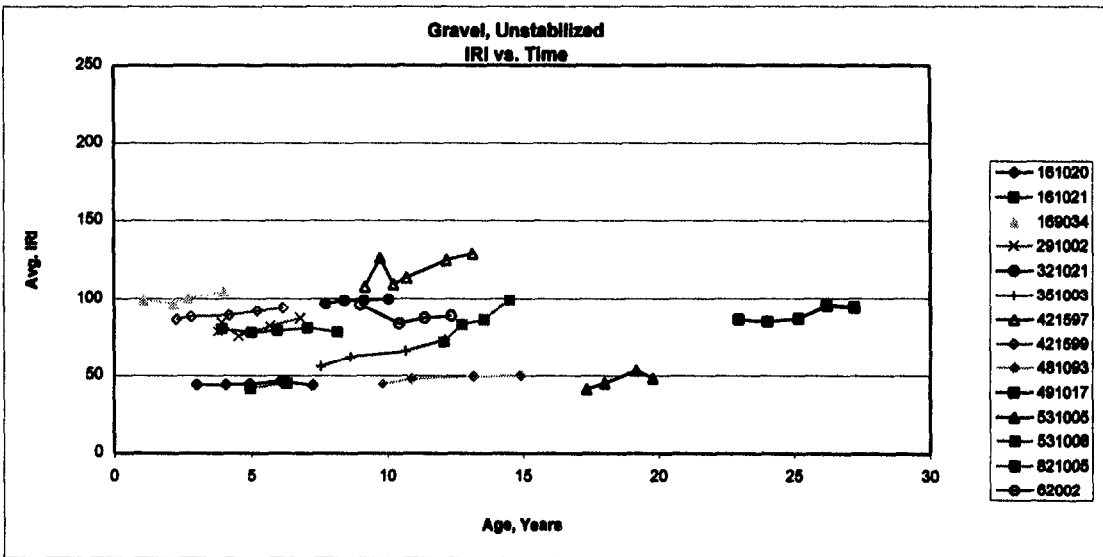
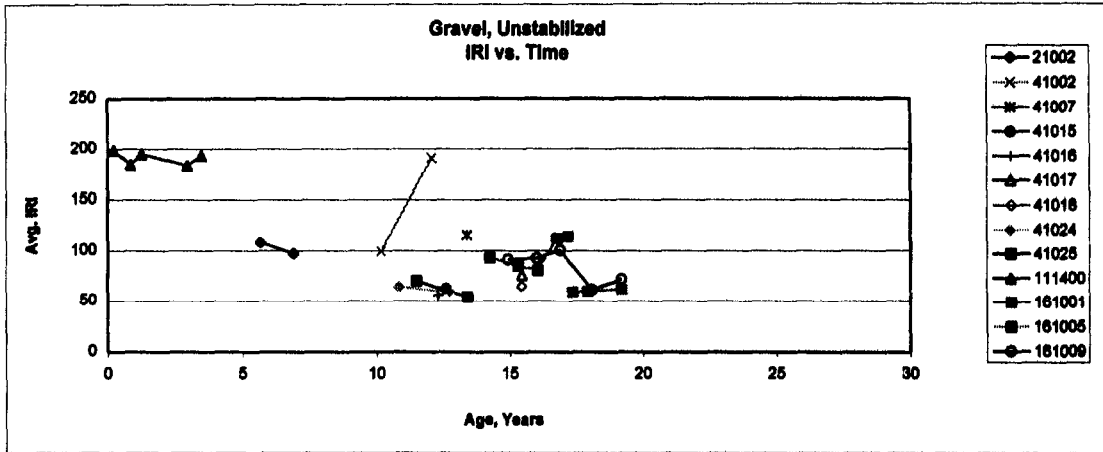


**Figure 49. Example of IRI versus time for GPS sites with gravel subgrades.**



Upon review of these comparisons, those trends which reflected steeper slopes (IRI versus time) were singled out for further review. The following is a listing of the GPS test sections that were considered for additional review:

GPS TEST SECTIONS				
Clay Unstabilized	Clay Stabilized	Sand Unstabilized	Sand Stabilized	Silt Unstabilized
082008	191044	041036	404088	481092
182008	482108	124154	483689	316700
283085	481181	261012	483739	
473104	483729	271087		
481056		283081		
481174		283087		
811804		451008		
283089		481048		
489005		906405		
481065		271029		
		483769		
		481169		
		281802		
		283091		
		836454		
		482172		

Those GPS test sections with steeper slopes (higher rates of increasing roughness) were reviewed for layer configurations and thicknesses. From this evaluation, it was observed that those sections in the unstabilized clay group with the steeper slopes all had a treated base material that was constructed on top of an untreated subgrade. All others in the unstabilized clay category without treated base materials were found to have relatively flat slopes. This observation somewhat supports the idea that full-depth pavements placed on expansive clays have inferior performance characteristics, as compared to flexible pavements with unbound granular base/subbase materials and/or stabilized subgrades.

**6.3.2 IRI vs. Fatigue Cracking.** A second set of comparisons were performed for IRI versus fatigue cracking. The primary focus of this comparison was for test sections with relatively low to no fatigue cracking and relatively high IRI values. Only test sections having clay or sand subgrades with stabilization were included in this comparison. The other group did not exhibit fatigue cracking. These comparisons included 35 of the 270 total GPS test sections included in the studies. These comparisons were inconclusive as to the benefits of subgrade stabilization,

but it was noted that a majority of the test sections having high IRI values had not experienced fatigue cracking.

#### **6.4 Effect of Stabilized Subgrades on Pavement Properties**

Material and pavement properties were also studied between the different GPS sections to determine any potential effects on the use of stabilized subgrades on pavement response and performance. Although some differences were noted, the data for pavements with stabilized subgrades are too limited to state conclusively that the noted differences are attributable to the use of stabilized or treated subgrades, rather than to some other factor. These results are briefly discussed below:

- Backcalculated subgrade moduli. As previously discussed, the backcalculated subgrade moduli for pavements with stabilized subgrade layers were found to be slightly smaller than the subgrade moduli for those pavements without stabilized subgrades.
- Moisture Contents and Percent Compaction. Moisture contents and percent compactions for the subgrade soils were reviewed to determine if the stabilized subgrade layer provides protection for the subgrade soils. The results and observations made from these comparisons are all based on the assumption that the pavements were constructed at the optimum moisture content and compacted near the maximum dry unit weight of the material.

Figure 50 is a histogram of the differences between actual moisture contents [W(act)] and optimum moisture content [W(opt)] of the subgrade soils beneath stabilized subgrade layers, and a plot of these moisture differences versus percent compaction. These subgrade soils are primarily clayey and sandy type soils. As shown, the majority of the subgrade soils have moisture contents that are higher than the optimum values.

Figures 51 and 52 show the same data, but for subgrade soils supporting pavements without stabilized subgrade layers for both sand and clay subgrades, respectively. As shown, the differences in moisture contents (actual minus optimum values) for the sandy subgrades without stabilization (figure 51) tended to be on the dry side of optimum, whereas the subgrade soils beneath a stabilized layer tended to be toward the wetter side of optimum (figure 50).

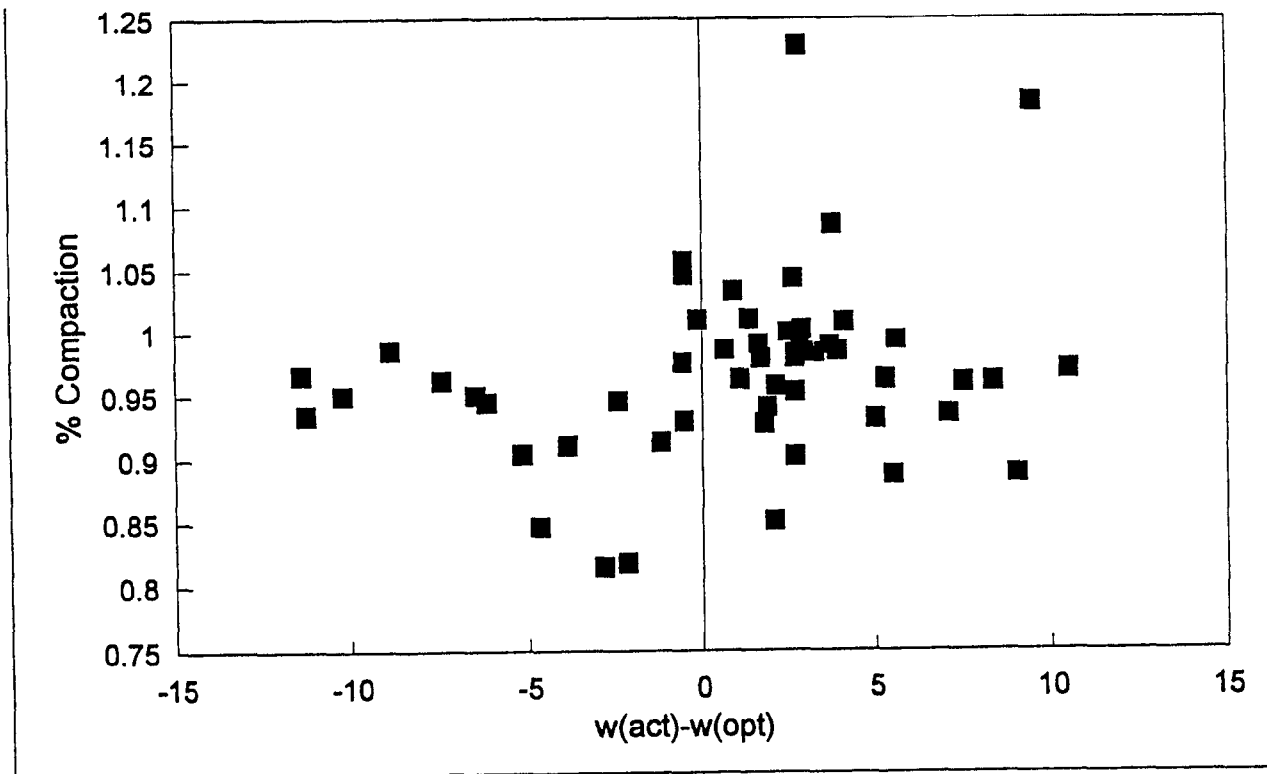
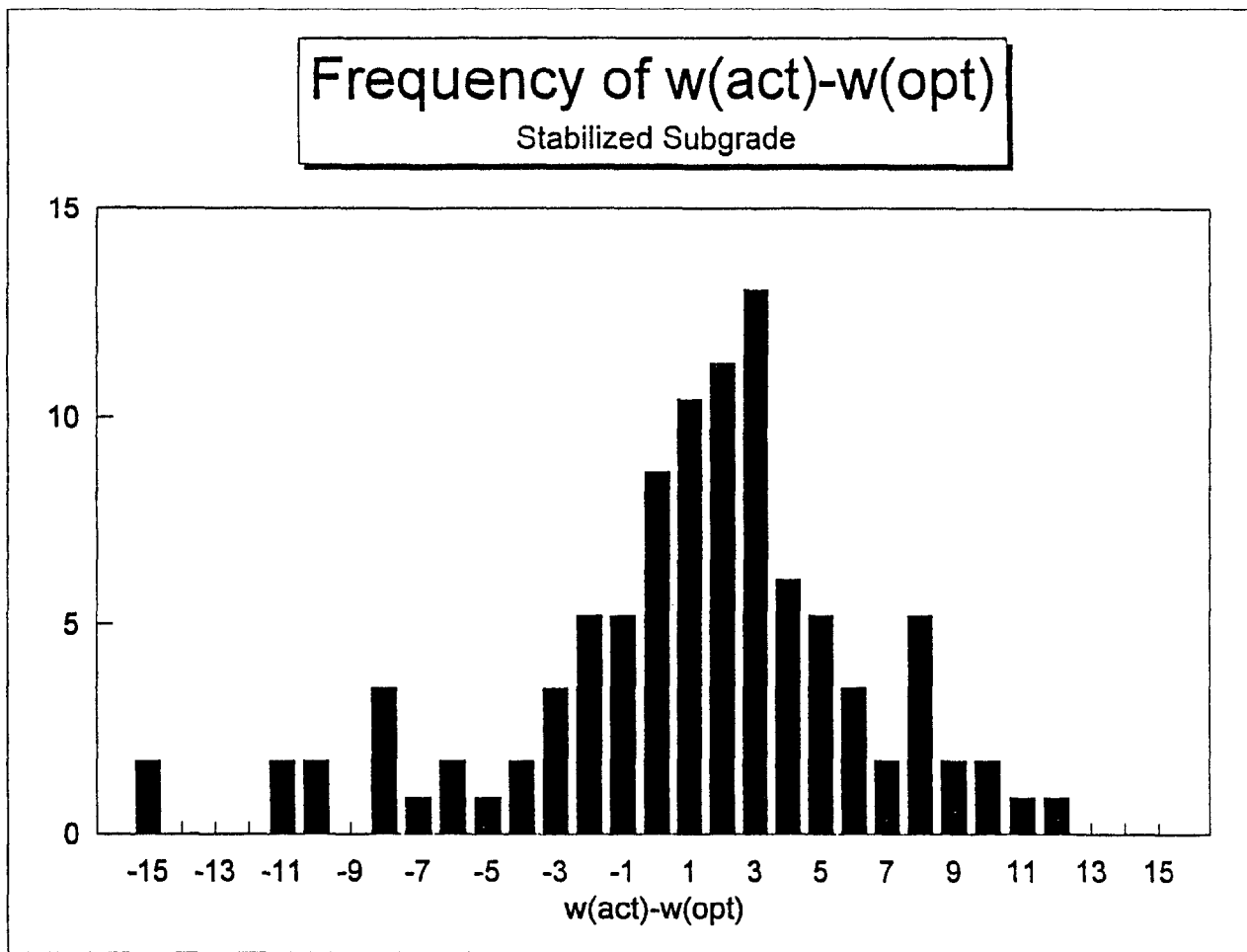
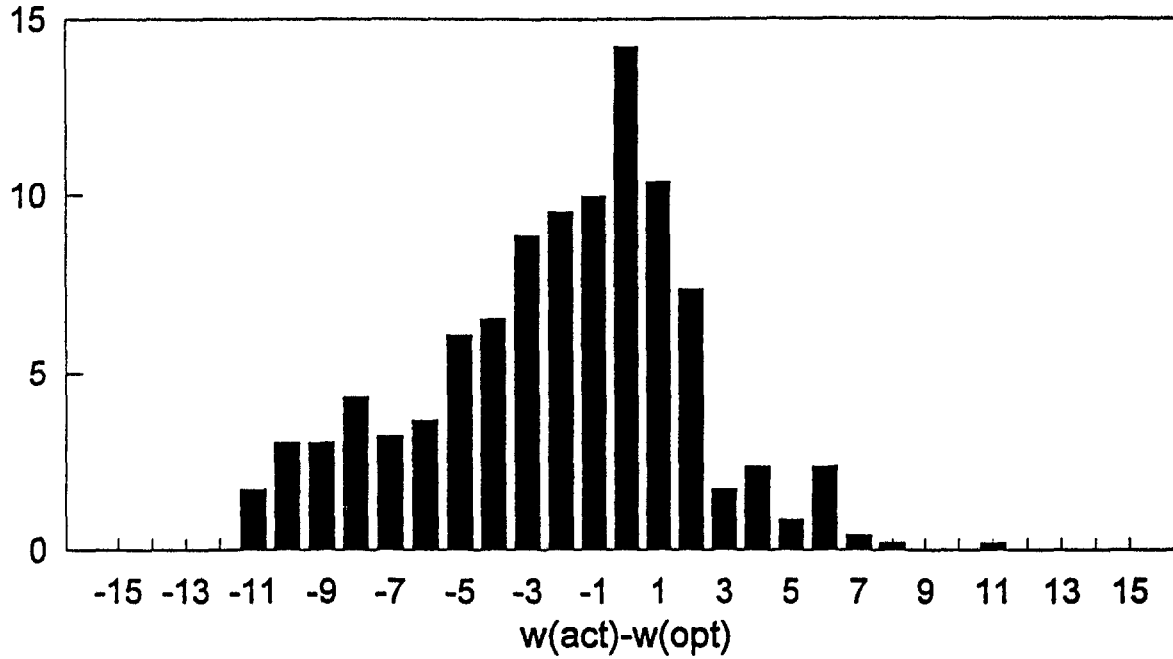


**Figure 50. Histogram and comparison of selected volumetric properties of subgrade soils beneath a stabilized subgrade layer.**

# Frequency of $w(\text{act})-w(\text{opt})$

Sand Subgrade



# % Compaction vs. $w(\text{act})-w(\text{opt})$

Sand Subgrade

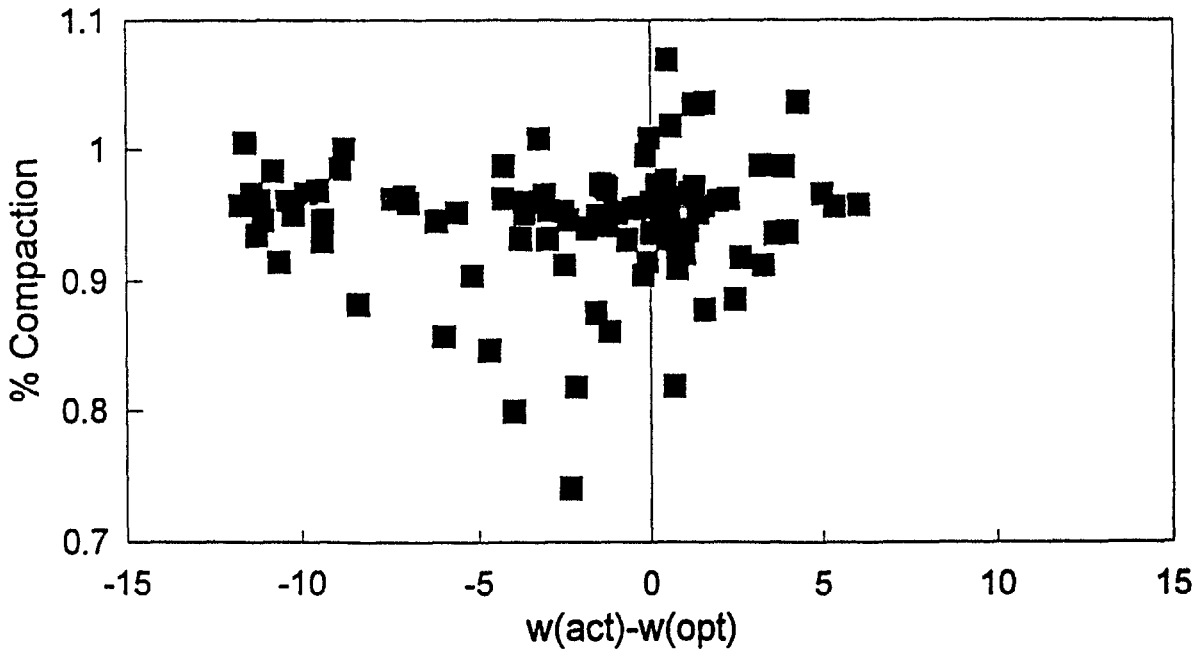
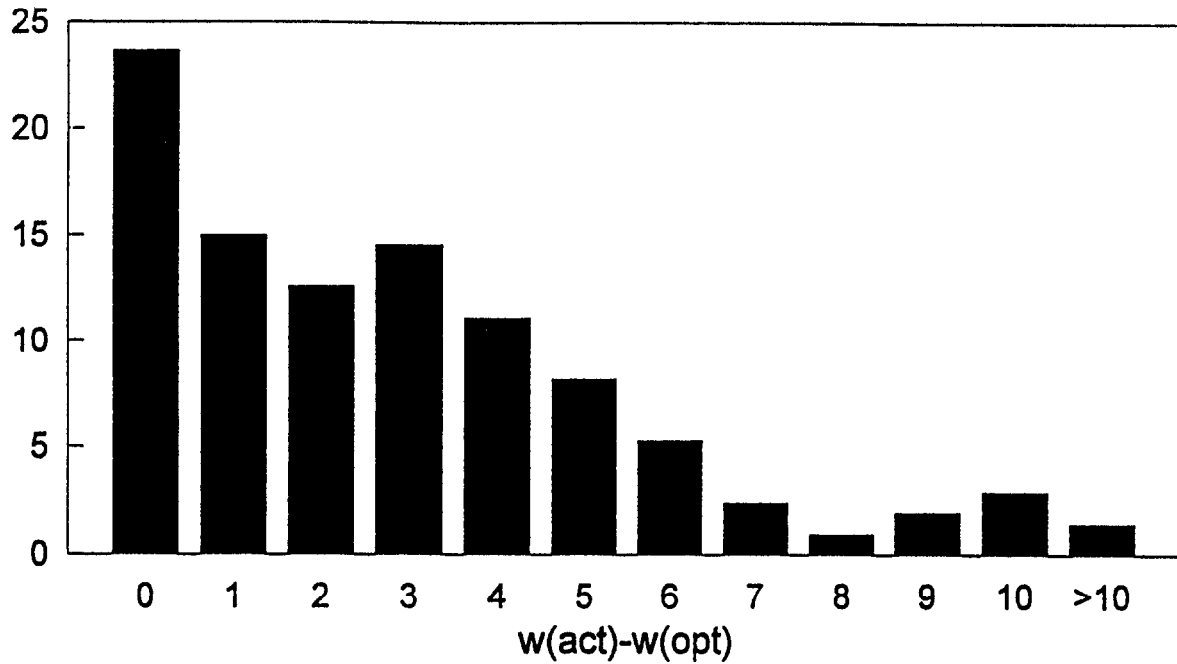


**Figure 51. Histogram and comparison of selected volumetric properties of sandy subgrades supporting pavements without any stabilized subgrade layer.**

# Frequency of $w(\text{act})-w(\text{opt})$

Clay Subgrade



# % Compaction vs. $w(\text{act})-w(\text{opt})$

Clay Subgrade

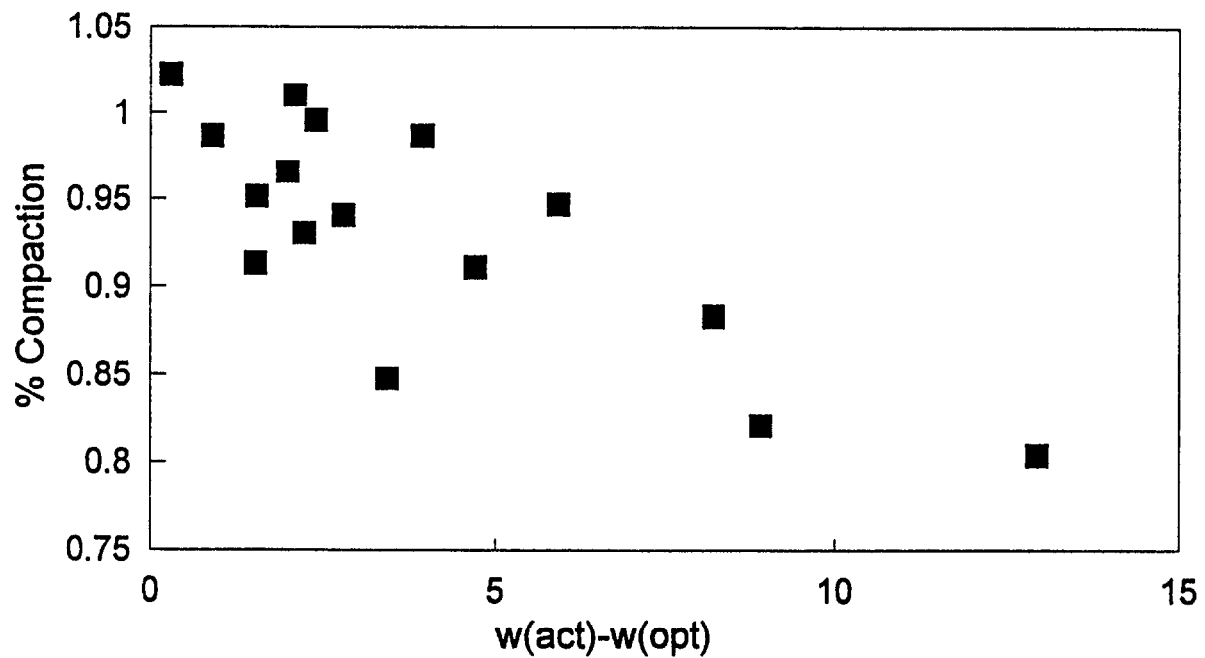


Figure 52. Histogram and comparison of selected volumetric properties of clay subgrades supporting pavements without any stabilized subgrade layer.

More importantly, there is a significant difference in the moisture contents for the clay subgrades with and without a stabilized layer. As shown in figure 52, almost all of the moisture contents for the clay subgrades without a stabilized layer are well above optimum conditions. Figure 52 also illustrates that as the moisture content increases, the percent compaction decreases, indicating possible volume change in the subgrade clay (based on the assumption mentioned above). The rate of change in IRI values with time for pavements with clay subgrades was consistently higher than for those pavements with other types of subgrade (figure 46), which should also coincide with any volume change in the underlying soils.

**Observation:** Full-depth pavements built directly on expansive soils (plasticity index exceeding 35) appear to have inferior performance characteristics, as opposed to those pavements where the asphalt concrete was placed on a granular base/subbase or stabilized material. In addition, the use of a stabilized subgrade on expansive clay soils appears to help maintain the moisture content in the clay subgrade near optimum conditions, resulting in slightly lower rates of change in IRI with time.

- **Dissipated Work.** Dissipated work was calculated using FWD deflection data measured at these sites. In general, greater values of dissipated work (i.e., more potential damage) were measured on those pavements without stabilized subgrades, as opposed to those pavements with stabilized subgrades. Figure 53 shows the dissipated work for two comparable asphalt concrete pavements in the Southern Region, one with and one without stabilized subgrades. As shown, the dissipated work is slightly greater for the pavement without the stabilized subgrade.

In summary, although some difference were noted, there are insufficient data to clearly indicate that the use of stabilized subgrades provides a definite improvement in pavement performance and properties, other than to provide a platform to facilitate construction. The one possible exception is for clay subgrades. Although the effects cannot be quantified at this time, the data indicate some minor improvements in performance (through IRI measurements) and moisture content that are closer to the optimum conditions of the subgrade soils. While the results are logical and consistent with expectations, the discrepancies between the number of test sites within sets of data for different soil types and number of stabilized subgrades preclude any positive statements on these results.

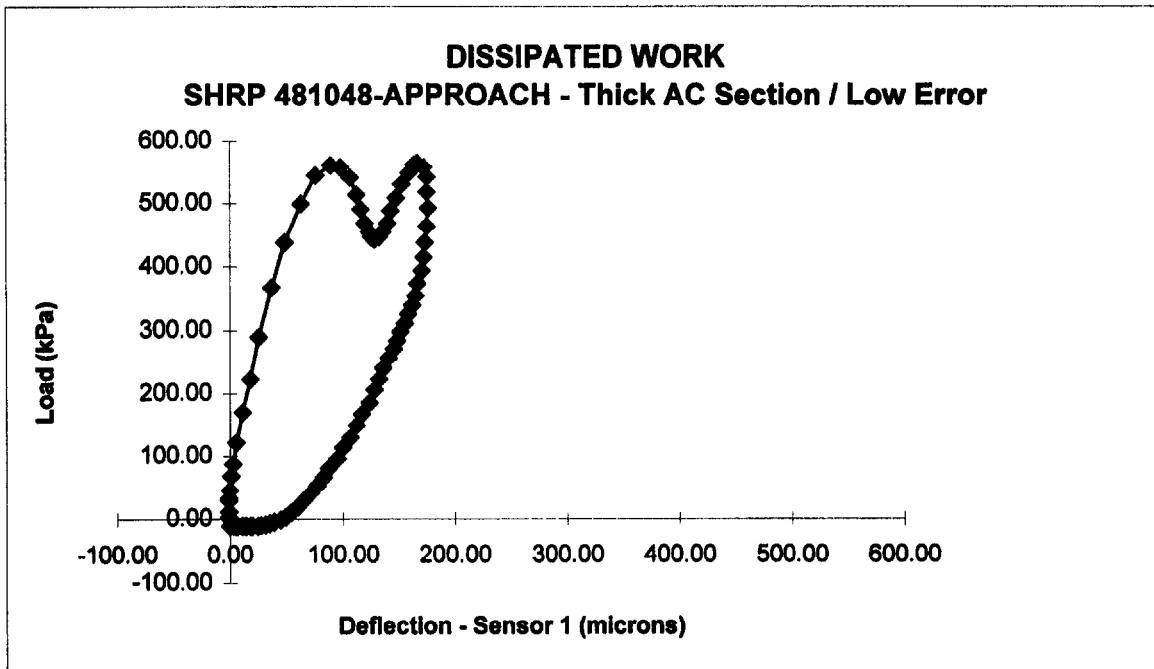
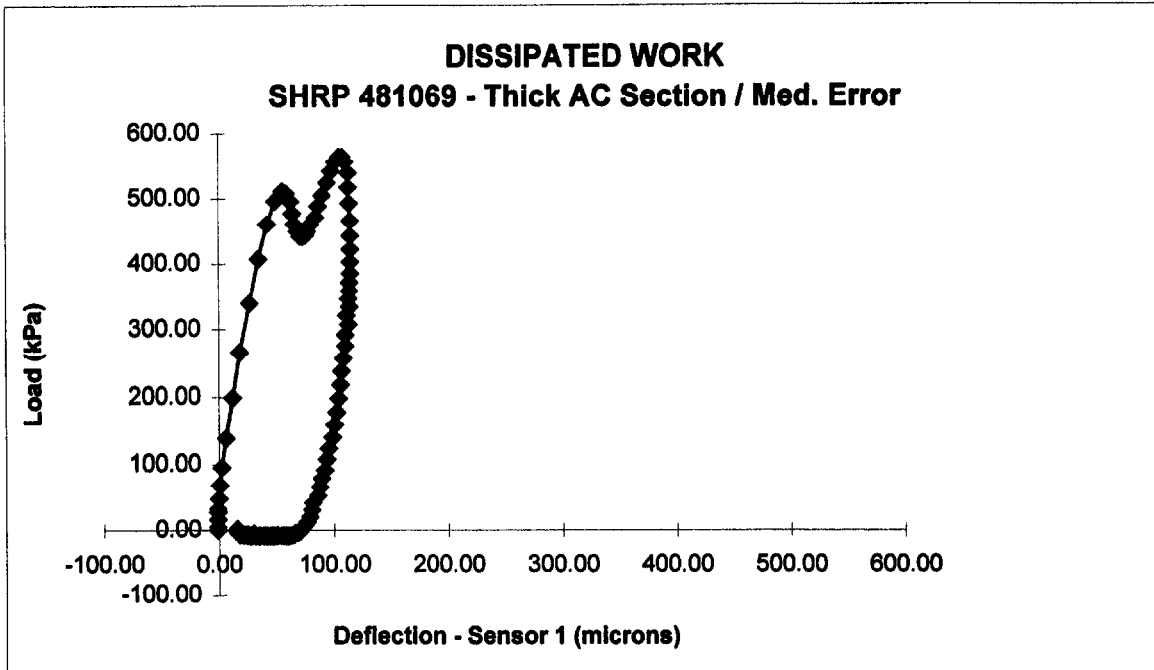


**Figure 53. Examples of the dissipated work determined from the deflection-time histories recorded during deflection testing on a pavement without a stabilized subgrade layer as compared to a pavement with a stabilized subgrade.**

## **7. SEASONAL VARIATION OF PAVEMENT MATERIALS**

Structural layer coefficients are the primary input values for determining the thickness requirements of flexible pavements using the 1986 and 1993 AASHTO Design Guide. The layer coefficient is a design parameter used to express the empirical relationship between structural number and thickness, and is a measure of the material's load-carrying capability within the pavement structure. Figure 54 shows the mean and range of values for the layer coefficients that are being used by various SHA's in the U.S. that use some version of the AASHTO Design Guide.

As layer coefficient is an empirical value that cannot be measured directly in the laboratory, the 1986 and 1993 AASHTO Design Guide provides relationships between various material properties and structural layer coefficient. Research and field studies, however, indicate many factors influencing the layer coefficients. In fact, the guide states that:

“The agency's experience must be included in implementing the results from the procedures presented. For example, the layer coefficient may vary with thickness, underlying support, position in the pavement structure, etc.”

One of the more common parameters for distinguishing among structural capacities between the different layer types is the elastic or resilient modulus. However, there are no procedures within the design guide to compensate for seasonal variation of resilient moduli for pavement layers, as for subgrade soil characterizations. In actuality, the asphalt concrete resilient moduli do vary with pavement temperatures and the resilient moduli of unbound base and subbase materials vary with stress state, moisture content and/or decompaction, similar to subgrade soils. These changes in physical properties and resilient moduli by season are not accounted for directly in the 1986 and 1993 guide.

Specifically, the design guide recommends that the elastic modulus of asphalt concrete materials be measured at a temperature of 20 °C (68 °F) to estimate the structural layer coefficient for dense-graded asphalt concrete surface courses. At 20 °C (68 °F), most mixes have layer coefficients that always exceed 0.44, especially if the instantaneous resilient modulus is used (5). The guide does not state whether the total or instantaneous resilient modulus should be used to determine the layer coefficient for asphalt concrete mixtures. The greater the elastic modulus, the larger the structural layer coefficient.



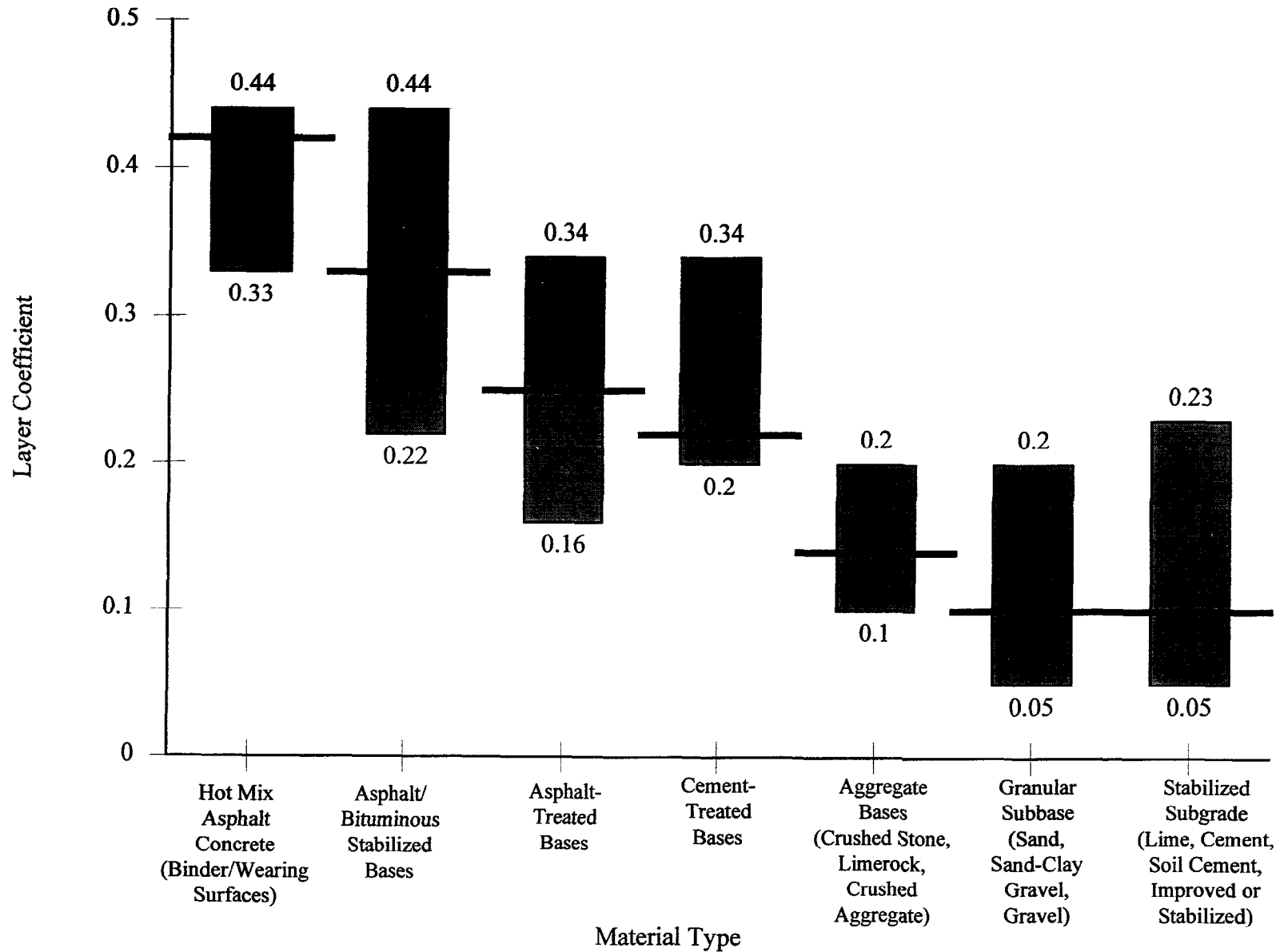


**Figure 54. Range and average values for layer strength coefficients of those SHA's using the 1972 or 1986/93 AASHTO procedures for flexible pavement design (2).**

Thus, the stiffer the mix, the better the material, or the thinner the material that needs to be provided. This obviously does not correspond to actual field performance from the warmer climates to the colder climates. Similarly, numerous studies have shown that the resilient moduli of unbound granular base and subbase materials vary with moisture content. Thus, part of this study was to develop procedures that take into account the damage caused by seasonal variation of moisture contents and/or temperatures for the different layers for flexible pavement design.

## **7.1 Seasonal Effects on Pavement Materials**

Seasonal variation has always been recognized as a significant consideration in the selection of design parameters for pavement design. However, recommendations are provided in the guide for seasonally adjusting only the subgrade design moduli. The stiffness coefficients used for the pavement structural layers are determined from a resilient modulus that is representative of the critical part of the year. As such, 64 GPS test sites were established within the LTPP Seasonal Monitoring Program (SMP) for evaluating the effects that seasonal variations (or changes in the weather) have on pavement response and material properties (as measured through deflection testing with the FWD). Deflection testing has been and is being conducted at each of these test sections, 1 day each month, along with the collection of all of the associated weather data to document the impact of weather on the structural capacity of these pavement sections. Using the data from these sites, evaluations on the effect of seasonal changes on pavement behavior can be investigated. By comparing variations in the test results with the guidelines provided in the guide, the magnitude and occurrence of deficiencies become quite apparent.

**7.1.1 Data Used in Evaluations.** NDT is conducted monthly at each of the seasonal test sites to measure changes in the pavement's response (and associated layer material properties) with changes in the weather. The seasonal sites used in the evaluations for this research activity were limited to 21 flexible seasonal sections for which at least 8 months of data were available.

Estimates of layer moduli were determined using the WESDEF backcalculation software. Testing was conducted over 61 m (200 ft) of each GPS site (at a spacing of approximately 7.5 m [25 ft]). However, test data variability along the pavement structure was averaged out to focus more directly on the seasonal variation (month-to-month changes in the measured deflection basin). Average moduli for each layer were then summarized by month and normalized to the month of June for comparison purposes. Figures 55, 56, and 57 show examples of the change in the normalized backcalculated moduli by month for asphalt concrete mixtures, base/subbase materials and subgrade soils, respectively. As shown, these seasonal differences in the surface

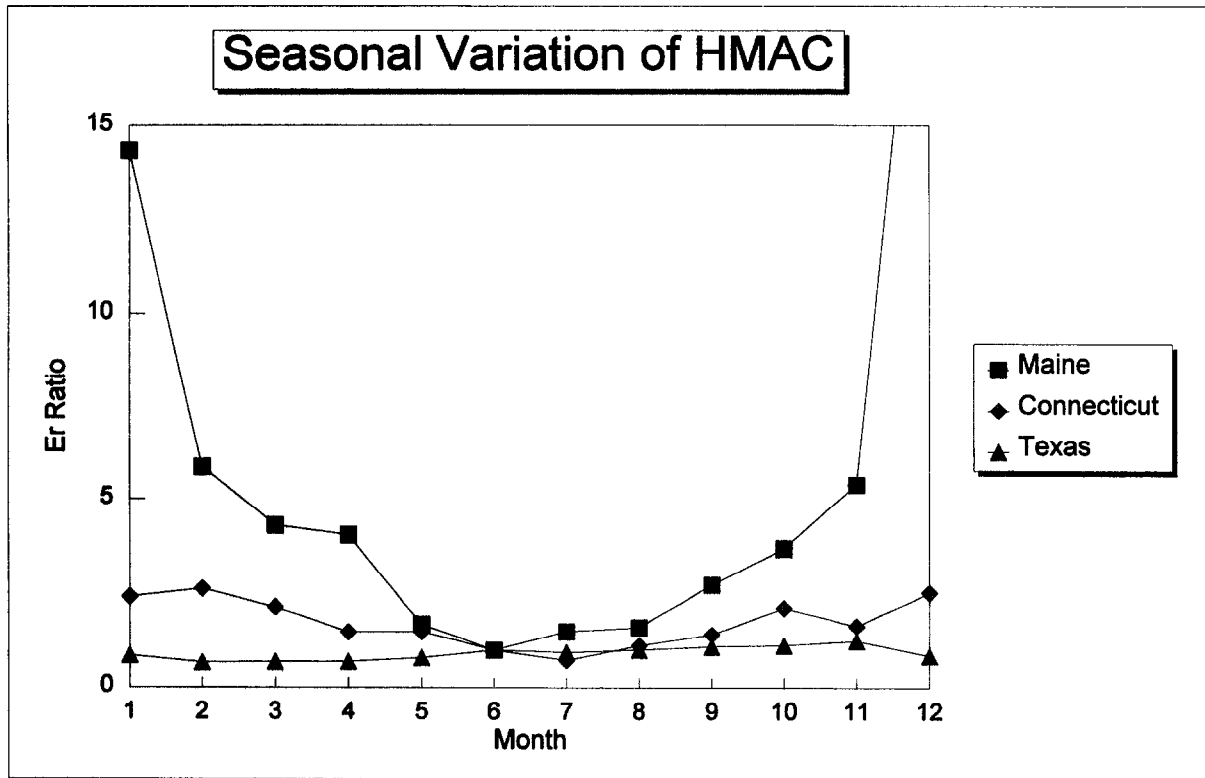


**Figure 55. Seasonal variation of the normalized backcalculated layer moduli for asphalt concrete mixtures at three of the seasonal sites.**

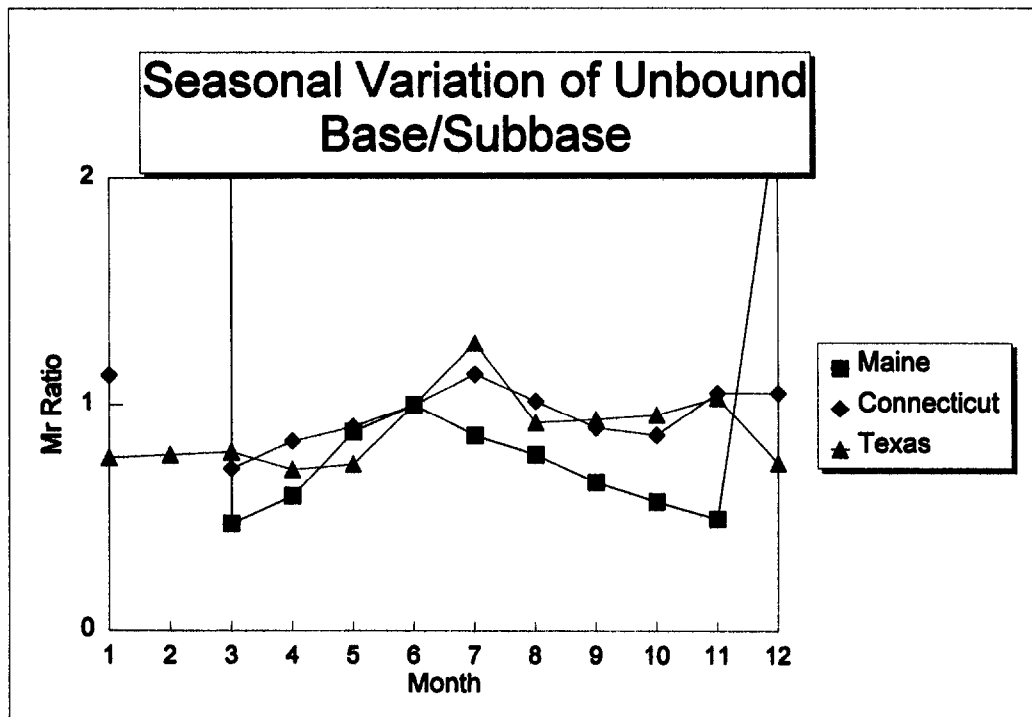


**Figure 56. Seasonal variation of the normalized backcalculated layer moduli for unbound granular base/subbase materials at three of the seasonal sites.**

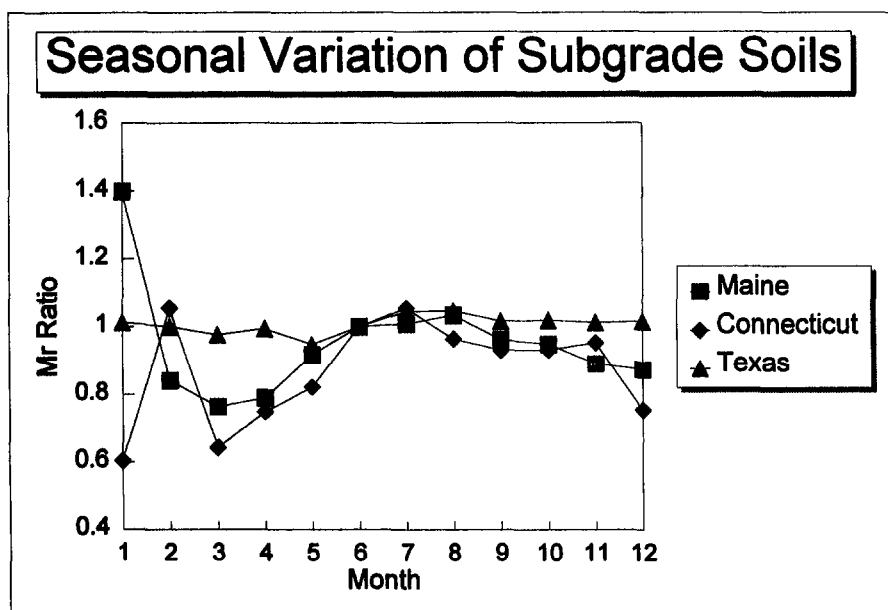


**Figure 57. Seasonal variation of the normalized backcalculated layer moduli for the subgrade soils at three of the seasonal sites.**

and base/subbase layers can be quite large, and can significantly exceed those differences in the subgrade for which seasonal differences are considered.

**7.1.2 Limitations of Evaluation.** The 21 flexible seasonal sites used in these evaluations are fairly evenly distributed across the four environmental regions. Thus, each region has less than 10 sites, limiting the different conditions and pavement types that can be studied in detail. This is actually not perceived to be that significant of a limitation, but it may ultimately be desirable to substantiate some of the findings presented in this report with additional testing at other locations.

There were several sections for which a full year of data were unavailable. Although more data will be available in the future, this limited the number of sites available for this analysis. As long as 8 months of data were available, with no more than 2 consecutive months of data missing, the data were included and used in this study.

The most significant limitation, however, was the lack of actual performance comparisons due to limited traffic data. Although the current data can be readily used to identify differences in design that seasonal changes can create, it would ultimately be interesting to evaluate the actual distinctions in performance differences (which can be attributable to seasonal variability). As these other data elements become available for these sections, this will be an area of continued interest.

## 7.2 Asphalt Concrete Materials

The guide recommends that the following relationship<sup>1</sup> be used to determine the structural layer coefficient for asphalt concrete mixtures ( $a_1$ ).

$$a_1 = 0.40 \text{Log} \left[ \frac{E_{RT}}{450} \right] + 0.44 \quad (16)$$

where:

$E_{RT}$  = The total resilient or elastic modulus, in ksi, of asphalt concrete mixtures.

---

Note 1: Equation 16, as used in the AASHTO Guide was developed using English units. As such, it is required that ksi be used in equation 16 to calculate the structural layer coefficient for asphalt concrete surface mixtures.

The total resilient modulus of the asphalt concrete ( $E_{RT}$ ) is to be measured at a temperature of 20 °C (68 °F), regardless of the environment. In actuality, the asphalt concrete resilient moduli vary with pavement temperature (see figures 8 and 55), but no consideration is given to local environmental conditions. Most mixes typically have stiffnesses at 20 °C (68 °F) that are considerably greater than the commonly assumed coefficient of 0.44. The average value used by most SHA's is 0.42 (figure 54). This implies that the same asphalt concrete mixture placed in southern Texas and northern Minnesota at equal thicknesses will have equal performance, or that the softer mixtures (lower moduli) typically used in the colder climates need to be thicker for the same traffic level. Obviously, the use of the same asphalt concrete mixtures for these two areas with diversely different environments results in differences in performance.

To compensate for different environments, various studies have used fatigue cracking to calculate an equivalent annual elastic modulus for the asphalt concrete materials. Various fatigue-cracking relationships have been developed and reported in the literature. Two of the more commonly used relationships, both of which used the AASHO Road Test data as the initial basis for development, are listed below (27, 30).

- AASHTO (30)<sup>2</sup>

$$\text{Log } N_f = 15.947 - 3.291 \text{ Log } (\epsilon_t / 10^{-6}) - 0.854 \text{ Log } (E^* / 10^3) \quad (17)$$

- Modified AASHTO (27)

$$\text{Log } N_f = \text{Log } K_1 + K_2 \text{ Log } \epsilon_t \quad (18)$$

where:

$$\begin{aligned} K_1 &= 7.87 \times 10^{-7} (E_{RT} / E_{70}) \\ K_2 &= 1.75 - 0.252 \text{ Log } K_1 \\ E^* &= \text{The complex modulus, in psi, of the asphalt concrete mixture (for this research activity, the total resilient modulus was used instead, because the complex moduli were unavailable).} \\ \epsilon_t &= \text{Tensile strain at the bottom of the asphalt concrete layer.} \end{aligned}$$

---

Note 2: Equation 17 was derived using English units. As such, it is required that psi be used in equation 17 to calculate the number of allowable wheel-load applications.

- $E_{70}$  = Modulus of the asphalt concrete mixture at a reference temperature of 21 °C (70 °F).
- $N_f$  = Allowable number of wheel-load applications to a failure level of 10-percent fatigue cracking within the wheelpath, or 5-percent, based on total area.

As part of this research activity, the procedure proposed by Von Quintus et al. (5) was used to determine the equivalent annual modulus for the asphalt concrete mixtures at each GPS site. The repeated-load indirect tensile test results included in the LTPP data base were used along with the pavement temperatures measured at the mid-depth of the asphalt concrete layer to determine the seasonal total resilient moduli. The equivalent annual resilient modulus or the design modulus  $[E_{RT}(\text{Design})]^3$  was determined in accordance with the following equation.

$$E_{RT}(\text{Design}) = \frac{\sum_{i=1}^k E_{RT}(T)_i \times DF_i}{\sum_{i=1}^k DF_i} \quad (19)$$

where:

- $DF_i$  =  $7.4754 \times 10^{10} [E_{RT}(T)]^{-1.908}$  (20)
- $DF_i$  = Damage factor for fatigue cracking in season i.
- $E_{RT}(T)_i$  = The total resilient modulus in psi (using indirect tensile loading conditions) for the average mid-depth pavement temperature (T) in °F for season i.
- k = Number of seasons (equal traffic assumed for each season).

It should be noted that the laboratory resilient moduli measured at 5 °C (41 °F) are believed to be questionable (discussed in chapter 3). As a result of this concern, only those sites where the mid-depth temperature of the asphalt concrete layer significantly exceeded 5 °C (41 °F) were used in this study. In other words, the sites used were primarily located in the Southern Region.

Asphalt concrete tensile strains were computed at the bottom of the asphalt concrete layer. Figure 58 graphically compares the asphalt concrete tensile strains (calculated with elastic layer

---

Note 3: Equation 20 was developed using English units. As such, it is required that psi be used in equations 19 and 20 to calculate the design modulus. The design modulus can then be converted to SI units.



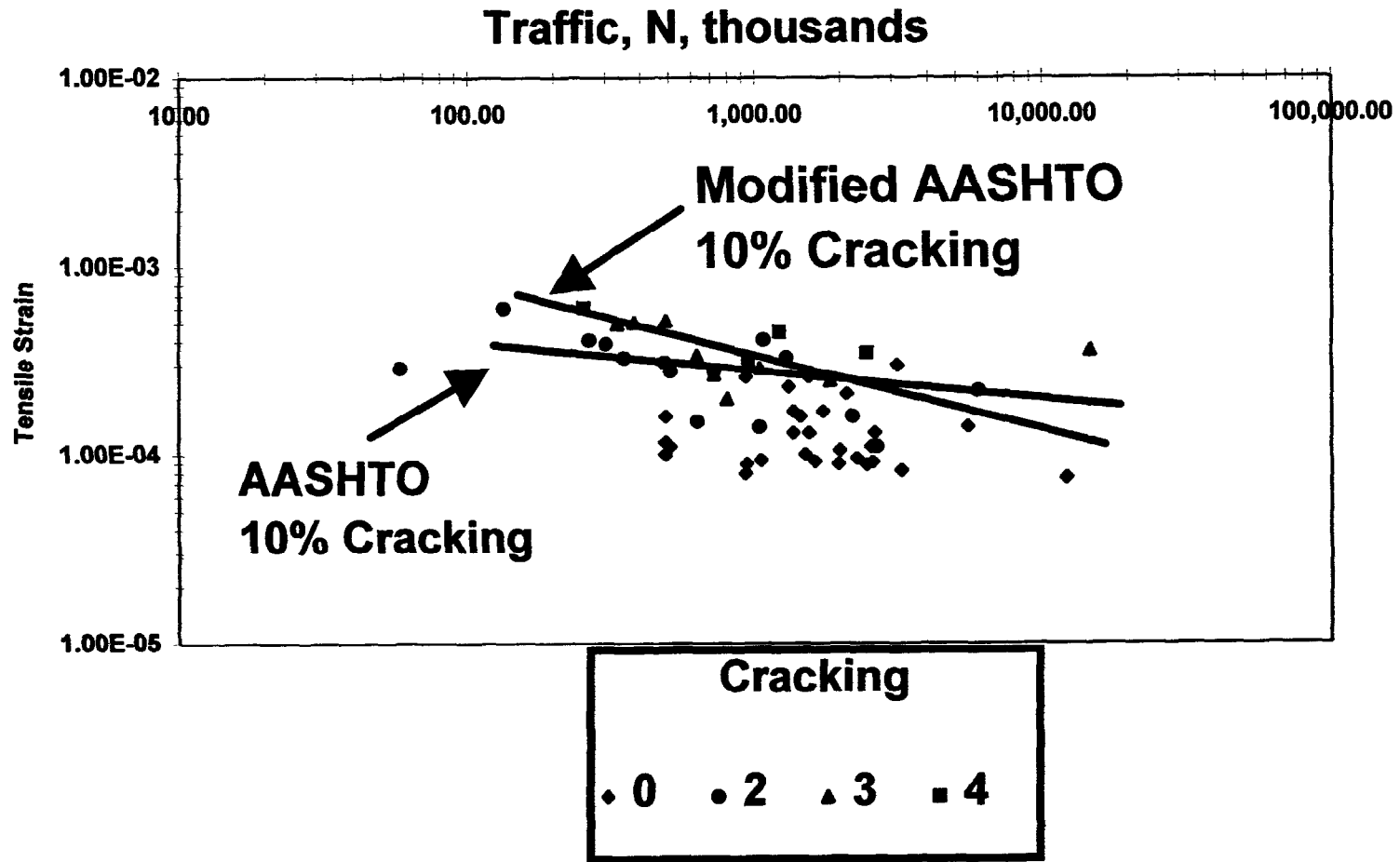


**Figure 58. Relationship between asphalt concrete tensile strains calculated with elastic layer theory of the total number of 80-kN (18-kip) ESAL's.**

theory) and the total accumulated 80-kN (18-kip) ESAL's at each site to the two fatigue failure criteria, noted as AASHTO and Modified AASHTO (equations 17 and 18). As shown, those sites with greater than 10-percent area fatigue cracking (cracking categories 3 and 4) generally fall above the AASHTO fatigue-cracking relationship and those sites with minimal to no fatigue cracking (cracking categories 0 and 2) are below the 10-percent area fatigue cracking.

Although differences do exist, as expected for evaluating fatigue properties, use of the LTPP data provides additional support on the applicability and use of equations 16 and 17. In addition, these results also suggest that use of the fatigue damage factors (equation 20) provides a reasonable comparison to the fatigue-cracking observations. Use of this procedure allows an equivalent annual modulus to be determined for asphalt concrete mixtures that are directly dependent upon the environmental conditions at a specific site. Use of these fatigue-damage factors, however, has not been validated or confirmed for designs based on a serviceability criterion.

**Observation:** Fatigue-damage factors can be used to calculate an equivalent annual or design total resilient modulus for asphalt concrete mixtures. However, these damage factors are not necessarily applicable to designs based on a serviceability criterion.

### 7.3 Unbound Base and Subbase Materials

As for the structural layer coefficients for asphalt concrete mixtures, the layer coefficients for unbound granular base and subbase materials are empirical values that cannot be measured directly in the laboratory. The guide does provide a relationship that equates the resilient modulus of the granular base material to the layer coefficient as given below:

$$a_2 = 0.249(\log_{10}M_R) - 0.977 \quad (21)$$

where:

- $a_2$  = Structural layer coefficient of the granular base.
- $M_R$  = Resilient or elastic modulus, in psi, of the unbound granular base.

Drainage coefficients (as discussed in chapter 4) have also been added to adjust for anticipated exposure to moisture and the quality of drainage. However, variability of the base modulus for varying drainage and moisture conditions by season is not accounted for in the guide. As noted for the asphalt concrete, most granular base materials have moduli considerably greater than the

modulus for a coefficient of 0.14, which is the value assumed by most SHA's (figure 54). The greater the elastic modulus, the larger the structural layer coefficient. Thus, the stiffer the material, the better the material or the thinner the layer of material that needs to be provided. However, the layer moduli and corresponding layer coefficients can vary, significantly increasing or decreasing the structural capacity of a given pavement structure (figure 56). This is a well-documented problem where spring thaw is common (going from very stiff structures to very weak or soft structures).

Using the backcalculated moduli from the deflection testing program, structural coefficients for the base materials can be calculated using equation 21. The results of these calculations are provided in table 14. As shown, these values vary considerably over the course of a year (and for most sections, are quite different from the AASHO Road Test value of 0.14). It should be reiterated, however, that these values are based on estimates from the above equation using backcalculated moduli. Equation 21 was developed and based on laboratory measured values representing the most critical part of the year. This is emphasized to note that some of the difference between the values calculated and the value from the AASHO Road Test are likely due to differences between backcalculated and laboratory moduli. Seasonal variations are still readily apparent, as shown in figure 59.

The sections in the freeze environments show definite "spikes" in the layer coefficients ( $a_2$ ) during the winter months. Obviously, one would not design for coefficients representative of the winter months. It is equally important to note, however, that where extreme seasonal variations exist, the use of average values can lead to erroneous designs. Of those sites listed in table 14, only three have average layer coefficients less than 0.14; most are significantly greater than 0.14.

Recognizing that an extensive testing effort would be required in the laboratory, nondestructive testing on a representative structure in the spring or critical season should be the most efficient method for establishing a base-layer coefficient for design purposes (see table 14) based on a serviceability criterion. Minimal testing of representative pavement structures should be conducted during their weak seasons to establish the design values for base structural layer coefficients when using the AASHTO serviceability criteria. Unfortunately, there are too few GPS seasonal sites to statistically determine the relative damage factors for granular base materials based on a serviceability criterion. The following summarizes the granular layer coefficients for each seasonal site by material and month(s) of its occurrence (values are from table 14).

Table 14. Calculated base stiffness coefficients.

	Date	a2		Date	a2		Date	a2		Date	a2		Date	a2
08SA	Jan-94	0.20	25SA	Dec-93	0.36	30SA	Jan-94	0.45	48SE	Nov-93	0.33	56SA	Jan-94	0.23
CA	Feb-94	0.19	MA	Feb-94	0.70	MT	Feb-94	0.64	TX	Dec-93	0.31	WY	Mar-94	0.10
	Mar-94	0.21		Mar-94	0.24		Mar-94	0.12		Jan-94	0.32		Apr-94	0.11
	Apr-94	0.19		Apr-94	0.15		Apr-94	0.13		Feb-94	0.32		May-94	0.12
	May-94	0.19		May-94	0.40		May-94	0.11		Mar-94	0.34		Jun-94	0.11
	Jun-94	0.32		Jun-94	0.19		Jun-94	0.12		Apr-94	0.33		Jul-94	0.11
	Jul-94	0.33		Jul-94	0.36		Jul-94	0.12		May-94	0.33		Aug-94	0.11
	Aug-94	0.34		Aug-94	0.19		Aug-94	0.14		Jun-94	0.35		Sep-94	0.11
	Sep-94	0.39		Sep-94	0.11		Sep-94	0.13		Jul-94	0.35		Nov-94	0.15
	Nov-94	0.59		Oct-94	0.07		Oct-94	0.12		Aug-94	0.36		Dec-94	0.63
	Dec-94	0.63		Nov-94	0.13		Nov-94	0.13		Sep-94	0.37			0.18
		0.33		Jan-95	0.42		Dec-94	0.61			0.34			
					0.28			0.23						
09SA	Feb-94	0.69	27SA	Dec-93	0.75	33SA	Mar-94	0.10	48SF	Dec-93	0.21	83SA	Dec-93	0.65
CO	Mar-94	0.09	MN	Jan-94	0.75	NH	Apr-94	0.14	TX	Jan-94	0.22	MB	Feb-94	0.58
	Apr-94	0.10		Mar-94	0.26		May-94	0.13		Feb-94	0.21		Mar-94	0.22
	May-94	0.12		Mar-94	0.09		Jun-94	0.12		Mar-94	0.20		Mar-94	0.04
	Jun-94	0.12		Apr-94	0.09		Jul-94	0.13		Apr-94	0.22		Apr-94	0.13
	Jul-94	0.14		May-94	0.20		Aug-94	0.11		May-94	0.28		Apr-94	0.22
	Aug-94	0.14		Jun-94	0.18		Sep-94	0.14		Jun-94	0.29		Jun-94	0.09
	Sep-94	0.12		Jul-94	0.18		Oct-94	0.10		Jul-94	0.30		Jul-94	0.05
	Oct-94	0.10		Aug-94	0.18		Nov-94	0.13		Aug-94	0.31		Aug-94	0.00
	Nov-94	0.11		Sep-94	0.18		Dec-94	0.13		Sep-94	0.30		Sep-94	0.01
	Jan-95	0.16		Oct-94	0.15		Jan-95	0.13			0.25		Oct-94	0.02
		0.17		Nov-94	0.19			0.12					Nov-94	0.01
					0.19									0.17
16SB	Feb-94	0.48	27SB	Dec-93	0.41	48SA	Oct-93	0.31	48SG	Dec-93	0.10	87SA	Jan-94	0.43
ID	Mar-94	0.20	MN	Jan-94	0.58	TX	Dec-93	0.30	TX	Jan-94	0.11	ON	Mar-94	0.26
	Apr-94	0.20		Mar-94	0.52		Jan-94	0.30		Feb-94	0.09		Apr-94	0.13
	May-94	0.18		Mar-94	0.21		Feb-94	0.29		Mar-94	0.09		May-94	0.12
	Jun-94	0.38		Apr-94	0.16		Mar-94	0.29		Apr-94	0.09		Jun-94	0.14
	Jul-94	0.35		May-94	0.15		Apr-94	0.30		May-94	0.06		Jul-94	0.17
	Aug-94	0.37		Jun-94	0.15		May-94	0.31		Jun-94	0.06		Aug-94	0.19
	Sep-94	0.42		Jul-94	0.15		Jun-94	0.38		Jul-94	0.07		Sep-94	0.15
	Nov-94	0.53		Aug-94	0.16		Jul-94	0.38		Aug-94	0.08		Oct-94	0.16
	Dec-94	0.76		Oct-94	0.15		Aug-94	0.33		Sep-94	0.05		Dec-94	0.18
		0.39		Nov-94	0.15		Sep-94	0.31		Oct-94	0.05		Feb-95	0.40
					0.25			0.32		Nov-94	0.06			0.21
											0.08			
23SA	Jan-94	0.77	27SC	Dec-93	0.74	48SB	Nov-93	0.10	50SA	Jan-94	0.74	90SA	Dec-93	0.77
ME	Feb-94	0.74	MN	Feb-94	0.75	TX	Dec-93	0.10	VT	Mar-94	0.74	SK	Jan-94	0.73
	Mar-94	0.15		Mar-94	0.23		Jan-94	0.06		Mar-94	0.22		Feb-94	0.75
	Apr-94	0.15		Mar-94	0.19		Feb-94	0.05		Apr-94	0.19		Mar-94	0.69
	May-94	0.15		Apr-94	0.20		Mar-94	0.07		May-94	0.20		Apr-94	0.09
	Jun-94	0.20		May-94	0.20		Apr-94	0.07		Jun-94	0.20		May-94	0.16
	Jul-94	0.19		Jun-94	0.19		May-94	0.07		Jul-94	0.21		Jun-94	0.15
	Aug-94	0.18		Jul-94	0.18		Jul-94	0.05		Aug-94	0.19		Jul-94	0.17
	Sep-94	0.17		Aug-94	0.17		Aug-94	0.03		Sep-94	0.19		Aug-94	0.16
	Oct-94	0.16		Sep-94	0.19		Sep-94	0.02		Oct-94	0.18		Sep-94	0.16
	Nov-94	0.14		Oct-94	0.18			0.06		Nov-94	0.19		Oct-94	0.15
	Dec-94	0.29		Nov-94	0.23					Dec-94	0.40		Nov-94	0.18
		0.27			0.29						0.31			0.35

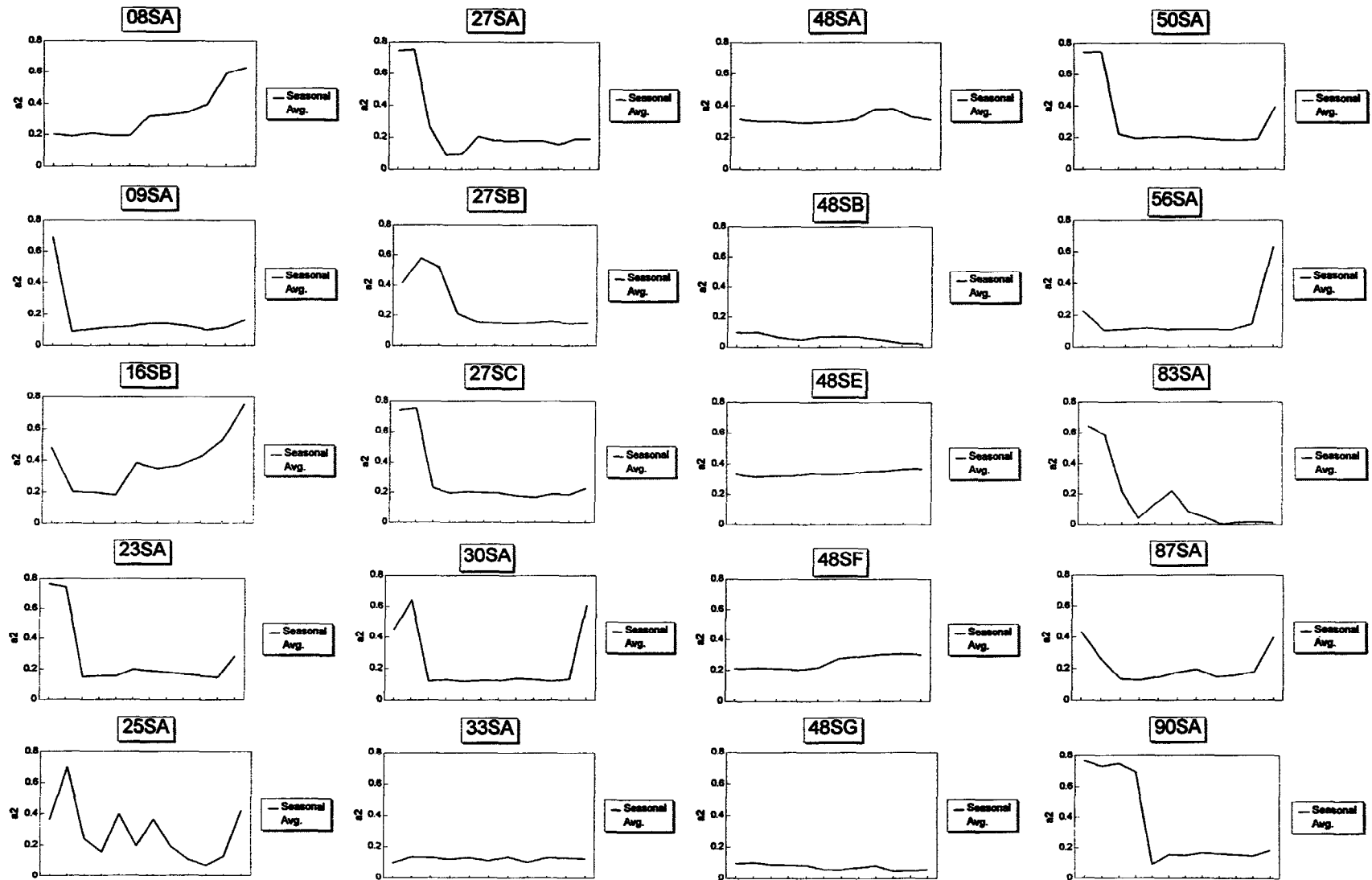


Figure 59. Plots of base stiffness coefficient by season.

Site	Lowest Layer Coefficient	Month of Occurrence
CA-08SA	0.19	April-May
CO-09SA	0.09	March
ID-16SB	0.18	May
ME-23SA	0.14	November
MA-25SA	0.07	October
MN-27SA	0.09	March-April
MN-27SB	0.15	May-July, Oct.-Nov.
MN-27SC	0.17	August
MT-30SA	0.11	May
NH-33SA	0.10	March
TX-48SA	0.29	February-March
TX-48SB	0.02	September
TX-48SE	0.31	December
TX-48SF	0.20	March
TX-48SG	0.05	September-October
VT-50SA	0.18	October
WY-56SA	0.10	March
MB-83SA	0.01	September
ON-87SA	0.12	May
SK-90SA	0.09	April

The true benefit associated with quantifying actual layer coefficient values is in identifying those cases where the layer coefficient is less than the commonly assumed value of 0.14. An oversight of this nature can significantly reduce the life of a pavement structure. As shown, 11 of the 20 sites have layer coefficients less than a value of 0.14, and some of these are significantly less than 0.14, indicating an extremely weak base material. Many of these sites only have one measurement (identified as month of occurrence) with the lowest layer coefficient, whereas other sites have two or more measurements with the lowest values. This length of time should have an effect on the design resilient modulus, which becomes extremely important in using mechanistic-empirical design procedures. These low base coefficients suggest pavements with poor performance characteristics or extensive levels of distress, which is not the case for

most of the seasonal sites. Using the coefficients associated with the base material in its weakest condition may be too conservative and inappropriate.

As such, the LTPP seasonal sites were used to develop relative damage factors based on fatigue cracking for calculating a design or equivalent resilient modulus for granular base materials, similar to the relative damage factors for the subgrade soils. Equation 17 was used to determine the seasonal damage and the equivalent annual resilient modulus of the base layer. The resulting equation is listed below<sup>4</sup>.

$$u_f = 1.885 \times 10^3 (M_R)^{-0.721} \quad (22)$$

$$M_R(\text{Base}) = \frac{\sum_{i=1}^k (M_R)_i \times (U_p)_i}{\sum_{i=1}^k (U_p)_i} \quad (23)$$

Thus, equation 23 can be used to calculate an equivalent annual modulus of the granular base/subbase layer based on a fatigue-cracking design criterion of the asphalt concrete surface. Currently, there is insufficient data in the LTPP data base to confirm and validate this theoretical development. As such, these damage factors should not be used for designs based on a serviceability criterion without confirming and validating their use. It should be noted and understood that these damage factors (equation 22) do not take into account overstressing or decompaction of granular base/subbase materials previously discussed in chapter 3.

#### 7.4 Subgrade Soils

Subgrade support is an extremely important design parameter in the AASHTO Pavement Design Equations (as in all pavement design procedures). Consequently, considerable focus is given to this parameter. In fact, most (if not all) of the compensation for seasonal variability is handled through the selection of the design moduli for the subgrade soil. Chapter 5 discussed

---

Note 4: Equations 22 and 23 were derived using English units. As such, it is required that psi be used in calculating the equivalent annual resilient modulus of unbound aggregate base/subbase layers. The equivalent annual resilient modulus can then be converted to SI units.

characterization of the subgrade soils for design. With the data from the LTPP seasonal test program, the seasonal variability at these seasonal sites can be evaluated using the backcalculated subgrade elastic moduli.

Subgrade moduli were backcalculated from deflection basin data using the WESDEF program. It should be reiterated that the guide clearly states, "...the effective roadbed soil resilient modulus determined from this chart applies only to flexible pavements designed using the serviceability criteria. It is not necessarily applicable to other resilient modulus-based design procedures." With no means of verifying that each of these sections conforms to this criteria, this issue must be considered in the evaluation of the results. The procedure, as described in section 2.3.1, establishes an estimate of relative damage ( $u_r$ ) for each of the seasonal moduli values provided (figure 45). The relationship provided in the guide is given below:<sup>5</sup>

$$u_r = 1.18 \times 10^8 \times M_R^{-2.32} \tag{24}$$

where:

$u_r$  = Relative damage based on a serviceability design criterion.

$M_R$  = Roadbed soil resilient modulus in psi.

The results of these calculations are provided in table 15. These resulting relative damage values are, in turn, averaged and the average relative damage value is then used to establish the design roadbed soil resilient modulus.

To evaluate the effectiveness of this approach for accommodating the seasonal variability, structural numbers (SN) were determined using the AASHTO equation and each of the individual monthly moduli, the design modulus, and the simple average modulus. Ratios of each SN value were plotted versus the SN value corresponding to the design moduli (following the guide). These plots are shown in figure 60.

As shown, there are frequent "spikes" on the sections in the freeze environments where the ratio drops well below equality (a ratio of 1). This implies that in these instances, the procedure recommended in the guide results in a required SN considerably greater than that required for those periods when the subgrade is extremely stiff (or frozen). This is to be expected, but as with

---

Note 5: Equation 24, as used in the AASHTO Design Guide, was developed using English units. As such, it is required that psi be used in calculating the Roadbed Soil Resilient Modulus. The Roadbed Soil Resilient Modulus can then be converted to SI units.



**Table 15. Backcalculated subgrade moduli and associated data (see footnote 5).**

Date				Date				Date				Date				Date								
Average Subgrade Mr		Relative Damage Uf	SN	Average Subgrade Mr		Relative Damage Uf	SN	Average Subgrade Mr		Relative Damage Uf	SN	Average Subgrade Mr		Relative Damage Uf	SN	Average Subgrade Mr		Relative Damage Uf	SN					
08SA CA	Jan-94	15018	0.02	2.52	25SA MA	Dec-93	21875	0.01	2.24	30SA MT	Jan-94	15090	0.02	2.52	48SE TX	Nov-93	31346	0.00	1.99	56SA WY	Jan-94	18663	0.01	2.36
	Feb-94	14769	0.03	2.53		Feb-94	26126	0.01	2.12		Feb-94	11086	0.05	2.76		Dec-93	31378	0.00	1.99		Mar-94	16730	0.02	2.44
	Mar-94	14824	0.02	2.53		Mar-94	19869	0.01	2.31		Mar-94	9115	0.08	2.91		Jan-94	32570	0.00	1.97		Apr-94	17513	0.02	2.41
	Apr-94	14753	0.03	2.54		Apr-94	21525	0.01	2.26		Apr-94	9673	0.07	2.86		Feb-94	29425	0.01	2.04		May-94	17006	0.02	2.43
	May-94	14732	0.03	2.54		May-94	22499	0.01	2.22		May-94	9201	0.08	2.90		Mar-94	32311	0.00	1.97		Jun-94	18375	0.02	2.37
	Jun-94	12472	0.04	2.66		Jun-94	24128	0.01	2.17		Jun-94	9332	0.07	2.89		Apr-94	30407	0.00	2.01		Jul-94	19345	0.01	2.33
	Jul-94	12262	0.04	2.68		Jul-94	25404	0.01	2.14		Jul-94	9294	0.07	2.90		May-94	31088	0.00	2.00		Aug-94	19533	0.01	2.33
	Aug-94	12231	0.04	2.68		Aug-94	25406	0.01	2.14		Aug-94	9539	0.07	2.88		Jun-94	28016	0.01	2.07		Sep-94	18520	0.01	2.37
	Sep-94	11346	0.05	2.74		Sep-94	23662	0.01	2.19		Sep-94	9409	0.07	2.89		Jul-94	42219	0.00	1.79		Nov-94	16734	0.02	2.44
	Nov-94	7332	0.13	3.09		Oct-94	25292	0.01	2.14		Oct-94	8347	0.09	2.98		Aug-94	43349	0.00	1.78		Dec-94	19004	0.01	2.35
	Dec-94	6257	0.18	3.22		Nov-94	21655	0.01	2.25		Nov-94	8570	0.09	2.96		Sep-94	43163	0.00	1.78			18142	0.02	2.39
		12363	0.05	2.63		Jan-95	17222	0.02	2.42		Dec-94	7545	0.12	3.07			34116	0.00391	1.83			18047	2.40	
		10592.4	2.74	Dec-94	22888	0.01	2.21		9683	0.07	2.83			32886.4	1.93									
						22355	2.24			9298.57	2.87													
09SA CO	Feb-94	53963	0.00	1.64	27SA MN	Dec-93	24936	0.01	2.15	33SA NH	Mar-94	23445	0.01	2.20	48SF TX	Dec-93	8794	0.08	2.94	83SA MB	Dec-93	19855	0.01	2.32
	Mar-94	30217	0.00	2.02		Jan-94	144836	0.00	1.08		Apr-94	48498	0.00	1.70		Jan-94	10022	0.06	2.84		Feb-94	41110	0.00	1.81
	Apr-94	35570	0.00	1.91		Mar-94	68979	0.00	1.49		May-94	37064	0.00	1.88		Feb-94	9704	0.07	2.86		Mar-94	79694	0.00	1.40
	May-94	39160	0.00	1.84		Mar-94	37719	0.00	1.87		Jun-94	33304	0.00	1.95		Mar-94	10020	0.06	2.84		Mar-94	54707	0.00	1.63
	Jun-94	44785	0.00	1.76		Apr-94	25193	0.01	2.14		Jul-94	33848	0.00	1.94		Apr-94	9003	0.08	2.92		Apr-94	39745	0.00	1.83
	Jul-94	51427	0.00	1.67		May-94	18194	0.02	2.38		Aug-94	35986	0.00	1.90		May-94	8573	0.09	2.96		Apr-94	18757	0.01	2.36
	Aug-94	46231	0.00	1.74		Jun-94	23003	0.01	2.21		Sep-94	40616	0.00	1.82		Jun-94	9081	0.08	2.91		Jun-94	14385	0.03	2.55
	Sep-94	45376	0.00	1.75		Jul-94	21583	0.01	2.25		Oct-94	36606	0.00	1.89		Jul-94	11088	0.05	2.76		Jul-94	14969	0.02	2.52
	Oct-94	47184	0.00	1.72		Aug-94	22029	0.01	2.24		Nov-94	519740	0.00	0.52		Aug-94	11522	0.04	2.73		Aug-94	15439	0.02	2.50
	Nov-94	39020	0.00	1.85		Sep-94	23382	0.01	2.20		Dec-94	23043	0.01	2.21		Sep-94	10999	0.05	2.76		Sep-94	15693	0.02	2.49
	Jan-95	32990	0.00	1.96		Oct-94	19785	0.01	2.32		Jan-95	197308	0.00	0.93			9881	0.0661	2.75		Oct-94	15876	0.02	2.48
		38827	0.00	1.86		Nov-94	19047	0.01	2.35			93587	0.00	1.98				9722.77	2.84		Nov-94	15930	0.02	2.48
		41737	1.85		19047	0.00756	2.35		34616	1.86							15930	0.01426	2.48					
						24752.2	2.22											18833.6	2.37					
16SB ID	Feb-94	17590	0.02	2.40	27SB MN	Dec-93	13520	0.03	2.60	48SA TX	Oct-93	17590	0.02	2.40	48SG TX	Dec-93	11260	0.05	2.74	87SA ON	Jan-94	31360	0.00	1.99
	Mar-94	14289	0.03	2.56		Jan-94	19587	0.01	2.32		Dec-93	16387	0.02	2.46		Jan-94	11338	0.05	2.74		Mar-94	26985	0.01	2.10
	Apr-94	13686	0.03	2.59		Mar-94	34723	0.00	1.92		Jan-94	15950	0.02	2.48		Feb-94	11059	0.05	2.76		Apr-94	20679	0.01	2.29
	May-94	13437	0.03	2.61		Mar-94	24966	0.01	2.15		Feb-94	15909	0.02	2.48		Mar-94	10955	0.05	2.77		May-94	20520	0.01	2.29
	Jun-94	11936	0.04	2.70		Apr-94	19386	0.01	2.33		Mar-94	15865	0.02	2.48		Apr-94	11018	0.05	2.76		Jun-94	23979	0.01	2.18
	Jul-94	13098	0.03	2.63		May-94	16896	0.02	2.43		Apr-94	17846	0.02	2.39		May-94	10430	0.06	2.80		Jul-94	24164	0.01	2.17
	Aug-94	12654	0.04	2.65		Jun-94	18772	0.01	2.36		May-94	18960	0.01	2.35		Jun-94	10549	0.05	2.80		Aug-94	27279	0.01	2.09
	Sep-94	12102	0.04	2.69		Jul-94	17661	0.02	2.40		Jun-94	22444	0.01	2.23		Jul-94	11685	0.04	2.71		Sep-94	24737	0.01	2.16
	Nov-94	11617	0.04	2.72		Aug-94	16938	0.02	2.43		Jul-94	22655	0.01	2.22		Aug-94	11961	0.04	2.70		Oct-94	24024	0.01	2.18
	Dec-94	14806	0.02	2.53		Oct-94	15568	0.02	2.50		Aug-94	21624	0.01	2.25		Sep-94	11806	0.04	2.71		Dec-94	92901	0.00	1.32
		13521	0.03	2.60		Nov-94	15234	0.02	2.51		Sep-94	21280	0.01	2.26		Oct-94	11668	0.04	2.72		Feb-95	88745	0.00	1.34
			13232.4	2.57			15234	0.01645	2.51			18774	0.01543	2.39		Nov-94	11506	0.04	2.73			36852	0.01	2.29
						17706.5	2.44			18202.4	2.38			11269	0.04725	2.74		26293	2.17					
														11237	2.74									
23SA ME	Jan-94	50133	0.00	1.68	27SC MN	Dec-93	38341	0.00	1.86	48SB TX	Nov-93	13889	0.03	2.58	50SA VT	Jan-94	23760	0.01	2.19	90SA SK	Dec-93	50670	0.00	1.68
	Feb-94	92868	0.00	1.32		Feb-94	89766	0.00	1.34		Dec-93	14583	0.03	2.54		Mar-94	24742	0.01	2.16		Jan-94	114657	0.00	1.20
	Mar-94	33383	0.00	1.95		Mar-94	50199	0.00	1.68		Jan-94	13014	0.03	2.63		Mar-94	21769	0.01	2.25		Feb-94	141421	0.00	1.09
	Apr-94	25200	0.01	2.14		Mar-94	31525	0.00	1.99		Feb-94	19115	0.01	2.34		Apr-94	16641	0.02	2.45		Mar-94	184757	0.00	0.96
	May-94	25975	0.01	2.12		Apr-94	26945	0.01	2.10		Mar-94	15947	0.02	2.48		May-94	17420	0.02	2.41		Apr-94	45729	0.00	1.74
	Jun-94	31691	0.00	1.98		May-94	27934	0.01	2.07		Apr-94	14982	0.02	2.52		Jun-94	16993	0.02	2.43		May-94	21226	0.01	2.27
	Jul-94	32118	0.00	1.98		Jun-94	31534	0.00	1.99		May-94	15064	0.02	2.52		Jul-94	17530	0.02	2.41		Jun-94	21471	0.01	2.26
	Aug-94	31370	0.00	1.99		Jul-94	30743	0.00	2.01		Jul-94	18328	0.02	2.37		Aug-94	17549	0.02	2.41		Jul-94	23936	0.01	2.18
	Sep-94	29942	0.00	2.02		Aug-94	31061	0.00	2.00		Aug-94	18582	0.01	2.36		Sep-94	17653	0.02	2.40		Aug-94	23857	0.01	2.18
	Oct-94	27602	0.01	2.08		Sep-94	27538	0.01	2.08		Sep-94	18682	0.01	2.36		Oct-94	18268	0.02	2.38		Sep-94	22731	0.01	2.22
	Nov-94	26301	0.01	2.11		Oct-94	26635	0.01	2.11			16219	0.02157	2.40		Nov-94	18002	0.02	2.39		Oct-94	22022	0.01	2.24
	Dec-94	26630	0.01	2.11		Nov-94	26022	0.01	2.12				15756.5	2.47		Dec-94	17728	0.02	2.40		Nov-94	21159	0.01	2.27
	36101	0.00	1.97		26022	0.00443	2.12						19004	0.01	2.41		21159	0.00595	2.27					
		30463	2.06			31160.3	2.03							18515	2.37			27444	2.10					

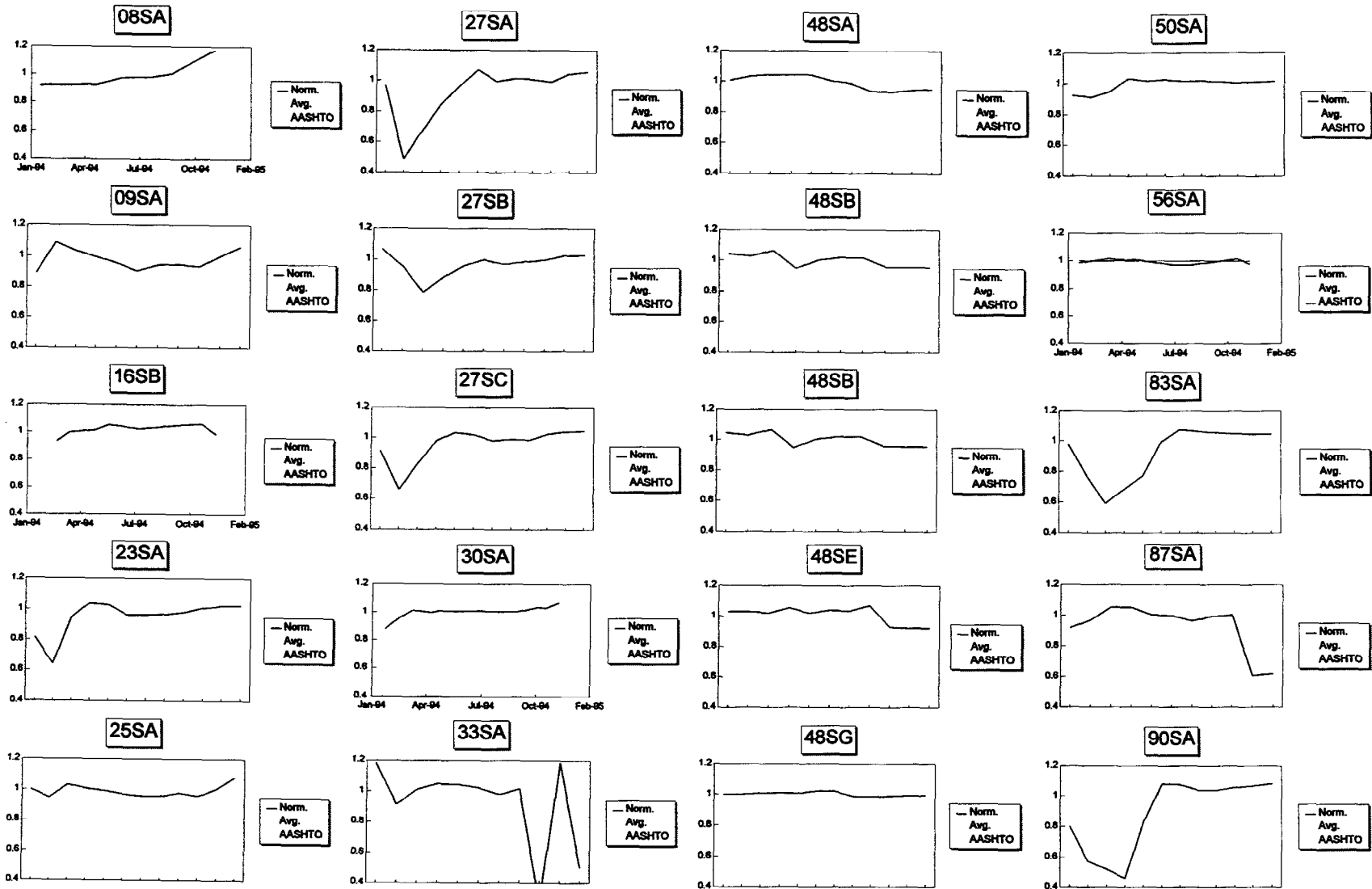


Figure 60. Ratio of SN based on seasonal subgrade Mr to the SN based on the guide.

the similar scenario with the unbound granular base materials, one would not design for moduli representative of the winter months (or even moduli generated from nondestructive testing during the summer when the subgrade is relatively dry and stiff). It is equally important to note, however, that where extreme seasonal variations exist, simple average values can also lead to erroneous designs.

The cases of particular concern, however, are when the ratio is greater than equality. This indicated occasions when the SN value required for a particular month is actually above that predicted from the seasonally adjusted moduli value recommended in the guide. In most instances, these errors do not exceed 10 percent. However, there are some cases noted where the monthly prediction is off by as much as 20 percent.

For design purposes using the original AASHO design equation, the subgrade resilient moduli (as with the base structural layer coefficients) should be measured from the testing conducted on representative subgrade soil specimens in their weakest state. As can be seen from the plots in figure 60, this is typically the spring season (March and/or April).

Minimal testing of representative pavement structures should be conducted during their weak seasons (typically March and April) to estimate the design values for the subgrade modulus (as with the base layer coefficients). If laboratory testing is to be used for establishing the resilient modulus of the roadbed subgrade soil, consideration should be given to duplicating the moisture-content levels that might be expected during the spring, as noted in the guide. However, to accurately establish this correction factor, the designer must conduct some field testing to establish the in situ moisture conditions during these seasons of weakness. Recognizing the level of effort that laboratory testing requires, it again would appear that nondestructive testing on a representative structure should prove to be the most efficient method for establishing a roadbed soil resilient modulus for design purposes.

Although the procedure included in the guide appears to be relatively effective (within 10 percent at selecting a design subgrade modulus), it requires considerably more nondestructive testing than simply focusing on the weakest season. Collection of an entire years worth of NDT is understandably a sizeable task, but more importantly, the weighted averaging process still allows for inadequate designs.

Damage factors for the subgrade soils were also determined theoretically to ensure that there is sufficient cover to prevent overstressing and excessive permanent deformation in the subgrade.

Equation 14 was used as the failure criteria, along with data from the SMP sites, to develop a relationship between subgrade resilient moduli and damage factors,  $U_{rs}$ , as given below:<sup>6</sup>

$$U_{rs} = 4.022 \times 10^7 [M_R]^{-1.962} \quad (25)$$

Thus, equation 25 can be used to calculate an equivalent annual modulus of the subgrade soil based on permanent deformation in the subgrade. Presently, there is insufficient data to validate this theoretical development. As expected, however, the damage factors based on a serviceability criterion (equation 24) are different than those based on minimizing permanent deformations in the subgrade from wheel loads.

With advances in technology, such as nondestructive deflection testing, and the wealth of data becoming available through the LTPP Program and similar studies, there will be many opportunities for exploring some of these enhancements and their effects on pavement designs and predicting performance. As pointed out in the guide, seasonal variability must be adequately accounted for. These studies reiterate the importance of avoiding the use of material properties in design that represent ideal conditions (or conditions when the paving materials are relatively dry and stiff, or frozen). However, these studies also point out the relative effects of using simple averaging (or even weighted averages as in the case of the subgrade moduli). With the complete sets of seasonal data available from these test sections, and simple evaluations like those conducted here, designers should now be able to focus their energies on establishing their design parameters based on spring evaluations (or when moisture contents are at their peak and moduli are at their lowest), using designs based on a serviceability criterion. This research activity has also presented methods to determine design layer moduli for specific distresses (or performance measures) that are required for mechanistic-empirical design procedures.

---

Note 6: Equation 25 was developed using English units. As such, it is required that psi be used to calculate the damage factors.

## **8. FWD DEFLECTION-TIME DATA AND PAVEMENT PERFORMANCE**

### **8.1 Background**

Wave propagation NDT methods were largely initiated by the U.S. Air Force for nondestructive pavement evaluations in the late 1960's. However, a procedure was not formally adopted by the Air Force for routine pavement evaluations until 1978 (32). Initially, loads were applied to the pavement by a steady-state vibrator, but this use of NDT was limited because of the equipment size and complexity and data analysis requirements.

During the latter 1970's, transient wave propagation behavior became better understood, and more reliable instrumentation for measuring the pavement response was available. At that time, impulse loading equipment also began to replace the steady-state vibrator, and by the early to mid-1980's, wave propagation methods were becoming more common for use in pavement evaluations. Although these methods have not been completely standardized or accepted by SHA's and other industry groups, they are now being used more extensively for research and forensic purposes.

For these types of tests, deflection-time histories of motion from an applied dynamic load are recorded by several receivers or sensors placed on the pavement surface. By computing the surface-wave travel time between adjacent receivers, as produced by different frequencies, a dispersion curve is obtained relating phase velocities to frequencies (or wavelengths). This type of testing does include the FWD, which has the most widespread use, because of its ability to impose high-amplitude dynamic loads.

### **8.2 Load-Deflection Response Data**

**8.2.1 Application of Impact Load.** Load application becomes a critical issue in a static analysis, because only the peak load is used to backcalculate layer moduli, which is relatively constant for a specific drop height. It is common practice that the measured peak load (or pressure) be corrected (or adjusted) to a standard load for ease of use in backcalculating layer moduli.

The load pulse generally occurs over a time of about 15 ms to about 35 ms. Although the time of the load pulse is fairly constant, the shape of the load pulse does vary. Both the loading time and load pulse shape can have an effect on the measured peak deflection basins, especially for

viscoelastic materials. This is graphically illustrated in figures 61 through 64, different deflection-time plots with the type of load pulse measured. For example, figures 63 and 64 clearly show differing creep effects from the applied load.

**8.2.2 Peak Deflection Time.** Peak deflections are normally used to backcalculate the elastic moduli of pavement materials and subgrade soils. However, these peak deflections occur at different times between the sensors used to measure the deflection basins. Figures 61 through 64 illustrate some of the time differentials between the peak deflections measured at sensors 1 through 7 with the FWD.

As a cursory review of the limited number of GPS sites considered for demonstrating the use of the deflection-time data, the ratio of the sensor distance from the applied load to the time to peak deflections measured at each sensor (or speed in terms of inches per millisecond) was calculated. Figure 65 summarizes the differences in slope (or speed of peak deflections) between different months of the year for some of the LTPP SMP sites and a comparison of some random GPS test sections.

A plot of sensor distance from the applied load and time of peak deflection is included in appendix A for those limited number of GPS sites reviewed. Table 16 summarizes the calculated slopes for each GPS site. In general, the speed is a function of the surface material and surface temperatures. On average, the speed is greater for PCC-surfaced pavements [50 to 150 cm/ms (20 to 60 in/ms)] than for asphalt concrete-surfaced pavements [25 to 90 cm/ms (10 to 35 in/ms)], and the speed is greater for asphalt concrete-surfaced pavements when the measurements are taken during the winter months, as opposed to the summer months.

**8.2.3 Response Recovery Time.** Another parameter reviewed from these data is the recovery time for the induced deflections; in other words, the time required to recover all of the deflection. Using sensor 1, the time to recover all of the peak deflection generally varies from about 25 ms to over 60 ms. In fact, for some of the sites, all of the deflection still had not been recovered even at 60 ms. Using the deflection-time plots, the pavement can be categorized into two basic types of response. These are:

- Elastic.
- Viscoelastic.

The elastic and viscoelastic properties of the pavement structure can be illustrated by reviewing the deflection-time data measured with the FWD. Figures 66 through 68 show these different

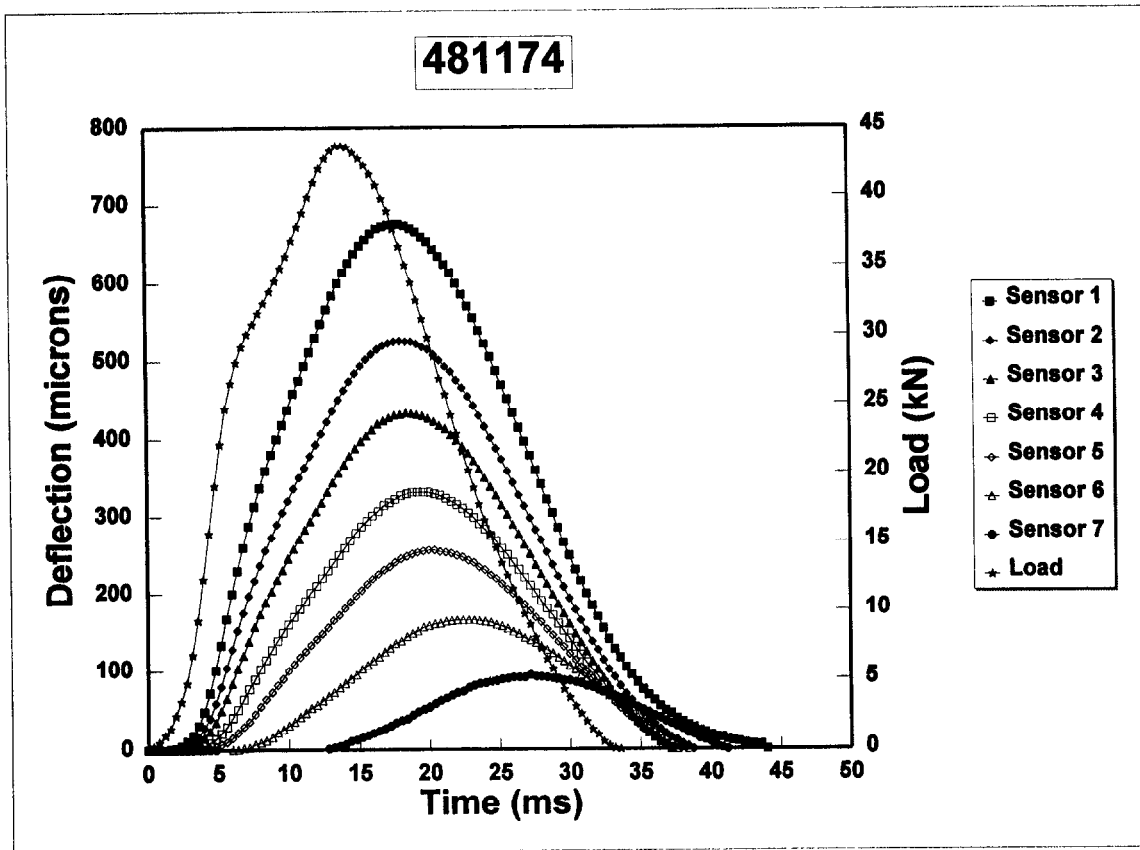


**Figure 61. FWD load pulse type "A" and the deflections measured by each sensor at GPS site 481174.**

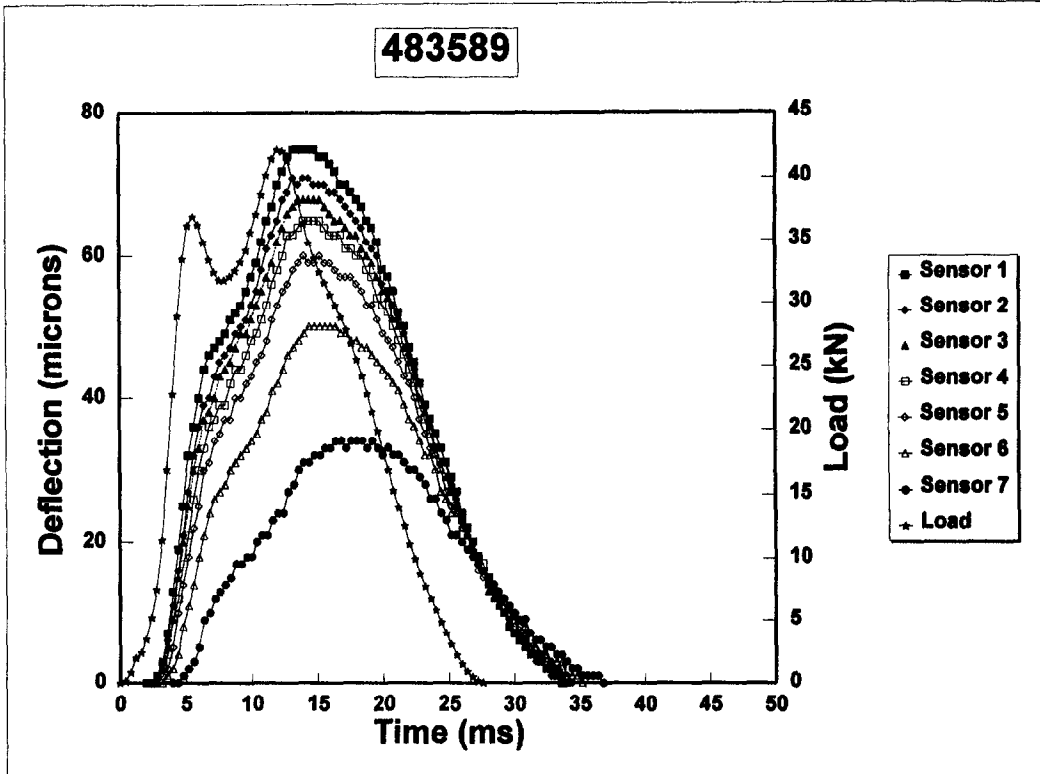


Figure 62. FWD load pulse type "B" and the deflections measured by each sensor at GPS site 483589.

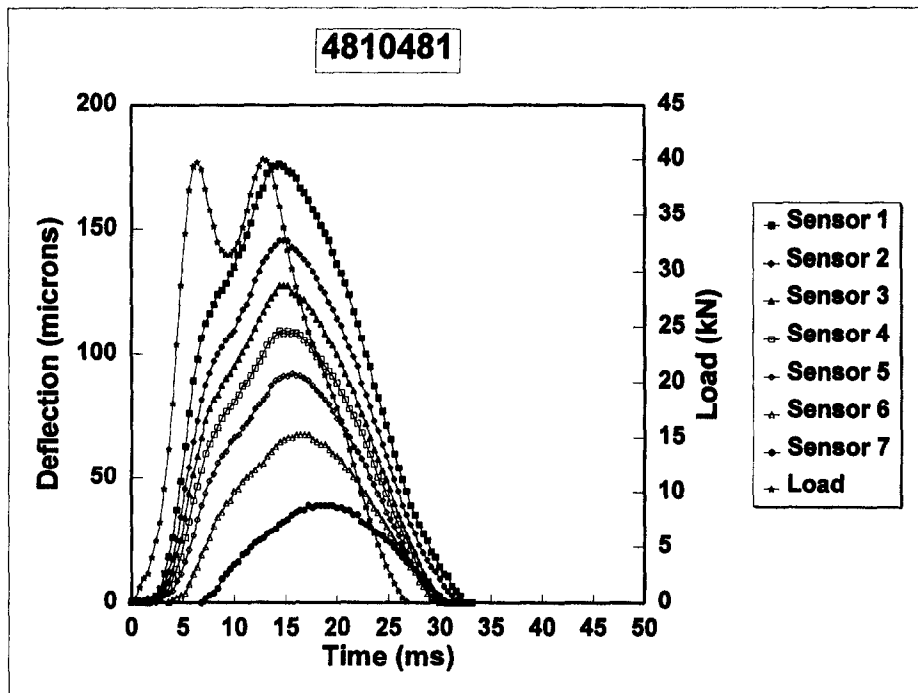
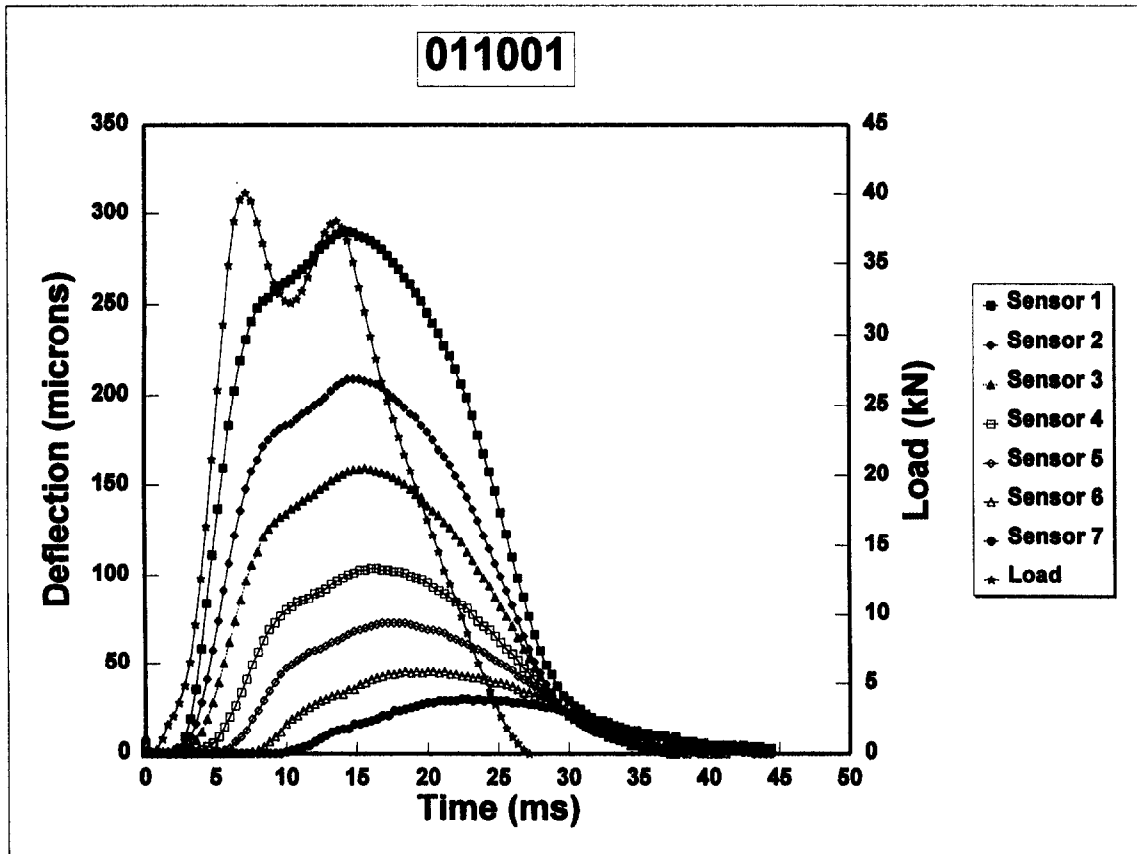
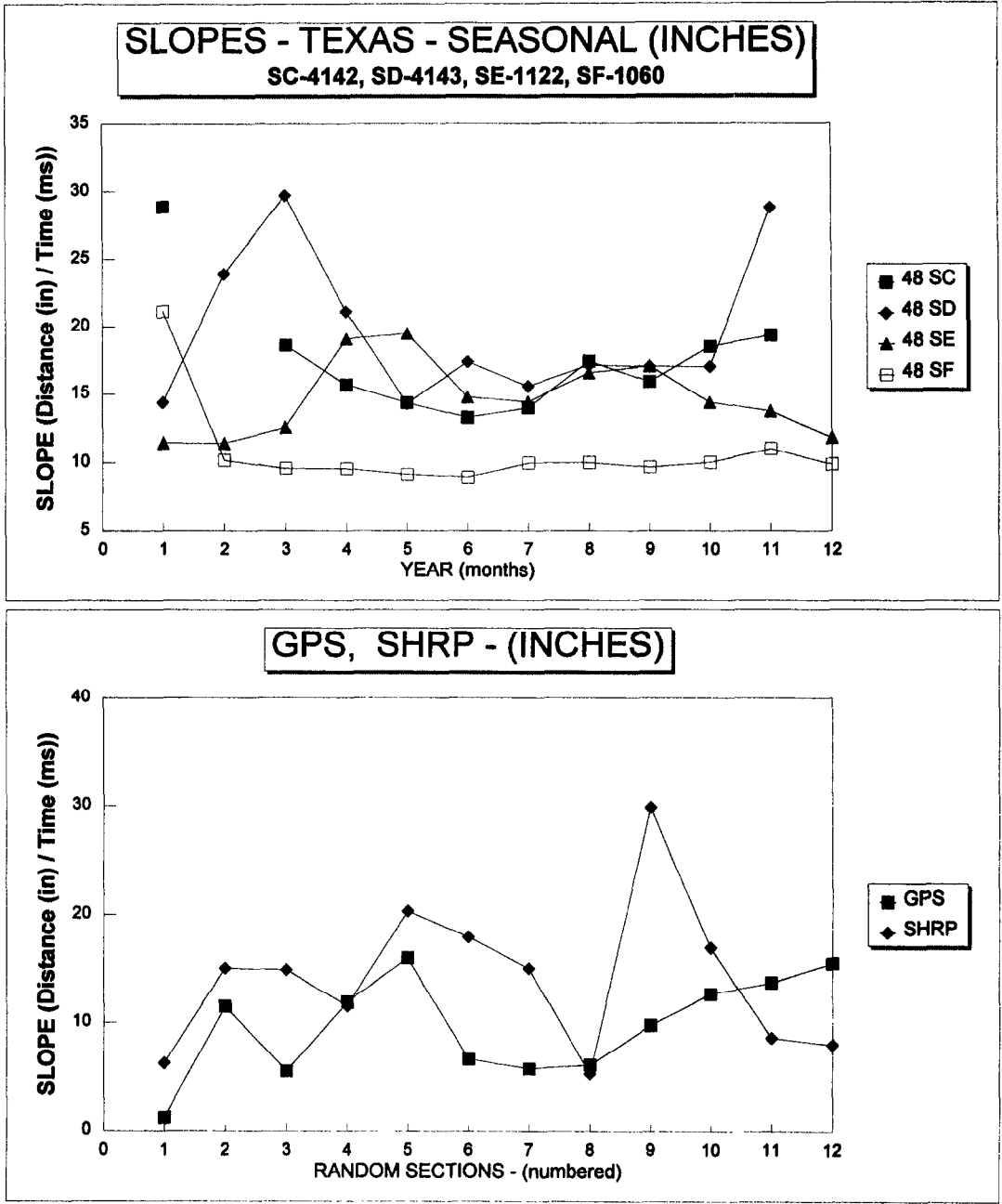


Figure 63. FWD load pulse type "C" and the deflections measured by each sensor at GPS site 4810481.





**Figure 64. FWD load pulse type "D" and the deflections measured by each sensor at GPS site 011001.**



1 in = 2.54 cm

**Figure 65. Average slope or speed (in inches per millisecond) of the peak deflections measured by each sensor during FWD testing of selected SMP and GPS test sections.**

**Table 16. Average slope of the relationship between sensor distance  
from the load and time to peak deflection.**

<b>TOTAL SLOPE - USING INCHES 0,8,12,18,24,36,60</b>					
	<b>48 - 4142</b>	<b>48 - 4143</b>	<b>48 - 1122</b>	<b>48 - 1060</b>	
	<b>48 SC</b>	<b>48 SD</b>	<b>48 SE</b>	<b>48 SF</b>	
<b>01 JAN</b>	28.85593220339	14.352227	11.41341546886	21.10278372591	1
<b>02 FEB</b>		23.888889	11.4016449623	10.1724137931	2
<b>03 MAR</b>	18.59482758621	29.716157	12.55119453925	9.572020248504	3
<b>04 APR</b>	15.65543071161	21.094527	19.05660377358	9.560952825782	4
<b>05 MAY</b>	14.33831376734	14.296296	19.4696969697	9.137444578799	5
<b>06 JUN</b>	13.24902723735	17.351664	14.73946784922	8.914285714286	6
<b>07 JUL</b>	13.96632366698	15.536332	14.39537329127	9.990407673861	7
<b>08 AUG</b>	17.39361702128	17.099448	16.54205607477	10	8
<b>09 SEP</b>	15.87654320988	16.990358	17.04545454545	9.665300546448	9
<b>10 OCT</b>	18.49348534202	16.990358	14.34675834971	10.01700680272	10
<b>11 NOV</b>	19.33694181326	28.796680	13.72611464968	11.00952948183	11
<b>12 DEC</b>			11.82067077344	9.888186679631	12

<b>SHRP</b>		<b>GPS</b>	
<b>01-1001-2</b>	6.25	<b>48-0001-B3</b>	1.226366610332
<b>01-4125-2</b>	15.01626898048	<b>48-1047-A3</b>	11.47659854977
<b>05-3058-1</b>	14.8536036036	<b>48-1056-C3</b>	5.511624463202
<b>05-3058-2</b>	11.54217643271	<b>48-1070-B1</b>	11.88926174497
<b>05-3074-1</b>	20.32352941176	<b>48-1092-B3</b>	15.97931873479
<b>05-4019-1</b>	17.89950576606	<b>48-1109-B1</b>	6.642327811683
<b>05-4019-2</b>	15.01750291715	<b>48-1174-A0</b>	5.762630312751
<b>05-4021-2</b>	5.263570309161	<b>48-1174-A3</b>	6.086304271091
<b>05-4023-1</b>	29.85915492958	<b>48-1178-B3</b>	9.755700325733
<b>05-4046-2</b>	16.91933240612	<b>48-3003-D1</b>	12.64449722882
<b>12-3996-1</b>	8.598014888337	<b>48-3589-A1</b>	13.71621621622
<b>12-4096-2</b>	7.991126070991	<b>48-4142-A1</b>	15.5

1 in = 2.54 cm

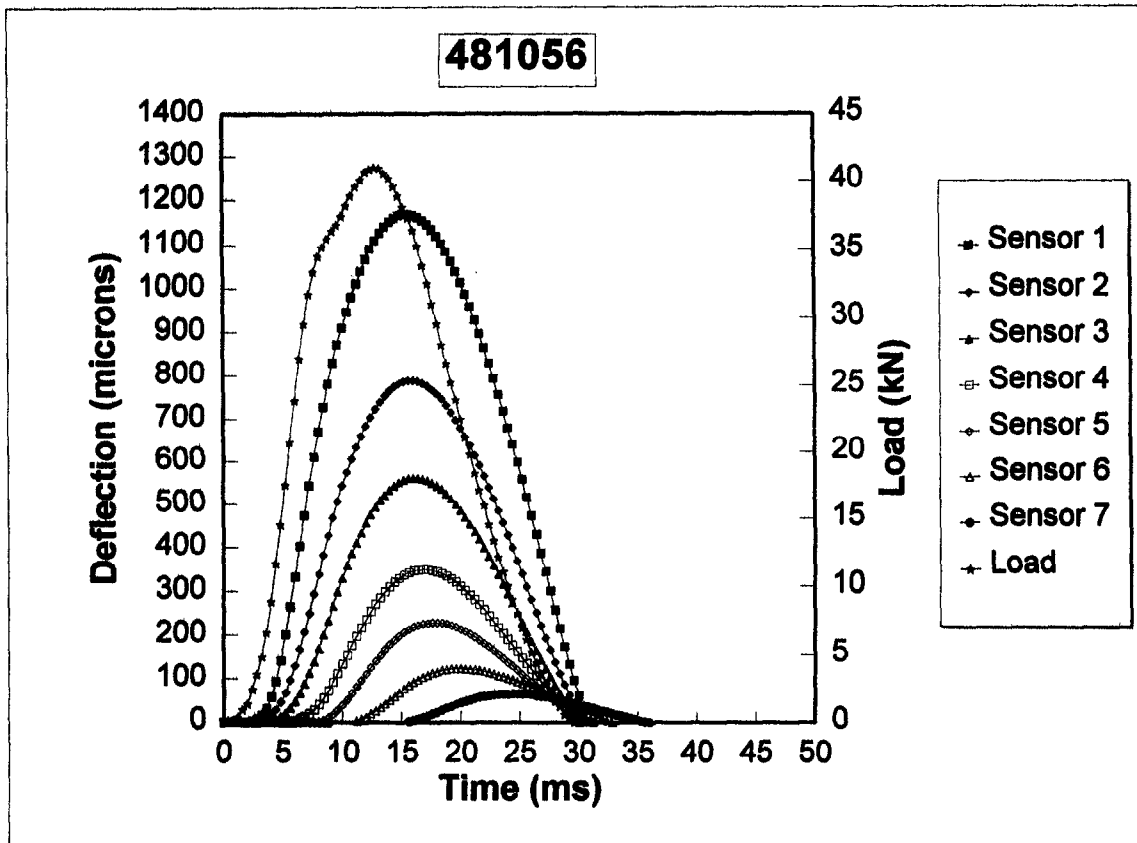


**Figure 66. Typical FWD deflection-time data from testing performed on an asphalt concrete pavement with elastic behavior, GPS site 481056.**

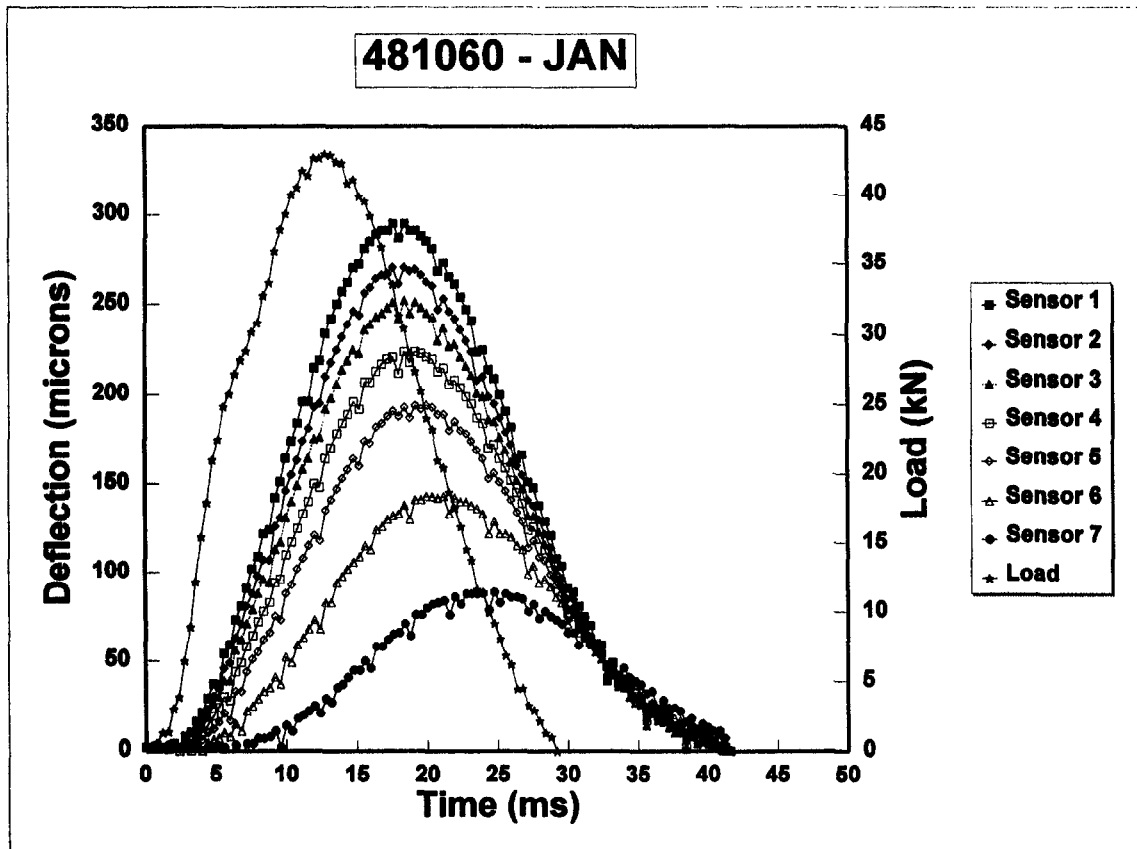


**Figure 67. Typical FWD deflection-time data from testing performed on an asphalt concrete pavement with some viscoelastic behavior, GPS site 481060.**

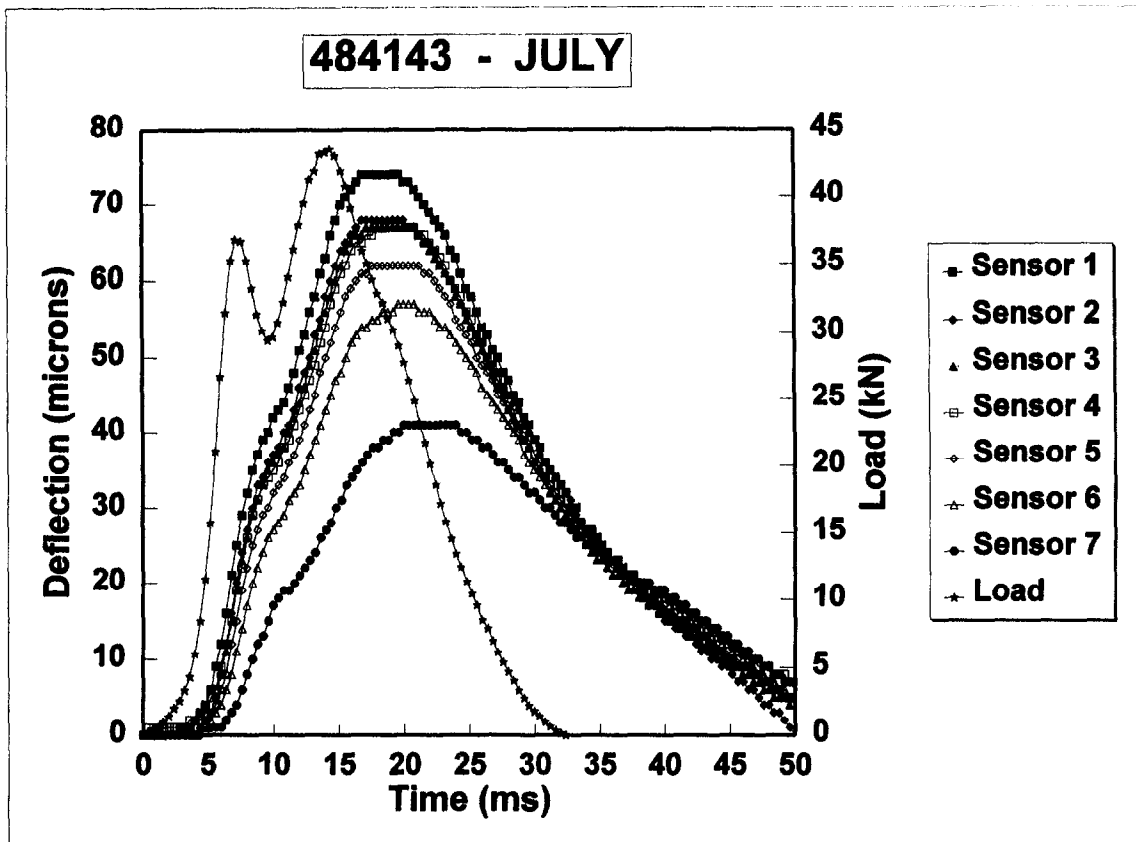


**Figure 68. Typical FWD deflection-time data from testing performed on a PCC pavement with viscoelastic behavior, GPS site 484143.**

types of pavement response characteristics. Figure 66 shows the response for a pavement section that is basically elastic, while figures 67 and 68 show pavements that are viscoelastic.

A pavement that behaves elastically will recover most or all of the induced deflection immediately after the load pulse reaches zero, as shown in figure 66. GPS test section 481056 (figure 66) is a thin (less than 51 mm (2 in) in thickness) asphalt concrete-surfaced pavement. Asphalt concrete mixtures are viscoelastic materials, but the surface for this test section is so thin that the viscoelastic properties are insignificant in relation to the total measured deflection.

A highly viscoelastic pavement will take time to recover the induced deflection after the load pulse reaches zero, as shown in figures 67 and 68. As shown, the maximum load and peak deflections are not coincident, and it takes over 20 ms past the end of the load pulse for the pavement to recover the deflection. GPS test section 481060 (which is also an SMP site, figure 67) is a relatively thick (19 cm (7.6 in) in thickness) asphalt concrete-surfaced pavement. The time difference between peak load and peak deflection is very prevalent.

GPS test section 484143 (another SMP site, figure 68) is a PCC-surfaced pavement. PCC pavements (and certainly PCC mixtures) are normally assumed to be elastic, as compared to asphalt concrete-surfaced pavements. However, figure 68 clearly shows viscoelastic properties in terms of the recovered deflection being highly time-dependent.

In conclusion, the differences between the elastic and viscoelastic responses of a pavement structure, as measured by the FWD, may begin to explain some of the differences normally observed and reported between the laboratory and backcalculated moduli of a pavement material and/or subgrade soil. These observed differences should be studied in depth in future data analysis studies regarding the LTPP data base; especially when developing mechanistic-empirical pavement performance models.

### **8.3 Dissipated Work**

An important property of materials that defines the viscoelastic and inelastic characteristics of materials is the dissipated work or dissipated energy of the material. Dissipated energy is simply defined as the area included in the loaded and unloaded portion of the stress-strain curve (i.e., referred to as the hysteresis loop). Dissipated energy has been used in the asphalt concrete fatigue area for many years by a few agencies. Similarly, the FWD load-deflection-time data can be used to measure the dissipated work during the loading and unloading of the pavement from the FWD impact load.

**8.3.1 Pavement Structural Characteristics.** Dissipated work, as measured by the FWD, was calculated for several LTPP-GPS sites during similar time periods (summer months). Figures 69 through 71 show examples of the hysteresis loop used to calculate dissipated work for different types of pavements, varying from very thin to very thick or soft to stiff. Based on a review of selected sites, the hysteresis loop and dissipated work do vary extensively by structure and pavement type. In general, however, there is much less dissipated work measured on PCC-surfaced pavements, as opposed to those measurements taken on asphalt concrete-surfaced pavements. Table 17 summarizes the dissipated work for a few of the GPS sites by surface type (asphalt concrete- and PCC-surfaced pavements).

Dissipated work was evaluated on a seasonal basis using some of the LTPP SMP sites. Figure 72 shows the variation in dissipated work by month for three SMP sites in Texas (1 = January and 12 = December). These are the same sites used for figures 69 through 71 for the month of July. As shown in figure 72, for the most part, dissipated work is independent of season or month. However, these sites are in Texas where the properties are more uniform throughout the year (i.e., no frost penetration into the subgrade and no spring thaw occurring in the base and underlying subgrade). It is expected that the dissipated work will be significantly different between seasons for those sites where frost penetration and spring thaw occur.

**8.3.2 Pavement Performance Comparisons.** Dissipated work should be directly related to the rate of pavement deterioration and/or damage. This becomes an extremely important parameter in evaluating pavement structures for defining remaining life and rehabilitation requirements. It is hypothesized that the dissipated work calculated from the FWD load-deflection-time data is proportional, if not directly related, to pavement damage in terms of fatigue cracking and other types of distress, excluding permanent deformation (rutting) that is confined to the asphalt concrete surface layer.

Various sites were selected with varying IRI values, distress magnitudes, and traffic levels to determine if, in fact, there is a relationship between dissipated work and pavement performance or the rate of pavement deterioration. These data are shown in figure 73 and do indicate that the greater the dissipated work, the more pavement distress (both in magnitude and severity) and the more different types of distresses that were observed at these sites. Thus, dissipated work appears to be a material or pavement response parameter (or property) that can be used to evaluate the performance behavior of pavement structures. More importantly, dissipated work can be measured directly with the FWD.



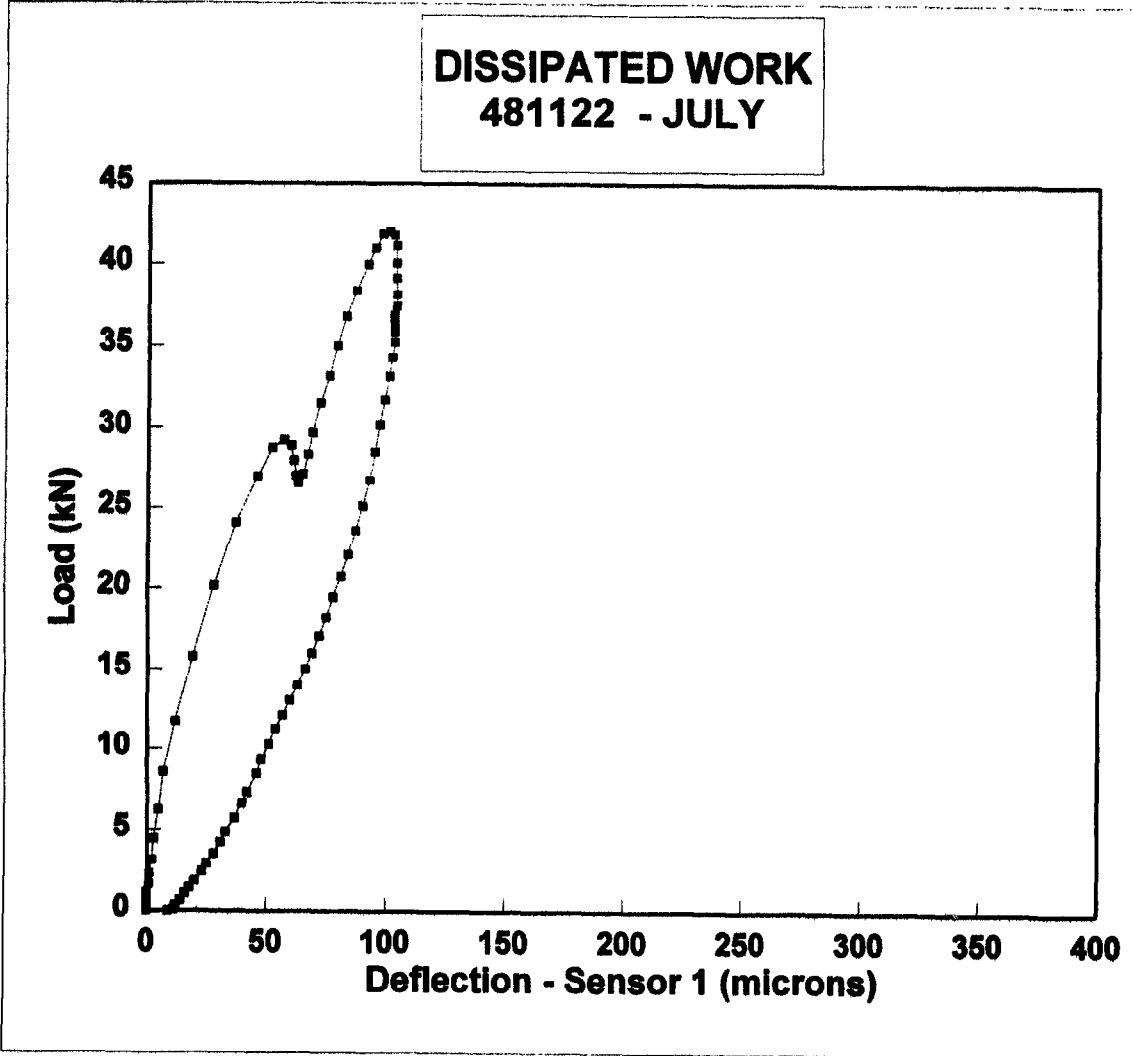


**Figure 69. Hysteresis loop as measured by the FWD at GPS site 481122 (asphalt concrete-surfaced pavement) in July.**

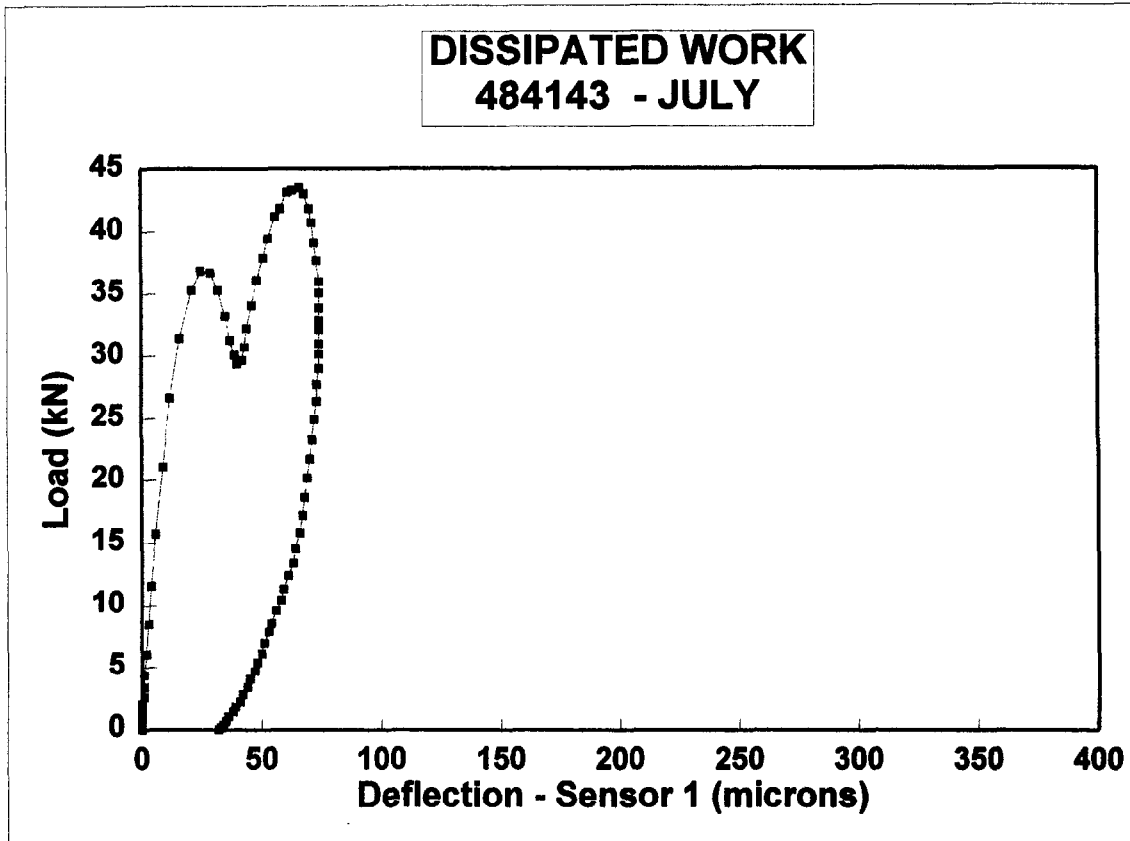


**Figure 70. Hysteresis loop as measured by the FWD at GPS site 484143 (PCC-surfaced pavement) in July.**

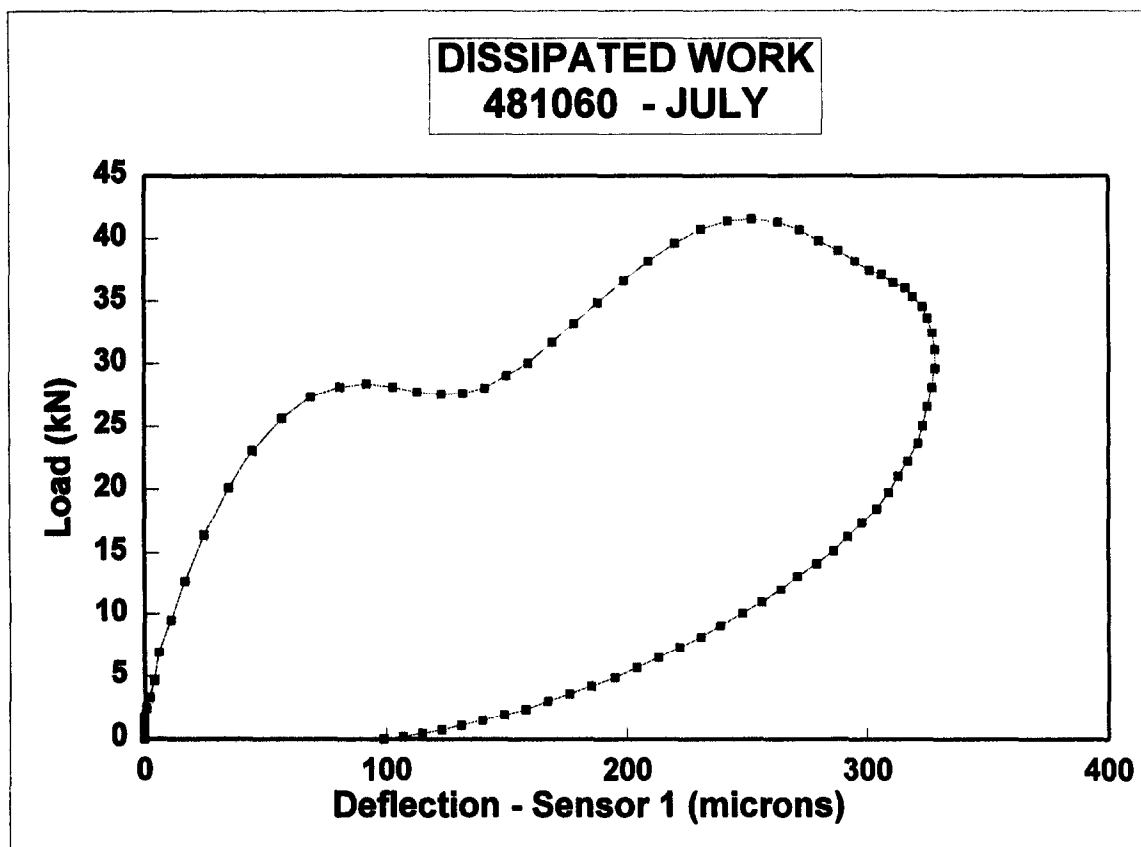


**Figure 71. Hysteresis loop as measured by the FWD at GPS site 481060 (asphalt concrete-surfaced pavement) in July.**

**Table 17. Dissipated work calculated from the loading and unloading (the hysteresis loop) of the pavement structure during FWD testing by type of surface.**

GPS Site Number	Dissipated Work, kN-microns	
	Asphalt Concrete-Surfaced Pavement	PCC-Surfaced Pavement
01 1001	5,354	
01 4125	2,623	
05 3058 (1)	4,239	
05 3058 (2)	4,598	
05 3074		4,209
05 4019 (1)		1,928
05 4019 (2)		1,528
05 4021		1,493
05 4023		4,131
05 4046		2,227
12 3996	4,451	
12 4096	4,184	
12 4109		2,902
12 4138		2,022
35 1003	1,967	
40 4086	4,930	

**Table 17. Dissipated work calculated from the loading and unloading (the hysteresis loop) of the pavement structure during FWD testing by type of surface (continued).**

GPS Site Number	Dissipated Work, kN-microns	
	Asphalt Concrete-Surfaced Pavement	PCC-Surfaced Pavement
47 9025	3,747	
48 0001	997	
48 1047	6,321	
48 1048 (1)	3,819	
48 1048 (2)	3,939	
48 1056	22,129	
48 1069	2,915	
48 1070	1,600	
48 1092	4,235	
48 1109	6,135	
48 1174 (1)	14,195	
48 1174 (2)	10,298	
48 1178	4,093	
48 3003		2,878
48 3589		1,663
48 3769 (1)	5,536	
48 3769 (2)	9,925	
48 4142		1,556
48 5323		2,459
<b>Range of Values</b>	<b>997-22,129</b>	<b>1,493-4,131</b>

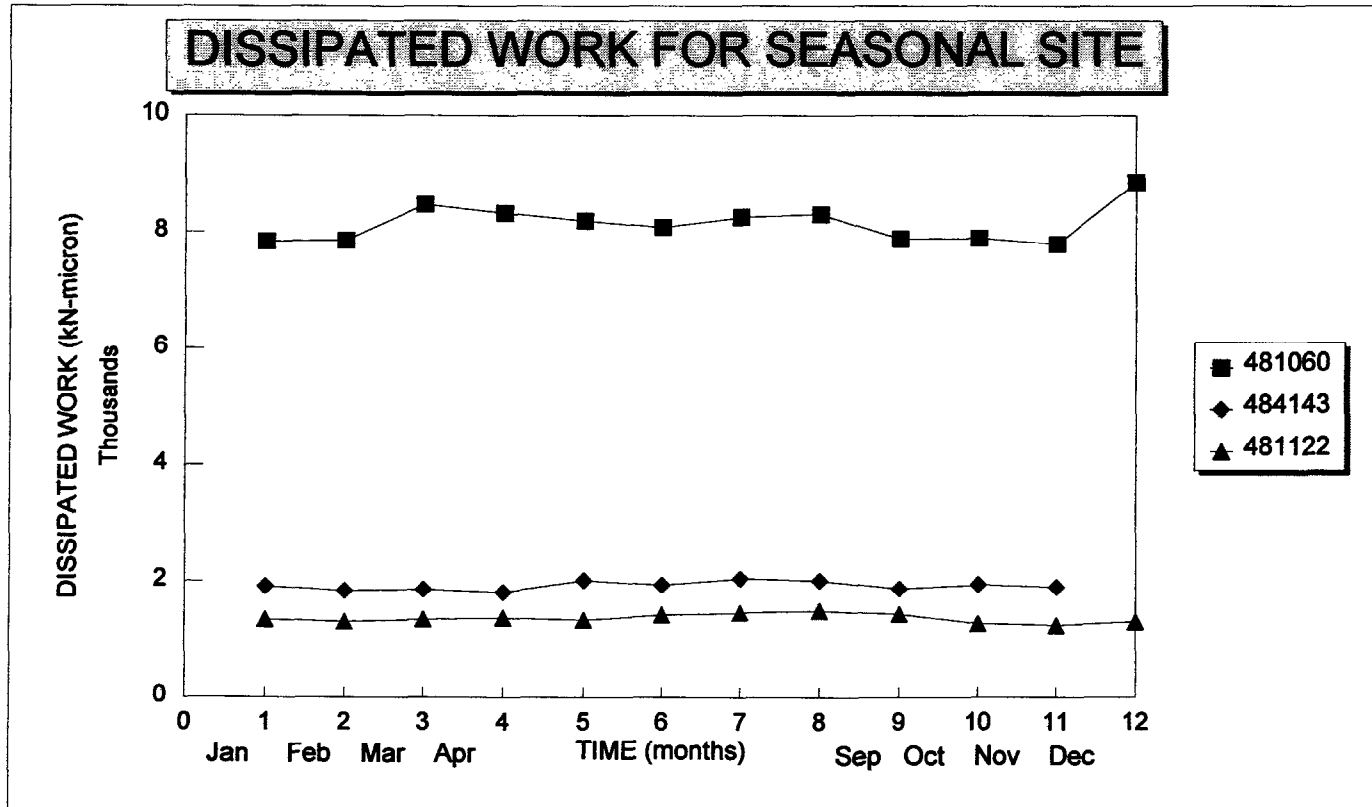


**Figure 72. Dissipated work by month, as measured during FWD deflection testing at three seasonal sites in the southern region.**

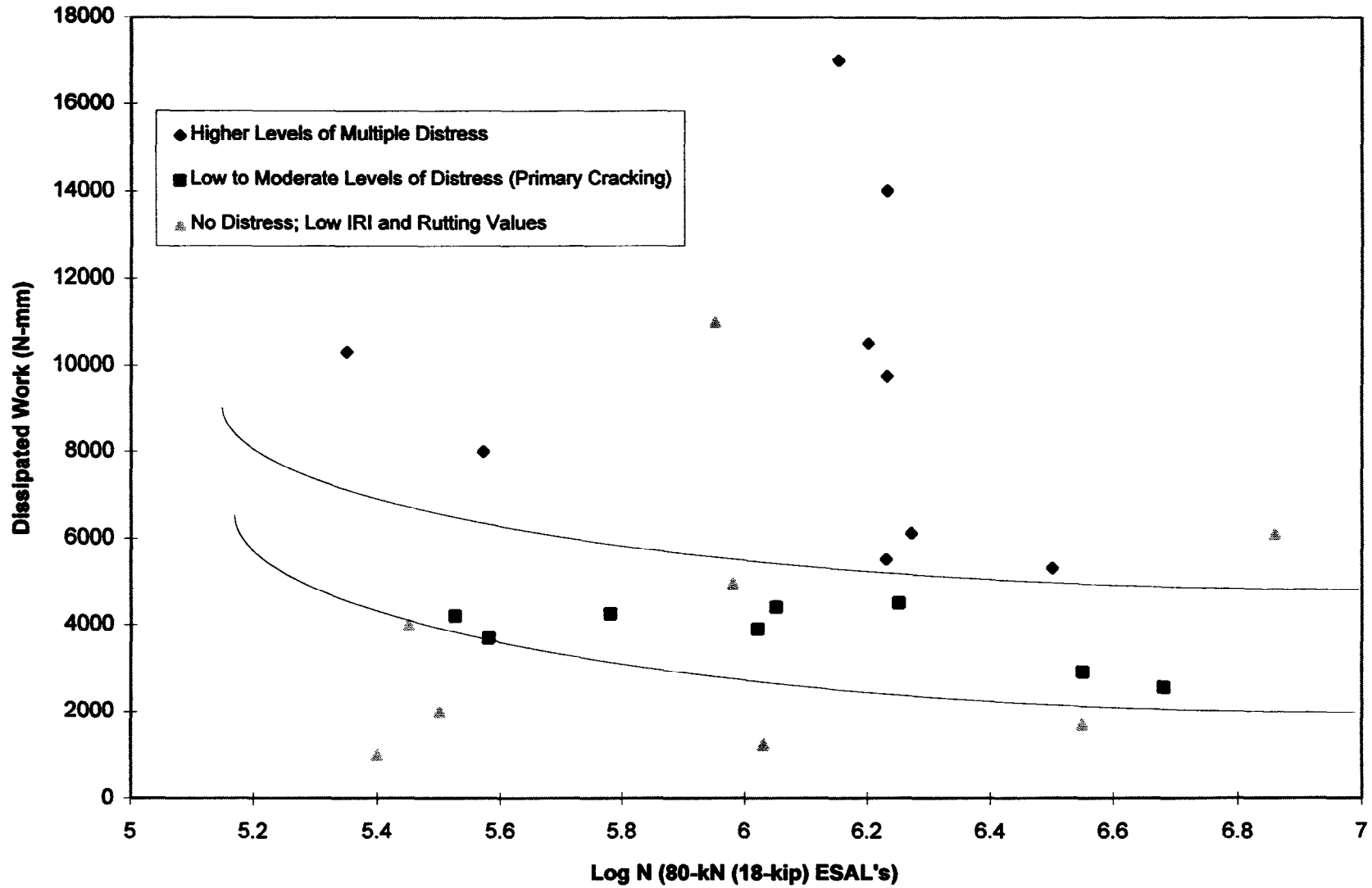


**Figure 73. Comparison of dissipated work to pavement condition for different traffic levels for selected GPS sites in the southern region.**

## **8.4 Summary**

In summary, the deflection-time history data collected within the LTPP program represents an invaluable data source and critical data element that has yet to be thoroughly investigated and utilized as to its potential for use in pavement diagnostic studies. This report has attempted to show some of the different parameters that can be used from the deflection-time data and the benefit of using these data for pavement diagnostic studies and pavement classifications. The authors strongly recommend that agencies begin to use these data sets to their full potential, especially with the national increased awareness of using mechanistic-empirical design procedures. These data should represent a key parameter in the development of these new design procedures that are being planned by AASHTO by the year 2002.



## 9. CONCLUSIONS AND RECOMMENDATIONS

The overall goal of this research effort was to enhance implementation of the 1993 AASHTO Design Guide through improved material characterizations and a better understanding of those inputs that are not well defined. To accomplish this activity, the study focused on using the LTPP data base to answer several pavement/material characterization questions and issues that are related to pavement design and evaluation. These included identifying differences between backcalculation and laboratory measurements of resilient moduli; subgrade characterization and the effects of subgrade stabilization on pavement performance; validity of the drainage coefficients and the effect on pavement performance of incorporating positive drainage features in pavement structures; and the consideration of seasonal variation of material properties for the design of pavement structures. The following conclusions and recommendations obtained from these studies are basically subdivided into two parts: (1) findings from the data analyses, and (2) concerns or potential problems with the LTPP data base.

### 9.1 Findings From the Data Analyses

One of the most important findings from this study is confirmation that the LTPP data base represents an invaluable resource to pavement engineers and the industry for study of controversial issues and to answer pavement design questions and/or issues. Use of this data base has provided important insight and support for certain design parameters and procedures recommended by the guide, but has also identified areas requiring revision.

Another very important finding from these studies relates to the dangers of using resilient moduli determined through the use of different techniques (i.e., the difference in values calculated from deflection basins using different backcalculation programs and the difference in backcalculated values from those measured in the laboratory). Testing for and calculations of resilient moduli for use in design procedures should be consistent with those used in developing the design procedure. The basis for the development of the design procedures must be known, so that values consistent with its development are used in design.

#### 9.1.1 Material Testing and Characterization Issues

- **Resilient Modulus.** The ratios between instantaneous ( $E_{RI}$ ) and total ( $E_{RT}$ ) resilient moduli for asphalt concrete mixtures determined from the LTPP data base are similar to those ratios determined from other studies. The ratio of  $E_{RT}/E_{RI}$  approaches 1.0 at temperatures less than 5 °C (41 °F) and begins to increase for temperatures greater than 5 °C (41 °F). At the colder temperature, the material is approaching the assumptions for

an elastic material, but at the higher test temperatures, the effects of recovery time become very important. Thus, at higher test temperatures, these values cannot be used interchangeably.

- The same constitutive equation (equation 5) can be used to represent the response of all unbound pavement materials and subgrade soils. This equation is similar to the constitutive model included in the Superpave program to represent material response and behavior.
- The nonlinear elastic coefficients and exponents of the constitutive equation (equation 5) for unbound materials were correlated to selected physical properties measured on the subgrade soils. Relationships were found between the nonlinear elastic coefficients and selected properties, and were summarized in table 11. The more important properties include moisture content, optimum moisture content, percent compaction, and maximum dry unit weight of the soil. These are the same properties that were found to be the most critical from other laboratory studies (table 10). However, the use of these relationships between nonlinear elastic properties and physical properties (summarized in table 11) can result in large errors in the estimation of resilient moduli of the subgrade soils. Thus, it is recommended that these correlations only be used for planning purposes and that actual repeated-load triaxial laboratory tests be conducted or nondestructive deflection testing be performed to determine the resilient modulus of the subgrade soils for pavement design.
- **Temperatures.** For characterizing asphalt concrete mixtures, the temperature determined at the mid-depth of the asphalt concrete layer should be used in determining the total resilient modulus ( $E_{RT}$ ) of the asphalt concrete mixture. There is less variability in the measurements for determining total resilient modulus, because the recovery time can be well defined in the data acquisition system.
- **Stress States and At-Rest Earth Pressures.** For characterizing unbound base/subbase materials, the total stress state should be determined at a depth one-quarter the thickness of the base/subbase layer below its surface for determining the in situ resilient modulus for predicting the structural response of the pavement structure.
- For characterizing the subgrade soils, the total stress state should be determined at a depth of 46 cm (18 in) below the surface of the subgrade. It is important that the at-rest stress state be considered with that induced by wheel loads in relating moduli from laboratory testing to backcalculated moduli for all unbound pavement materials and subgrade soils.

Omission of the at-rest stress state can lead to more significant differences between those moduli calculated from deflection basins and those measured in the laboratory.

### **9.1.2 Backcalculation of Layer Moduli for Design Purposes**

- Differences between the laboratory measured and backcalculated layer moduli were found for different pavement layers and materials. These are briefly noted below:
  - For asphalt concrete mixtures, the backcalculated moduli [E(FWD)] are significantly greater than the laboratory [E<sub>RT</sub>(IDT)] measured values. Asphalt concrete is a viscoelastic material and differences in the applied load between the laboratory and FWD become important, especially at higher temperatures. The ratios of E(FWD)/E<sub>RT</sub>(IDT) are dependent upon pavement and testing temperatures. These resulting ratios range from 1.0 at 5 °C (41 °F) to 4.0 at 40 °C (104 °F). For designing asphalt concrete pavement structures using the AASHTO guide, all backcalculated elastic moduli should be converted to equivalent laboratory measured values, using the ratios presented in chapter 3. In addition, the total resilient modulus should be used rather than the instantaneous value. For mechanistic-empirical design procedures, the modulus value used depends on the technique that was used to measure the modulus of the asphalt concrete mixtures.
  - For unbound pavement materials and subgrade soils, the backcalculated moduli are consistently higher than the laboratory measured values. The ratios of E(FWD) to M<sub>R</sub> (laboratory) are dependent upon pavement type. Currently, there were insufficient data to quantify any differences in these ratios that are dependent upon material type. The greatest effect on these ratios was found to be pavement type. More importantly, the ratios determined from these analyses are significantly greater than the recommended C values included in the guide. From the results conducted within this study, it is recommended that those values included in the guide not be used, provided that the total stress states, including the at-rest stress condition, are considered in determining the resilient modulus for a specific layer and material. When using the guide, the backcalculated moduli must be converted to an equivalent laboratory value.

- **Drainage and Pavement Performance.** Based on the analyses conducted with the available data, the drainage coefficients included in the guide were not substantiated. More importantly, the benefits of positive drainage features in either asphalt concrete- or PCC-surfaced pavement were not substantiated. Some of the problems in identifying the potential benefit of subsurface drainage features may be related to the assumption that the positive drainage system is functioning properly. Thus, it is strongly recommended that those sites with positive drainage features be inspected by video inspection techniques to confirm that these drainage features are, in fact, functioning.
- **Subgrade Stabilization and Characterization.** Full-depth pavements built directly on expansive soils appear to have inferior performance characteristics, as opposed to those pavements where the asphalt concrete material was placed on a granular base/subbase or stabilized material. Also, the use of a stabilized subgrade on expansive clay soils appears to help maintain the moisture content in the clay subgrade near optimum conditions, resulting in slightly lower rates of change in the IRI value with time.
- The effects of stabilized subgrades on performance could not be established with the available data. In addition, the use of the serviceability-based relative damage concept and the applicability of the subgrade vertical compressive strains criteria could not be validated. The subgrade modulus in the original AASHO design equation, however, represents the soil in its weakest condition, and did not account for seasonal variation. These analyses appear to be indicating that use of the equivalent annual resilient modulus under the serviceability criteria may be inappropriate. Thus, it is strongly recommended that the testing and monitoring of the GPS and seasonal sites be continued and improvements in the accuracy of the monitored traffic data be implemented to provide the data needed to establish the accuracy and validity of the damage concept for seasonal variation of subgrade moduli using the serviceability criteria, and the effect that stabilized subgrades may have on performance.
- **Damage Factors.** Damage factors were determined for calculating an equivalent annual resilient modulus of the subgrade soil based on permanent deformation in the subgrade. These permanent deformation damage factors, however, were not confirmed, because of insufficient data and/or inappropriate assumptions. These damage factors for permanent deformation are different from those based on a serviceability criterion. Again, they should not be used interchangeably. Performance monitoring and response testing of the GPS and SPS sites should be continued to allow evaluation of these values.

- Fatigue damage factors can be used to calculate an equivalent annual or design total resilient modulus for asphalt concrete mixtures. However, these damage factors are not necessarily applicable to designs based on a serviceability criterion.
- Damage factors for the unbound granular materials and subgrade soils were determined from this study for specific types of pavement distress. These damage factors can be used to calculate an equivalent annual modulus for these materials. However, these damage factors are not necessarily appropriate for use with designs based upon a serviceability criterion. Presently, there are insufficient data to confirm and validate this theoretical development. Although this may appear to be too conservative, resilient moduli for granular base materials representing its weakest condition should be used for designs based on a serviceability criterion.
- **Deflection Time-History Data and Dissipated Work.** The deflection-time history data measured during FWD testing can be used to determine the elastic and viscoelastic response properties of both PCC- and asphalt concrete-surfaced pavements. From these data, dissipated work can be calculated. Dissipated work was found to be dependent on the pavement cross section and material types, and is believed to be directly proportional to the rate of deterioration of different pavement structures. Although dissipated work was not used directly in these analyses, it is strongly recommended that the dissipated work be used to determine its relationship to various distresses and the rate of deterioration of pavement structures.

## 9.2 Potential Concerns/Problems With the LTPP Data Base

- **Asphalt Concrete Resilient Moduli Measured at 5 °C (41 °F).** The resilient moduli of the asphalt concrete mixtures measured at 5 °C (41 °F) are believed to be in error. The moduli measured at 5 °C (41 °F) are only slightly greater than the values measured at 25 °C (77 °F) and, in some cases, are even less than those measured at 25 °C (77 °F). These test results are significantly different than those reported from other material studies. It is strongly recommended that these data be closely reviewed to identify why the values measured at 5 °C (41 °F) are significantly different from those values reported from other studies. In addition, the relationship between the total resilient modulus measured at 25 °C (77 °F) and the indirect tensile strength measured at 25 °C (77 °F) is significantly different than reported for similar mixtures in other studies.
- **Backcalculation of Layer Moduli.** Elastic layer theory cannot be used to accurately backcalculate the layered elastic moduli of pavement structures identified as having

"problem deflection basins." It is recommended that these deflection measurements be verified as to their accuracy and, more importantly, to identify the cause of these types of basins (Types I, II and III as shown in figures 19 through 21). It is also strongly recommended that the data quality checks include a step or process during deflection testing on the roadway to identify those basins, so that the onsite conditions can be checked. These problem basins were definitely dependent upon pavement type and occurred more frequently for test sections within the dry-freeze environment.

- **Damage Factors.** Insufficient data exist to validate the damage factors for the different pavement layers to consider seasonal variation in the design of flexible pavements. It is highly recommended that the SPS and seasonal monitoring sites be continued to collect performance and distress data, as well as pavement response data, to obtain the necessary data to evaluate the concept of using relative damage factors for pavement structural design, especially for developing mechanistic-empirical design procedures.
- **Drainage Coefficients.** Insufficient data exist to validate the use and applicability of the drainage coefficients recommended for use by the guide. However, one reason for the inconclusive finding noted above may be a result of the assumption that the drainage features are functioning as designed and are being maintained. It is recommended that video inspection techniques be used to confirm the adequacy of any positive drainage features built into the pavement structure, especially for the more important SPS projects.

## References

1. American Association of State Highway and Transportation Officials, *AASHTO Guide for Design of Pavement Structures*, Washington, DC, 1993.
2. National Cooperative Highway Research Program, *Catalog of Current State Pavement Design Features and Practices: Systems for Design of Highway Pavements*, NCHRP Project 1-32, Interim Report Submitted by ERES Consultants, Inc., November 1995.
3. Daleiden, Jerome F., et al., *Evaluation of the AASHTO Design Equations and Recommended Improvements*, Report No. SHRP-P-394, Strategic Highway Research Program, National Research Council, Washington, DC, 1994.
4. Simpson, Amy L., et al., *Sensitivity Analyses for Selected Pavement Distresses*, Report No. SHRP-P-393, Strategic Highway Research Program, National Research Council, Washington, DC, 1994.
5. Von Quintus, H.L., et al., *Asphalt-Aggregate Mixture Analysis System: AAMAS*, NCHRP Report No. 338, National Cooperative Highway Research Program, National Research Council, Washington, DC, March 1991.
6. Baladi, G.Y., *Integrated Material and Structural Design Method for Flexible Pavements*, Report No. FHWA/RD-88/109, Federal Highway Administration, September 1987.
7. Von Quintus, Harold L., *Case Study Report - Premature Flexible Pavement Failure Analysis, Impact of Tire Pressures*, Report No. TT-4/1, Prepared for the Texas Transportation Institute, Texas A&M University, Florida DOT State Project No. 99000-1712, March 1991.
8. Von Quintus, Harold L., J. Brent Rauhut, and Thomas W. Kennedy, "Comparisons of Asphalt Concrete Stiffness as Measured by Various Testing Techniques, *Proceedings*, Volume 51, Association of Asphalt Paving Technologists, 1982.
9. Lytton, Robert L., et al., *Development and Validation of Performance Prediction Models and Specifications for Asphalt Binders and Paving Mixes*, Report No. SHRP-A-357, Strategic Highway Research Program, National Research Council, Washington, DC, 1993.
10. Santha, B. Lanka, "Resilient Modulus of Subgrade Soils: Comparison of Two Constitutive Equations," *TRR No. 1462*, Transportation Research Board, National Research Council, Washington, DC, 1994, pp. 79-90.

11. Strategic Highway Research Program, *Manual for FWD Testing in the Long Term Pavement Performance Study: Operational Field Guidelines, Version 2.0*, March 1993.
12. Strategic Highway Research Program, National Research Council, *Analysis of Section Homogeneity, Non-Representative Test Pit and Section Data, and Structural Capacity: FWDCHECK, Version 2.00, Volume I - Technical Report*, Report No. SHRP-P-633, Washington, DC, 1993.
13. Roesse, J., *Computer Program UTFWIBM*, The University of Texas at Austin, Texas, 1987.
14. Magnuson, A.H., *Computer Analysis of Falling Weight Deflectometer Data, Part I: Vertical Displacement Computations on the Surface of a Uniform (One-Layer) Half-Space Due to an Oscillating Surface Pressure Distribution*, Research Report No. 1215-1F, Texas Transportation Institute, Texas A&M University, College Station, Texas, 1988.
15. Von Quintus, Harold L. and Brian Killingsworth, *Backcalculation of Layer Moduli of LTPP General Pavement Study (GPS) Sites*, Publication No. FHWA-RD-97-076, Federal Highway Administration, Washington, DC, July 1997.
16. Michalak, C.H. and Scullion, T., *MODULUS 4.2: User's Manual*, Research Report 1939-1, Texas Transportation Institute, 1993.
17. Foinquinos, R., *FWD-DYN: A Computer Program for Forward Analysis and Inversion of Falling Weight Deflectometer Data*, Research Report 1970-1F, Center for Transportation Research, 1993.
18. May, R.W. and H.L. Von Quintus, *The Quest for a Standard Guide to NDT Backcalculation*, STP 1198, American Society for Testing and Materials, December 1994.
19. Strategic Highway Research Program, *SHRP Layer Moduli Backcalculation Procedure - Software Selection*, SHRP Technical Report, Strategic Highway Research Program, July 1991.
20. American Society for Testing and Materials, *Nondestructive Testing of Pavements and Backcalculation of Moduli*, Second Volume, STP 1198, Editors: Harold L. Von Quintus, Albert J. Bush, III and Gilbert Y. Baladi, December 1994.
21. Rhode, G. and Scullion, T., *MODULUS 4.0: A Microcomputer-Based Procedure for Backcalculating Layer Moduli From FWD Data*, Research Report 1123-1, Texas Transportation Institute, 1990.



22. Alexander, D.R., et al., "Multilayer Elastic Program for Backcalculating Layer Moduli in Pavement Evaluation," In *Nondestructive Testing of Pavements and Backcalculation of Moduli*, ASTM STP 1026, ASTM, Philadelphia, Pennsylvania, 1989, pp. 171-188.
23. Rada, G.R., et al., "Layer Moduli From Deflection Measurements: Software Selection and Development of Strategic Highway Research Program's Procedure for Flexible Pavement," *TRR No. 1377*, Transportation Research Board, National Research Council, Washington, DC, 1992.
24. PCS/Law Engineering, *SHRP's Layer Moduli Backcalculation Procedure*, SHRP-P-655, Strategic Highway Research Program, National Academy of Science, 1993.
25. Mohseni, A. and Rada, G., *Initial Analysis of SHRP Backcalculation Results*, Draft Report, PCS/Law, June 1993.
26. Barker, W.R. and W.N. Brabston, *Development of a Structural Design Procedure for Flexible Airport Pavements*, FAA Report No. FAA-RD-74-199, U.S. Army Corps of Engineers Waterways Experiment Station, Federal Aviation Administration, September 1975.
27. Rauhut, J.B., R.L. Lytton, and M.I. Darter, *Pavement Damage Functions for Cost Allocation, Volume 1: Damage Functions and Load Equivalence Factors*, Report No. FHWA/RD-84/018, Federal Highway Administration, June 1984.
28. Claessen, A.I.M., J.M. Edwards, P. Simmer, and P. Uge, "Asphalt Pavement Design - The Shell Method," *Proceedings*, Fourth International Conference on Structural Design of Asphalt Pavements, Volume 1, August 1977.
29. Simpson, A., J. Daleiden, and B. Hadley, "Rutting Analysis From a Different Perspective," *TRR No. 1473*, Transportation Research Board, National Research Council, Washington, DC, July 1995.
30. Finn, F.N., C. Saraf, R. Kulkarni, K. Nair, W. Smith, and A. Abdullah, *Development of Pavement Structural Subsystems*, NCHRP Report No. 291, National Cooperative Highway Research Program, Transportation Research Board, National Research Council, Washington, DC, December 1986.
31. Baladi, Gilbert Y. and Francis X. McKelvey, *Mechanistic Evaluation and Calibration of the AASHTO Design Equations and Mechanistic Analysis of the SHRP Asphalt-Surfaced Pavement Sections*, Report No. SHRP-P-678, Strategic Highway Research Program, National Research Council, Washington, DC, 1994.
32. Nielsen, J.P. and G.T. Baird, *Evaluation of an Impulse Testing Technique for Nondestructive Testing of Pavements*, Report No. CEEDO-TR-77-46, Civil and Environmental Engineering Development Office, Tyndall Air Force Base, Florida, September 1977.